The Role of 17beta-Estradiol on 2,3,7,8-Tetrachlorodibenzo-p-dioxin-mediated Oxidative DNA Damage in Liver Cell Models

dem Fachbereich Chemie der Universität Kaiserslautern
zur Erlangung des akademischen Grades
"Doktor der Naturwissenschaften"
eingereichte Dissertation

(D386)

vorgelegt von
Diplom Lebensmittelchemikerin
Manuela Göttel

Betreuung:

Prof. Dr. Dr. Dieter Schrenk,
Technische Universität Kaiserslautern

Der experimentelle Teil der vorliegenden Arbeit entstand im Zeitraum von Mai 2005 bis Dezember 2008 im Fachbereich Chemie, Fachrichtung Lebensmittelchemie und Toxikologie an der Technischen Universität Kaiserslautern sowie in der Lebensmitteltoxikologie an der Universität von Burgund in Dijon.

Eröffnung des Promotionsverfahrens: 07. Januar 2009

Tag der wissenschaftlichen Aussprache: 10. Dezember 2009

Prüfungskommision:

Vorsitzender: Prof. Dr. Werner Thiel

1. Berichterstatter: Prof. Dr. Dr. Dieter Schrenk

2. Berichterstatter: Prof. Dr. Marie-Christine Chagnon

ACKNOWLEDGEMENTS

First of all, I greatly want to thank my principal supervisor Prof. Dr. Dr. Dieter Schrenk for his support and the opportunity to perform my doctoral thesis in his lab and work on such an interesting toxicological topic. The presentation of my research results during international toxicology congresses such as EUROTOX or SOT were a great experience. I also want to thank Prof. Schrenk for supporting my wish to organize a stay abroad to perform parts of my research work in France.

Likewise, I profoundly want to thank Prof. Dr. Marie-Christine Chagnon at the laboratory of Food Toxicology at the University of Burgundy in Dijon, France for having accepted me to work in her research group for several months. The possibility to establish cooperation between the two labs even afterwards further added to the immeasurable experience. I am thankful for her support, extensive advice, and fruitful discussions.

I would also like to thank Prof. Dr. Werner Thiel for accepting the responsibility of leading the board of examiners.

Thanks to all members of Prof. Schrenk's, Prof. Eisenbrand's, and Prof. Richling's research groups for the nice working atmosphere and the exchange and cooperation between the groups. I want to thank all the colleagues for the great time we spent together, even outside the lab. Especially, I want to thank my friends Yvonne Fery, Yufanyi Ngiewih, Nicole Raquet, and Sven Triebel with whom I shared a lot of fun at the lab and beyond.

Special thanks to our technicians for their expert technical support: Monika Gross for her record-worthy isolation of rat hepatocytes and her organizing talent, Andreas Kamychnikow for his Best Western support, and Wilja Daub for any kind of technical assistance.

Thanks to Anita Strohauer for her friendliness and help with any kind of problems. Thanks as well to Rainer Scheuermann, who continuously spread his good humor in the lab, keep your smile! Thanks to Ari Vetter for his availability when technical problems occured, especially with the comet software. Thanks to Sylvia Schmidt, without your company in the comet lab many of the endless comet assay hours would have been much less exciting, and to Phillip Bellion for the helpful discussions on the GSH assay.

Many thanks to all my internship students for their contribution to this work in any way: Christina Pachel, Maria Tsaneva, Martin Chopra, and Estelle Renard.

Merci beaucoup to all the colleagues and friends in Dijon. *Je vous remercie énormément* for having welcomed and integrated me in such a friendly fashion. It was always a great pleasure working with you.

In particular I would like to thank Isabelle Severin for her valuable and extensive advice on genotoxicity tests, Coralie Dumont for her friendship and support in the transfection assays, Ludovic LeCorre for the fruitful discussions, especially during the last months, and Laurence Dahbi for the numerous scientific discussions. Catherine Berges and Willy Potier deserve my gratefulness, among other things, for helping me out with dry ice for the transport of the uncounted samples that travelled between Kaiserslautern and Dijon. Many thanks to all of you for the *pauses café conviviales,* which I always enjoyed.

I also want to express many thanks to Hélène Poirier at the laboratory of Nutrition at the University of Burgundy in Dijon for providing me deep insights into the method of qPCR, for her time and patience, and many helpful ideas.

My best wishes to Prof. Bernd Epe at the laboratory of pharmacy at the University of Mainz, who kindly provided us with repair-deficient $OGG1^{-/-}/csb^{mut/mut}$ mice. Special thanks to Markus Fussher, who performed the alkaline elution technique with me, for his support and help.

Dr. Karl-Heinrich Fritzemeier (Bayer Schering, Germany) has to be thanked for kindly providing us with the anti-estrogen ZK 191 703 and for answering my questions.

I would like to acknowledge the financial support in the award of a Doctoral Scholarship (Landesgraduiertenförderungsgesetz (LGFG) Rheinland-Pfalz) and a Foreign Exchange Scholarship (Deutscher Akademischer Austauschdienst (DAAD)).

I am most grateful to my friends, especially to Anja and Jamie, for encouraging me throughout this work, for their support and motivation.

Thanks to *Portugal. The Man*, *Muse*, and *Black Rust* for the inspiring music.

Without the constant support and help of my parents and my family this doctoral thesis would not have been possible.

Special thanks to Benjamin: your support and encouragement always kept me going!

LIST OF ABBREVIATIONS

[3H]-thymidine	tritium-labelled thymidine
µg	microgram [unit]
µL	microliter [unit]
µM	Micromolar
17beta-HSD	17β-hydroxysteroid dehydrogenase
2-AAF	2-acetylaminofluorene
2-OHE2/4-OHE2	2-/4-hydroxyestradiol
8-MOP	8-methoxypsoralen
8-oxo-dG	8-hydroxy-2'-deoxyguanosine
3-MC	3-methylcholanthrene
Ade	Adenine
AF	activation functions
aFGF	acidic fibroblast growth factor
AhR	aryl hydrocarbon receptor
AhRC	aryl hydrocarbon receptor complex
AhRR	aryl hydrocarbon receptor repressor
AMP	adenosine monophosphate
AR	autoradiography
ARNT	aryl hydrocarbon nuclear translocator
ATP	adenosine triphosphate
ATSDR	Agency for Toxic Substances and Disease Registry
BaP	benzo(a)pyrene
BER	base excision repair
β-gal	beta-galactosidase
bHLH	basic-helix-loop-helix
bp	base pair
Brg1	Brahma/SWI2-related gene 1
BROD	benzyloxyresorufin *O*-debenzylase
BSA	bovine serum albumin
bw	body weight
cAMP	cyclic adenosine monophosphate
CBP	cAMP response element binding protein
CE	catechol estradiol
cDNA	complementary DNA
ChIP	chromatin immunoprecipitation
CHO	chinese hamster ovary cells
COMT	catechol-O-methyltransferase
CPRG	chlorophenol-red β-D-galactopyranoside
csb	cockayne syndrome B
CT	treshold cycle
CYP	cytochrome P450-dependent mono-oxygenases
DBD	DNA binding domain
DCF	2',7'-dichlorofluorescein
dCMP	deoxycytidine monophosphate
DEN	diethyl-N-nitrosamine
dG	deoxyguanosine
DMEM	Dulbecco's modified Eagle's medium
DMSO	dimethylsulfoxide
DNA	deoxyribonucleic acid

dNTP	deoxynucleotide triphosphate
DRIP	vitamin D receptor interacting protein
dRPase	deoxyribophosphodiesterase
DSB	double-strand break
dsDNA	double-stranded DNA
DTNB	5,5'-dithiobis-2-nitrobenzoic acid
E.coli	escherichia coli
e.g.	for example
E1	estrone
E2	17beta- estradiol
E3	estriol
EGF	epidermal growth factor
Endo	endonuclease
EndRet	endoplasmatic reticulum
ER	estrogen receptor
ERE	estrogen response elements
ERE	estrogen response element
EROD	7-ethoxyresorufin-O-deethylase
et al.	and others
EtOH	ethanol
EtRes	7-ethoxyresorufin
FAD	flavin adenine dinucleotide
Fapy	formamidopyrimidine/4,6-diamino-5-formamidopyrimidine/2,6-diamino-4-hydroxy-5-formamidopyrimidine
FBS	fetal bovine serum
Fen1	flap endonuclease I
FMN	flavin mononucleotide.
FPG	Formamidopyrimidine (Fapy)-DNA glycosylase
GC-MS	gas chromatography mass spectrometry
GPx	glutathione peroxidases
GR	gluthatione reductase
GSH	glutathione (reduced form)
GSSG	oxidized glutathione/glutathione disulfide
GST	glutathione-S-transferases
Gua	guanine
Gy	gray [unit]
h	hour [unit]
h .../r ...	human .../rat ...
H_2DCFDA	2', 7'-dichlorodihydrofluorescein diacetate
HAH	halogenated aromatic hydrocarbon
HAP1	human 5'AP-endonuclease
HAT	histone acetyltransferase
HGF	hepatocytes growth factor
HhH	helix-hairpin-helix
HPLC-ECD	high performance liquid chromatography with electrochemical detection
HSD	hydroxysteroid dehydrogenase
HSP	heat shock protein
i.e.	that is
i.p.	intraperitoneal
I3C	indole-3-carbinol
IARC	International Agency for Research on Cancer
ICZ	indolo-(3,2,-b)-carbazole
iXRE	inhibitory xenobiotic responsive element
kDa	kilodaltons [unit]
kg	kilogram [unit]
ko	knockout
L	liter [unit]

LBD	ligand binding domain
LMP	low melting point
LOAEL	lowest observed adverse effect
LSC	liquid scintillation counting
Luc	luciferase
mA	miliampere [unit]
MAPK	mitogen activated protein kinase
MB-COMT	membrane-bound COMT
MEM	minimum essential medium
MFO	mixed function oxidase
MGMT	O6-methylguanin-DNA –methyltransferase
min	minutes [unit]
mL	milliliter [unit]
mM	millimolar
MMS	methyl methanesulfonate
mRNA	messenger-ribonucleic acid
MROD	methoxyresorufin *O*-dealkylase
NADH	nicotinamide adenine dinucleotide
NADPH	nicotinamide adenine dinucleotide phosphate
NER	nucleotide excision repair
ng	nanogram [unit]
NHEJ	Non-homologous end joining
nm	nanometer [unit]
nM	nanomol [unit]
NMPA	normal melting point agarose
NOAEL	no observed adverse effect level
NQO	4-nitroquinoline-N-oxide
NTP	National Toxicology Program
OGG1	7,8-dihydro-8-oxoguanine-DNA glycosylase
oligo(dT)	oligodeoxythymidylic acid
or HPLC-MS	high performance liquid chromatography mass spectrometry
OTM	olive tail moment
PAGE	polyacrylamide gel electrophoresis
PAH	polycyclic aromatic hydrocarbon
PAS	Per-ARNT-SIM
PBS	phosphate buffered saline
PBSCMF	phosphate buffered saline (magnesium and calcium free)
PCB	polychlorinated biphenyls
PCDD	polychlorinated dibenzo-p-dioxins
PCDF	polychlorinated dibenzofuran
PCNA	proliferating cell nuclear antigen
PCR	polymerase chain reaction
Per	period
pg	picogram [unit]
pH	potentia hydrogneii [unit]
PHf	primary hepatocytes from female rats
PHm	primary hepatocytes from male rats
pM	picomolar [unit]
Pol	polymerase
POP	persistent organic pollutant
PROD	pentoxyresorufin *O*-dealkylase
PVDF	polyvinylidene fluoride
Q	quinone
qPCR	quantitative polymerase chain reaction
QR	quinone reductase
r/h ...	rat/human ...
REP	relative potency value

RFC	replication factor C
RNA	ribonucleic acid
ROS	reactive oxygen species
rpm	revolustions per minutes
rRNA	ribosomal RNA
RT	reverse transcription
SAH	S-adenosylhomocysteine
SAM	S-adenosylmethionine
S-COMT	soluble COMT
SDS	sodium dodecyl sulfate
SHE	syrian hamster embryo
SIM	single-minded
siRNA	small interfering RNA
SOD	superoxide dismutase
SQ	semiquinone
SRC	steroid receptor coactivator
SSB	single-strand break
SULT	sulfotransferase
Taq	thermus aquaticus
TBH	tert-butyl hydroperoxide
TBS	tris buffered saline
TCDD	2,3,7,8-tetrachlorodibenzo-p-dioxin
TDI	tolerable daily intake
TEF	toxic equivalency factor
TEQ	toxic equivalent
TGF	transforming growth factor
tGSH	total glutathione level
TIF	transcriptional intermediary factor
TK	thymidine kinase
TM	melting temperature
TRAP	thyroid hormone receptor-associated protein
tRNA	transfer RNA
TSH	thyroid stimulating hormone
UDP	uridine diphosphate
UDPGT	UDP glucuronosyltransferases
UDS	unscheduled DNA synthesis
UV	ultraviolet radiation
v/v	volume per volume
w/o	without
w/v	weight per volume
WHO	World Health Organisation
wt	wild-type
XAP2	hepatitis B virus X-associated protein 2
xg	gravitational acceleration [unit]
XRCC	X-ray repair cross-complementing factor
XRE	xenobiotic responsive element

DEUTSCHE ZUSAMMENFASSUNG

2,3,7,8-Tetrachlorodibenzo-p-dioxin (TCDD) ist ein ubiquitär in der Umwelt vorkommendes humanes Kanzerogen. Es bestehen reichlich Hinweise darauf, dass TCDD über den aktivierten Arylhydrocarbon Rezeptor (AhR) und dadurch vermittelte Induktion der Cytochrome P450 CYP1A1 und CYP1B1 antiestrogene Wirkung ausübt und in den Estrogenrezeptor alpha (ERalpha) vermittelten Signalweg eingreifen kann. In der vorliegenden Arbeit wurde die Hypothese überprüft, ob eine gesteigerte Aktivierung des Estradiolmetabolismus durch die TCDD induzierten Enzyme CYP1A1 und CYP1B1 zu oxidativen DNA Schäden in Leberzellen führen kann. Außerdem wurde die mögliche Modulation durch 17beta-Estradiol (E2) untersucht. Die ausgewählten spezies- und geschlechtsspezifischen AhR-responsiven Leberzellmodelle, die Hepatomzelllinien HepG2 (human) und H4IIE (Ratte) sowie primäre Rattenhepatozyten von männlichen und weiblichen Wistar Ratten, zeigten eine Induktion von CYP durch TCDD. Die basale und TCDD-induzierte Expression von CYP1B1, welches als Schlüsselenzym im Estradiolmetabolismus E2 in das reaktivere und gentoxische 4-Hydroxyestradiol überführt, war am besten in den primären Rattenhepatozyten ausgeprägt. Die CYP-abhängige Induktion von reaktiven Sauerstoffspezies (ROS) konnte nur in Rattenzellen gezeigt werden und lässt diese als bessere Stimulatoren des Estradiolmetabolismus über den reaktiveren CYP1B1-vermittelten Reaktionsweg vermuten. Estradiol selbst induzierte ROS nur in primären Rattenhepatozyten, was gleichzeitig mit einer Induktion von CYP1B1 mRNA verbunden war. Zum ersten Mal wurde in dieser Arbeit die Rolle von TCDD und E2 auf oxidative DNA Schäden im Comet Assay *in vitro* an Leberzellen untersucht und brachte beide Substanzen als Induktoren oxidativer DNA Basenmodifikationen nur in den primären Rattenhepatozyten hervor. Die direkte DNA schädigende Wirkung der beiden Hauptestradiolmetaboliten, 4-Hydroxyestradiol und 2-Hydroxyestradiol, trat ebenfalls nur in primären Rattenhepatozyten auf und zeigte, dass E2 die DNA im gleichen Ausmaß schädigte. Die Induktion oxidativer DNA Schäden durch E2 konnte allerdings nicht vollständig mit der metabolischen Umwandlung von E2 durch CYP1A1 und CYP1B1 erklärt werden und muss weiter untersucht werden. Die endogene Expression geringer Mengen an ERalpha mRNA in Rattenhepatozyten und das Fehlen von ERalpha in den Hepatomzelllinien wurde zum Anlass genommen, die Effekte von ERalpha in transfizierten HepG2 zu untersuchen. Durch die Überexpression von ERalpha zeigte E2 eine steigernde Wirkung auf die AhR-vermittelte transkriptionelle Aktivität als mögliche Regulation von E2 Levels. Im Gegenzug reduzierte TCDD die durch E2 aktivierte ERalpha Signalwirkung und bestätigte die antiestrogene Wirkung von TCDD. Eine solche Modulation durch die Kobehandlung von TCDD mit E2 konnte in allen anderen Experimenten nicht beobachtet werden und die Rolle endogener ERalpha Levels muss im Weiteren untersucht werden.

TABLE OF CONTENTS

1. INTRODUCTION

Cancer is the leading cause of death worldwide. Lung, stomach, colon, liver, and breast cancer are among the most frequent cancers leading to death each year. In 2004, liver cancer caused the death of 610 000 persons worldwide, which makes it the fourth fatal disease after lung, stomach, and colon cancer. The cellular changes result in the transformation of cells into tumors which are dependent on the genetic disposition, but also other factors such as the diet, or the exposure to environmental contaminants e.g. dioxins play a major role. (WHO, 2009)

Dioxins are a large family of halogenated aromatic hydrocarbons (HAHs), termed polychlorinated dibenzo-p-dioxins (PCDDs). PCDDs are released into the environment as by-products during various combustion processes, such as waste incineration or production of certain pesticides or chemicals, and can ubiquitously be found in the environment. They are ubiquitously found in soil, sediments, air, animals, and human tissues and are known to accumulate throughout the food chain because of their lipophilic character and slow metabolism *in vivo*. The general population can be exposed to PCDDs by inhalation, ingestion, and dermal contact. Apart from occupational and accidental exposures to PCDDs, more than 90% of the human exposure occurs through the diet by eating meat, milk, eggs, fish, and related products, since the compounds accumulate in animal fat. (IARC, 1997)

The prototype compound of PCDDs is 2,3,7,8-tetrachlorodibenzo-p-dioxin (TCDD), a highly toxic and persistent organic pollutant (POP, Stockholm Convention) which is ubiquitously present in the environment, in the food chain, or human samples (Agent Orange Association of Canada, 2009). Mean background levels of TCDD in human tissues are in the range of 2-3 ng/kg fat (IARC, 1997).

TCDD exerts its toxic effects via the activation of the arylhydrocarbon receptor (AhR) signaling pathway and subsequent altered gene expression including cytochromes P450 (CYP) 1A1, 1A2, and 1B1 (Whitlock et al., 1996; Mimura and Fujii-Kuriyama, 2003). It was classified as a human carcinogen by the International Agency for Research on Cancer and the liver carcinogenesis is one of the major concerns related to TCDD exposure (IARC, 1997). In initiation-promotion studies TCDD was not found to be genotoxic but a potent liver tumor promotor. TCDD acts as a more potent hepatocarcinogen in female than in male or ovariectomized rats (Kociba et al., 1978; Lucier et al., 1991). The sex difference

led to the hypothesis of an estrogen-dependent mechanism of TCDD-induced carcinogenesis in rats, associated with increased levels of 8-oxo-hydroxyguanine (8-oxo-G), a hallmark of oxidative DNA damage (Wyde et al., 2001; Tritscher et al., 1996).

It was shown that TCDD elicits its anti-estrogenic effects by interfering in the metabolism of hormones such as estrogens via the induction of biotransformation enzymes (Safe et al., 1998). Exposure to estrogens such as 17beta-estradiol (E2) is primarily associated with an increased risk of breast cancer (Clemons and Goss, 2001). However, E2 was also associated with liver carcinogenesis and it has been postulated to act as a promoter by estrogen receptor-mediated growth stimulation via co-mitogenic effects (Ni and Yager, 1994).

As the metabolism of the major estrogen estradiol occurs mainly in the liver, which is also the major target organ of the xenobiotic metabolism, the present study was conducted to further elucidate the role of E2 in TCDD-mediated oxidative DNA damage in *in vitro* liver cell models.

2. THEORETICAL BACKGROUND

2.1. DIOXINS AND TCDD

Polychlorinated dibenzo-p-dioxins (dioxins) and polychlorinated dibenzofurans (furans) (PCDD/PCDF), polybrominated dibenzo-p-dioxins, and polychlorinated biphenyls (PCBs) are termed as halogenated aromatic hydrocarbons (HAHs), and are among the most important toxic persistent environmental pollutants (persistent organic pollutants, POPs). The most toxic and potent compound of this group of structurally related chemicals, which have a common mechanism of action and induce the same spectrum of effects, is the dioxin-type molecule 2,3,7,8-tetrachlorodibenzo-p-dioxin (TCDD). The chemical structures of a representative PCDD and PCDF are shown in Figure 1. Moreover, these substances are ubiquitously found in the environment, as they are highly persistent and accumulate in the food chain because of their chemical stability, lipophilicity and their resistance to degradation.

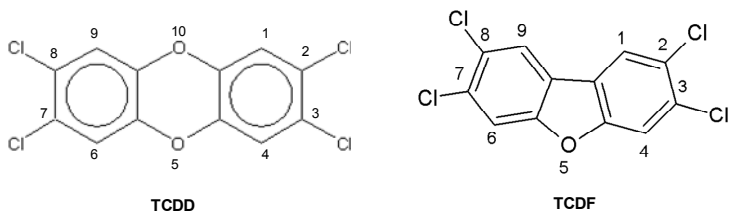

Figure 1: Chemical structure of the PCDD 2,3,7,8-tetrachlordibenzo-p-dioxin (TCDD) and the PCDF 2,3,7,8-tetrachlorodibenzofuran (TCDF), including the ring numbering.

There exist 75 possible PCDD isomers and 135 possible PCDF congeners. Not all of these isomers are toxic, as their toxic potency depends on the structure-activity relationship. In more general terms, toxic congeners have halogen atoms in three or four of the lateral ring positions. (Poland and Knutson, 1982)

2.1.1. PRODUCTION AND EXPOSURE

TCDD and its related compounds are not commercially synthesized, but are formed and released into the environment as trace contaminants of various chemical combustion processes or natural processes. PCDDs including TCDD are inadvertently produced in thermal processes with free chlorines such as during paper pulp bleaching, waste incine-

ration, metal production, and wood combustion. (Silkworth and Brown, 1996; ATSDR, 1998)

Dibenzodioxins and dibenzofurans were produced during the synthesis of chlorophenols and chlorophenoxy broad-spectrum herbicides that were widely used in the 1960s and 1970s to control weeds and as a defoliant during the Vietnam War (Agent Orange). Mixtures of PCDDs and PCDFs have also been identified as contaminants in these products. During the synthesis of 2,4,5-trichlorophenol used to manufacture the broad-spectrum herbicide and defoliant 2,4,5-trichlorophenoxyacetic acid, TCDD was formed. (Poland and Knutson, 1982)

TCDD itself has no commercial applications but is synthesized as a research chemical. It was tested as a flame-proofing agent, an insecticide, and a wood destroying fungicide, but was never commercially used for these purposes (ATSDR, 1998). Besides occupational exposure, accidental exposure to dioxins can occur during industrial accidents. In 1976, the so-called Seveso disaster (Italy) has resulted in the highest known exposure to TCDD in residential populations (Warner et al., 2002). Exposure to humans is nearly entirely through the diet particularly milk and other dairy products, fish and meat (IARC, 1997).

2.1.2. PHARMACOKINETICS

After oral administration of radio-labeled TCDD, it was found to be stored primarily in the liver and to a lesser extent in the fat tissue and is eliminated in feces and a smaller amount in the urine (Rose et al., 1976). The biological half-life of TCDD differs a lot between humans and rodents. The whole body-half-life was estimated to be 5.8 – 11.3 years in humans (Olson, 1994) compared with generally 10 to 30 days in rodents (rat, guinea pig, hamster). (IARC, 1997)

Consequently, following chronic low-dose exposure, TCDD accumulates at a higher rate in human tissue compared to experimental animals. Lipophilicity increases with more chlorination and controls absorption and tissue partitioning. Metabolism is the rate-limiting step for elimination. Since persistent compounds are slowly metabolized and eliminated, they bioaccumulate as a result. (WHO, 1998)

2.1.3. TOXIC EQUIVALENT FACTORS (TEFS)

TCDD is the most toxic and potent congener of the group of HAHs. In order to express the relative biological potency and toxicity of other congeners in relation to the lead compound TCDD the concept of toxic equivalency factors (TEFs) has been established. (van den Berg et al., 2000)

The TEF estimates the toxic potency of a compound relative to the toxicity of TCDD, for which the factor of 1 was assigned. The TEF concept has the purpose of facilitating human risk assessment and regulatory control of exposure to complex PCDD, PCDF, and PCB mixtures. The consensus WHO TEF values were derived based on all available scientific data using a tiered approach in which *in vivo* studies were given more weight than *in vitro* data. The Relative Potency Value (REP) refers to substances for which the relative potency to TCDD was obtained based on a single *in vitro* or *in vivo* study.

TEF values are used to calculate toxic equivalent (TEQ) concentrations in biological samples including human tissues and food. The inclusion criteria for a compound in the TEF concept were elaborated as follows:

- obligatory structural relationship to PCDDs and PCDFs
- binding to the Ah receptor
- exert AhR-mediated biochemical and toxic responses
- persisting and accumulating in the food (Ahlborg et al., 1994)

Modulating effects of compounds that are not AhR ligands are not considered in the TEF concept. Based on the TEF approach, the World Health organization established a tolerable daily intake (TDI) of 1-4 TEQ pg/kg bw/day for dioxins and dioxin-like compounds by applying a safety factor of 10 to the range of selected lowest observed adverse effect levels (LOAELs) of 14-37 pg TCDD/kg bw/day. (WHO, 1998)

2.1.4. TCDD AND ITS TOXIC EFFECTS

TCDD as the prototypical and most potent HAH exerts a number of species- and tissue-specific biochemical and toxicological responses. The most important TCDD-mediated effects are summarized in the following Table (Table 1). Some of its toxic effects, which are crucial for this work, are illustrated and focused on in more detail in thesubsequent sections.

Table 1: Overview of biochemical and toxic effects of TCDD. (Safe, 2001; WHO, 1998; Denison and Heath-Pagliuso, 1998)

<table>
<tr><td>Immunotoxicity:
Immune suppression, thymic involution</td><td>Induction of Gene Expression:
Phase 1 and Phase 2 drug metabolizing enzymes</td></tr>
<tr><td>Dermal Toxicity:
Chloracne, hyperkeratosis</td><td rowspan="2">Endocrine Disruption:
Alterations in endocrine homeostasis, interaction with estrogen receptor (AhR/ER cross talk)</td></tr>
<tr><td>Tumor Promotion</td></tr>
<tr><td>Hepatotoxicity</td><td rowspan="3">Modulation of cell growth:
Proliferation and differentiation,
inhibition of apoptosis</td></tr>
<tr><td>Wasting Syndrome</td></tr>
<tr><td rowspan="2">Teratogenicity:
Cleft palate, hydronephrosis, embryotoxicity</td></tr>
<tr><td>Lethality</td></tr>
</table>

2.1.4.1. CARCINOGENICITY

TCDD has been classified as a human carcinogen by the National Toxicology Program (NTP) and the International Agency for Research on Cancer (IARC, 1997). The primary supporting data for its carcinogenic effects are derived from animal carcinogenicity studies and mechanistic studies with TCDD. Additionally, human epidemiology data provide evidence that both animals and humans have a similar mechanism of action towards toxicological responses to TCDD and that there is a causal relationship between exposure to TCDD and cancer. (Schmidt and Bradfield, 1996)

Since 1977 many independent animal studies of TCDD have found this compound to be carcinogenic in a dose-dependent fashion and induce tumors in several species like rats, mice, and hamsters. Tumors occur in both sexes in various strains at multiple sites and from multiple routes of dosing. Increased incidences of cancers in laboratory animals include liver, thyroid, lymphatic, respiratory tract, adrenal cortex, hard palate, nasal turbinates, tongue, and skin. (Huff et al., 1994; Knerr and Schrenk, 2006)

In three chronic studies in two mouse strains oral administration of TCDD over 52–104 weeks increased the incidence of hepatocellular adenomas and carcinomas in both males and females (Tóth et al., 1979; Della Porta et al., 1987; NTP, 1982a). In one of these expe-

riments follicular cell adenomas of the thyroid, lymphomas, and subcutaneous fibrosarcomas were observed in female mice, whereas a trend for dose-related increase in lung tumors was found in male mice (NTP, 1982a).

In rats TCDD's carcinogenic effect was characterized dose-dependently in the liver (Poland and Knutson, 1982; Kociba et al., 1978). In a two-year TCDD feeding study of male and female Sprague Dawley rats, female rats showed an increased incidence of hepatocellular hyperplastic nodules and hepatocellular carcinomas at the highest dietary level (100 ng/kg bw/day). Squamous cell carcinomas of the hard palate, nasal turbinate, tongue, and lung were found in both sexes. Hence, female rats were more sensitive than males to hepatocarcinogenic effects of TCDD. The lowest observed adverse effect of TCDD in the Kociba study was the development of hepatic adenomas in rats at an intake of 10 ng/kg bw/day. TCDD also caused thyroid tumors in male rats (Kociba et al., 1978). The induction of liver UDP glucuronosyltransferases (UDPGTs) by TCDD is responsible for the increased excretion of thyroid hormone. The subsequent feedback mechanism results in an increase in thyroid stimulating hormone (TSH), stimulating proliferation of thyroid follicular cells. (Barter and Klaasen, 1992; WHO, 1998)

In a second two-year study in female Sprague Dawley rats increased incidence of cholangiocarcinomas and hepatocellular adenomas of the liver, cystic keratinizing epithelioma of the lung, and gingival squamous cell carcinomas of the oral mucosa were noted (Walker et al., 2006). Application of TCDD for 104 weeks to the clipped skin of mice increased the incidence of dermal fibrosarcomas in mice (NTP, 1982b). Administration of TCDD (intraperitoneal (i.p.) or subcutaneous injection at 4 week intervals for 13 months) to hamsters resulted in test substance-related occurrences of squamous skin cell carcinomas (Rao et al., 1988).

TCDD is a tumor promotor as shown in initiation-promotion studies. Administration of TCDD following initiation with known carcinogens enhanced the incidence of skin papillomas, lung adenomas, liver adenomas, and hepatoblastomas in mice. Extensive examination of liver tumor promotion showed that TCDD acts as a liver tumor promotor in rats and mice. In several rat strains TCDD enhanced the incidence of hepatic lesions of female rats after initiation with N-nitrosamines such as diethyl-N-nitrosamine (DEN). (Pitot et al., 1980; Dragan and Schrenk, 2000; Viluksela et al., 2000; Moennikes et al., 2004)

Short-term studies indicate the lack of direct DNA-damaging effects including covalent binding to DNA by TCDD, which underlines that TCDD is not acting as an initiator (Turteltaub et al., 1990; Randerath et al., 1990). Studies on liver tumor promotion in the female rat liver support a non-genotoxic mechanism for the induction of neoplasms by TCDD.

The processes involved in carcinogenicity induced by TCDD do have a no observed adverse effect level (NOAEL), which in the rat liver is at an exposure level of 1 ng TCDD/kg bw/day (Kociba et al., 1976). The ability of TCDD to enhance proliferation via co-mitogenic action and to inhibit apoptotic processes in enzyme-altered liver foci, or to induce oxidative DNA damage in nuclear rat liver DNA further supports an indirect mechanism of carcinogenicity (Schrenk et al., 1992; Stinchcombe et al., 1995; Wyde et al., 2001).

2.1.4.2. GENOTOXICITY

Equivocal findings in *in vivo* and *in vitro* genotoxicity studies of TCDD in human and animal cells indicated that TCDD is not believed to be mutagenic (IARC, 1997). TCDD failed to induce mutations in the Ames test in the presence and in the absence of exogenous metabolically active S9-mix (Mortelmans et al., 1984). The *in vitro* Unscheduled DNA Synthesis (UDS) assay performed in cultures of human mammary epithelial cells derived from five women showed no induction of DNA repair activity after treatment with TCDD (Eldridge et al., 1992). However, a mixture of organochlorine compounds containing TCDD increased sister chromatide exchange formation in human lymphocytes (Nagayama et al., 1994).

DNA single-strand breaks were induced dose- and time-dependently in the liver of single dosed TCDD-treated female Sprague Dawley rats using the alkaline elution technique (Wahba et al., 1989). Additionally, DNA single-strand breaks were detected in rat peritoneal lavage cells (Alsharif et al., 1994a) and in human breast cancer cell lines by means of the comet assay (Lin et al., 2007). Nevertheless, there is no evidence of direct binding of TCDD to DNA (IARC, 1997; Randerath et al., 1990). In human studies following *in vivo* exposure, no positive results of TCDD or other PCDD congeners have been reported upon chromosome aberration (IARC, 1997). The weight of evidence of these experimental data suggests that TCDD is not acting as a direct genotoxic agent.

2.1.5. AHR SIGNALING PATHWAY

The aryl hydrocarbon receptor (AhR) is a ligand-activated transcription factor and a member of the basic-helix-loop-helix/Per-ARNT-SIM (Per: Period, ARNT: aryl hydrocarbon nuclear translocator, SIM: single-minded; bHLH/PAS) family, which is structurally distinct from the nuclear receptor superfamily (see section 2.2.5). Other members of this family include ARNT and the AhR repressor (AhRR) (Hankinson, 1995). AhR mediates the toxicological effects of dioxins and the schematic AhR signaling is demonstrated in Figure 2.

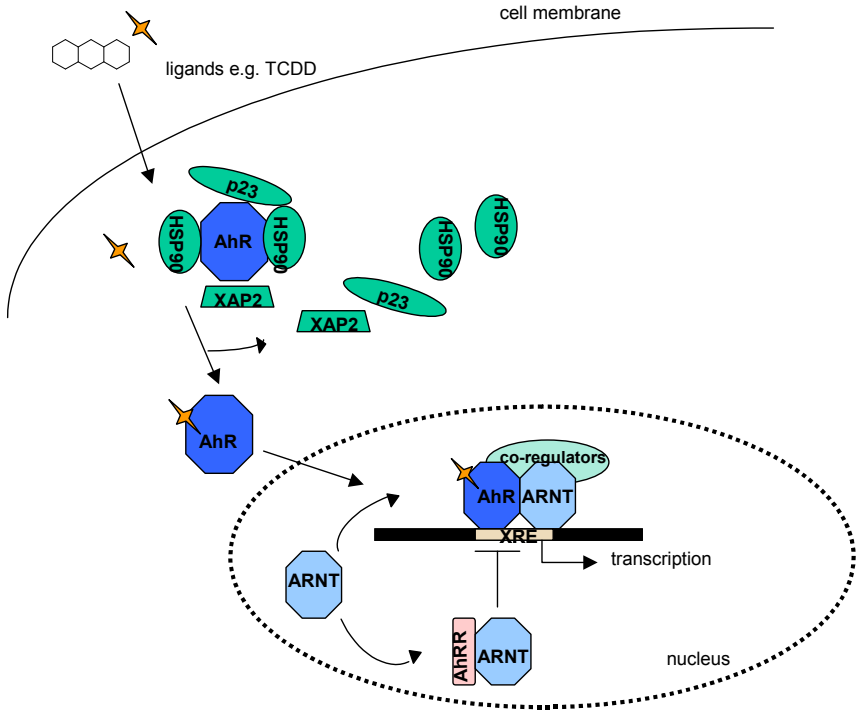

Figure 2: Mechanism of transcriptional activation by AhR and negative feedback regulation by AhRR (according to Mimura and Fujii-Kuriyama et al., 2003).

The unliganded AhR is present in the cytosol as part of a complex with two heat shock protein 90 molecules (HSP90), immunophilin-like protein (XAP2) and co-chaperone p23. XAP2 and p23 are thought to stabilize the HSP90-complex. (Meyer and Perdew, 1999). Ligand binding to the PAS B region of the AhR (see section 2.1.6) induces conformational changes and triggers subsequent translocation of the AhR complex into the nucleus. The AhR dissociates from its HSP90 complex and then dimerizes with its partner molecule, the AhR nuclear translocator (ARNT), in the nucleus. Ligand-bound AhR/ARNT complex (AhRC) recognizes an enhancer element designated xenobiotic responsive element (XRE) located in the promotor regions of AhR target genes. The core consensus nucleotide sequence of XRE is determined to be 5'-TNGCGTG-3' and is present in multiple copies within the enhancer. (Whitlock et al., 1996). In order to activate transcription, co-activators are recruited such as the histone acetyltransferase p300/CBP (cAMP (cyclic adenosine monophosphate) response element binding protein) (Kobayashi et al., 1997), chromatin remodeling factor Brahma/SWI2-related gene 1 (Brg1) (Wang and Hankinson, 2002), and the mediator vitamin D receptor interacting protein/thyroid hormone receptor-associated protein (DRIP/TRAP) complex (Wang et al., 2004). Moreover, binding of the AhR/ARNT heterodimer to XREs facilitates the association of another transcription factor Sp1 to its cognate recognition sequence in the promotor region (Kobayashi et al., 1996).

Phosphorylation state is also important for transactivation and binding activity to the XRE (Whitlock et al., 1996). The AhR/ARNT heterodimer induces the expression of target genes encoding for xenobiotic metabolizing enzymes responsible for activation (Phase 1) such as CYP1A1, CYP1A2, CYP1B1 and for elimination (Phase 2) such as NADP(H)-oxidoreductase, glutathione-S-transferase-Ya (GST-Ya), UDP-glucuronosyltransferase (UDPGT). Additionally, genes involved in cell proliferation (TGF-β, IL-1β, and PAI-2), cell cycle regulation (p27, jun-B) and apoptosis (Bax) are known to be induced by AhR ligands. (Mimura and Fujii-Kuriyama, 2003)

Moreover, the AhR repressor (AhRR) functions as a negative regulator of AhR by competing with AhR for dimerization with ARNT and binding to XRE sequence. It is localized in the nucleus and forms a heterodimer with ARNT constitutively. Together, AhR and AhRR form a regulatory feedback mechanism. (Mimura et al., 1999)

2.1.6. FUNCTIONAL STRUCTURE OF AHR

The AhR was identified for the first time from mouse liver in 1976 (Poland et al., 1976). Members of the bHLH/PAS family possess characteristic structural motifs (Figure 3). At the NH_2 terminal end the protein contains a bHLH motif that is involved in DNA binding and dimerization processes. Additionally, it contains the nuclear localization and export signals. Adjacent to this region the PAS domain is located containing two sub-domains, PAS A and PAS B, which influence protein-protein interactions, DNA recognition, and ligand binding. The ligand binding domain (LBD) partly overlaps with the PAS B region and with the binding site for HSP90. In addition to the PAS B region, HSP90 also interacts with bHLH region to mask the nuclear localization signals, thus keeping the AhR in the cytosol until ligand binding. The C-terminal segment displays a transactivation domain, consisting of multiple stimulatory and inhibitory subdomains. (Whitlock, 1999)

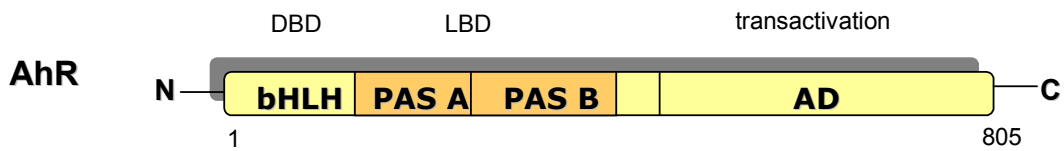

Figure 3: Schematic functional domains of AhR. DBD, DNA binding domain; LBD, ligand binding domain; bHLH, basic helix-loop-helix; PAS, Per-ARNT-Sim; AD, activation domain (adapted from Whitlock, 1999).

2.1.7. SPECTRUM OF AHR LIGANDS

Most if not all of TCDD's toxic effects are mediated by the AhR. Many effects of TCDD are only observed following long-term chemical exposure (Poland and Knutson, 1982). However, the broad substrate-specificity, which is linked to induction of a variety of detoxifi-

cation enzymes, confers a rather adaptive advantage to the organism.
The planar and lipophilic metabolically stable halogenated aromatic hydrocarbons (HAHs) such as the polyhalogenated dibenzo-p-dioxins, dibenzofurans, and biphenyls represent the most potent class of AhR ligands with high AhR binding affinities in the picomolar to nanomolar range. The metabolically more labile polycyclic aromatic hydrocarbon (PAHs) such as 3-methylcholanthrene or benzo(a)pyrene (BaP) exert lower binding affinity (nanomolar to micromolar range). (Denison and Nagy, 2003). These HAHs and PAHs belong to the 'classical' AhR ligands as opposed to the 'non-classical' AhR ligands that can be further subdivided into synthetic and naturally occurring ligands.

Among the synthetic non-classical chemicals benzimidazole drugs (Krusekopf et al., 1997) and pesticides such as carbaryl (Ledirac et al., 1997) can be grouped. A variety of naturally occurring AhR inducers have been described, pointing out the broad substrate specificity of AhR ligands, even though the majority of these ligands are weak CYP1A1 inducers compared to TCDD. A number of dietary plant compounds such as I3C (indole 3-carbinole) (Bjeldanes et al., 1991), curcumin (Ciolino et al., 1998), and carotinoids (Gradelet et al., 1996) competitively bind to the AhR and induce AhR-dependent gene expression. A major class of natural AhR ligands is that of indoles including I3C and tryptophan which can convert in the mammalian digestive tract to more potent AhR agonists, i.e. indole-derived products (Heath-Pagliuso et al., 1998, Perdew and Babbs, 1991). The natural AhR ligand with the highest AhR agonist affinity as identified to date is indolo-(3,2,-b)-carbazole (ICZ), an acidic condensation product formed from I3C (Bjeldanes et al., 1991).

Flavonoids represent the largest group of naturally occurring dietary AhR ligands comprising flavones, flavanols, flavanones and isoflavones most of which are antagonists but agonists such as quercetin also exist (Ciolino et al., 1999). Many of these flavonoids are substrates for CYP1A1 and CYP1B1 (Doostdar et al., 2000).

The continuous and persistent expression of specific genes in target cells might be an explanation for the adverse effects mediated by high affinity ligands whereas the relatively weak PAH ligands lead to only transient activation of AhR-signaling pathway, thus producing less toxic effects compared to TCDD. (Denison and Nagy, 2003)

The occurrence of nuclear AhR complexes in untreated cells in culture supports the existence of endogenous AhR ligands (Singh et al., 1996; Chang and Puga, 1998). To date, the identified endogenous chemicals which activate the AhR gene battery exert very weak AhR binding affinity compared to TCDD. However, a high affinity endogenous AhR ligand has not yet been able to be detected. Moreover, the exact nature of the responsible chemicals remains to be determined. A variety of weak endogenous ligands has been

identified including indoles, tetrapyroles, and arachidonic acid metabolites among others. These endogenous physiological AhR ligands are rapidly degraded by the concomitantly induced detoxifying enzymes but would act as transient inducers of AhR-dependent gene expression indicating a role of AhR in cell proliferation and differentiation or cell cycle programming. (Denison and Nagy, 2003)

2.1.8. CYTOCHROME P450S

The most important superfamily of enzymes involved in oxidative Phase 1 reactions of the xenobiotic metabolism are the cytochrome-P450-dependent mono-oxygenases (CYPs). Members of the cytochrome P450 superfamily are hemeproteins found in plant tissues and in a wide range of species from bacteria to vertebrates located predominantly in the endoplasmic reticulum. Their name 'P450' was originally taken from the characteristic light absorption peak of the proteins at 450 nm when they are reduced and complexed with carbon monoxide. (Murray, 2000)
CYPs are constitutive and inducible oxidative enzymes that catalyze the oxidation of a wide range of lipophilic substrates at the expense of molecular oxygen (O_2) and nicotinamide adenine dinucleotide phosphate (NADPH) primarily for detoxification reaction. The iron-containing hemeproteins consist of heme B as the prosthetic group providing four ligands to the iron. The fifth ligand is a thiolate anion (S^-) from a cysteine residue and the position of the sixth ligand is taken by the oxygen atom of a water molecule (Halliwell and Gutteridge, 1999). Structurally, cytochromes P450 consist of several domains:

- a hydrophobic N-terminus, which acts as a membrane anchor to either smooth endoplasmic reticulum or mitochondria,
- a substrate-binding site,
- an oxygen binding site, and
- a free hydrophilic C-terminal.

The whole mono-oxygenase enzyme system consists of two components (Figure 4): cytochrome P450 and a flavoprotein, NADPH-cytochrome P450-reductase (cytochrome reductase), which are closely bound to each other in the membranes of the smooth endoplasmic reticulum, the nucleus, or mitochondria (Eisenbrand and Metzler, 2002). During the CYP-catalyzed reaction, one atom of O_2 is transferred onto the substrate and the other atom is used to form H_2O, a reaction that is termed mixed-function oxidase or mono-oxygenase reaction. The cytochrome reductase transfers a single electron to the heme-iron (Fe^{3+}) of the cytochrome P450. The resulting oxidized cytochrome P450 (Fe^{2+})

binds molecular oxygen (O_2) as the sixth ligand. The transfer of a second electron by cytochrome oxidoreductase or alternatively cytochrome b_5 results in activated oxygen and the production of a water molecule. Activated oxygen is carried onto the substrate. The oxidized substrate can further be subjected to Phase 2 conjugation reactions catalyzed by detoxifying enzymes including glutathione s-transferases, glucuronyl transferases etc.(Forth et al., 2005)

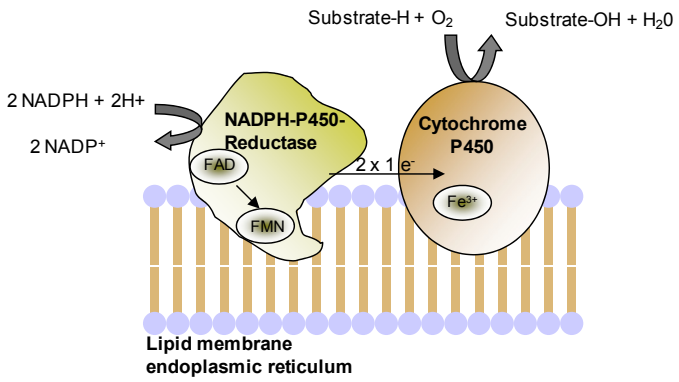

Figure 4: Microsomal mono-oxygenase reaction. The enzyme system consists of NADPH-P450-reductase and cytochrome P450, closely bound to each other and anchored in the lipid membrane of the endoplasmic reticulum. The lipophilic substrate binds to cytochrome P450 in the oxidized state. Flavoprotein NADPH-P450-oxidoreductease transfers a single electron to heme-iron (Fe^{3+}) at the expense of NADPH. The resulting heme-iron Fe^{2+}-complex also binds molecular oxygen (O_2). The transfer of a second electron leads to oxidized substrate and production of a water molecule (H_2O). NADPH: nicotinamide adenine dinucleotide phosphate, reduced form; FAD: flavin adenine dinucleotide; FMN: flavin mononucleotide. (According to Forth et al., 2005)

Besides the inactivation of substrates, also activation processes to form reactive intermediates may occur which can cause cellular damage. Thus, cytochromes P450 are also considered to play a central role in tumor development and progression (Gonzalez and Gelboin, 1994). The liver as the main organ of xenobiotic metabolism is especially rich in cytochromes P450, with the highest cytochrome P450 activity found in hepatocytes. To date, there exist 18 CYP mammalian gene families, among them the four families CYP1, 2, 3, and to a lesser extent CYP4, whose primary role is the metabolism of exogenous compounds from the diet, drugs or environmental toxicants. Another group of important CYP families is constitutively expressed in endocrine glands and is involved in steroid hormone synthesis (CYP11, CYP17, CYP19). (Murray, 2000; Nebert and Dalton, 2006)

Each P450 gene family has an assigned number based on the similarity to their nucleic acid and amino acid sequence homology and is divided into subfamilies (capital letters) and subsequent members of each subfamily (numbers). Some examples of representative inducers and substrates of these families 1-4 are summarized in Table 2. CYP3A4 is quantitatively the main CYP in human liver. CYPs can also be found in extra-hepatic tissues, particularly in those that are exposed to exogenous chemicals such as the small intestine, kidney, and lung (Murray et al., 1988; Halliwell and Gutteridge, 1999).

Table 2: Examples of members of the human cytochrome P450 families 1-4 mainly responsible for the metabolism of xenobiotics with representative inducers and substrates (according to Murray, 2000 and Halliwell and Gutteridge, 1999).

P450 family	P450 sub-family	Isoenzyme	Inducer	Substrate
CYP1	CYP1A	CYP1A1	TCDD, 3-MC	7-Ethoxyresorufin, benzpyrene (PAHs)
	CYP1B	CYP1B1	TCDD	PAHs, estradiol, heterocyclic amines
CYP2	CYP2B	CYP2B1	Phenobarbital, aroclor	Acetylenes, olefins
CYP3	CYP3A	CYP3A4	Rifampicin	Estradiol, methadone, testosterone, aflatoxin
CYP4	CYP4A	CYP4A1	Clofibrate, other peroxisome proliferators	Prostaglandins, fatty acids

The three mammalian CYP1 genes, i.e. CYP1A1, CYP1A2 and CYP1B1 are regulated by the AhR, which is activated by the binding of coplanar PAHs and HAHs. Many substrates for CYP1 enzymes are also AhR ligands. Whereas CYP1A2 in turn mainly metabolizes aromatic amines, CYP1A1 and CYP1B1 can metabolize PAHs (Nebert et al., 2004). The relevance of CYP1A1 and CYP1B1, which also play an important role in the E2 metabolism, is outlined in more detail in section 2.2.8.

2.1.8.1. CYP1A1 AND CYP1B1

In humans and in the rat constitutive CYP1A1 expression is negligible. However, high levels of CYP1A1 mRNA, protein, and enzyme activity are inducible following exposure to numerous lipophilic, co-planar substrates such as PAHs. Many of the inducers are in turn metabolized by CYP1A1. (Nebert et al., 2004)

Inducible CYP1A1 activity is ubiquitously detectable in almost every tissue such as the lung, liver, brain, gastrointestinal tract, lymphocytes, and heart (Anzenbacher and Anzenbacherova, 2001). Historically, CYP1A1 is the classical isoenzyme for the activation of procarcinogenes such as the PAH benzo(a)pyrene (BaP) to ultimate carcinogens. In the first place the carcinogenic PAH 3-methylcholanthrene (3-MC) was discovered as the original inducer of CYP1A1. Later on TCDD was found to be the most potent inducer and is therefore considered as the prototype. The placement of TCDD's four lateral chlorine

atoms is responsible for the compound's metabolic resistance to oxygenation by CYP1A1, so that it can produce a sustained induction and persist in the cell. (Whitlock et al., 1996)

CYP1B1 is a new member of the human CYP1 gene family and was cloned in 1994 (Sutter et al., 1994). There is only a low degree of similarity of nucleic acid and amino acid sequence (about 40%) with CYP1A1 and CYP1A2 (Murray et al., 2001). However, CYP1B1 is most closely related to CYP1A1 and 1A2. Similar to the other members of the CYP1 family, CYP1B1 is induced by PAHs, dioxins, and other typical ligands through the AhR system and in turn it metabolically activates a number of polycyclic aromatic amines, heterocyclic amines, aromatic amines, and nitropolycyclic hydrocarbons to pro-mutagens. CYP1B1 is predominantly found in a number of extrahepatic human tissues including heart, kidney, prostate, ovary, colon, uterus, and mammary gland which is of interest especially in hormone-mediated carcinogenesis. (Shimada et al., 1996)

The rat and human CYP1B1 predicted that nucleic acid amino acid sequences are 80% identical. However, there are considerable species differences regarding regulation and tissue-specific expression. CYP1B1 is over-expressed in a wide range of human tumors (Murray et al., 1997) but it is also highly expressed in hormone-related organs such as the adrenal glands, mammary, uterus, testes, and ovary. This tissue distribution suggests an endogenous physiological function for CYP1B1. In organs, in which CYP1B1 is expressed to a lesser extent, such as liver and kidney, it may rather play a role in detoxification processes, since it is inducible by TCDD (Walker et al., 1995).

Besides the AhR-mediated pathway of transcription by AhR agonists, an alternative procession of CYP1B1 transcription was suggested. The human CYP1B1 mRNA contains multiple polyadenylthion sites and both mouse and rat CYP1B1 have been reported to be also regulated by cyclic AMP (cAMP)-mediated pathways. (Brake and Jefcoate, 1995)

An important discovery was the role of human CYP1B1 as a 4-hydroxylase in estradiol metabolism (Hayes et al., 1996). Several CYPs such as CYP1A1 and CYP1B1 have been demonstrated to catalyze the two main metabolites in the E2 metabolism (see section 2.2.8). Compared to human CYP1B1, mouse CYP1B1 was not found to hydroxylate 17beta-estradiol (Savas et al., 1997).

2.1.9. AhR/ER Cross Talk

TCDD has been reported to induce hepatocellular carcinogenesis in female but not male Sprague Dawley rats and the tumorigenic response in females was considered estrogen-dependent (Kociba et al., 1978). In the same study TCDD showed anti-tumorigenic activity in multiple age-dependent spontaneous endocrine related tumors including pituitary

adenoma (both sexes), pituitary adenocarcinoma, interfollicular adenoma of the thyroid (female), or pheochromocytoma of adrenals (males). Decreased formation of benign uterine tumors and benign neoplasm of the mammary gland in female rats exposed to TCDD suggested that TCDD interacts with the estrogen receptor (ER). There is extensive evidence that TCDD elicits anti-estrogenic activity via the action of the AhR. This is strongly supported by numerous studies in various breast cancer cell lines. Several possible mechanisms for the endocrine disrupting actions have been proposed:

- Inhibition of 17beta-estradiol (E2)-induced cell proliferation and DNA synthesis e.g. by specifically blocking the E2-induced transition from G1 to S phase (Wang et al., 1998).
- Inhibition of E2-dependent gene and protein expression such as pS2, cathepsin D, vitellogenin etc. The activated AhR may inhibit the binding of the E2/ER complex to an estrogen response element (Safe, 2001).
- TCDD induces degradation of ERalpha through activation of proteasome (Wormke et al., 2003).
- TCDD-mediated down-regulation of ER levels via a repressor site in the promotor region of ER genes (e.g. Safe and Wormke et al., 2003).
- Increased E2 metabolism by the induction of CYP1 by TCDD (Cavalieri et al., 2006).
- Increased co-mitogenic action of TCDD by estrogens (Schrenk et al., 1992).

Consequently, this AhR/ER cross talk is considered to play a crucial role in TCDD- and E2-dependent mechanisms of carcinogenesis.

2.2. ESTROGENS AND ESTRADIOL

Estrogens are a group of steroid hormones functioning as the primary female sex hormones but also have a physiological role in the male reproductive tract. The most potent active natural representative of this group of steroids is 17beta-estradiol (E2). The three major naturally occurring estrogens are estrone (E1), E2, and estriol (E3). Estrogens consist of 18 C-atoms. The steran molecule is the basic chemical structure of the estrogens consisting of an aromatic 6-C ring A and three additional saturated 6-C rings B, C, and D (Figure 5). In contrast to androgens, there is no angular methyl group situated between the A and B ring.

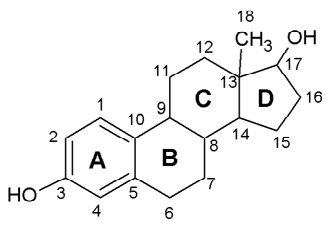

Figure 5: Chemical structure of estradiol (E2) including ring numbering and designation of rings A to D.

The biological activity is dependent on their binding affinity to specific estrogen receptors (see section 2.2.4).

Estrogens exert diverse biological effects such as female sexual differentiation and development, the control of the menstrual cycle, the maintenance of bone density, and proliferation of the endometrium in the uterus, arterial vasodilatation, and neuroprotective actions. Besides the ovary (granulosa and theca cells) and placenta, which are primarily responsible for the production of estrogens in humans, estrogens are produced in minor concentrations by the adrenal glands and testes (Leydig cells). Furthermore, they can also be formed by aromatization of androgens in fat tissue. The conversion of testosterone to estradiol and of androstenedione to estrone is catalyzed by the enzyme aromatase. For the transport in the plasma, estrogens are bound to the sexual hormone binding globulin (SHBG). Plasma estrogen concentrations vary between species and according to sex, age, and the stage of the estrous cycle in women (Silbernagel and Despopoulos, 2003; Forth et al., 2005). Different physiological serum concentrations of estradiol in different species in both sexes are presented in Table 3.

Table 3: Physiological serum concentrations of estradiol in different species and phases. ([a] DePaolo and Masoro, 1989; [b] Sarkar et al., 2000; [c] Silbernagel and Despopoulos, 2003)

Species, Strain	**Sex, Age, Timing**	**Reference Range**
Mice	Female, Basal	1-5 pg/mL[a]
Rats	Female, Basal	< 10 pg/mL[a]
	Female, 2nd Diestrus Day	20-30 pg/mL[a]
	Female, Proestrus	40-50 pg/mL[a]
Rats, Long Evans	Female, basal	about 50 pg/mL[b]
	Female, ovariectomized	< 20 pg/mL[b]
Human	Male	0.05 ng/mL[c]
	Female, ovulation	0.4 ng/mL[c]
	Female, other cycle phases	0.06-0.2 ng/mL[c]
	Female, gestation	7-14 ng/mL[c]

2.2.1. BIOSYNTHESIS

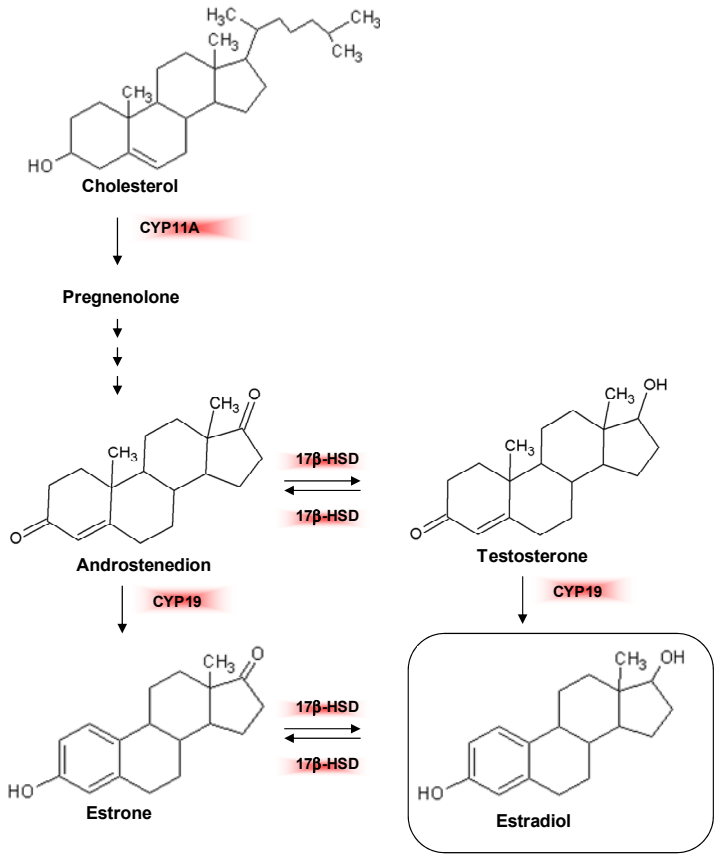

Figure 6: Simplified steps in biosynthesis of steroid hormones and estradiol. Steroid hormones are biosynthesized from cholesterol. Estradiol is formed by both CYP19 and 17beta—hydroxysteroid dehydrogenase (17β-HSD) from androstenedione via testosterone or estrone. (According to Tsuchiya et al., 2005)

The biosynthesis of estrogens from cholesterol involves a series of enzymatic steps catalyzed by either dehydrogenases or CYP enzymes (Figure 6). First CYP11A catalyzes pregnenolone formation from cholesterol by hydroxylation and cleavage of the side chain between C-20 and C-22. This prohormone can further be converted into progesterone (a gestagen) or 17alpha-hydroxypregnenolon by dehydrogenases or CYP17 respectively. In subsequent reactions, involving CYP17 enzymes and dehydrogenases, testosterone is formed. The enzyme aromatase (CYP19) catalyzes the aromatization of the A ring and elimination of the C-19 atom so that androgens are converted into estrogens. Thus, androgens are the obligatory precursors of estrogens. Estrone reacts to potent estradiol by 17beta-hydroxysteroid dehydrogenase (17beta-HSD). (Forth et al., 2005; Tsuchiya et al., 2005)

2.2.2. CARCINOGENICITY

The evidence for the carcinogenic activity of estrogens including 17beta-estradiol in animals and in humans has been sufficient to consider the natural hormone as a carcinogen (IARC, 1987; IARC, 1999). In rodent tumor models estradiol induced various tumor types in many organ sites following oral or subcutaneous administration of pharmacological doses of E2. Hence, E2 increased the incidence of mammary, pituitary, uterine, cervical, vaginal, testicular, lymphoid, and bone tumors in mice (Huseby, 1980; Highman et al.,

1980; Highman et al., 1981; Nagasawa et al., 1980). The incidence of mammary and/or pituitary tumors was increased in rats after dosing E2 (Noble et al., 1975; Shull et al., 1997). In outbred hamsters, malignant kidney tumors occurred in intact and castrated males and in ovariectomized but not intact females (Kirkman, 1959).

In humans elevated circulating estrogen levels caused by hormone medications or by enhanced endogenous estrogen production increase the risk of breast cancer and uterine cancer. Thus, prolonged exposure to estrogen unopposed by progestin, a synthetic progestagen used for hormonal contraception or hormone replacement therapy, is an accepted risk factor for endometrial cancer (Greenwald et al., 1977; Key and Pike, 1988). Even if many cohort studies failed to identify an association between serum estrogens and breast cancer risk, presumably due to inappropriate study designs (Wysowski et al., 1987; Garland et al., 1992), more recent epidemiological studies were able to reveal strong relationships between breast cancer risk and plasma or urinary estrogen concentrations (Adlercreutz et al., 1994; Toniolo et al., 1995). Contrarily to protective effects in the uterine, estrogens in combination with progestin do not inhibit but increase breast cancer risk, since the latter acts as a mitogen for mammary ductal epithelial cells (Colditz et al., 1995).

The carcinogenic action of E2 is mainly associated with mammary and uterine cancer development. However, long-term exposure of women to high levels of synthetic estrogens such as ethinylestradiol has also been linked to increased risk of hepatic tumors (Baum et al., 1973; Palmer et al., 1989). Likewise, in the liver E2 has been found to have co-mitogenic effects in cultured rat hepatocytes mediated through an ER-dependent mechanism. E2 enhanced the mitogenic action of liver growth factors like epidermal growth factor (EGF), transforming growth factor-α (TGF-α), hepatocytes growth factor (HGF), hepatopoietin B, and acidic fibroblast growth factor (aFGF) on stimulated DNA synthesis. (Ni and Yager, 1994). Furthermore, the estrogen co-mitogenesis in cultured hepatocytes could be inhibited by tamoxifen (Yager and Shi, 1991).

2.2.3. GENOTOXICITY

Estradiol has the potential to cause genotoxicity via its reactive metabolites 2-and 4-hydroxyestradiol after metabolic conversion. Bacterial gene mutation tests (Ames) with E2 were negative with or without metabolic activation by S9-mix. (Dhillon and Dhillon, 1995; Lang and Reimann, 1993). Likewise, E2 was negative in mutation tests with mammalian cells (Drevon et al., 1981; Tsutsui et al., 1987 and 2000) except for one assay (Kong et al., 2000). The positive results in this study with V79 cell line however lacked a dose-

response relationship and the mutagenic concentrations were within the physiological range (Kong et al., 2000). Estradiol and its catechol metabolites, in particular 4-hydroyestradiol, induced cell transformation using Syrian hamster embryo (SHE) fibroblasts (Tsutsui et al., 1987 and 2000). Concerning non-mutational DNA lesions estradiol has been studied in a variety of *in vitro* and *in vivo* systems using different endpoints of genotoxicity. Estradiol and its two main catechol metabolites can cause DNA damage as observed in DNA ^{32}P-postlabeling in the following order of potency: 4-OHE2 > 2-OHE2 > E2 (Hayashi et al., 1996). E2 treatment leads to increased DNA strand breaks in the male Syrian hamster kidney, which is consistent with the finding of renal cancers in this species (Han and Liehr, 1994). Additionally, DNA strand breaks were found in the MCF-7 breast cancer cell line and human peripheral lymphocytes *in vitro* (Yared et al., 2002; Anderson et al., 1997). DNA adduct formation was found in the liver of male but not female rats after oral E2 administration for 2 weeks (2 mg/kg bw) (Feser et al., 1996) and in the liver and kidney of Syrian hamsters after single dose injection (Liehr et al., 1987). Two out of three *in vitro* tests for Sister Chromatide Exchange using human peripheral lymphocytes were positive after treatment with estradiol and at concentrations above 25 µg/L, which were negligible for human relevance (see Table 3) (Dhillon and Dhillon, 1995; Ahmad et al., 2000; Banduhn and Obe, 1985). Negative and positive chromosomal aberration tests have been reported. Positive results were obtained in *in vitro* tests using human lymphocytes (Dhillon and Dhillon, 1995; Ahmad et al., 2000), V79 cells (Sato et al., 1992), and CHO cells (Kochhar, 1985). Negative results of *in vitro* chromosome aberration were observed in human lymphocytes by others (Stenchever et al., 1969; Banduhn and Obe, 1985). As far as induction of micronuclei is concerned, positive results have been shown in a number of studies *in vitro* in MCF-7 cells and in SHE cells (Yared et al., 2002; Schnitzler et al., 1994). However, other *in vivo* mouse micronucleus tests in spermatids (Pylkkänen et al., 1991) and mouse bone marrow (Morita et al., 1997) were negative.

Though inconclusive, results depending on the endpoint and cell type used, estradiol showed genotoxic properties *in vivo* and *in vitro* mostly at high concentrations. This cannot be taken as evidence for a genotoxic potential in humans under normal conditions. Almost exclusively positive tests appear with the metabolite 4-hydroxyestradiol and to a lesser extent with 2-hydroxyestradiol, suggesting that the balance of the E2 metabolic pathway (see section 2.2.8) determines whether the formation of the reactive E2 metabolites shifts towards a genotoxic potential of E2. (Joosten et al., 2004)

2.2.4. ESTROGEN RECEPTORS

For a long time it was believed that estrogen action was mediated exclusively through one intracellular ligand-activated transcription factor that regulates a set of genes, now known as the estrogen receptor alpha (ERalpha). ERalpha was the first ER cloned and isolated from MCF-7 human breast cancer cells in the late 1980s. (Walter et al., 1985). In 1996 another subtype of ERs was discovered in rat prostate, named ERbeta, which possesses many similar functions but also bears some unique functions of its own. Both receptors share a high degree of sequence identity (see section 2.2.5). (Kuiper et al., 1996)

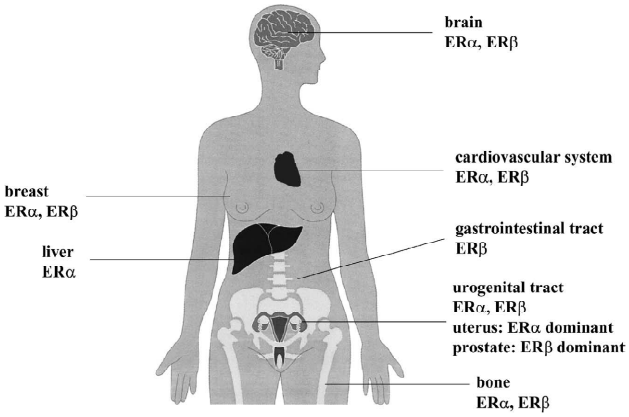

Figure 7: Distribution of ERalpha and ERbeta in different tissues the human body (adapted from Pearce and Jordan, 2004)

They are widely distributed throughout the human body with distinct and overlapping expression patterns in a variety of tissues (Figure 7). In the uterus, liver, kidney, and heart ERalpha is highly expressed. ERbeta exhibits a more limited expression pattern and is primarily detected in the ovary, prostate, lung, gastrointestinal tract, bladder, hematopoietic system, and central nervous system. The two subtypes are also co-expressed in a number of tissues including the mammary gland, certain brain regions, cardiovascular system, urogenital tract, and bone. ERalpha is the main subtype in the liver, whereas ERbeta is the main ER in the colon. Within the same tissue both ERs can be localized in distinct cellular subtypes, e.g. in the ovary ERalpha is mainly present in the theca cells and interstitial cells whereas ERbeta is predominantly found in the granulosa cells (Sar and Welsch, 1999).The expression in rats is similar to that in the human body. (Pearce and Jordan, 2004)

2.2.5. FUNCTIONAL STRUCTURE OF ER

Estrogen action is mediated by binding one of the two specific ERs, ERalpha and ERbeta. Members of the nuclear receptor family share a common domain structure with distinct functional domains A to E as designated in Figure 8 (Mangesldorf et al., 1995). The ligand binding domain (LBD) is located in the C-terminal E/F domain. Furthermore, E/F domain contributes to receptor dimerization. Next to the C-terminal domain the hinge (D) domain

is located bearing the nucleus location signal. In the center of the receptor there is a highly conserved zinc finger-based DNA binding domain (DBD). This C domain specifically recognizes its cognate estrogen response elements (EREs) in the target gene promotors. (McKenna et al., 2002). The transactivation activities of both receptors are mediated by two separate but not mutually exclusive transcription activation functions (AFs) allowing the receptor to stimulate transcription of genes. The N-terminal A/B domain encodes activation function 1 (AF-1) and is a constitutive ligand-independent activation function. The C-terminal ligand-dependent activation function AF-2 is located in the ligand binding domain (LBD). (Nilsson and Gustaffson, 2000)

The autonomous AF-1 is constitutively active but is masked in the absence of a ligand. In contrast, AF-2 is dependent on ligand binding through ligand-dependent conformational change and subsequent formation of a hydrophobic surface, which is required for interaction with co-regulators. (McKenna et al., 2002)

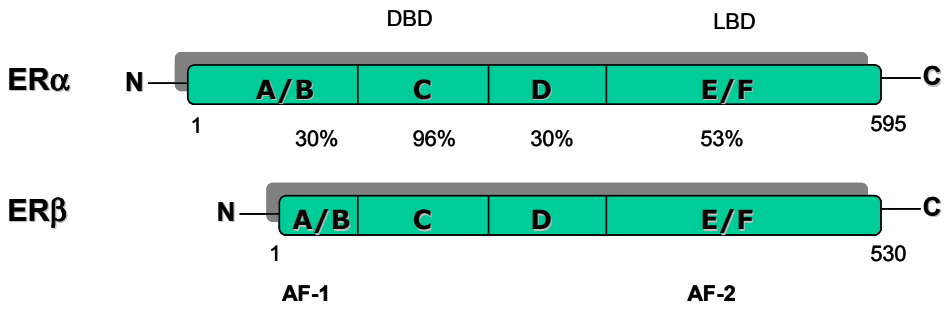

Figure 8: Structure and homology between human ERalpha and the long form of ERbeta. AF, activation function; DBD, DNA binding domain; LBD, ligand binding domain. (Adapted from Pearce and Jordan, 2004)

AF-1 domain is very active in ERalpha but the activity of AF-1 in ERbeta is minimal (Barkhem et al., 1998). The DNA binding domain of ERalpha and ERbeta is highly homologous. Hence, both receptors interact with identical DNA response elements and bind to the different EREs with similar specificity and affinity (Nilsson and Gustaffson, 2000).The LBD also exhibits a high degree of homology and therefore both receptors exert similar affinities for the endogenous estrogen 17beta-estradiol (E2). However, there are also some subtype specific ligands. (Sun et al., 1999). AF-2-mediated transcriptional activities are dependent on interaction with cofactor proteins. The activity of each AF is promoter- and cell type- specific. (Berry et al., 1990)

2.2.6. ER SIGNALING PATHWAY

The estrogen receptors ERalpha and ERbeta belong to the nuclear receptor superfamily of ligand-regulated transcription factors (Pettersson and Gustaffson, 2001). Both ER subtypes regulate gene expression in two ways: classical (genomic) and non-genomic signaling (summarized in Figure 9).

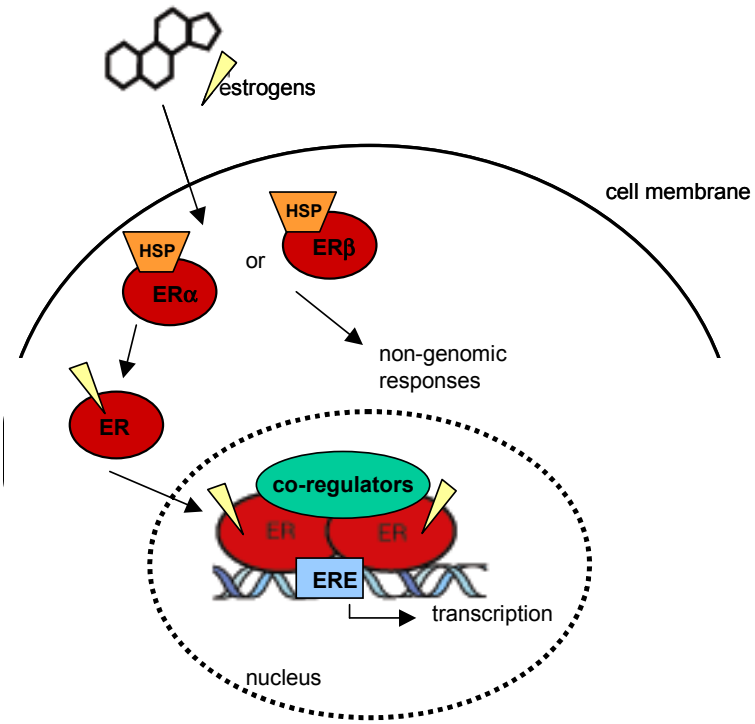

Figure 9: Estrogen signaling pathway in cells. Estradiol can bind to either estrogen receptor alpha (ERα) or beta (ERβ). Upon ligand binding, ERs translocate to the nucleus and bind to cognite estrogen response elements to regulate transcription. ERs are also known to regulate non-genomic signaling pathways. ERE, estrogen response element; HSP, heat shock protein. (According to Weatherman, 2006; Hall et al., 2001)

The classical pathway acts via direct DNA binding to estrogen response elements (ERE). Thereby, biological actions of estrogens are mediated by binding to one of the two specific estrogen receptors. In the absence of hormones ER is sequestered with other intracellular proteins, mainly heat shock proteins such as HSP90, forming an inhibitory complex that masks DNA binding regions and stabilizes the inactive receptor in the cytoplasm. Ligand binding induces conformational changes within the receptor, which promotes dissociation of heat shock proteins leading to dimerization and translocation into the nucleus. Ligand-bound ER dimer then interacts with co-regulatory proteins and recruits other transcription factors in order to bind to DNA sequences termed EREs located in the regulatory regions of responsive target genes. Subsequently, transcription of estrogen-regulated genes such as e.g. cathepsin D, ps2, vitellogenin is activated. (Mangelsdorf et al., 1995)

ERs can bind to DNA as homo-and heterodimers. In cells expressing both subtypes ERbeta often acts as a dominant inhibitor of ERalpha-dependent transcriptional activity. Quite a

number of co-regulatory proteins are known for ERs, comprising co-activator and co-repressors. (Mangelsdorf et al., 1995)
Following agonist binding, interaction with co-activators is triggered. Co-activators relevant for AF-2 activity are members of the p160 protein family, i.e. steroid receptor coactivator-1 (SRC-1), transcriptional intermediary factor 2 (TIF2), and AIB1 (amplified in breast cancer I) (Leo and Chen, 2000). P160 proteins recruit further transcription activators and histone acetyltransferase (HAT) complexes that modify histone tails covalently and contain p300 and CBP (cAMP binding protein). Modifications include acetylation, methylation, phosphorylation, and ubiquitination at the amino-terminal histone tails (Strahl and Allis, 2000).These chromatin structure remoduling complexes loosen chromatin structure in promotor regions and thus facilitate binding to promotor regions. The thyroid receptor–associated protein 220 (TRAP220) is a component of mediator complexes that regulate transcriptional control by direct interaction of both ERalpha and ERbeta with the transcription machinery e.g. to RNA polymerase II. (Kang et al., 2002; Rosenfeld et al., 2006). Remarkably, cofactor selectivity of AF-1 and AF-2 regions is not identical, so that different protein complexes may be formed at both AF regions.

Estrogen receptor signaling may also occur via ERE-independent mechanism. Both receptors can regulate genes that do not contain EREs in their regulatory regions via protein-protein interactions by tethering to other DNA-bound transcriptions factors, such as activating protein 1 (AP-1) and specificity/stimulating protein 1 (Sp1). Cellular response through this direct non-genomic signaling pathway is specific to ER isoform and promotor. ER alpha and ERbeta can exhibit opposing actions in the regulation of several promotors and specific response elements. (Paech et al. 1997, Saville et al., 2000)

Furthermore, estrogens can activate a putative membrane transduction pathway that generates rapid tissue responses. ERs can directly interact with other cytosolic proteins e.g. protein tyrosine kinase SRC can be activated which subsequently initiates MAPK (Mitogen activated protein kinase) cascade. (Kato et al., 1995)

2.2.7. MECHANISMS OF CARCINOGENESIS

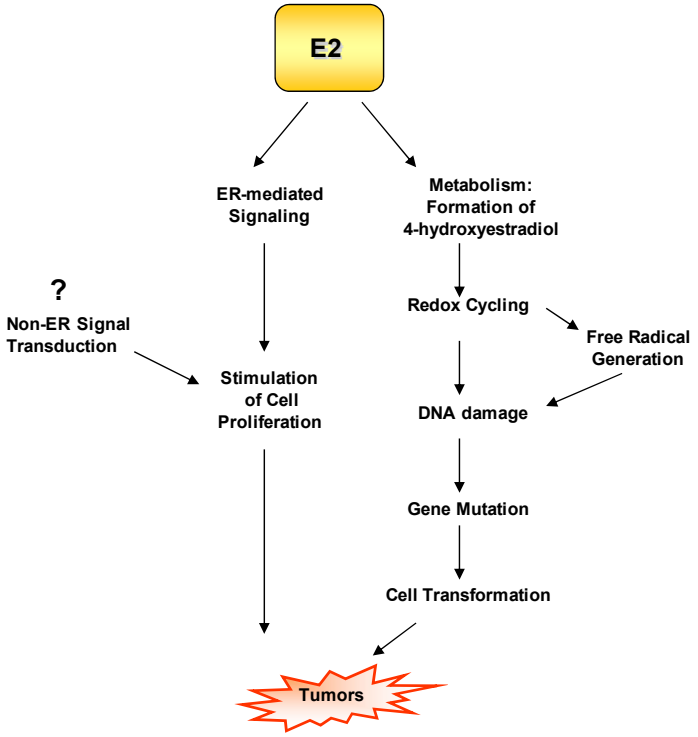

Figure 10: Proposed mechanisms of E2-induced carcinogenesis either by stimulation of proliferation as a response of hormone-dependent action with the estrogen receptor (ER) or by DNA-damaging effects during E2 metabolism. Stimulation of cell proliferation may also be possible by non-ER signal transduction. (Modified from Liehr, 2001 and Yager, 2000).

There are two proposed mechanisms of carcinogenesis of estradiol characterized by interplay of mutagenic/genotoxic and hormonal effects, which are summarized in Figure 10 (Liehr, 2001).

On the one hand estradiol as a hormone may stimulate cell proliferation via binding of ER and the subsequent estrogen signaling pathway.

On the other hand estradiol may act as a procarcinogen that induces genotoxicity via the reactive 4-hydroxyestradiol metabolite and the associated metabolic redox cycling between the corresponding quinone and hydroquinone forms. The semiquinone intermediates are free radicals, which generate more oxygen radicals inducing multiple forms of DNA damage. Additionally, the quinone intermediates may bind covalently to DNA and form potentially mutagenic DNA adducts or apurinic sites.

2.2.8. OXIDATIVE METABOLISM OF ESTROGENS

The metabolism of estrogens mainly occurs in liver, but also in extrahepatic tissues (Cavalieri et al., 2006). The estrogens E1 and E2 are obtained via aromatization of 4-androstene-3,17-dione and testosterone respectively catalyzed by CYP19 (aromatase) as described before (see Figure 6). E1 and E2 are biochemically interconvertible by the enzyme 17beta–estradiol dehydrogenase. Both estrogens are metabolized to catechol estrogens (CE) by two major pathways, which are explained in the following using E2 as example (Figure 11).

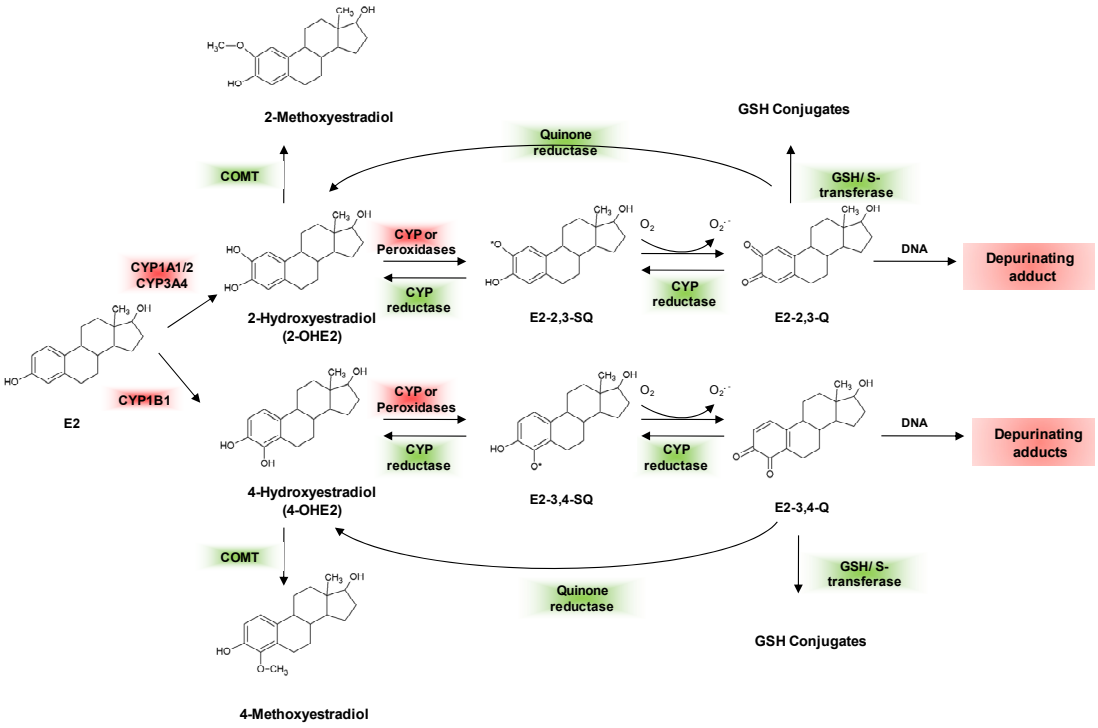

Figure 11: Cytochrome P450-mediated metabolic pathways of estradiol (E2). E2 is metabolized to 2- and 4-hydroxyestradiol (2-and 4-OHE2). The catechol metabolites can be O-methylated to monomethoxy estradiol metabolites by catechol O-methyltransferase (COMT). 2-and 4-OHE2 undergo metabolic redox cycling to generate free radicals such as superoxide radical anion (O_2^{*-}) and the reactive semiquinone (SQ) and quinone (Q) intermediates which cause DNA damage. (Adapted according to Cavalieri et al., 2006 and Tsuchiya et al., 2005)

E2 is metabolized to 2-hydroxy CE (2-OHE2), which is predominantly catalyzed by CYP1A1, but also CYP1A2, and CYP3A4. The formation of the 4-hydroxylated estradiol (4-OHE2) is catalyzed by CYP1B1. (Lee et al., 2003; Shou et al., 1997)

These two catechol estrogen forms are among the major metabolites of E2. Generally, the 2-OHE2 is the major CE formed, since approximately 80% of estradiol is biotransformed to 2-hydroxyestradiol and 20% to 4-hydroxyestradiol (Weisz et al., 1992). However, increases in the level of CYP1B1 e.g. by induction of TCDD can render the minor CE metabolite 4-OHE2 as the major one (Spink et al., 1994; Hayes et al., 1996).

To a lesser extent estrogens are also converted by several CYP isoforms to a large number of other hydroxylated metabolites via 6alpha-, 6beta-, 7alpha-, 12beta-, 15alpha-, 15beta-, 16alpha-, and 16beta-hydroxylation *in vitro* and *in vivo* (not shown in Figure 11) (Lee et al., 2001 and 2002).

The CEs are capable of metabolic redox cycling and are further oxidized by organic hydroperoxide-dependent CYP1A enzymes or other peroxidases to the respective quinone (Q)

forms E2-2,3-Q and E2-3,4-Q releasing free radicals. The semiquinone free radical is an intermediate of this metabolic conversion. In the presence of O_2 the semiquinone radical is oxidized to CE-Q which forms superoxide anion radicals, and then H_2O_2. Hydroxyl radicals are produced in the presence of Fe^{2+} (see also section 2.3.1). CE-quinones can be converted back to the catechol form via stepwise reduction catalyzed by NADPH-dependent CYP reductase directly by quinone reductase.

In addition to the direct free radical-initiated DNA damage that can occur due to the redox cycling of CE, quinone intermediates may form depurinating DNA adducts *in vivo* and *in vitro*. It is hypothesized that these DNA adducts may generate apurinic (AP) sites leading to mutations, which may initiate E2-dependent cancers. (Cavalieri et al., 2000). The 4-hydroxylated estradiol metabolite has been shown to exhibits greater carcinogenic potency than 2-OHE2, since 4-OHE2 induced kidney tumors in male Syrian hamsters, whereas 2-OHE2 did not (Liehr et al., 1986; Li and Li, 1987). Since both metabolites have similar redox potentials (Mobley et al., 1999; Cavalieri et al., 2006), the greater potency of 4-OHE2 cannot be attributed to the redox cycling. Instead, E2-3,4-Q formed by 4-OHE-2 had a higher reactivity in the formation of depurinating DNA adducts compared to E2-2,3-Q (Zahid et al., 2006). Treatment of rat mammary gland with E2-3,4-Q resulted in the formation of the 4-OHE2-1N3Ade and 4-OHE2-1-N7Gua depurinating adducts (Mailander et al., 2006). N3Ade adducts depurinate rapidly, leading to premutagenic apurinic (AP) sites, whereas N7Gua adducts depurinate relatively slowly, slowing accurate DNA repair. These results suggest, that E2-3,4-Q may be the major carcinogenic metabolite of estrogens. (Zahid et al., 2006; Mailander et al., 2006; Cavalieri et al., 2006)

In general, CEs and reactive semiquinones and quinones are inactivated by conjugating reactions such as glucuronidation and sulfation. The most common pathway of inactivation occurs by *O*-methylation catalyzed by the ubiquitous catechol-*O*-methyltransferase (COMT) (Ball and Knuppen, 1980; Rogan et al., 2003). 2-Hydroxyestradiol is methylated by COMT at a faster rate than 4-OHE2 (Emons et al., 1987; Zhu and Liehr, 1993; Goodman et al., 2002). Additionally, the resulting 2-methoxyestradiol has an inhibitory effect on cell proliferation (Klauber et al., 1997; Fotsis et al., 1994). Protection at the quinone level can occur by conjugation of CE quinones with glutathione (GSH) alone or catalyzed by glutathione-S-transferases (GSTs). A second inactivating process for CE quinones is their reduction back to CE by NADPH-quinone reductases (QR) or NADPH-CYP-reductases. If these inactivation pathways are insufficient due to excessive production of the metabolites or a lack of deactivation enzymes, competitive catalytic oxidation of semiquinones and quinones can occur. Then, CE-Q may lead to initiation of cancer. (Cavalieri et al., 2000 and 2006; Rogan et al., 2003). Since the specific formation of the minor metabolite 4-OHE2

may be important for the pathway leading to estrogen-induced cancer, the CYP1B1 enzyme is considered as a key player in this process.

2.2.8.1. CATECHOL-*O*-METHYLTRANSFERASE

Since COMT is the predominant conjugating enzyme in the E2 metabolism it is discussed in more detail. COMT is a magnesium-dependent enzyme that catalyzes the transfer of a methyl group from the methyl donor S-adenosylmethionine (SAM) to one hydroxyl moiety of the catechol ring of a substrate, generating S-adenosylhomocysteine (SAH) in the process. Catechol substrates include catecholamine neurotransmitters, xenobiotic catechols, and catechol estrogens (Axelrod and Tomchick, 1958). *O*-Methylation of CEs results in methoxyestrogens, thus lowering the ability of CEs to be converted to more reactive semiquinone and quinone metabolites (Dawling et al., 2001; Yager, 2000). The COMT enzyme, which is involved in hepatic and extra-hepatic O-methylation, occurs in two distinct forms. It can be found either in the cytoplasm as a soluble protein (S-COMT), which constitutes the predominant expressed COMT form, or in association with membranes as a membrane-bound protein (MB-COMT) (Malherbe et al., 1992). The amino acid sequence of S-COMT and MB-COMT is identical, except for an NH_2-terminal extension of 50 hydrophobic amino acids in MB-COMT that serves as an anchor to the membrane (Bertocci et al., 1991; Ulmanen and Lundström, 1991). Both protein forms occur constitutively but differ in tissue expression. S-COMT is the predominant form in nearly all tissues, whereas MB-COMT generally accounts for about 10% of total enzyme activity (Jeffery and Roth, 1984; Grossman et al., 1985). Thus, in normal breast tissue as well as MCF-7 breast cancer cells S-COMT constitutes more than 90% of total COMT activity (Tenhunen et al., 1994).

Polymorphisms have been identified in the COMT gene (Lachman et al., 1996), and a low-activity form of the enzyme has been associated with increased estrogen-induced breast cancer in women. Thus, COMT genotype is hypothesized to define differences in metabolizing estrogen, possibly explaining interindividual differences. (Lavigne et al., 1997; Thompson et al., 1998)

2.3. OXIDATIVE DNA DAMAGE

2.3.1. OXIDATIVE STRESS AND ROS

Radical species are molecules or molecular fragments containing one or more unpaired electrons in atomic or molecular orbitals. Unpaired electrons account for the considerable reactivity of the free radicals resulting in a short half-life (e.g. nanoseconds). Oxygen-derived radicals are the most important class of radical species generated in aerobe organisms, known as reactive oxygen species (ROS). (Valko et al., 2004). The toxicity of such reactive species may be explained by its reaction with other radicals or non-radical molecules. Non-radical ROS such as hydrogen peroxide (H_2O_2) are easily converted into radicals (Pryor, 1986). ROS are products of naturally occurring processes in cellular metabolism. They either serve essential biological functions or are byproducts of metabolic processes. (Valko et al., 2004; Halliwell and Gutteridge, 1999). Table 4 summarizes the major ROS implicated in cellular processes.

Table 4: Reactive oxygen species: radical and non-radical molecules

Name	**Symbol**
Hydroxyl	$^{\bullet}OH$
Superoxide anion	$O_2^{\bullet -}$
Alkoxyl	$RO^{\bullet}$
Peroxyl	$ROO^{\bullet}$
Nitroxyl	$NO^{\bullet}$
Hydrogen peroxide	H_2O_2
Singlet oxygen	$^1O_2$
Ozone	O_3
Hypochlorous acid	HOCl

The imbalance in the generation and removal (antioxidant defense) of radical species, in favor of the former leading to potential damage of cellular structures, is termed as oxidative stress (Seis, 1991). Endogenous sources of ROS formation include:

- mitochondria,
- xanthine oxidase–mediated catabolism of purines,
- metabolism of xenobiotics by the cytochrome P450 system,
- peroxisomes involved in the oxidation of fatty acids, and
- macrophage-activated oxygen uptake during inflammation. (Valko et al., 2006)

During cellular respiration in the mitochondria the reduction of molecular oxygen (O_2) to water occurs in the electron transport chain via cytochrome c oxidase-catalyzed reaction (Figure 12). The four sequential single-electron reduction steps of O_2 result in the formation of reactive oxygen species as partially reduced intermediates, such as superoxide anion radical ($O_2^{\bullet -}$), hydrogen peroxide (H_2O_2), and the hydroxyl radical ($^{\bullet}OH$).

Minor amounts of these ROS can escape the electron transport chain (1–3%) and damage cellular components. (Kelly et al., 1998; Benzi et al., 1992)

$$O_2 \xrightarrow{e^-} O_2^{\bullet -} \xrightarrow{e^-,\ 2H^+} H_2O_2 \xrightarrow[-\ OH^-]{e^-} {}^{\bullet}OH \xrightarrow{e^-,\ H^+} H_2O$$

Figure 12: Sequential four single-electron reduction steps from molecular oxygen to water. (According to Valko et al., 2004)

Beneficial roles of ROS involve immune-mediated defense reactions. During the respiratory burst of leukocytes in host defense, monocytes, neutrophils, and macrophages can produce radicals, such assuperoxide anion radicals, which serve as cytotoxic agents against pathogenic organisms. (Conner and Grisham, 1996)

The hydroxyl radical is one of the most potent oxidants known with an *in vivo* lifetime of only a few nanoseconds (Pryor, 1986). It can be produced by the reaction of superoxide anion radical and hydrogen peroxide in the Haber-Weiss reaction (Figure 13).

$$2\,O_2^{\bullet -} + 2H^+ \longrightarrow H_2O_2 + O_2$$

$$O_2^{\bullet -} + H_2O_2 \longrightarrow {}^{\bullet}OH + {}^{-}OH + O_2$$

Figure 13: Haber Weiss reaction

Transition metals (e.g. iron and copper) often serve as catalysts in this kinetically slow reaction, which is then known as Fenton reaction (Figure 14).

$$O_2^{\bullet -} + Fe^{3+} \longrightarrow O_2 + Fe^{2+}$$

$$Fe^{2+} + H_2O_2 \longrightarrow {}^{\bullet}OH + {}^{-}OH + Fe^{3+}$$

$$O_2^{\bullet -} + H_2O_2 \longrightarrow {}^{\bullet}OH + {}^{-}OH + O_2$$

Figure 14: Fenton reaction

The cytochrome P450-catalysed mono-oxygenase system is an established source of ROS. In addition, NADPH-dependent formation of ROS generates in particular superoxide radicals, which dismutate to hydrogen peroxide. Through the induction of cytochrome P450 enzymes, the production of ROS is stimulated. During catalysis of the electron transfer from the NADPH-cytochrome P450 reductase onto the cytochrome P450, electrons can leak onto the oxygen molecules forming superoxide anion radicals in addition to the mono-oxygenation of the substrate. This unintended leakage of electrons is also called uncoupling. The extent of the uncoupling is dependent on the isoenzyme and the substrate. (Kuthan and Ullrich, 1982; Bösterling and Trudell, 1981)

Figure 15 shows the normal steps of the mono-oxygenase reaction. Shortly, substrate binds to ferric-cytochrome P450 and subsequently leads to an increased reducibility of the hemeprotein. Cytochrome P450 is a one-electron acceptor and NADPH-cytochrome P450 reductase will rapidly reduce the hemeprotein at the expense of NADPH. Subsequently, oxygen binds to the ferrous cytochrome P450, and the oxy-cytochrome P450 formed may uncouple or may accept a second electron from the reductase. With a number of cytochrome P450 isoforms, the second electron is the more effectively input from the reductase via an electron transfer protein, cytochrome b5. Some substrates increase the affinity for cytochrome b5, which was shown to be able of transferring a reducing equivalent to ferric cytochrome P450 from NADH. The reduction of the oxycytochrome P450 brings the oxygen to the redox state of hydrogen peroxide complexed to the cytochrome P450. A water molecule and the oxidized substrate are generated during these reactions.

The role of cytochrome b_5 is considered to provide the second electron at a faster rate for product oxidation than for the release of superoxide anion by decreasing the release of the superoxide anion radical, while decreasing or without influencing NADPH consumption. Thus, the enhancing effect of coupling stabilizes the oxycytochrome P450 complex. (Schenkman and Jansson, 2003)

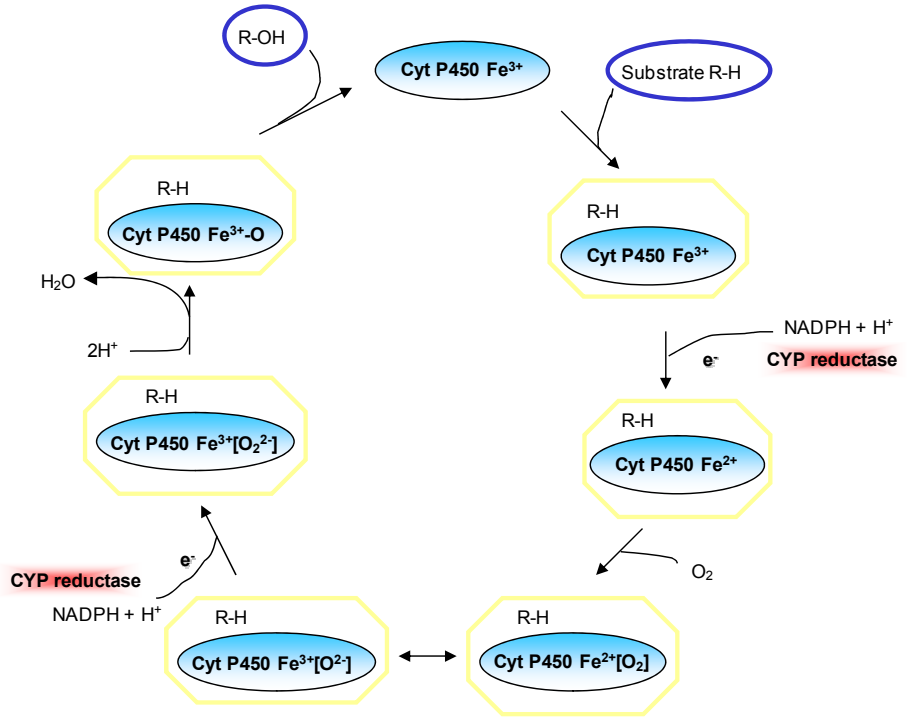

Figure 15: Steps in the cytochrome P450 cycle during mono-oxygenase reaction. Two single-electron transfers from NADPH-cytochrome P450 reductase (CYP reductase) to cytochrome P450 in order to reduce molecular oxygen (O_2) and lead to subsequent substrate oxidation. (According to Eisenbrand and Metzler, 2005)

Additionally, the NADPH-CYP reductase is involved in the so-called redox-cycling of various quinoid compounds, acting as a one-electron donor for endogenous or exogenous quinones to produce free semiquinone radicals. Within this cycle, a one-electron reduction via NADPH-cytochrome P450 reductase yields the reactive semiquinone radical, which can be reduced directly to the more stable hydroquinone in a second catalyzed one-electron transfer reaction. Semiquinone may also readily re-oxidize in a non-enzymatic reaction in the presence of molecular oxygen, which leads to formation of ROS such as superoxide anion radicals. (Bolton et al., 2000). The redox cycling mechanism is presented in Figure 16 using the example of menadione, a known redox cycler.

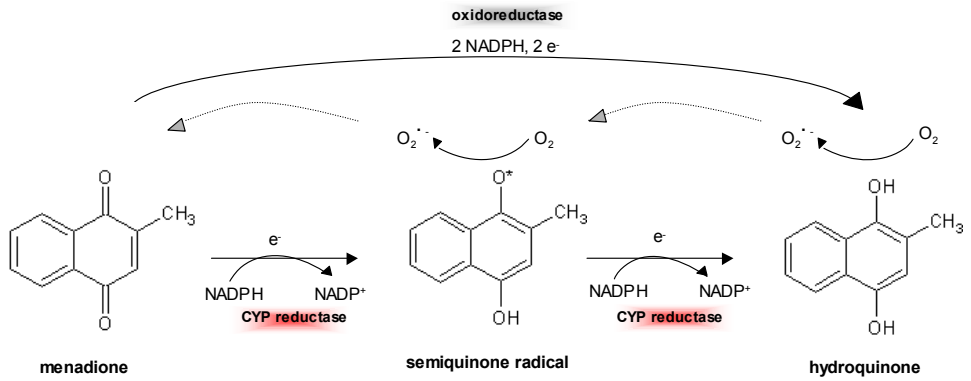

Figure 16: Schematic redox cycling of menadione, representative of the one- and two-electron transfer of quinones. In two sequential reduction steps NADPH-cytochrome P450 reductase (CYP reductase) catalyzes the formation of the reactive semiquinone radical and the more stable hydroquinone. NADPH-oxidoreductase (oxidoreductase) catalyzes directly the formation of hydroquinone. Under aerobic conditions the reactive quinone forms can be re-oxidized in a non-enzymatic reaction producing ROS. (Modified from Morrisson et al., 1984)

Menadione is a naphthochinone derivative, which belongs to the group of K vitamins (Forth et al., 2005). The flavoprotein NADPH-oxidoreductase can directly catalyze the two-electron reduction to the more stable hydroquinone. The oxidoreductase may therefore be able to protect the cells from the toxic effects of menadione by competing with the one-electron reduction pathways. Already catalytic amounts of quinones are sufficient to produce ROS, which are assumed responsible for the cytotoxic and DNA-damaging effects of menadione observed in primary rat hepatocyte cultures. (Morrison et al., 1984)

2.3.2. ANTIOXIDANT DEFENSES

The cell is well equipped with numerous enzymatic antioxidant defenses systems that aim at protecting the cell from oxidative damage.

Superoxide radical is not known to directly react with cellular components like protein, sugars, or nucleic acids. It is depleted in a dismutation reaction, which in biological systems can be accelerated by superoxide dismutases (SODs), an enzyme that rapidly scavenges $O_2^{\bullet -}$(Figure 17).

$$2\,O_2^{\bullet -} + 2H^+ \xrightarrow{\text{SOD}} H_2O_2 + O_2$$

Figure 17: Dismutation reaction of superoxide anion radical to hydroperoxide catalyzed by superoxide dismutase (SOD).

There exist three SOD isoforms in eukaryotes. Manganese SOD (Mn-Sod), containing a manganese prosthetic group, resides in the mitochondria and protects mitochondrial membranes, proteins, and DNA from the generated ROS from the respiratory chain. Copper/zinc SOD is a cytosolic SOD, and the extracellular SOD is secreted and binds to the plasma membrane acting in

the extracellular matrix. (Fridovich, 1995). SOD enzymes work in conjunction with H_2O_2-removing enzymes, such as catalase and glutathione peroxidases (GPx) (Michiels et al., 1994)

Hydrogen peroxide is removed by catalase, a manganese or heme-containing enzyme, which rapidly dismutates H_2O_2 to water and oxygen (Figure 18).

$$2\,H_2O_2 \xrightarrow{\text{Catalase}} 2\,H_2O + O_2$$

Figure 18: Catalase-mediated dismutation of hydrogen peroxide to water.

Catalase mainly is found in peroxisomes, but also in mitochondria and the cytosol. Additionally, it was reported, that catalase metabolizes alkyl peroxides.

Glutathione peroxidase (GPx) catalyzes the reduction of organic peroxides to the corresponding alcohol and water with glutathione (GSH) as a cofactor and is present in the cytosol and the mitochondria. GSH provides the reducing equivalents as a non-enzymatic antioxidant and as a consequence is oxidized to glutathione disulfide (GSSG). Glutathione reductase (GR) reduces oxidized glutathione (GSSG) to regenerate GSH at the expense of NADPH (Figure 19).

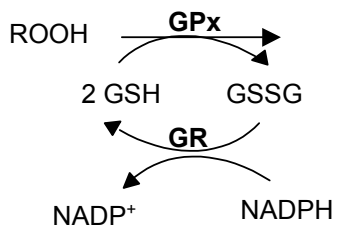

Figure 19: Antioxidant pathway of glutathione peroxidase (GPx) and recycling of GSH. Organic peroxides can be reduced by GPx with GSH as the reducing cofactor. Glutathione reductase (GR) reduces oxidized glutathione (GSSG) to regenerate GSH. (De Leve and Kaplowitz, 1991)

The main GPx isoforms are selenium-containing enzymes. Moreover, in addition to catalases cytosolic GPxs have also high affinity for H_2O_2, which is removed by coupling its reduction to water with the oxidation of reduced glutathione. (Kelly et al., 1998; Halliwell and Gutteridge, 1999)

Glutathione is a thiol-containing tripeptide consisting of L-g-glutamyl-L-cysteinyl-glycine, which is present in all mammalian cells at millimolar concentrations (De Leve and Kaplowitz, 1991) (Figure 20).

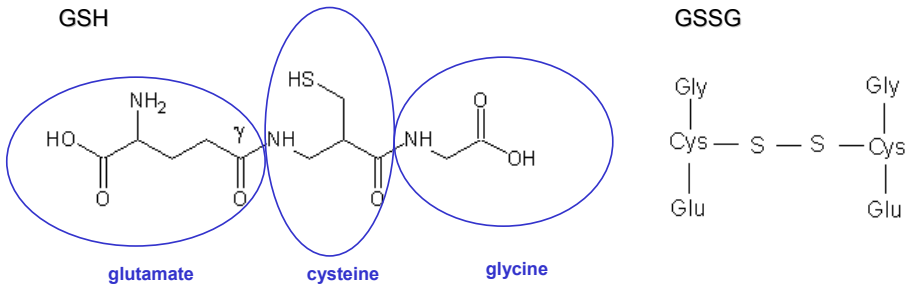

Figure 20: Structures of reduced glutathione (GSH) and oxidized glutathione (GSSG). The GSH tripeptide (glutamic acid-cysteine-glycine) can be reduced and two GSH molecules form GSSG, as the thiol groups of cysteine are oxidized to from a disulphide bridge. (According to De Leve and Kaplowitz, 1991 and Halliwell and Gutteridge, 1999).

It is synthesized predominantly in the liver based on the amino acids via two successive adenosine triphosphate (ATP)-dependent steps, comprising enzymatic ligation of L-glutamate and L-cysteine and the subsequent addition of glycine to the C-terminal end of gamma-glutamylcysteine via glutathione synthetase. (Rebrin and Sohal, 2008; De Leve and Kaplowitz, 1991)

GSH provides antioxidant protection as it can also directly reduce a number of ROS including singlet oxygen, hydroxyl radical, and superoxide anion radical, whereby it is oxidized to GSSG. The cysteine thiol moiety is essential for the antioxidant activity, as the thiol groups are oxidized to form a disulphide bridge, joining two GSH molecules together (Figure 20) (Halliwell and Gutteridge, 1999). As a result of oxidative stress, depletion of the intracellular GSH pool occurs which can lead to increased oxidative cell injury. Glutathione reductase has an important function in maintaining high intracellular ratios of GSH/GSSG. GR reduces oxidized glutathione (GSSG) in the presence of NADPH in order to regenerate GSH. This regeneration of GSH is also essential for its role as a co-substrate for GPx-mediated action (Figure 19). (Meister and Anderson, 1983; Kelly et al., 1998)

If the ability of the cell to recycle GSH by GR is overcome due to severe oxidant stress, the accumulated GSSG is actively transported out of the cell to maintain the redox state for the cell. The export of GSSG was also reported in the liver. GSSG plasma levels thus well reflect the intracellular redox state. (Sies et al., 1972; Lew et al., 1985). Unlike the plasma membrane, the mitochondrium, which is under permanent physiological oxidant stress, is unable to transport GSSG out of the compartment (Olafsdottir and Reed, 1988). Thus, the organelle is considered to be susceptible to the consequence of a pro-oxidant shift.

The ratios of reduced to oxidized glutathione (GSH/GSSG) are the primary determinants of the cellular redox state. Under physiological conditions in mammalian cells these GSH/GSSG ratios are high, with high GSH concentrations in the liver (up to 7-8 mM in the

rat liver) as the main target organ of the xenobiotic metabolism. (Halliwell and Gutteridge, 1999)

Normally, in healthy cells more than 98% of intracellular total glutathione is present as the reduced thiol form (GSH), termed as GSH status, since glutathione reductase will rapidly reduce any oxidized glutathione (DeLeve and Kaplowitz, 1991). Oxidative stress can lead to GSH depletion and affect the GSH status, leading to an imbalance in the anti-oxidative capacity of the cells.

2.3.3. OXIDATIVE DNA DAMAGE IN CARCINOGENESIS

As a consequence of the formation of ROS, one human cell has been estimated to be exposed to approximately $1.5x10^5$ oxidative attacks every day (Beckman and Ames, 1997). Cellular damage resulting from ROS is called oxidative damage. Since ROS are continuously formed in living cells, cellular damage occurs if the antioxidant defense systems cannot provide adequate protection (Halliwell and Gutteridge, 1999; Loft and Poulsen, 1996).

DNA is the most susceptible cellular target to one-electron oxidation processes by various ROS and reactive nitrogen species. Moreover, it has been hypothesized that endogenous DNA damage by ROS plays a major role in carcinogenesis, mutagenesis, and aging. The DNA damage is challenged by endogenous and exogenous agents. Exogenous environmental factors include nutritional components, pollutants, radiation, or chemicals that affect DNA damage. (Loft and Poulsen, 1996; Collins, 1999; Cadet et al., 2000; Halliwell and Gutteridge, 1999). As a result of DNA damage cells have several defense systems in order to repair the damage or to eliminate the damaged cells. Damaged DNA can interfere directly with cell signaling and growth (Cerutti et al., 1994). A DNA modification that remains unrepaired or misrepaired can be fixed permanently when the cell undergoes division. If this manifested DNA damage, i.e. mutation, is related to critical genes such as oncogenes or tumor suppressor genes initiation and/or progression may result. Thus, ROS may act at several steps in the multistage carcinogenesis process (Loft and Poulsen, 1996). DNA damage can cause a temporary arrest of cell cycle progression, allowing DNA repair to take place prior to replication. There exist specific and non-specific repair mechanisms which can remove DNA alterations, thus restoring intact DNA (Wood et al., 2005). Irreparable DNA damage can also be implicated in apoptosis (the programmed cell death) as a further protective mechanism to prevent carcinogenesis. (Krokan et al.,1997)

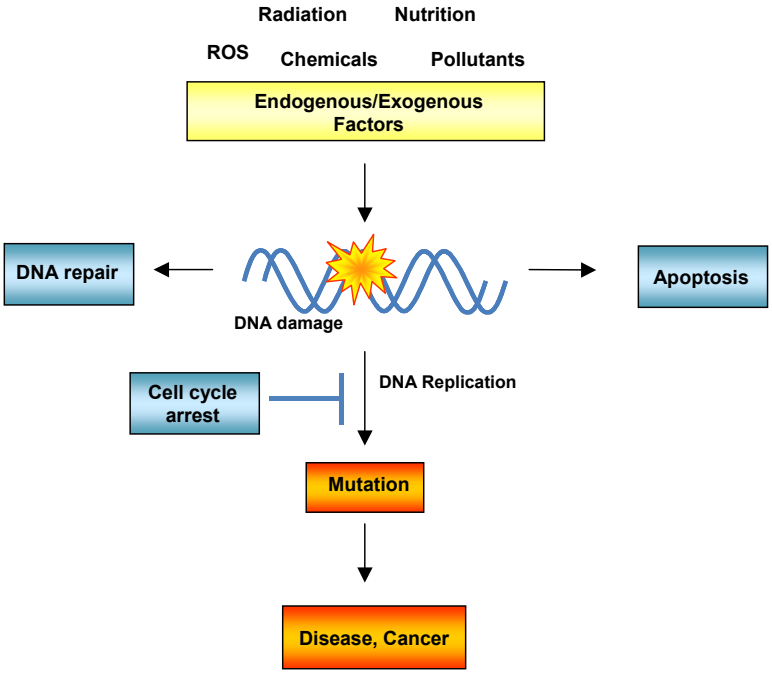

Figure 21: Schematic presentation of the role of the maintenance of DNA integrity following DNA oxidation in carcinogenesis (according to Krokan et al., 1997 and Collins, 1999).

Consequently, several processes and factors coordinate and cooperate to maintain the integrity of the genome. Figure 21 gives an overview of all these processes. In cells there is a balance between the continuous generation of oxidative DNA modifications by ROS, depending on the ratio of ROS formation to antioxidant defense systems, and the protective repair mechanisms that prevent mutations and increased levels of DNA lesions. Any change in this steady state level of oxidative DNA modifications may elevate the mutation frequencies and the cancer incidence. (Epe, 2002)

2.3.4. OXIDATIVE DNA BASE MODIFICATIONS

Various DNA base products of interaction with reactive oxygen and free radical species have been identified (Cadet et al., 2002; Cooke et al., 2003).

Susceptible sites of DNA structure for oxidative damage include the purine and pyrimidine bases and the sugar-phosphate backbone, whereas the reaction with the nitrogenous bases dominates (Dizdaroglu et al., 2002). The different forms of DNA damage involve modification of purine and pyrimidine bases as one of the major classes of oxidative DNA damage, but also single-or double-strand DNA strand breaks (SSBs or DSBs), apurinic/apyrimidinic sites (AP sites), and DNA cross-links (Valko et al., 2006). The hydroxyl radical ($^{\bullet}OH$) is the primary oxidant responsible for DNA damage, because neither H_2O_2 nor peroxyl radicals can directly react with DNA. The oxidation of DNA bases via hydroxyl radical leads to hydroxylation, ring-opening, or fragmentation. OH-adduct radicals of DNA bases are generated via an addition reaction to double bonds of DNA bases. Besides, $^{\bullet}OH$ reacts with the sugar moiety of DNA (2'deoxyribose, dRib) by abstracting an H-atom from

each of the carbon atoms forming various sugar products, DNA strand breaks, and base-free sites by a variety of mechanisms. Modified sugars are either released from DNA and form a DNA strand break or remain bound to DNA with one or both phosphates. (Dizdaroglu et al., 2002). The apparently most studied and abundant oxidative modification of DNA bases involves the C-8 hydroxylation of guanine. The lesions most commonly used as biomarkers are 8-hydroxy-2'-deoxyguanosine (8-OHdG, also called 8-oxo-dG) and 2,6-diamino-4-hydroxy-5-formamidopyrimidine (FapyGua) (Epe, 1995; Cadet et al. 1997). Figure 22 illustrates the mechanism of formation of guanine products from the C8-OH adduct radical, which is formed by attack of $^{\bullet}$OH to the C-8 position of guanine. 8-oxo-dG is formed after addition of the hydroxyl radical to the C-8atome of guanosine, whereas alternatively FapyGua is produced via opening of the imidazol ring. Analogous reactions of adenine yield 8-hydroxyadenine (8-OH-Ade) and 4,6-diamino-5-formamidopyrimidine (FapyAde). Both types of products are formed in the absence and presence of oxygen. However, reducing agents increase the ring-opened products formamidopyrimidines, whereas the formation of 8-hydroxypurines is preferred in the presence of oxygen. (Dizdaroglu et al., 2002). 8-oxo-G gives rise to GC→TA transversion as a consequence of stable mispairing with adenine (Wood et al., 1990; Cheng et al., 1992). This type of mutation is found increased in bacteria and eukaryotic cells that are deficient in the repair of 8-oxo-G (Klungland et al., 1999; Minowa et al, 2000). These lesions can be detected in the DNA or assayed in urine. Specific analytical methods for the detection of the biomarkers of oxidative damage after DNA acidic hydrolysis include the following techniques: HPLC-ECD (high performance liquid chromatography with electrochemical detection), GC-MS (gas chromatography mass spectrometry), or HPLC-MS/MS (ESCODD, 2002). Further examples of typical oxidative DNA damages are shown in Figure 23.

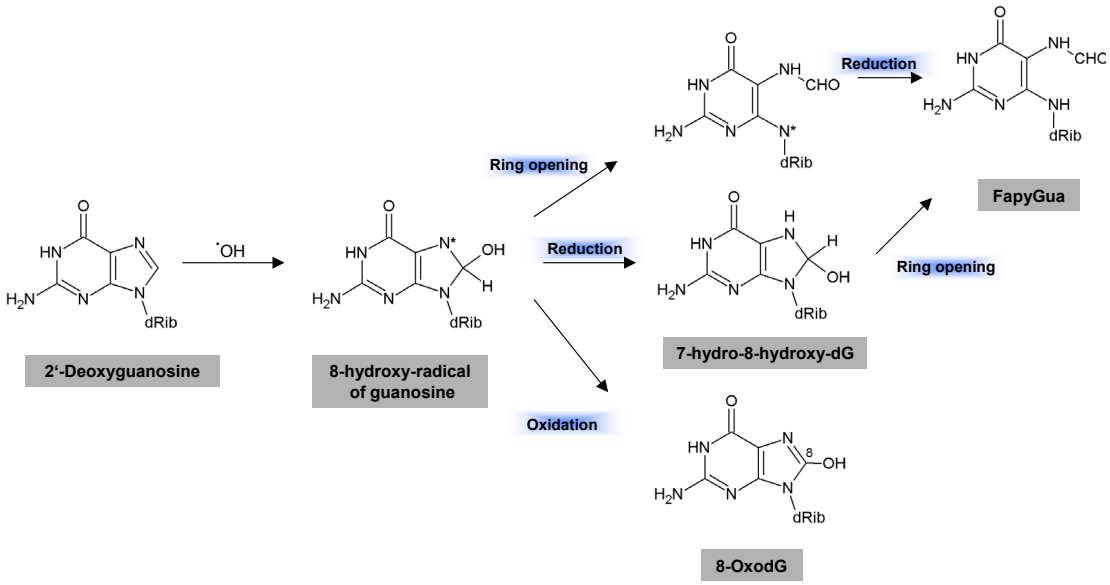

Figure 22: Reaction of 2'-deoxyguanosine with hydroxyl radical (•OH) and formation of the common DNA lesions 8-hydroxy-2'-deoxyguanosine (8-oxo-dG) and 2,6-diamino-4-hydroxy-5-formamidopyrimidine (Fapy-Gua). (According to Valko et al, 2006; Kelly et al., 1998; Dizdaroglu et al., 2002)

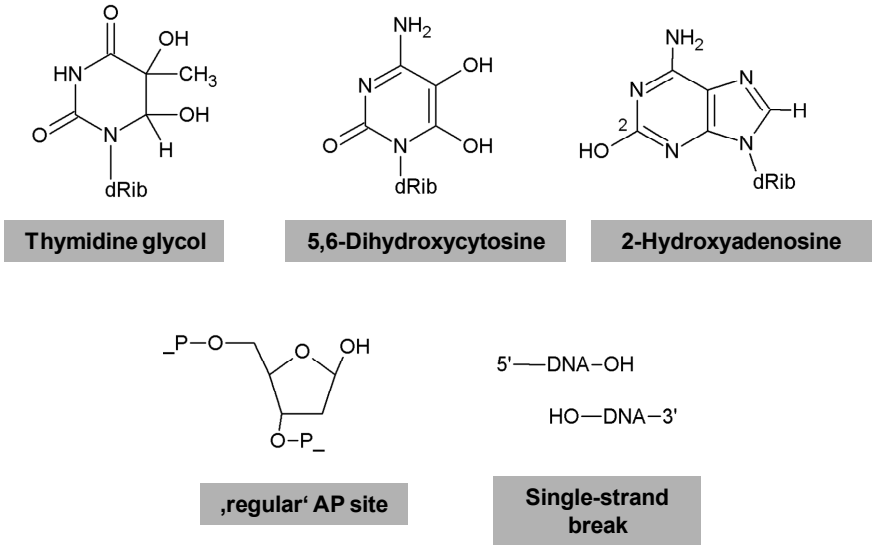

Figure 23: Chemical structures of various DNA base modifications induced by ROS (according to Epe et al., 1993).

2.3.5. DNA REPAIR

There exist a number of specific and non-specific DNA repair systems in humans, which are necessary to remove DNA lesions derived from endogenous and exogenous sources. This is important, since even under normal cellular conditions a measurable amount of cellular damage exists in mammalian cells. With respect to endogenous DNA damage, the DNA is constantly damaged. It undergoes 'spontaneous' decomposition, such as loss of purines, deamination of cytosine, hydrolysis, non-enzymatic methylation of DNA bases, and oxidative DNA damage by ROS (Halliwell and Gutteridge, 1999).

As oxidative DNA modifications have mutagenic potential, intact and effective DNA repair systems are essential to minimize toxic reactions (Wood et al., 1990). The high efficiency, which is a prerequisite of the DNA repair systems, becomes more clear if one considers that every human cell consist $6x10^9$ base pairs which are distributed to 46 chromosomes that have to be protected from DNA damage (Forth et al., 2005). Oxidative DNA base modifications are thought to be predominantly eliminated by base excision (Krokan et al., 1997; Hartwig and Schwerdtle, 2002). Since in the course of this study formation of oxidative stress and oxidative DNA damage was investigated, the focus in the following will be on the base excision repair (BER).

The most important repair mechanisms known to date are as follows (Wood et al., 2005):

- Direct Reversal of DNA damage repair:
  - Repair via O6-methylguanine-DNA –methyltransferase (MGMT)
  - Repair of 1-methyladenine or 3-methylcytosine via dioxygenases (ABH2 and ABH3) (Duncan et al., 2002)
- Base excision repair (BER):
  - Single-nucleotide BER (short-patch pathway)
  - Poly-nucleotide BER (long-patch pathway)
- Nucleotide excision repair (NER):
  - Global genomic repair
  - Transcription-coupled NER
- Mismatch Repair
- Double-strand break repair
- Homologous recombination

- Non-homologous end joining (NHEJ)

2.3.5.1. BASE EXCISION REPAIR (BER)

Oxidative DNA lesions including DNA strand breaks and AP sites as well as other types of spontaneous DNA base alterations are mainly eliminated by BER (Hartwig and Schwerdtle, 2002; Krokan et al., 1997). There exist two base excision repair (BER) sub-pathways in mammalian cells (Figure 24) that are characterized by the number of nucleotides synthesized into the excision patch: the 'single-nucleotide' BER pathway (one nucleotide incorporated) and the 'poly-nucleotide' BER (several nucleotides incorporated) BER pathway (Forth et al., 2005). Both of these sub-pathways involve excision of a damaged base and/or nearby nucleotides and DNA synthesis to fill the excision gap (Nilsen and Krokan, 2001).

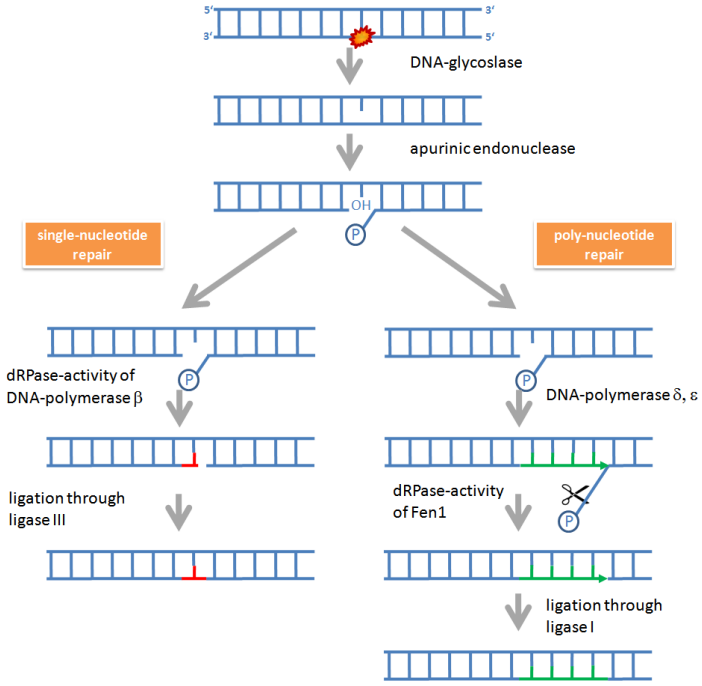

Figure 24: Alternative BER pathways: short-patch and long-patch BER (according to Slupphaug et al., 2003 and Forth et al., 2005).

The specificity of the BER system is determined by the enzymes that initiate the repair pathway, the N-glycosylases. They act specifically on one substrate or a class of substrates (McCullough et al., 1999). These N-glycosylases hydrolyze the N-glycosylic bond between the target base and deoxyribose-phosphate backbone, thereby releasing a free base and leaving an apurinic/apyrimidinic (AP) site in DNA (Barnes et al., 1993).

Single-nucleotide BER is suggested to be the major BER pathway in human cells, performing between 78 and 90% of all BER (Bennett et al., 1997; Sobol et al., 1996). During this short-patch BER the abasic site is converted into a single-strand break via the human

5'AP-endonuclease (HAP1, also called APE1), which is the major AP endonuclease (Nilsen and Krokan, 2001; Barzilay and Hickson, 1995). The deoxyribophosphodiester moiety is removed by the dRPase activity of Polβ (Deterding et al., 2000). Thereby a 3'-OH end is generated which serves as a substrate for DNA polymerase β (Polβ) and ligase III, which reseal the single-strand nick in eukaryotic cells (Kubota et al., 1996). While Polδ or Polε have been shown to substitute for Polβ with regard to DNA synthesis, no backup repair exists for the dRPase activity of Polβ (Dianov et al., 1999). The X-ray repair cross-complementing factor-1 (XRCC1) interacts as a scaffolding protein with Polβ via its N-terminal region, and with DNA ligase III via its C-terminal region (Kubota et al., 1996; Nash et al., 1997).

The long-patch BER, which repairs e.g. DNA single-strand breaks, involves replacement of mainly 2 up to 8 nucleotides starting from the damaged site. In eukaryotes the short DNA sequence is removed by flap endonuclease I (Fen1). Polδ or Polε are involved in the repair, and DNA ligase I reseals the open ends. (Nilsen and Krokan, 2001)
The proliferating cell nuclear antigen (PCNA) is implicated in the appropriate positioning of Fen1 and stimulates its nuclease activity to release the oligonucleotide containing the dRP moiety (Wu et al., 1996). Furthermore, PCNA is also involved in Polδ or Polε – dependent synthesis. Polδ or Polε is dependent on PCNA and replication factor C (RFC) (Stucki et al., 1998).

2.3.5.2. REMOVAL OF 8-OXO-G BY REPAIR GLYCOSYLASES

The known glycosylases directed against oxidized bases are all bifunctional (Slupphaug et al., 2003). This means that they combine two enzymatic functions and exert both glycosylase and AP lyase activity leading directly to a single-strand break. The analysis of the repair of 8-OH-guanine in mammalian cell-free extracts showed that this DNA modification is eliminated preferentially by the short-patch pathway of BER. However, long-patch BER can substitute for it when the components of the short-patch are saturated or missing. (Fortini et al., 1999)

Among the repair enzymes the DNA glycosylase isolated from Escherichia coli (E.coli), the formamidopyrimidine (Fapy)-DNA glycosylase (FPG), has been shown to recognize purines with an opened imidazol ring. Besides Fapy, the FPG protein (also named MutM) in E. coli catalyses the excision of further ring-opened purines and damaged purine bases such as the oxidation products 8-oxo-dG from double-stranded DNA. (Boiteux et al., 1992)

E.coli FPG is a 30 kDa enzyme containing a zinc finger motif (O'Connor et al, 1993). In addition to its N-glycosylase activity (abasic site nicking), this protein also has a deoxyribose excising activity that cleaves both the 5'- and 3'-phosphodiester bonds at an AP site

by successive b- and d-elimination reactions, resulting in a 1-base gap leaving both the 3' and 5' DNA ends phosphorylated (Bhagwat and Gerlt, 1996). Further processing requires a 3'-phosphatase contributed by endonuclease IV (EndoIV) to produce a primer for DNA polymerase (Agnez et al., 1996). However, when adenine is misincorporated opposite 8-oxo-G, the adenine-specific DNA glycosylase MutY is responsible for the removal of adenine in an effort to avoid the G→T transversion mutation. The complete repair of the lesion is not accomplished until dCMP pairs with 8-oxo-G and thus creates a substrate for FPG. (Michaels et al., 1992)

FPG enzyme activity is not restricted to 8-oxo-guanine detection, which is probably the most important biological substrate of FPG, or formamidopyrimidines (ring-opened purines). It possesses broad substrate specificity. FPG also catalyzes the excision of other forms of DNA damage such as AP sites and ring-opened N-7 guanine adducts. (Epe et al., 1993; Tchou et al., 1994; Li et al., 1997; Tudek et al., 1998; Speit et al., 2004)

Purified repair glycosylases such as the bacterial FPG protein are widely used for the quantification of endonuclease-sensitive modifications. If the digestion is carried out on intact cellular DNA such as carefully lysed cells, the single-strand breaks produced in cellular DNA can be measured using one of the following very sensitive techniques:

- The comet assay (Collins et al., 2004)
- The alkaline elution assay (Epe and Hegler, 1994)
- The alkaline unwinding assay (Hartwig et al., 1996)

Since the comet assay and the alkaline elution technique were performed in this study, the techniques are described in more detail in Materials and Methods(see section 4).

Up to now there is no known sequence homolog for the bacterial FPG glycosylase in eukaryotic cells. However, functional homologs have been cloned from yeast and human cells by several groups in 1997. The most important enzyme for the repair of 8-oxo-G in mammalian cells is the 7,8-dihydro-8-oxoguanine-DNA glycosylase OGG1 protein. (Boiteux and Radicella, 2000; Bruner et al., 2000). OGG1 encodes a 43 kDa protein that lacks a zinc finger domain, but contains a helix-hairpin-helix (HhH) motif similar to those in EndoIII or MutY (Nash et al., 1996). It is a glycosylase with AP lyase activity, which is specific for Fapy and 8-oxo-G:C and 8-oxo-G:T but does not cleave at 8-oxo-G:A (van der Kemp, 1996). The human OGG1 gene encodes two major isoforms of the enzyme, a-hOGG1 and b-hOGG1, resulting from alternative mRNA splicing. Both isoforms contain mitochondrial targeting signals, while only a-hOGG1 contains a nuclear localization signal (Nishioka et al., 1999).

Since specific inhibitors of the repair of oxidative DNA modification are not known, the generation of OGG1$^{-/-}$ knockout mice provide an interesting tool to analyze the effects of decreased repair rates *in vivo* and *in vitro* (Klungland et al., 1999; Minowa et al., 2000). Hence, the background level of 8-oxo-G in the chromosomal DNA in the liver of untreated OGG1$^{-/-}$ knockout mice was significantly higher than in that of wild-type animals (Minowa et al., 2000). Furthermore, cells derived from OGG1$^{-/-}$ mice showed no detectable 8-OH-G glycosylase activity when measured using oligonucleotide substrates, implying that the mammalian OGG1 protein is required to initiate the BER pathway (Klungland et al., 1999). Inactivation of OGG1 in yeast resulted in increased spontaneous mutations, revealing a spontaneous mutator phenotype (Thomas et al., 1997).

Taken together it is strongly suggested that base excision repair (BER) of 8-OH-G by the FPG or OGG1 proteins protects the genome from the mutagenic action of endogenous ROS in prokaryotes or eukaryotes respectively.

3. PROBLEM DEFINITION AND OBJECTIVES

It was hypothesized that TCDD interferes with the regulation of estrogens resulting in reduced concentrations of circulating estrogens via enhanced metabolic activation of estradiol by TCDD-induced enzymes, particularly CYP1A1 and CYP1B1. TCDD may lead to the enhanced formation of ROS as an initiating event and subsequent oxidative DNA damage indirectly via the redox cycling of the CYP-activated reactive main catechol estradiol metabolites, 4-hydroxyestradiol (4-OHE2) and 2-hydroxyestradiol (2-OHE2), that possess themselves a genotoxic potential. The induction of CYP1B1 plays a key role in this process as it preferentially forms the minor 4-OHE2, which exhibits greater carcinogenic potency (Lee et al., 2003). Besides the induction of oxidative stress via enhanced E2 metabolism, TCDD can directly lead to the induction of ROS via massive CYP induction, which is believed to be associated with leakage of ROS during extensive induction of the CYP mono-oxygenase system. Furthermore, the extensive evidence of TCDD to elicit anti-estrogenic activity was associated with modulation of the ERalpha-mediated regulation and a number of mechanisms were proposed to describe these AhR/ERalpha cross talk mechanisms (Safe, 2001; Matthews and Gustaffson, 2006).

In the present study the indirect-genotoxic mechanism of TCDD and E2 was investigated in light of a possible potentiating effect of both compounds on oxidative DNA damage. The aim of this study was to further elucidate the mechanism of action of TCDD on E2 metabolism in liver cells using *in vitro* models. A better understanding in the way estradiol is involved in the mechanism of TCDD-induced rat hepatocarcinogenesis should be provided.

In order to better understand the effects of E2 on TCDD-mediated toxicity and underlying mechanisms, the following areas of concern were investigated:

- Four different AhR-responsive liver cell models, rat H4IIE and human HepG2 hepatoma cell lines and rat primary hepatocytes from male and female rats were chosen to cover species- and sex-specific effects. The choice of hepatoma cells lines versus primary hepatocytes cultures should enable to compare metabolic capabilities and molecular mechanism between tumorigenic and non-transformed liver cells.
- The influence of TCDD and/or E2 *in vitro* on AhR-regulated CYP gene expression, subsequent ROS formation, DNA damage, and the most important antioxidant

defense systems (GSH and catechol-O-methyltransferase) were examined. Not only the effects of single treatment, but also combined effects of both substances should be examined after 20 h or 48 h treatment time.

- In order to exclude possible cytotoxic effects of the test compounds in the different cell types, a cytotoxicity assay was performed. The Alamar Blue Assay, also known as the resazurin reduction assay, was chosen to obtain non-cytotoxic concentrations of TCDD, E2, or the co-treatments, as well as the catechol estradiols 2-OHE2 and 4-OHE2 for use in further experiments.
- An overview of expression levels of the major E2-metabolizing enzymes CYP1A1 and CYP1B1 was anticipated by performing quantitative (TaqMan) real-time RT-PCR, Western blot analysis, and EROD-activity assay to assess basal and induced mRNA, protein levels, and CYP1A activity respectively.
- The nuclear receptor status of AhR and ERalpha, which is responsible for the TCDD-and E2-mediated signaling pathways, was determined by TaqMan Real-time RT-PCR or Western Blot analysis.
- The fluorescence H_2DCFDA assay in cracked cells was established in order to assess the potential role of ROS formation by TCDD and/or E2 in cultured cells. The possible correlation with induction of CYP enzymes was addressed as well, e.g. by the additional use of a CYP1A inhibitor.
- The elimination of reactive E2 metabolites by conjugation reactions was investigated. Different approaches should determine the detoxification of E2 metabolites: mRNA expression levels of COMT using real-time RT PCR method and cellular contents of total GSH (i.e. reduced and oxidized form).
- It was planned to investigate the genotoxic potential of TCDD and/or E2 on the formation of DNA strand breaks by performing the comet assay with and without FPG to differentiate between oxidative DNA damage. In order to check if possible oxidative DNA lesions are due to DNA base excision repair, the Unscheduled DNA synthesis (UDS) assay was additionally performed.
- The role of ERalpha in AhR- and ER–mediated transcription processes were evaluated in transient transfection assays using HepG2 cell line. Likewise, the role of respective AhR and ER inhibitors had to be investigated.
- Additionally, the role of the over-expression of ERalpha for some of the critical endpoints such as gene expression profile and ROS formation also had to be investigated in HepG2 cells transiently transfected with ERalpha.

- Accompanying the *in vitro* experiments, the relevance of TCDD on accumulation and repair of oxidative DNA base modifications was planned to be assessed *in vivo* in repair-deficient OGG1$^{-/-}$/csb$^{mut/mut}$ knockout mice after administration of a single dose of TCDD. FPG-sensitive DNA modifications will be quantified by the alkaline elution technique.

4. MATERIALS AND METHODS

If not otherwise indicated, standard reagents were purchased from Sigma-Aldrich, Carl-Roth, Fluka, Merck, BioRad, or Invitrogen. Cell culture media and supplementations were obtained from PAA Laboratories.

Consumables were purchased from Greiner, Eppendorf, BioRad, B. Braun Melsungen AG, Thermo Fisher Scientific, VWR, Sarstedt, or Millipore.

Compositions of solutions and buffers as well as a list of equipment can be found in appendix 8.2.

4.1. CELL LINES

The hepatoma cell lines used for the experiments were obtained from ECACC (European Collection of Cell Culture, UK). All cells used were adherent cell lines growing in a monolayer.

4.1.1. HEPG2 HUMAN HEPATOMA CELL LINE

HepG2 is a human-derived hepatocyte carcinoma cell line established from the tumor tissue of a 15-year-old Caucasian Argentine boy with hepatocellular carcinoma in 1975. The HepG2 hepatoma cell line is a widely used advantageous human-derived permanent cell line, which resembles liver parenchymal cells and expresses a spectrum of certain Phase 1 and Phase 2 drug metabolizing enzymes (Knasmüller et al., 1998 and 2004; Knowles et al., 1980; Sassa et al., 1987; Diamond et al., 1980). The cells were described to not harbor a hepatitis B virus genome and to produce a variety of plasma proteins such as albumin, alpha2-macroglobulin, alpha1-antitrypsin, transferrin etc. With a doubling time of ca. 50-60 h, the adherent cells take several days to form a confluent monolayer and grow until then mainly in small aggregates (DSMZ GmbH, 2009).

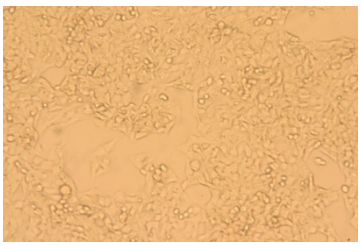

Figure 25: HepG2 cells in culture, almost grown to confluence.

4.1.2. H4IIE RAT HEPATOMA CELL LINE

H4IIE cells are adherent rat hepatoma cells that originate from Reuber H35 hepatoma cells. This cell line was established in 1964 and has a doubling time of 18-22 h, exhibiting high arylhydrocarbon hydroxylase inducibility. The cell line is useful for detecting picto-gram-quantities of planar polychlorinated organic compounds in environmental samples and food extracts. The cells have low basal CYP1A1 activity along with a high degree of responsiveness towards planar halogenated hydrocarbons. (Pitot et al., 1964; LGC Standards, 2009)

4.2. RAT AND MOUSE STRAINS

Animals were purchased from Charles River Laboratories (Sulzfeld, Germany). Knockout mice were kindly provided by Professor Dr. Bernd Epe (Institute of Pharmacy, Johannes Gutenberg University of Mainz, Germany). Upon arrival in the animal housing, animals were acclimatized for at least 4 days to get used to environmental conditions.

4.2.1. OUTBRED WISTAR RATS

Male and female Wistar rats were used for isolation of primary rat hepatocytes. The nomenclature of the rat strain is CrL:WI. The white albino rats were originated by the Wistar institute and given to Scientific Products Farm, Ltd. (predecessor of Charles River United Kingdom, CRUK) in 1974. Charles River was provided with the rat strain by CRUK in 1975. Wistar rats are a widely used rat model. (Charles River Laboratories, 2009)

4.2.2. INBRED C57BL/6 MICE

The nomenclature of the mice strain is C57BL/6NCrl. C57BL/6 was developed by C.C. Little in 1921 from a mating of Miss Abby Lathrop's stock that also gave rise to the strains C57BR and C57L. The strains 6 and 10 were separated in 1937. Charles River was provided

with the strain by the National Institutes of Health (NIH) in 1974. C57BL/6 mouse strain finds a broad research application and is a general multipurpose model, particularly for the generation of transgenic/knockout models. (Charles River Laboratories, 2009). C57/BL6 mice were ordered at the same body weight range than the knockout mice.

4.2.3. OGG1$^{-/-}$/CSB$^{MUT/MUT}$ DOUBLE KNOCKOUT MICE

The generation of the homozygous OGG1$^{-/-}$/csb$^{mut/mut}$ knockout mice was perfomed at Prof. Epe's laboratory facilities as follows: homozygous OGG1$^{-/-}$ mice (Klungland et al., 1999) were interbred with csb$^{mut/mut}$ mice (van der Horst et al., 1997) to produce an OGG1$^{-/-}$/csb$^{mut/mut}$ knockout mouse and F2 progeny was genotyped (Osterod et al., 2002). The single knockout mice used for mating to develop the double knockout mice were originally generated by DNA microinjection into blastocytes from C57BL/6J mice as described in the above mentioned papers.

4.2.4. MICE TREATMENT

For the alkaline elution assay (see section 4.7.3) homozygous OGG1$^{-/-}$/csb$^{mut/mut}$ knockout (ko) mice and C57BL/6J wild-type (wt) mice aged between 3 and 7 months were treated once by intraperitoneal (i.p.) injection with TCDD (1 µg/kg bw) or the vehicle control (DMSO 0.5% (v/v)) in corn oil. After duration of 96 h mice were sacrificed and primary hepatocytes isolated as described in section 4.3. Animals were chosen for the test groups by randomized selection and housed in steel cages (2-5 animals/cage). Number of animals assigned to the test groups in a randomized order are summarized in Table 5.

Table 5: Groups of animals and treatments.

	Ko		**Wt**	
	Vehicle	**TCDD (1 µg/kg bw)**	**Vehicle**	**TCDD (1 µg/kg bw)**
Animal numbers	3	4	3	3

4.3. ISOLATION OF PRIMARY CELLS

4.3.1. PREPARATION OF RAT HEPATOCYTES

Primary rat hepatocytes were isolated for primary culture from individual male or female Wistar rats (weighing 160-250 g) using a modification of the two-step in situ collagenase

perfusion technique described by Seglen (1976). Cell culture conditions are described in section 4.4.

Before the procedure, perfusion buffers were pre-warmed to 42°C in a water bath. The rat was anesthetized by intraperitoneal (i.p.) injection with 300 µL/100 g bw phenobarbital (equivalent to 100 mg/kg bw). The abdominal cavity was opened and the liver was exposed. A volume of 0.1 mL heparin solution (1000 U/mL) was injected into the vena cava inferior to prevent early blood coagulation. Both the inferior vena cava and vena porta hepatica were ligated for subsequent fixation of cannulae. A cannula was inserted into the hepatic portal vein and fixed. Vena cava inferior was cut with surgical scissors to allow blood and perfusion buffers to run off. In the first step, liver was perfused with EGTA-perfusion buffer I (flow: 40 mL/min) for up to 10 minutes. By deprivation of Ca^{2+} ions desmosomes, which bind liver cells to one another, are loosened. During this first perfusion step, diaphragm was laid open and a second cannula was inserted into the upper part of the vena cava superior. The cannula was equipped with a flexible tube to allow flow back of the perfusion solutions after vena cava inferior was successfully blocked by tightening the ligation. In a second step, liver perfusion is continued with Ca^{2+}-containing collagenase perfusion solution II (100 U collagenase/mL) for 5 to 10 minutes (flow: 40 mL/min). After perfusion, the liver was cut out of the animal and the liver capsula was removed. For this, complete liver was filtered through nylon filters of different mesh size (first 250 µM and then 100 µM) by adding pre-warmed washing buffer (200 mL). Cell suspensions were distributed to four 50 mL tubes and centrifuged (5 min, 350 rpm, room temperature). Supernatant was discarded and cell pellet resuspended in 100 mL washing buffer and three consecutive washing steps were performed. After the last washing procedure, cells were resuspended in 20 to 40 mL of washing buffer and kept at room temperature for cell counting and subsequent seeding. Only rat hepatocytes with a cell vitality of greater than 85% were used for experiments.

4.3.2. PREPARATION OF MOUSE HEPATOCYTES

Primary hepatocytes from mice treated with TCDD or vehicle control as described in section 4.2.4 were isolated using the modified two-step EGTA/collagenase perfusion technique (Seglen, 1976; Hengstler et al., 2000). Perfusion buffers were maintained at 37°C and gassed continuously with carbogene. Carbogene contains 5% CO_2 (v/v). During carbogene-equilibration, pH value drops down. Therefore, HEPES-buffer pH 8.5 is used for the preparation of EGTA buffer and collagenase buffer, adjusting the pH of the perfusion buffers to a value of 7.8.

Treated wild-type mice and knockout mice were sacrificed by inhalation of excess isoflurane in a saturated chamber. Immediately after expiration, the animal was prepared for perfusion. The abdominal cavity was opened and the liver and hepatic portal vein exposed. Cannulae were inserted into the hepatic portal vein and fixed with a ligation. Arteria carotis was cut with surgical scissors and the liver was perfused with EGTA buffer for 15 minutes (flow: 1 mL/min). Subsequently, the buffer was changed and perfusion was continued with collagenase-buffer (max. flow: 1 ml/min) for up to 30 minutes. At the end of the perfusion, the gallbladder was carefully removed. The liver was then excised and dissociated carefully in 10 mL of ice-cold suspension buffer by chopping it carefully into smaller pieces with the help of tweezers. The loosened mass was filtered through gauze (100 µM pore size) and centrifuged at 15xg for 10 min (4°C). The supernatant was discarded and the resulting cell pellet resuspended in 30 mL of cold suspension buffer. The washing step was performed twice again. Cells were stored on ice until further use. Freshly isolated hepatocytes were subjected to analysis by alkaline elution within 1 hour. Cell viability was determined with trypan blue exclusion as described in section 4.4.3 and ranged between 58-88%.

4.4. CELL CULTURE

4.4.1. CELL CULTURE CONDITIONS

Hepatoma cell lines as well as primary rat hepatocytes were cultured in phenol red-free Dulbecco's Modified Eagle's medium with glucose (1 g/L) supplemented with 10% fetal bovine serum^{Gold} (FBS^{Gold}), 1% penicillin/streptomycin (P/S; v/v), and 4 mM L-glutamine in a humidified atmosphere at 37°C, 5% CO_2, and 95% air. Hepatoma cell lines H4IIE (rat) and HepG2 (human) were grown as a monolayer in 75 cm^2 cell culture flasks. Routine monitoring has shown the hepatoma cells to be mycoplasma-free using PCR and the VenorGem Mycoplasma Detection kit (Minerva Biolabs).

4.4.2. MEDIUM RENEWAL AND CONTINUOUS CULTIVATION

Cultured cell lines were routinely maintained by subculturing them every seven days at $2.1*10^{-6}$ HepG2 cells and $0.5*10^{-6}$ H4IIE cells per 75 cm^2 cell culture flask. Culture medium was changed every two to three days and in particular the day after subculturing. For this, medium was removed from the culture flask (75 cm^2) and cells rinsed with 2 mL of trypsin/EDTA (1x) solution. Detachment solution was removed and an additional 1 mL of trypsin/EDTA solution added to the flask and well distributed on the cell monolayer. Cells

were incubated at 37°C for a few minutes (2-5 min) until the cells were detached from the surface. Immediately, fresh culture medium containing 10% FBS (12-15 mL) was added in order to inactivate the trypsin digestion reaction. Cells were individualized and suspended by pipetting up and down at least 20 to 40 times and were dispensed into new culture flasks.

4.4.3. DETERMINATION OF CELL NUMBER

Cell concentrations were determined via hemocytometer using trypan blue exclusion test. Neubauer counting chamber was used for cell lines and mice hepatocytes and a Fuchs-Rosenthal cell chamber for rat primary cells. Exemplarily, the Neubauer counting chamber is shown in Figure 26.

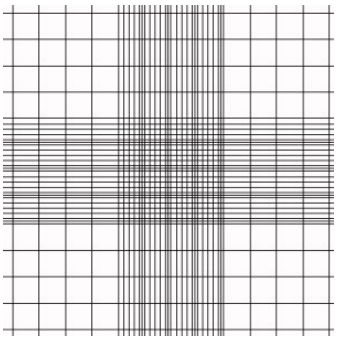

Figure 26: Neubauer counting chamber

Cell suspension of cell lines or mouse hepatocytes were dissolved at a ratio of 1:2 with trypan blue (0.4%) solution and placed on the hemocytometer. Trypan blue colors dead cells blue and leaves viable cells uncolored. Uncolored cells in 4 large squares consisting of 16 small squares were counted under the light microscope and the mean value of cells of the 4 large squares was calculated. The number of viable cells per ml was determined as follows:

$$\frac{cells}{mL} = \sum_{i=1}^{4} x_i * DF * 10^4$$

x: mean of viable cells of 4 large squares
DF: dilution factor (generally DF = 2)
104: hemocytometer-specific factor of the Neubauer chamber

To determine the total cell number, the cell number per mL was multiplied with the respective volume of the cell suspension. (Lindl, 2002)

Primary rat hepatocytes were counted in a Fuchs-Rosenthal cell chamber. Therefore, cell suspension (10 µL) was diluted at a ratio of 1:100 with washing buffer. Three areas consisting of 16 one square millimeter areas were counted and the total cell number was calculated according to the following equation:

$$total\ cell\ number\ per\ mL = \frac{n * 80 * 1000 * DF}{x}$$

n: total number of counted cells

80: hemocytometer-specific factor of the Fuchs-Rosenthal chamber
DF: dilution factor (generally DF = 100)

Cell viability was assessed by trypan blue dye exclusion test. For this 150 µL of the diluted cell suspension were mixed with 150 µL of the trypan blue solution (0.4%). Non-colored viable cells were counted and the corresponding viability factor (VF) is determined as follows:

$$VF = \frac{viable\ cells}{n}$$

n: total number of cells (see above)

The percentage of viable cells was determined by dividing the number of living (uncolored) cells by the total number of cells and multiplying by the factor 100:

$$\%\ viable\ (uncolored)\ cells = \frac{uncolored\ cells}{(colored + uncolored\ cells)} * 100$$

The number of viable cells per mL is expressed as the multiplication of the total number of cells per mL and the viability factor as follows:

$$viable\ cells\ per\ mL = \left(\frac{total\ cell\ number}{mL}\right) * VF$$

(Lindl, 2002; Schmitz, 2009)

4.4.4. FREEZING AND THAWING OF CELLS

Cultured cells were frozen in special freezing medium containing DMEM medium supplemented with 10% FBS and 10% DMSO. DMSO was used as a cryoprotector agent and permits the conservation of cell membranes integrity during the freezing process. Cells to be frozen were detached from the flasks by trypsination, counted, and then centrifuged (500 rpm, 5 min, room temperature). Approximately 2.5-4*10^6 hepatoma cells were suspended in 0.5-1 mL freezing medium per cryo tube. In order to allow progressive freezing, cryo tubes were first placed in a special cryo freezing-box containing cold 100% isopropanol (at 4°C) and kept at -80°C overnight to permit cells to gently and steadily cool down (about -1°C/min). The next day, cells were put in liquid nitrogen for storage. For thawing, cells frozen in liquid nitrogen were rapidly put at room temperature and were immediately dissolved in 15-30 mL normal DMEM culture medium (10% FBS). Subsequently, cells were centrifuged (3 min, 100 rpm, room temperature). Culture medium was removed and the pellet resuspended in 2 mL of fresh DMEM medium (10% FBS) and distributed to 75 cm^2 flasks containing already 12-15 mL of culture medium.

4.4.5. SEEDING OF CELLS

4.4.5.1. RAT HEPATOCYTES

Sterile, freshly isolated rat hepatocytes were seeded on collagenated well-plates or cell dishes. Cell plates were precoated with rat tail collagen solution (0.5 mg/L) and left to dry under UV light at sterile conditions overnight. Hepatocytes were seeded at a density of 0.1×10^6 cells per cm^2 in phenol red-free DMEM medium at 10% FBS supplemented with P/S (1%), and L-glutamine (4 mM) and allowed to attach under normal culture conditions. Four to 6 h after seeding, medium was replaced by fresh medium (DMEM 10% FBS), and cells were kept in DMEM (10% FBS) overnight before treatment.

4.4.5.2. CELL LINES

Hepatoma cells were seeded in normal cell culture medium (DMEM with 10% FBS) at the appropriate cell density depending on the plate format. The exact cell concentration seeded was chosen to achieve approximately 80% cell confluence at the end of the treatment time in the respective plate format dependent on the experiment

The final seeding concentrations used for each assay for the different cell types are indicated in Table 6.

Table 6: Concentration of cells seeded according to assay, format, and cell type. In brackets, the time of treatment is indicated.

			Seeded cell concentration (10^6 cells/mL) (treatment times in h)		
Assay, Method, Experiment	**format**	**Final volume/well (mL)**	**HepG2**	**H4IIE**	**PH**
Comet assay, UDS, Alamar Blue	96-well	0.1	0.5 (20)	0.015 (20)	-
H_2DCFDA, Alamar Blue	48-well	0.4	0.175 (20) 0.15 (48)	0.1 (20) 0.075 (48)	0.25 (20, 48)
EROD, Transfection	24-well	1	0,12 (48)	0,05 (48)	0.18 (20, 48)
Comet assay, tGSH	6-well	2	0.4 (20)	0.25 (20)	0.5 (20, 48)
Extraction of RNA microsomes, homogenate, tGSH	Ø 60 mm	4	0.375 (20) 0.45 (48)	0,2 (20) 0.25 (48)	0.625 (20, 48)
UDS	25 cm^2 flasks	5	-	-	0.5 (20)

4.4.6. TREATMENT WITH TEST COMPOUNDS

Twenty-four hours after seeding culture medium was removed and cells were treated over a period of 20 h or 48 h with the test substance in phenol red-free DMEM medium supplemented with 0.5% FBS (DMEM 0.5%).

Test substances were dissolved in either DMSO or ethanol (EtOH) and added to the serum-reduced medium so that the final solvent concentrations never exceeded 0.25% (v/v). Generally, cells were treated with concentrations of TCDD (1 nM and 10 nM; Pro-

mochem), 17beta-estradiol (10 nM and 100 nM) or its metabolite forms 4- or 2-hydroxyestradiol (10 nM, 100 nM, 1 µM, 3 µM, and 10 µM).

For co-treatments of TCDD with E2, both compounds were added simultaneously to the culture medium. Solvent-treated cells served as the negative control. The solubility of TCDD in EtOH 100% and the correctness of the concentration were checked analytically by Ökometric GmbH, Bayreuth. The final concentrations of solvent generally used for the different experiments are presented in the legends of the figures displayed in the results part (section 5). The respective positive controls, which respond to the different methods used, are described for each method separately.

4.5. BIOCHEMICAL ASSAYS

4.5.1. CYTOTOXICITY TEST: ALAMAR BLUE ASSAY

4.5.1.1. PRINCIPLE

The Alamar Blue (AB) assay, also termed resazurin reduction assay, was performed according to the procedure described by O'Brien and co-workers (2000). It is a simple and rapid test for *in vitro* measurement of cell proliferation and cytotoxicity based on metabolic cell activity. Oxidized Alamar Blue (resazurin) is a water soluble, non-toxic, and non-fluorescent blue colored dye. It is easily uptaken by cells and is reduced to a pink fluorescent dye (resorufin) in the medium by cell activity or mitochondrial enzymes (see Figure 27). (De Fries and Mistuhashi, 1995). There is a direct correlation between reduction of resazurin in the growth media and the proliferation of living cells. The reduction rate of Alamar Blue is dependent on the rate of metabolism of the cell line tested. Resorufin can be further reduced to colorless hydroresorufin. It has not been resolved whether the reduction reaction takes place intracellularly via mitochondrial enzyme activity, at the plasma membrane surface, or extracellularly in the medium as a chemical reaction.

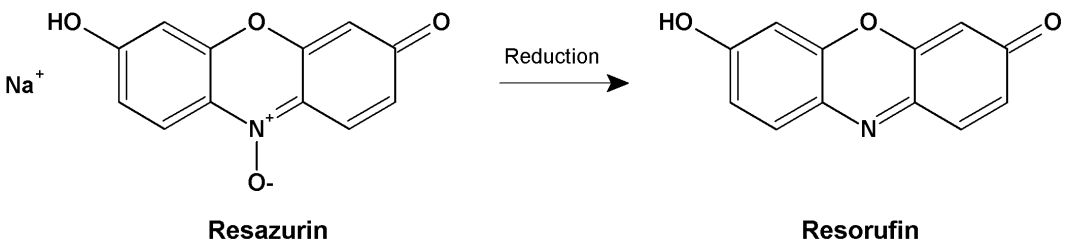

Figure 27: Reduction of resazurin (blue) to resorufin (pink). (According to O' Brien et al., 2000).

4.5.1.2. EXPERIMENTAL PROCEDURE

At the end of the cell treatment medium was removed, cells were rinsed with PBS, and 400 µL of AB solution (diluted 1/10 with DMEM without FBS) was added to each 48-well. If other well-plates were used, the volume was adjusted accordingly (e.g. 1 mL per well on a 6-well plate). After one hour incubation at 37°C in a humidified chamber fluorescence was measured at 540 nm excitation and 620 nm emission using Fluorescent Ascent microplate reader. Treatment with 0.1% sodium dodecyl sulfate (SDS) over the whole treatment time served as the positive control. A blank (non-cell control) was included in each experiment. The blank value is subtracted from fluorescence intensities. The mean of three replicates was then related to the negative control. The viability of cells was expressed as a percentage of survival compared to control cells (DMSO-treated 0.1%-0.25%).

4.5.2. CELLULAR ROS LEVELS: H_2DCFDA FLUORESCENCE ASSAY

4.5.2.1. PRINCIPLE

Since the use of the fluorogenic probe 2',7'-dichlorodihydrofluorescein diacetate (H_2DCFDA) was first described by Keston and Brandt (1965) as a fluorometric assay of hydrogen peroxide (H_2O_2), it has become a popular method for measuring formation of reactive oxygen species (ROS) in a variety of cell types for spectrofluorometric and flow-cytometric detection. The non-polar, non-ionic H_2DCFDA can easily cross the cell membrane (seeFigure 28). Once entered into the cell, cellular esterases hydrolyze its acetyl groups to form non-fluorescent 2',7'-dichlorodihydrofluorescein (H_2DCF). Deacetylated form of the probe is rapidly oxidized, generating the highly fluorescent product 2',7'-dichlorofluorescein (DCF). ROS formation is measured as increase in fluorescence which is associated with oxidation of the probe. (Bass et al., 1983; LeBel et al., 1992)

Though H_2DCFDA was originally used to detect H_2O_2, the probe is not specifically oxidized by H_2O_2 alone, but also by many other ROS forms. In fact, it remains unclear which ROS are responsible for the oxidation of H_2DCF. Apart from that, other constituents of the assay (e.g. buffers or culture media) or artifacts such as compounds other than ROS may be responsible for oxidation of H_2DCF. (LeBel et al., 1992; Brubacher and Bols, 2001)

In addition to that aspect, ROS that are stable (such as H_2O_2) are also capable of freely moving out of the cells. Thus, generation of DCF is not restricted to intracellular ROS production (Henderson and Chappell, 1993). The fact that the probe must first be de-acetylated in order to be susceptible to oxidation has also to be taken into account. As

inherent esterase activities vary greatly between different cell types, low cellular esterase activity may limit availability of H_2DCF and underestimate ROS production. (Brubacher and Bols, 2001)

In other words, up to date the assay is a simple, low cost fluorometric method which is easy to perform in order to obtain first hints of ROS production in cells following treatment with test compounds. Nevertheless, care has to be taken with interpretation of results as far as the origin of the detected ROS is concerned.

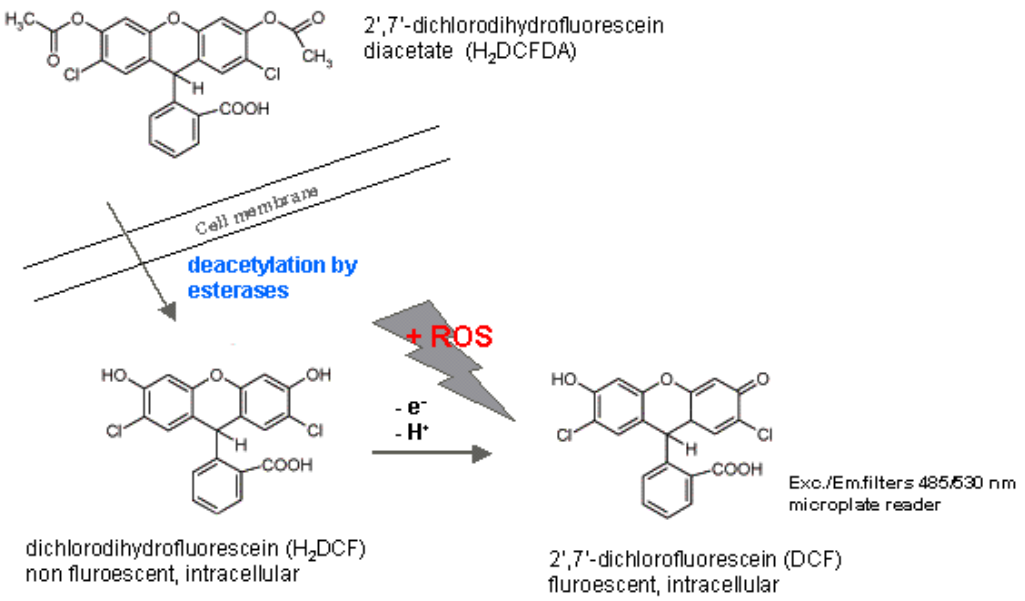

Figure 28: Proposed mechanism of entry of H_2DCFDA into cells. H_2DCFDA penetrates cell membrane and is deesterified to H_2DCF, which in the presence of ROS is subsequently oxidized to the fluorescent DCF. (According to LeBel et al., 1992)

4.5.2.2. EXPERIMENTAL PROCEDURE

The assay was performed according to LeBel et al. (1992) and Wang and Joseph (1999) with modifications. Following treatments for 20 h or 48 h, cells seeded in 48-well plates (or 24 well plates for transfected cells) were washed twice with PBS and frozen at -80°C. By means of three freezing/thawing cycles at -80°C and 4°C respectively, cell membranes were cracked. The protocol was carried out in the dark. Until loading of cells, cells and assay components were kept on ice.

For loading with the probe, cell membrane-cracked cells were incubated with a freshly prepared reaction mixture consisting of PBS, H_2DCFDA (5 µM/well) and esterases (0.05 U/well) at 37°C for 5 min in a microplate reader (Ascent Fluoroskan). Detailed composition of the master mix for the different plate formats can be viewed in Table 7. Then,

reaction was started by dispensing 10 µL/24-well of NADPH (33,5 µM/well) and fluorescence was measured in 5 min intervals for 30 min at 485 nm excitation and 538 nm emission.

Tert-butyl hydroperoxide (TBH) is an organic hydroperoxide and common pro-oxidant used to evaluate the effects of oxidative stress in cell lines and primary cultures, which was associated with rapid induction of glutathione (GSH), cellular lipid peroxidation, NADPH depletion, and altered Ca^{2+} homeostasis (Alia et al., 2005; Martin et al., 2001; Park et al., 2009). TBH was successfully shown to induce cellular ROS levels using the H_2DCFDA in colon carcinoma Caco 2 cell line (Bellion et al., 2008) and served as the positive control. It was added at a final concentration of 250 µM to the well containing untreated cells and the reaction mixture directly before the measurement in order to stimulate oxidative activity. In order to assess NADPH-independent formation of DCF, a no-NADPH control was always set up. Fluorescence intensities after 30 min (Ft30) were calculated as follows: Ft30 of the blank (cell-free control) was substracted from Ft30 of the sample and then related to an external calibration curve with DCF (ranging from 5 nM to 1 µM DCF/well). Therefore, DCF solutions (400 times higher concentrated) were prepared, diluted with reaction mixture accordingly in cell-free wells, and measured as described above. DCF production is linear to fluorescence increase, which allows for an expression of relative levels of ROS production in units of DCF fluorescence. Results are expressed as a percentage of DCF production (in nM) obtained with the control cells.

Table 7: H_2DCFDA reaction mixture prepared on ice for 48- or 24-well plates respectively.

Reagent	**MasterMix (per well)** **48-well plate**	**MasterMix (per well)** **24-well plate**
PBS	388 µL	776 µL
H_2DCFDA 2 mM	1 µL	2 µL
Esterase 48.6 U/mL	9.5 µL	2 µL
NADPH 13.4 mM	10 µL	20 µL
Final volume/well	400 µL	800 µL

4.5.3. 7-ETHOXYRESORUFIN-O-DEETHYLASE (EROD) ASSAY

4.5.3.1. PRINCIPLE

For the determination of monooxygenase activities several substrates on the basis of derivatives of phenoxazones are available to specifically assess CYP450 enzyme activities in liver tissues and cells.

The method commonly used to measure CYP1A activity is the 7-ethoxyresorufin-O-deethylase (EROD) assay. For this, the derivative of phenoxazone, namely 7-ethoxyresorufin, is specifically dealkylated by CYP1A1, yielding the highly fluorescent resorufin. Alkoxyresorufin-O-dealkylase substrates can be used to distinguish isoforms of P450 induced by various types of xenobiotics. Consequently, monooxygenase activity can be used as a marker for a given CYP450.

In the following protocol, EROD assay was performed in intact cells according to the method of Donato and co-workers (1993). Substrates are directly added to cultured cells to be metabolized and the resorufin formed is fluorimetrically quantified in microplates. Protein contents were determined in parallel by applying the fluorescamine assay. (Kennedy and Jones, 1994; Kennedy et al., 1995).

Fluorescamine reacts rapidly and stoichiometrically at neutral pH with amino acids, peptides, and proteins to the highly fluorescent derivatives. Fluorescamine itself as well as its hydrolysis products of excess substrate are non-fluorescent. (Udenfried et al., 1972). Reactions of 7-ethoxyresorufin and fluorescamine to fluorescent products are shown in Figure 29.

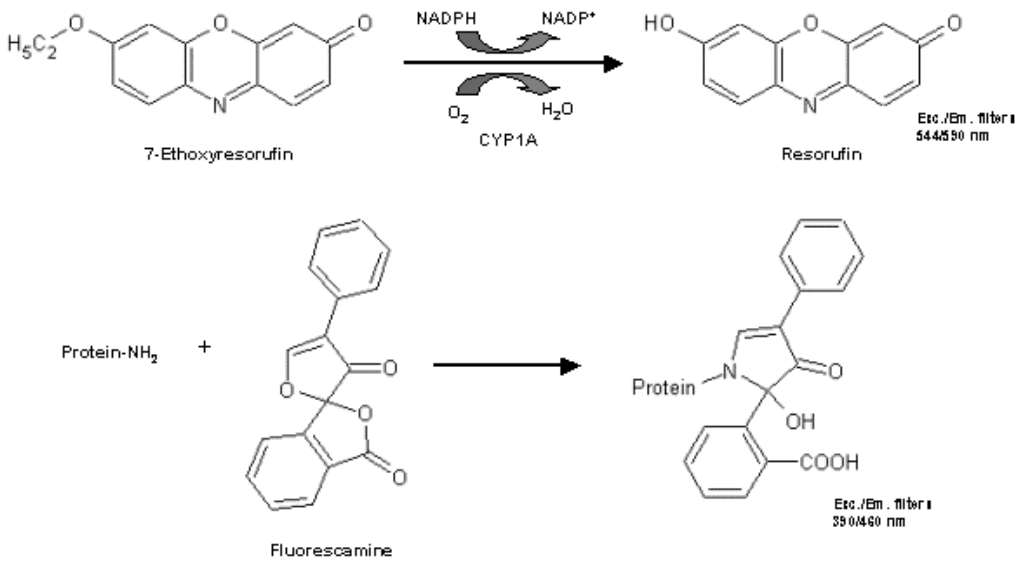

Figure 29: Reaction of ethoxyresorufin to resorufin by CYP1A (upper reaction) and reaction of protein with fluorescamine (according to Kennedy et al., 1995).

4.5.3.2. EXPERIMENTAL PROCEDURE

After 48 h treatment of the cells in 24-well plates the treatment medium was removed and cells were washed twice with PBS. The assay was started by adding a volume of 700 µL of the reaction mixture containing the substrates 7-ethoxyresorufin (EtRes) (8 µM/well) and dicoumarol (10 µM/well) in the appropriate culture medium without FBS (see Table 8). The addition of dicoumarol prevents further metabolism of the resorufin formed by the cytosolic enzyme diaphorase. For the resorufin standard curve (see Table 9) wells containing no cells but reaction mixtures were used. TCDD 1 nM served as the positive control for this test, as it is known to induce CYP1A activity at very low levels (Hasspieler et al., 2006).

Table 8: Reaction mixture for EROD assay.

Component	Volume per well (µL)
EtRes 0.5 mM	11.2
Dicoumarol 2 mM	3.5
DMEM w/o phenol red w/o serum	685.3
Finale volume	700

Table 9: Scheme for pipetting resorufin standard curve per well.

Standard	Resorufin (pM/well/mL)	Resorufin 2.7 µM (µL)	Resorufin 27 µM (µL)	MeOH (µL)
Blank	0	0	-	200
1	5.4	2.2	-	197.8
2	13.5	5.5	-	194.5
3	27	11	-	189
4	54	22	-	178
5	108	44	-	156
6	270	-	11	189
7	540	-	22	178
8	1080	-	44	156

After incubation of cells at 37°C for 60 min under normal cell culture conditions, the reaction medium from each well was transferred to a new 24-well plate. At this stage, the well plate containing the medium supernatants could be further processed or kept at -80°C. Subsequently, ß-glucuronidase was added to the medium and incubated in a shaking incubator at 37°C overnight in order to achieve hydrolysis of potential resorufin conjugates. The next morning, 200 µL of methanol was added per well to stop enzyme reaction. A standard curve of resorufin was prepared by adding resorufin and methanol as indicated in Table 9. EROD activity of supernatants was measured in 24-well plates using a plate reader (Fluoroscan Ascent FL) with an excitation wavelength of 544 nm and an emission wavelength of 590 nm for resorufin.

After collecting supernatants for resorufin determination cells attached on the well plate were washed twice with PBS and stored at -80°C until needed for determination of proteins.

The cells were thawn and lysed with 200 µL of SDS 1% per well. Plates were incubated for 10 min on a shaker at room temperature. First Na-acetate buffer 50 mM (pH 8) was added to each well (700 µL/well). Then, fluorescamine solution 300 µg/mL was added (300 µL/well) and cells were incubated in the dark for 15 min. Protein content was quantified at 405 nm excitation to 465 nm emission for fluorescamine. Total protein was quantified against a BSA calibration curve and a blank, which were performed simultaneously using the wells without cells. Following addition of SDS, standards were prepared on the 48-well plate. Na-acetate buffer was added together with BSA standards as indicated in Table 10, and after incubation time with fluorescamine the measurement was carried out as described above. (Donato et al., 1993; Kennedy and Jones, 1994; Kennedy et al., 1995)

Table 10: Scheme for pipetting BSA standard curve per well.

Standard	**BSA (µg/well)**	**BSA 1 mg/mL (µL)**	**Na-phosphate 50 mM, pH 8 (µL)**
Blank	0	0	700
1	25	25	675
2	50	50	650
3	100	100	600
4	150	150	550
5	300	300	400
6	500	500	200

Contents of resorufin and protein were calculated according to the standard curves and specific EROD activity per well in pM per minute and per mg was determined according to the following equation:

$$EROD\ activity = \frac{pm\ resorufin\ per\ well}{well\ reaction\ time\ (60\ \text{min.})} * mg\ protein\ per\ well$$

4.5.4. DETERMINATION OF TGSH AND GSSG

4.5.4.1. PRINCIPLE

Oxidation of the tripeptide glutathione (y-glutamylcysteinylglycine, GSH) in cells leads to the formation of glutathione disulfide (GSSG). Intracellular glutathione is effectively maintained in the reduced state by GSSG reductase linked to the NADPH/NADP$^+$ system. (Baker et al., 1990)

GSH is conveniently assayed by an enzymatic recycling procedure in which GSH or GSSG in the presence of glutathione reductase leads to the continuous reduction of 5,5'-dithiobis-2-nitrobenzoic acid (DTNB) by NADPH. Detection of the chromophoric product 2-nitro-5-thiobenzoic acid (TNB) can be monitored spectrophotometrically at 412 nm (see Figure 30).

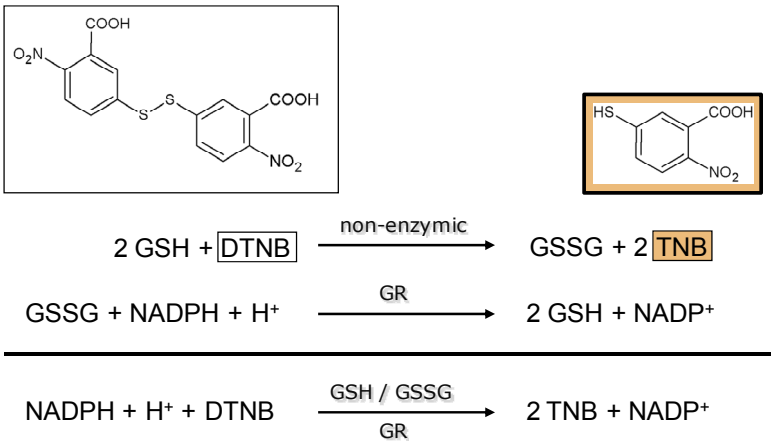

Figure 30: Glutathione reductase-catalyzed reduction of sulfhydryl reagent 5,5'-dithiobis-2-nitrobenzoic acid (DTNB) to the chromophoric product 2-nitro-5-thiobenzoic acid (TNB) (according to Akerboom and Sies, 1981).

The reaction rate is proportional to the concentration of total GSH (tGSH, reduced and oxidized glutathione), since all the other reaction compounds are added in excess. Quantification is achieved by parallel measurements of a standard curve of known GSH concentrations. Because both GSH (reduced form) and GSSG (oxidized form) are measured by this method, the data are usually expressed in tGSH = GSH + 2 GSSG. In order to selectively quantify reduced and oxidized forms of glutathione, GSH can be masked and thus the assay be made specific for GSSG. Therefore, reduced GSH is inactivated by the addition of 2-vinylpyridine (Griffith, 1980). Total Glutathione (tGSH) and GSSG are measured in a kinetic assay as described in Akerboom and Sies (1981) with modifications according to Gallagher et al. 1994. For tGSH determination in a 96-well plate, the assay was adapted as mentioned in the protocol of Schaefer et al. (2006).

4.5.4.2. EXPERIMENTAL PROCEDURE

Cell suspensions grown in 60 mm petri dishes (at least three dishes per treatment) were washed twice with PBS. Cells were trypsinized and reaction stopped by adding 1 mL of

FBS (10%)-containing culture medium. Detached cells were transferred to a 15 mL tube and centrifuged (10 min, 4°C, 1000 rpm). Supernatant was discarded. Pellet was re-suspended in freshly prepared 2 mL of a phosphate buffer (solution A + B; sodium phosphate (125 mM) containing EDTA (6.3 mM), pH 7.5), then pipetted in a 2 ml microtube, and centrifuged again (10 min, 4°C, 2000 rpm). The pellet was re-suspended in 370 µL phosphate buffer (solution A + B). Aliquots (20 µL) were used for protein quantification in the Bradford assay (as described in section 4.5.5) and could be kept at -80°C for at least one week.
The remaining cell suspension (350 µL) was used for protein precipitation by adding an equal volume of 5-sulfosalicylic acid (5-SSA, 10%). The precipitated solution was either used immediately for glutathione quantification or stored at -80°C for seven days. Since GSH oxidizes rapidly at pH values above 7.0, the samples were precipitated under acid conditions in order to maintain proper disulfide redox status. In addition to that effect, sample acidification also ensured cell lysis and subsequent release of free thiols and disulfides. (Gallagher et al., 1994)

For tGSH determination in a 96-well plate lysed cells were centrifuged (15 min, 4°C, 13000 rpm). Centrifugation supernatants (10 µL) were added to 190 µL/well of a freshly prepared reaction mixture containing 164 µL solution A + B, 20 µL DTNB (6 mM), 4 µL NADPH (20 mM), and 2 µL GSR (50 U/mL) per well. TNB formation was measured at room temperature in a microplate reader (MWG, Sirius HT injector) at 412 nm after 2 min reaction time. GSH standard solutions (320 µM, 160 µM, 100 µM, 50 µM, 20 µM, 10 µM, 5 µM) were prepared by diluting in 5-SSA 5% starting from the GSH stock solution 1 mM. A volume of 10 µL GSH standard solutions was used for measurements leading to the following GSH concentrations per well: 16 µM, 8 µM, 5 µM, 1 µM, 0.5 µM, 0.25 µM. A blank measurement lacking GSH (10 µL of 5-SSA 5%) was run in parallel and the background level of product formation was subtracted from all sample values. Each experiment was performed in duplicate.

Prior to photometric determination of GSSG, 500 µL of supernatants were transferred into a new 1.5 mL microtube. GSH was readily derivatized with 20 µL of 2-vinylpyridin and 100 µL of triethanolamine (TEA) 50%. GSH was inactivated in a thermomixer at 26°C and 600 rpm for 1 h. The addition of 2-vinylpyridine followed by neutralization with TEA prevented oxidation of GSH in the sample (Baker et al., 1990). Aliquots (20 µL) of GSH-inactivated samples were assayed as described above (using 154 µL of phosphate buffer (solution A + B appropriately) and submitted to photometric determination at 412 nm and 25°C after 10 min reaction time. GSSG standards (1.25-40 µM) were prepared likewise in 5-SSA 5% from stock solution (1 mM) and aliquots of 20 µL for measurements led

to the following GSSG concentrations per well: 4 µM, 2 µM, 1 µM, 0.5 µM. 0.25 µM, and 0.125 µM.

Each experiment was performed in duplicate. Sample contents of tGSH and GSSG were determined by relation to the standard curve generated with known amounts of GSH or GSSG and were expressed as µMol/mg protein normalized to solvent control. The total GSH content of the sample (tGSH = GSH + 2 GSSG) was used to indicate the sum of freely soluble GSH and GSSG, but did not reflect glutathione present as mixed disulfides. GSH status was calculated as reduced GSH in percent of tGSH.

4.5.5. QUANTIFICATION OF PROTEINS: BRADFORD ASSAY

4.5.5.1. PRINCIPLE

Quantification of proteins with the method of Bradford (1976) involves the binding of an acidic solution of Coomassie Brilliant Blug G-250 to protein. The color dye's absorbance maximum shifts from 465 nm (red form) to 595 nm (blue form) upon the binding of proteins. It unspecifically binds basic and aromatic amino acid residues, especially arginine (Compton and Jones, 1985). It is a very rapid assay, as the dye binding process is complete after approximately 2 minutes and remains stable four 1 hour. Little or none interferences occur from cations such as sodium, potassium, or from carbohydrates. (Bradford, 1976)
The method was carried out according to the Bio-Rad Protein Assay Technical Bulletin with slight modifications (Bio-Rad, 1999).

4.5.5.2. EXPERIMENTAL PROCEDURE

Protein Assay Dye Reagent Concentrate (Bio-Rad) containing Coomassie Brilliant Blue G-250, methanol, and phosphoric acid was prepared by diluting one part of the dye with four parts of ddH_2O. Six dilutions of the protein standard bovine serum albumine (BSA) in concentrations ranging from 0-10 µg/well were prepared from BSA stock solution (0,5 mg/mL) and pipetted into separate wells of a 96-well microplate as indicated in table Table 11.
Samples were diluted 1/20 in ddH2O and 20 µL/well of each sample were used. Protein solutions were assayed in triplicate. A volume of 200 µL of diluted dye reagent were added per well. The microplate was incubated at room temperature for at least 5 min but no more than 1 h. The increase in absorption was monitored at 595 nm in a microplate reader (MWG, Sirius HT injector). The extinction value from the reagent blank was subtracted from the extinction values of samples. The concentration of BSA was plotted against the

corresponding absorbance resulting in a standard curve. Based on the standard curve, the protein concentration (µg/µL) in unknown samples was calculated.

Table 11: Pipette scheme for preparation of BSA standard curve for the Bradford assay.

protein/well (µg)	BSA 0.5 mg/mL (µL)	ddH_2O (µL)
0	0	100
1	10	90
2	20	80
4	40	60
6	60	40
8	80	20
10	100	0

4.6. MOLECULAR BIOLOGY

4.6.1. TOTAL RNA EXTRACTION

Most of the RNA is localized in the cytoplasm. Cytoplasmic RNA consists of ribosomal RNA (rRNA, 71%), transfer RNA (tRNA, 15%) and to a lesser extent of messenger RNA (mRNA, 3%). Total RNA was isolated from cells with the RNeasy Mini Kit from Qiagen according to the manufactor's instructions (RNeasy Mini Handbook, 2006). This method takes advantage of the binding properties of RNA to a silica-based membrane in combination with the speed of microspin technology. (Lottspeich and Engels, 2006)

The RNeasy isolation procedure results in purification of mRNA and is therefore an appropriate method for its subsequent use in the real-time RT-PCR (see section 4.6.2). Since most RNAs that are smaller than 200 nucleotides (i.e. 5.8S rRNA, 5S rRNA, and tRNAs, which constitute 15-20% of total RNA) do not bind to the RNeasy silica membrane, they are selectively excluded in the course of the extraction. RNA samples are easily contaminated or destroyed by the very stable and active enzyme ribonuclease (RNases) so that some precautions have to be considered when working with RNA: wearing gloves, cleaning of benches and pipettes with RNase AWAY solution, use of sterile and RNase-free plasticware, and the use of filter tips. All reaction steps were performed at room temperature and all centrifugation steps were carried out at the same speed at ≥ 8000x*g*

(≥ 10 000 rpm). Medium was removed from the cells grown in 60 mm diameter cell culture dishes and cells were washed twice with PBS and stored at -80°C until RNA extraction. First, cells were lysed and homogenized in the presence of highly denaturating guanidine-thiocyanate-containing buffer. For direct cell lysis 600 µL of buffer RLT (containing 1% (v/v) β-mercaptoethanol) were added to the cell culture dish. Therewith, RNases were immediately inactivated to ensure purification of the intact RNA. Cells were harvested with a sterile cell scraper and the cell lysate was directly pipetted onto a QIA-shredder spin column and centrifuged for 2 min at maximum speed. Addition of a volume of 600 µL ethanol 70% to the homogenized lysate provides appropriate binding conditions to the spin column. The lysate is mixed well by pipetting. The sample (up to 700 µL at a time) was then transferred to a silica-based membrane RNeasy Mini spin column and centrifuged for 15 s. Since total RNA was bound to the membrane, the flow-through was discarded. The column was washed by adding 700 µL of Buffer RW1 to the RNeasy column and centrifuged for 15 s. After that, the column was washed again twice by adding 500 µL of Buffer RPE and centrifuged. At the last centrifugation step, the tubes were centrifuged for 2 min in order to dry the RNeasy silica-gel membrane. The RNA was then eluted by adding 32 µLof RNase-free water to the RNeasy column. After centrifuging for 1 min, the total RNA was kept on ice and stored at -80°C for further use.

4.6.1.1. SPECTROPHOTOMETRIC QUANTIFICATION AND DETERMINATION OF RNA QUALITY

The determination of the concentration of RNA or DNA is based on the absorption maximum of nucleic acids at 260 nm. The aromatic rings of the bases are responsible for their absorption, which can be measured spectrophotometrically in the ultraviolet (UV) range. An absorbance of 1 unit at 260 nm (A260) corresponds to 44 µg of RNA per mL at a neutral pH. The purity of RNA can be estimated via the ratio of the absorption readings at 260 nm and 280 nm (A260/A280). Pure RNA has an A260/A280 ratio between 1.9 and 2.1. Contaminations for example with proteins that absorb light in the UV spectrum can influence the ratio. RNA possessing ratios smaller than 1.8 are indicative of protein contaminations and affect high quality of the RNA. (RNeasy Mini Handbook, 2006; Lottspeich and Engels, 2006). RNA samples were quantified with a NanoDrop 1000 spectrophotometer, which enables highly accurate analyses by disposing only 1 µL of the sample (Thermo Fisher Scientific Inc.). An A260/A280 ratio in the range of 1.8 to 2.3 was considered to be of a good quality for RNA.

4.6.1.2. RNA GEL ELECTROPHORESIS

In order to assess RNA integrity total RNA was separated according to its molecular weight during denaturizing agarose gel electrophoresis. Intact RNA showed two prominent bands, namely the ribosomal RNAs 28S and 18S, with a ratio of approximately 2:1. RNA was degraded when the bands appeared as a smear. A 1.5% agarose gel was prepared by melting agarose and RNase-free water in the microwave and adding 10% formaldehyde. Formaldehyde acts as a denaturation agent. The RNA (3 µL) was mixed with the same volume of ethidium bromide-containing RNA loading buffer. The mixture was heated for 20 min at 65°C to achieve RNA denaturation. The presence of 3-morpholino-1-propanesulfonic acid (MOPS) buffer, formaldehyde, and formamide in the loading buffer supports this effect. Samples were cooled on ice and then loaded into the pockets of the agarose gel. MOPS buffer (1x) was used as the electrophoresis buffer. Gel electrophoresis was conducted for 2-3 h at 80-90 V. Only intact total RNA, which resulted in sharp 28S and 18S rRNA bands with a 2:1 ratio as shown in Figure 31, was subjected to cDNA synthesis. (RNeasy Mini Handbook, 2006; Sambrook et al., 1989)

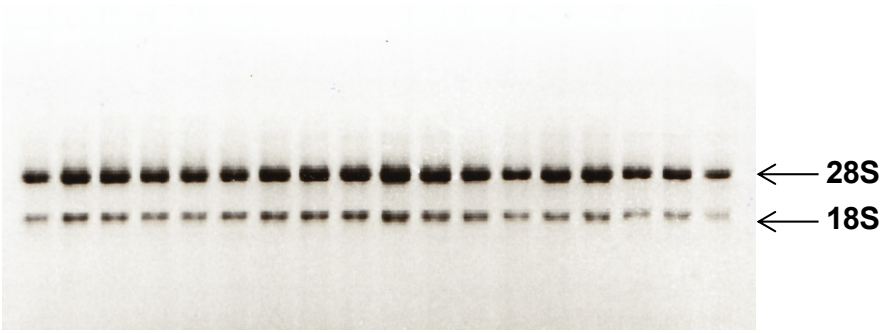

Figure 31: Representative RNA gel of several RNA samples.

4.6.2. REAL-TIME RT-PCR

4.6.2.1. PRINCIPLE

Since the Polymerase Chain Reaction (PCR) was invented in 1983 by Kary Mullis (Nobel Price awarded in 1993) (Mullis and Faloona, 1987), the PCR method has become a widely used technology with broad applications in fields such as molecular biology, diagnostics, and forensic analysis in order to amplify a specific DNA fragment exponentially and selectively (Holland et al., 1991). In general, the PCR procedure consists of three main reaction steps of temperature cycling that are repeated up to 40-50 times: denaturation, annealing of primers, and elongation. The reaction is started by heating to 92-98°C. High temperature is applied to separate the strands of the double helical DNA by disrupting the hydrogen bonds between complementary bases, resulting in single-stranded DNA. Lower-

ing the temperature to 50-60°C leads to hybridization of the primers (i.e. synthesized oligonucleotides of 15-30 bases with complementary DNA sequences to the targeted DNA) to the complementary base sequences of the single-stranded DNA template. During extension step temperature is raised to its optimum of 72-75°C. The DNA polymerase binds to the primer template and starts synthesis of the new DNA strand by incorporating the deoxynucleotide triphosphates (dNTPs). Utilizing Thermus aquaticus (Taq) polymerase, commonly an optimum temperature of 72°C can be used. Under optimum conditions the amount of DNA target is doubled at each extension step, leading to exponential amplification of the specific DNA fragment. (Kubista et al., 2006; Falbe and Regitz, 1995)

During conventional PCR the amplification is detected by DNA agarose gel electrophoresis, while during real-time PCR the amplification of nucleic acids is monitored in "real-time", i.e. when the reaction progresses, and is directly related to the starting number of DNA copies. By means of fluorescence techniques, which permit to measure fluorescence accumulation during the reaction, the real-time quantitative PCR (qPCR) detection was developed. Fluorescent signals, which are proportional to the amount of PCR product, can be generated by fluorescent dyes such as SYBR Green or by sequence-specific fluorescent oligonucleotide probes. (Salmon, 2002)

SYBR Green (see Figure 32) is the most frequently used intercalating dye and is capable of emitting fluorescence when bound to double-stranded DNA (dsDNA), but with a lack of specificity. Therefore, amplification products have to be verified by the use of a melt curve after every SYBR Green experiment. (Becker-Follmann and Baas, 2004). SYBR Green can be excited by blue light at a wavelength of 480 nm. It emits light at a maximum of 520 nm. (Wilhelm and Pingoud, 2003). TaqMan (Double-Dye probes) are fluorophore-labeled oligonucleotide hybridization probes that are used for sequence-specific detection and constitute a very specific detection method as PCR products can only be detected if the probes hybridize to the appropriate amplification products. Double-Dye oligonucleotides are coupled with a fluorescent reporter attached to the 5' end of the probe and a quencher molecule attached to the 3' end. Traditionally, FAM (6-carboxy-fluorescein) was used as the fluorophore and TAMRA (6-carboxy-tetramethyl-rhodamine) as the quencher. The fluorophore transfers its energy to the quencher and the energy is released from the quencher as fluorescence of a higher wavelength. (Pfaffl, 2009; Eurogentec, 2007). During the so-called TaqMan qPCR the 5'-3' exonuclease activity

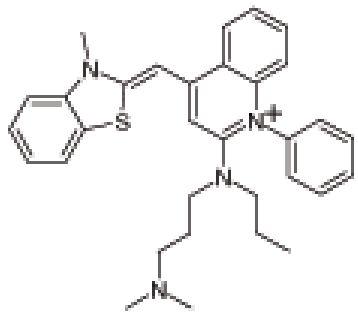

Figure 32: Molecular Structure of SYBR Green (Kubista et al., 2006).

of the thermostable enzyme Taq DNA polymerase and TaqMan probes are employed in the polymerase chain reaction in order to generate a specific detectable signal (Holland et al., 1991).

4.6.2.2. AMPLIFICATION CURVE

During PCR reaction exponential amplification occurs. The amplification plot obtained in a real-time PCR reaction is shown in Figure 33. The PCR cycle number is shown on the x-axis, and the detected fluorescence from the amplification reaction, which is proportional to the amount of amplified product, is shown on the y-axis. In the initial phase, fluorescence remains at background levels, and exponential product accumulation is not yet detectable (cycles 1-18 in Figure 33).The cycle at which the emission intensity of the sample rises above the background fluorescence is defined as CT (threshold cycle) and is inversely proportional to the target sequence concentration. (Pfaffl, 2001). The higher the target concentration, the lower the number of amplification cycles required to raise fluorescence above baseline (Lie and Petropoulos, 1998).

In the case of a 100% PCR efficiency, the amount of PCR product doubles in each cycle according to the following equation:

$$N = N_0 - 2^n$$

N: number of amplified molecules
N_0: number of molecules prior to amplification
^{n}: cycle number.

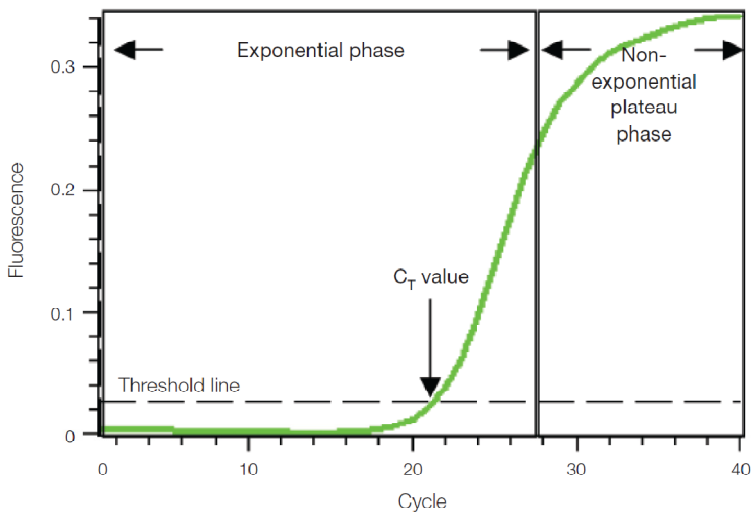

Figure 33: Real-time PCR amplification plot (Bio-Rad, 2006).

During the exponential phase amplified products can be quantified. When the reaction components become limited, reaction slows and enters saturation (plateau phase). In a typical real-time PCR experiment all response curves saturate at the same level. (Pfaffl, 2004; Becker-Follmann and Baas, 2004; Kubista et al., 2006)

4.6.2.3. DNA DIGESTION AND REVERSE TRANSCRIPTION

Reverse transcription (RT) followed by real-time PCR is a highly sensitive and powerful technique to analyze mRNA expression, even small changes and rare transcripts can be quantified. For this application RNA has to be transcribed into DNA. The resulting DNA strand is referred to as complementary DNA (cDNA). Extracted RNA samples (0.5 µg) were reverse-transcribed according to the instruction manual of the iScript cDNA Synthesis Kit (Bio-Rad) using oligo(dT) random hexamer primers. Prior to cDNA synthesis a DNA digestion step was performed in order to avoid artifacts from DNA targets, i.e. genomic DNA residual from RNA preparations. Deoxyribonuclease I, Amplification Grade (DNase I, Amp Grade, Invitrogen) purified from bovine pancreas digests single- and double-stranded DNA to oligodeoxyribonucleotides containing a 5'-phosphate. It eliminates DNA for RNA purification procedures prior to PCR amplification. The RNA sample (0.5 µg) was added to the reaction mix (see Table 12) and incubated for 15 min at room temperature. Higher temperatures or longer incubation times can lead to Mg^{2+}-dependent hydrolysis of the RNA. DNase I is inactivated by addition of 1 µL of EDTA 25 mM solution to the reaction mixture. After heating for 10 min at 65°C the RNA samples were put on ice and further subjected to reverse transcription.

Table 12: DNA digestion reaction mix (DNase I, Amp Grade, Invitrogen)

Component	Volume per reaction (µL)
RNA sample 5 µg (0.0625 µg/µL)	8
DNase I Reaction Buffer (10x)	1
DNase I, Amp Grade (1 U/µL)	1

The RT-reaction was carried out using iScript cDNA Synthesis Kit (Bio-Rad) following the manufactor's instructions. A master mix was prepared as listed in Table 13 and added to the RNA template from the DNA digestion step. A no-reverse transcriptase control reaction consisting of a non-RT-treated RNA sample (1 µL of nuclease-free water was added instead) was always run in parallel to ensure efficiency of the reaction.

Table 13: Master Mix Reverse Transcriptase reaction.

Component	Volume per reaction (µL)
5x iScript Reaction Mix	4
iScript Reverse Transcriptase	1
Nuclease-free water	4
RNA template from DNA digestion step	11
Total Volume	20

The samples were put in the iCycler and the thermocycling program was started (see Table 13).

Table 14: Thermocycling conditions for RT-Reaction with iScript cDNA Synthesis Kit (Bio-Rad).

Step	Temperature	Duration time
1	25°C	5 min
2	42°C	30 min
3	85°C	5 min
4	4°C	Hold

Afterwards, the obtained cDNA was diluted to 12.5 ng/µL (at a final volume of 20 µL) and was kept at -20°C for short-term storage and at -80°C for long-term storage.

4.6.2.4. REAL-TIME PCR

Real-time PCR was performed in a total volume of 25 µL per reaction on an iCycler iQ Real-Time PCR Detection System with iCycler Software version 3.1 (Bio-Rad) using a 96-well format. Each PCR reaction contained 25 ng (2 µL) of the diluted cDNA (12.5 ng/µL), 12.5 µL of AbsoluteTM QPCR SYBR® Green Fluorescein Mix (Thermo Scientific), 1 µL of the 5 µM primer mixes (forward and reverse primer 200 nM/well) and 9.5 µL of sterile pure water. When a fluorogenic probe was used, the qPCR Master Mix no ROX (Eurogentec, Belgium) with a primer mix containing the primer pairs (300 nM/well) and the fluorogenic probe (100 nM/well) were added instead (see Table 15). A no-template control was run for each primer pair. First, reverse transcribed cDNA was transferred to a 96-well PCR Plate (Thermo Scientific) and then the adequate volume of the Master Mix was added. PCR well plates were covered with optic seals and spinned down (1 min, 1000 rpm).

Table 15: Master Mix for a PCR reaction (25 µL)

Reagent	**MasterMix 25 ng cDNA template**	**MasterMix 50 ng cDNA template**
SYBR Green Mix 2x or qPCR MasterMix No ROX 2x	12.5 µL	12.5 µL
Primer Mix (5 µM) or TaqMan Primer Mix	1 µL	1 µL
Nuclease-free water	9.5 µL	7.5 µL
Final volume MM	23 µL	21 µL
cDNA (12,5 ng/µL)	2 µL	4 µL

The primers for h/r CYP1A1 were already validated and used in the laboratory previously. The other primer sets were designed using the free software primer 3 (Rozen and Skaletsky, 2000) and purchased from Eurofins MWG Operon. Fluorogenic probes were designed and obtained from Eurogentec. Primer Sequences for each gene are listed in Table 16. The housekeeping gene 36B4 was used as an estradiol-independent control, which was shown to not modify mRNA levels following estradiol treatment. The 36B4 mRNA is the mRNA for human acidic ribosomal phosphoproteine PO. (Laborda, 1991)

Optimized PCR consisted of 45 cycles at 95°C for 15 seconds followed by amplification at 58-60°C for 30 or 60 seconds. In the case of the ERalpha gene expression 50 cycles were run and 50 ng of cDNA template were used to achieve appropriate CT detection. For real-time PCR using SYBR Green fluorescein mix a melting curve emerging in a gradient, starting at the respective annealing temperature up to 90°C in increasing steps of 0.5°C, verified the single PCR product. The real-time thermal cycling program and the optimized annealing temperatures and annealing times of the different target genes are listed in Table 17 and Table 18.

Table 16: Overview of primer sequences, gene accession number, and amplicon size. FAM = 6-carboxy-fluoroscein, TAMRA = 6-carboxy-tetramethyl-rhodamine.

Gene	**Primer sequence (5'-3')**	**Gene Bank Accession No.**	**Amplicon size (bp)**
hCYP1B1	sense: GCT AAA CCC GCT GTC CAT CC anti-sense: CCG CCT CCG TTG CCT CAG probe: 6-FAM-ACC ACG CTC CTG CTA CTC CTG TCG G-TAMRA	NM_000104	100
rCYP1B1	sense: GAG TTG GTG GCA GTG TTG antisense: GCA TCG TCG TGG TTG TAC	NM_012940	130
h/rCYP1A1	sense: CCT CTT TGG AGC TGG GTT TG anti-sense: CCT GTG GGG GAT GGT GAA	NM_000499 NM_012540	227
h/rERalpha	sense: AAG ATC AAC GAC ACT TTG ATC CAC anti-sense: ATG CCT TTG TTA CTC ATG TGC C probe: 6-FAM-CTG GCC CAG CTC CTC CTC ATC CT-TAMRA	NM_000125 NM_012689	124
h/rAhR	sense: TCC ACA GTT GGC TTT GTT TGC anti-sense: TGT GAA GTC CAG TTT GTG TTT GG probe: 6-FAM-CTA CTC CAC TTC AGC CAC CGT CCATCCT-TAMRA	NM_001621 NM_013149	108
hCOMT	sense: ACA GTG CTA CTG GCT GGC TGA CAA anti-sense: GGC TGT CTT GGA ACT CAC TT	NM_007310	108
rCOMT	sense: GAG TCA CAA GCT TTA CAG GT anti-sense: GGC TGT CTT GGA ACT CAC TT	NM_012531	115
h36B4	sense: ACT TGC TGA AAA GGT CAA GG anti-sense: TTC CTT GGC TTC AAC CTT AG	M17885	128
r36B4	sense: TGC AGC TGA TAA AGA CTG GA anti-sense: CTG TAG ATG CTG CCA TTG TC	X15096	127

Table 17: Real-time PCR thermal cycling program.

Step	Cycle number	Temperature (°C)	time (min)
1) Enzyme activation	1x	95	15 min
2) Denaturation	45x/50x	95	15 s
Annealing		annealing temperature (58 – 60)	1 min
3) Final denaturation	1x	95	30 s
	1x	annealing temperature	30 s
4) Melt curve	80x	annealing temperature + 0.5	10 s
5) Hold	1x	4	∞

Table 18: Optimized annealing temperatures and annealing time.

Gene	Annealing temperature	Annealing time
hCYP1B1	60°C	1 min
rCYP1B1	60°C	1 min
h/r CYP1A1	58°C	1 min
h/r ERalpha	60°C	1 min
h/r AhR	60°C	1 min
h/r COMT	58°C	1 min
h 36B4	56°C	1 min
r 36B4	58°C	1 min

The comparative delta-delta CT method was used to determine relative expression levels between treatments. The cycle number at which the transcripts of the gene of interest were detectable (CT) was normalized to the cycle number of 36B4 detection, referred to as ΔCT. Subsequently, mean ΔCT value of the controls was subtracted from ΔCT of the treatment, providing the ΔΔCT value. The relative expression difference of a sample be-

tween a treatment and control normalized to the house keeping gene (ratio) was calculated by the equation below. (Pfaffl, 2004)

$$\Delta CT = CT\ target\ gene - CT\ HKG$$

$$\Delta\Delta CT = \Delta CT\ treatment - \Delta CT\ control$$

$$ratio = 2^{-\Delta\Delta CT}$$

Relative mRNA expression normalized to solvent control is useful to investigate treatment-related fold-inductions. In order to assess the mRNA levels non-normalized to control, the CT value of the target gene was normalized to the CT value of the housekeeping gene, but not related to control ($2^{-\Delta CT}$).

4.6.2.5. PRIMER VALIDATION AND MELTING CURVE

Standard curves applying serial dilutions of starting cDNA for each test gene primer set were generated to determine optimal annealing temperatures and times and to ensure that the efficiency of the amplification of the test gene and the housekeeping gene were approximately equal. The efficiency of a PCR assay has to be estimated for every primer pair by means of a standard curve.

The PCR conditions were optimized by determining a standard curve of the corresponding target cDNA. Serial dilutions (1:6) of a standard cDNA sample were performed starting with 50 ng per reaction input cDNA. Cell- and species-specific cDNA from TCDD-treated cells was used. Additionally, optimum annealing temperature for the primers had to be determined (see Table 18).

According to the dilution steps, a standard curve was obtained during the real-time PCR reaction. The concentrations of the cDNA were related to the CT cycles in a logarithmic scale. From this, the corresponding PCR efficiency (E) can be calculated from the resulting slope as follows:

$$E = 10^{-(\frac{1}{slope})}$$

Under optimum primer conditions PCR efficiency is at 100%, which corresponds to a value of E = 2.0. (Pfaffl, 2001; Pfaffl, 2004)

When real-time PCR was performed using SYBR Green, a melting curve analysis was performed subsequent to every PCR reaction in order to characterize the amplified sequences with respect to their melting temperature (TM) (Wilhelm and Pingoud, 2003).

4.6.3. PREPARATION OF MICROSOMES

4.6.3.1. PRINCIPLE

CYP enzymes are microsomal-type, integral membrane proteins that are bound to the membrane of the endoplasmic reticulum (EndRet). CYP enzymes are located in the EndRet of many animal tissues and plant tissues (Halliwell and Gutteridge, 1999). Thus, the microsomal fraction of cells was extracted for the investigation of protein levels of CYPs such as CYP1B1 and CYP1A1 enzymes.

The isolated microsomal fraction contains two main components, i.e. the rough and smooth microsomes. Rough microsomes arise from rough-surfaced EndRet; smooth microsomes derive mostly from the smooth EndRet, at least for liver tissues. Isolation of crude microsomes consists of both elements. (Dallner and Ernster, 1968). The endoplasmic reticulum consists of a network of interconnected tubules, vesicles, and sacs, which play a role in specialized cellular functions such as protein synthesis, sequestering of calcium, production of steroids, storage and production of glycogen, and insertion of membrane proteins. By definition microsomes are the parts of a tissue homogenate that can be sedimented by ultracentrifugation from mitochondrial supernatant. Serial centrifugation steps include low speed centrifugation at 1000xg and medium speed centrifugation at 12 000xg, thereby removing nuclei, cell debris, mitochondria, and lipids to obtain a post mitchochondria fraction. Ultracentrifugation of the supernatant at 100 000xg finally results in microsomal preparation. (Dallner, 1974; Sigma Protocol, 2005)

4.6.3.2. EXPERIMENTAL PROCEDURE

Microsomes (crude EndRet) were easily purified by homogenization of cultured cells and subsequent differential centrifugation following Sigma protocol for EndRet isolation with modifications (Sigma Protocol, 2005). After treatment with compounds cells grown in 60 mm-diameter petri dishes were washed twice with ice-cold PBS, and were then manually scraped into a microtube with 1 mL PBS. All steps were conducted on ice. The suspension was centrifuged (600xg, 5 min, 4°C). A volume of 500 µL sucrose solution 0.25 M, termed Isotonic Extraction Buffer (IEB 1x), containing 0.1% protease inhibitor cocktail was added to the supernatant. IEB 1x was prepared just before use and protease inhibitor cocktail containing selected protease and phosphatase inhibitors was added to prevent degradation of proteins in the cell extract. Cells were homogenized using a needle homogenizer (10 s.). All fractionation and homogenization procedures were performed in IEB 1x, since liver microsomal vesicle is completely permeable to sucrose thus having a less damaging effect on microsomal vesicles than many other suspension media under the conditions of ultracentrifugation (Dallner, 1974). The obtained homogenate was centri-

fuged at 1000xg for 10 min at 4°C and the resultant supernatants were then centrifuged at 12 000xg for 15 min at 4°C. The post mitochondrial supernatant was transferred to a special ultracentrifugation tube and subjected to ultracentrifugation (100 000xg, 60 min, 4°C). The crude pelleted ER was resuspended in 30-40 µL natrium phosphate buffer (50 mM, pH 7.6) with the help of a needle sonicator. The microsomes were stored at -80°C until further use. Protein concentrations for each sample of microsomes were determined using the Bradford method (1976) (see section 4.5.5).

4.6.4. PREPARATION OF CELL HOMOGENATES

Whole cell extracts were prepared for nuclear receptor protein analysis. Cells were washed twice with ice-cold PBS and were resuspended in 200 µL lysis buffer by scraping cells off manually and transferring them to a 1.5 mL microcentrifuge tube. Cells were incubated on ice for 30 min and homogenized using a needle sonicator (10 s). Cellular debris was pelleted by centrifugation (12 000x*g*, 30 min, 4°C). The supernatants were used for determination of protein by Bradford method (see section 4.5.5) and stored at -80°C.

4.6.5. SEMI-QUANTITATIVE PROTEIN DETERMINATION

4.6.5.1. PRINCIPLE

Western Blot (protein immunoblot) analysis is used to detect specific proteins in samples from whole tissue or cell culture. Homogenized subcellular protein fractions are separated according to their molecular weight shape, or isolectric point using polyacrylamide gel electrophoresis. In order to allow the proteins to migrate through the gel, they are maintained in a denatured state (Laemmli buffer containing strong reducing agent) and charged negatively by adding the anionic detergent sodium dodecyl sulfate (SDS) so that proteins move to the positively charged electrode through the acrylamide mesh of gel. The amount of bound SDS is relative to the size of the protein. After separation of the protein components by electrophoresis they can be transferred to a polyvinylidene fluoride (PVDF) or nitrocellulose membrane. This protein transfer is called blotting, and subsequently proteins bound to membranes can be detected using polyclonal or monoclonal antibodies specific to the protein of interest. The whole procedure of protein transfer and immunodetection of proteins is called Western blotting, contrarily to Southern and Northern blotting techniques, which are used to detect DNA and RNA respectively. (Lottspeich and Engels, 2006)

4.6.5.2. SDS-PAGE AND IMMUNOBLOTTING

Microsomal or homogenate samples were diluted (1/3) with Laemmli loading buffer (3x), mixed, and centrifuged. Denaturated protein samples were carefully loaded into the lanes of the polyacrylamide gels. One lane per gel is reserved for the marker protein, which is a commercially available mixture of proteins with defined molecular weights and staining to allow colored visible bands. The Precision Plus Kaleidoscope Protein standard (Bio-Rad) was mixed with 3x Laemmli loading buffer as described for the samples and provided a 10 band ladder with colored bands ranging from10 kDa up to 250 kDa. Respective resolving (10% acrylamide) and stacking (4% acrylamide) gels were prepared. Before loading of the samples, 1x electrophoresis buffer was poured into the Western blot tank. Denatured protein samples were electrophoretically separated in the polyacrylamide gels at a constant voltage of 90 V until the samples have passed the stacking gel. The voltage was then turned up to 120 V and the sample allowed separating. The run of the pre-stained molecular weight marker is used to determine the endpoint of the electrophoresis (about 1.5 h). After protein separation by SDS polyacrylamide gel electrophoresis (SDS-PAGE) separated proteins on the gels were transferred to a polyvinylidene fluoride (PVDF) membrane using semi-dry blotting technique (Western Blot). Prior to blotting the PVDF membrane was pre-wetted using 100% methanol for 10 min and the filter pads were soaked in blotting buffer. The filterpad sandwich, consisting of two filterpads/membrane/polyacrylamide gel/two filterpads, was assembled and placed into the semi-dry blotting apparatus. Blotting was performed at constant amperage (50 mA per membrane) in the presence of 1x blotting buffer for 90 min. The completeness of the protein transfer could be checked by staining the polyacrylamide gel using amido black solution and a subsequent washing step (about 1 h) in distaining solution. Non-specific binding sites were blocked by incubation of the PVDF membrane with 5% dried milk in tris buffered saline (TBS) supplemented with Tween-20 (TBS-T 1x) in a 50 mL centrifuge tube on a rotating mixer for 1 h (alternatively overnight at 4°C). After three washing steps for 5 min with TBS-T the membranes were incubated with the respective primary antibodies diluted in TBS-T for at least 1.5 h at room temperature (alternatively overnight at 4°C). The antibody was removed and three washing steps (5 min each) were performed with TBS-T. The membrane is then incubated with a horseradish peroxidase (HRP)-labeled secondary antibody (diluted in TBS-T) for up to 1 h at room temperature (details for the use of antibodies see Table 19). The secondary antibodies were removed and membranes were washed three times as described before.

Table 19: List of primary and secondary antibodies and its optimized use conditions for Western Blot analysis.

Primary antibody	Dilution	Incubation	Secondary antibody	Dilution	Incubation	Mol. weight
Rabbit polyclonal anti-CYP1A1 (Santa-Cruz Biotechnology)	1/1000	1.5 h	Goat anti-rabbit IgG-HRP (Santa-Cruz Bio-technology)	1/5000	1 h	56 kDa
Rabbit polyclonal anti-CYP1B1 (Santa-Cruz Biotechnology)	1/1000	1.5 h	Goat anti-rabbit IgG-HRP (Santa-Cruz Bio-technology)	1/5000	1 h	57 kDa
Mouse monoclonal anti-ERalpha (Abcam)	1/500	Overnight, 4°C; 1 h blocking	Goat anti-mouse IgG-HRP (Santa-Cruz Bio-technology)	1/5000	45 min	68 kDa
Rabbit polyclonal anti-CYP2D1 (Milli-pore)	1/1000	1.5 h	Goat anti-rabbit IgG-HRP (Santa-Cruz Bio-technology)	1/2000	1 h	57 kDa

Several attempts were performed to optimize the conditions of the method. The parameters chosen especially to improve detection of human CYP1B1 protein bands were as follows:

- Increasing amounts of microsomal protein sample per lane
- Use of two different first antibodies
- Dilutions of antibody (first and second antibody)
- Incubation time of antibodies
- Blocking time
- Exposure time to luminescence detection
- Different luminescence detection agents

4.6.5.3. CHEMILUMINESCENCE DETECTION

The immobilized protein bands of interest conjugated with horseradish peroxidase were detected using an enhanced chemiluminescence kit (CheLuminate-HRP Pico Detect, AppliChem). The chemiluminescent ready-to-use reagents were prepared just prior to use. A volume of Solution A was mixed in a 1:1 ratio with Solution B (stable H_2O_2 solution). Sufficient solution to cover the membrane was added and equilibrated for at least 5 min. Blots were placed protein side up on the lumi imager (Roche) and light intensity was detected (generally over 5-20 s for CYP1A1, 20-45 s for CYP2D1, 30-60 s for CYP1B1, and 10-15 min for ERalpha). HRP catalyzes the oxidation of luminol in the presence of H_2O_2. The intermediate luminol reaction product is in an excited state decaying to the ground state by emitting light. Enhancers such as phenolic compounds can amplify the light emission (see Figure 34). (AppliChem Product Information, 2002)

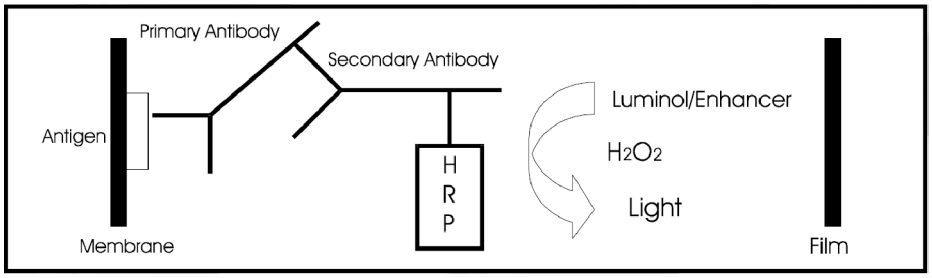

Figure 34: Principle of the protein detection procedure: HRP-linked proteins catalyze the oxidation of luminol in the presence of hydrogen peroxide (H_2O_2) and an enhancer. Oxidized luminol emits light by decaying back to the ground state. (AppliChem Product Information, 2002)

Densitometric analysis was performed using LumiAnalyst 3.1 (Roche) according to Boehringer Light Units (BLU). The densitometric intensity of the bands is related to the bands of the control protein (rat CYP2D1) and normalized against the DMSO solvent control

4.6.5.4. STRIPPING AND REPROBING OF MEMBRANES

Stripping the antibodies from the PVDF membrane allows the reuse of Western Blots for detection of another specific protein e.g. for normalization against a control protein, i.e. CYP2D1 for cells of rat origin to guarantee comparable loading efficiencies.

After the first chemiluminescent detection the membrane was kept in TBS-T buffer to avoid drying of the membrane. Membranes were washed four times for 5 min in TBS-T buffer. Then, it was subjected to 60 mL of the stripping buffer and incubated for 30 min at 50°C. Subsequently, the membrane was washed again in TBS-T (six times for 5 min). The membrane was reused starting at the blocking step following the normal Western blot protocol as described above.

4.6.6. TRANSIENT TRANSFECTION AND LUCIFERASE ACTIVITY

4.6.6.1. PRINCIPLE

Exogenous DNA can be taken up by eukaryotic cells under appropriate conditions. A wide variety of transfection methods have been developed to facilitate this process. Most commonly used transfection techniques include the use of calcium phosphate, liposome fusion, diethylaminoetyhl dextrane (DEAE-dextrane), lipofection, retroviruses, electrophoration, and microinjection. However only a portion of the DNA becomes localized in the nucleus and thus target genes can be expressed for several days (transient transfection). In general, one or two days after transfection process cells are lysed and reporter gene products of the test promotor analyzed. This technique can also be used to obtain stable expression of various genes after inclusion of the expression plasmid into chromosomal DNA. For selection of stably transfected cells the expression vector used has to possess a resistance gene marker expressed in transfected cells. Nevertheless, the spontaneous entry of intact DNA into cells is a highly inefficient process dependent on the size and charge of DNA, and the cell's various enzymatic and membrane barriers. (Felgner et al., 1987; Lottspeich and Engels, 2006)

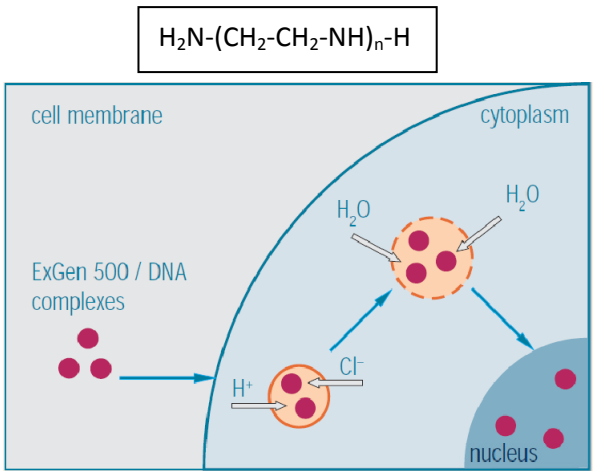

Figure 35: Structure of ExGen 500 B. Mechanism of action: ExGen500/DNA complexes are endocytosed. 'Proton-sponge' effect buffers endosomal pH by proton accumulation and chloride influx. Induced endosomal swelling and rupture leads to DNA translocation. (Ferrari et al., 1997 and Fermentas Brochure, 2007)

ExGen 500 (Fermentas) is a non-viral, non-liposomal, gene delivery transfection reagent. It consists of a linear form of polyethylenimine, a cationic organic polymer that possesses a high cationic charge density potential. Thereby, the reagent can easily condense DNA and deliver genes. In Figure 35 the structure and mechanism of action is illustrated. ExGen500 interacts with DNA and forms stable, highly diffusible complexes which enter the cytoplasm by endocytosis.

Every third atom of the ExGen 500 backbone is a protonable amino nitrogen atom, which makes the polymeric association an effective 'proton sponge'. This property buffers endosomal pH by accumulation of protons and passive chloride influx to the endosome containing the complexes. Subsequent osmotic swelling promotes endo-

somal rupture, allowing translocation of DNA to the nucleus. This 'proton sponge' protects DNA from lysosomal degradation. (Behr, 1996; Ferrari et al., 1997; Fermentas Brochure, 2007)

All transient transfection assays were performed in cooperation with Prof. Marie-Christine Chagnon's laboratory of Food Toxicology at the University of Burgundy in Dijon, France. The effect of exogenous ERalpha on ER- or AHR-mediated signaling following exposure to TCDD and/or E2 was determined using HepG2 cells transiently transfected with hERalpha and an ER- or AhR-responsive luminescent reporter gene. In order to investigate AhR/ER cross talk the transfections were performed with and without hERalpha and additionally selective inhibitors of AhR and ER function were applied. HepG2 cells were transiently transfected using ExGen500 reagent (Fermentas).

4.6.6.2. REPORTER GENES AND EXPRESSION PLASMIDS

Plasmids pRST7-hERalpha and ERE-TK-Luc were kindly provided to the department of Food Toxicology at the University of Burgundy (Dijon, France) by Dr. D. McDonnell (Ligand Pharmaceutical, San Diego, USA). Control plasmids pCMVβ-Gal and pSG5 were kindly provided by Dr. M. Cherkaoui-Malki (LBMC, University of Burgundy, Dijon, France). The pCMVβ-Gal contains the beta-galactosidase gene and is used to check transfection efficiency, whereas pSG5 served as the vector control to obtain the same amount of DNA concentration for each transfection process. The reporter gene plasmid pGL3-XRE-Luc was constructed previously in the laboratory by Dr. J. Racky (Racky et al., 2004). The pGL3-XRE-Luc reporter gene construct contains a 485 bp fragment of the rat CYP1A1 gene including two XREs (Baumgart et al., 2005). The ERE-TK-Luc reporter plasmid contains a single copy of the vitellogenin ERE fused up-stream of the Herpes simplex thymidine kinase (TK) promoter sequence linked to the luciferase (Luc). The pRST7-hERalpha expression plasmid consists of a 1590 bp fragment of the human ERalpha-encoding sequence. (Tzukerman et al., 1994).

4.6.6.3. EXPERIMENTAL PROCEDURE

For transient transfection assays HepG2 cells were seeded in 24-well plates and maintained in DMEM medium w/o PR supplemented with 10% dextrane-coated charcoal fetal bovine serum (DCC-FBS). Cells were allowed to attach for 24 h. Each plasmid was diluted in 0.15 M NaCl to a final concentration of 100 ng/µL. First, plasmid mixes were prepared as follows: 100 ng ERE-TK-Luc or XRE-Luc, 100 ng hERalpha, 100 ng pCMVβ-Gal, and pSG5 to a final concentration of 0.5 µg DNA. For transfections when hERalpha was omitted, the amount of pSG5 was adjusted to 0.5 µg DNA accordingly. Plasmid mixes were vortexed gently and 2 µl/well of Exgen500 diluted in NaCl 0.15 M (1/7.5) was added to DNA. After

vortexing the microtubes were incubated for 10 min at room temperature. The Ex-gen500/DNA mixture was then added to 9 volumes of Opti-MEM medium without phenol red (Invitrogen) and pipetted to the wells (300 µL/well). In order to achieve even distribution of the complexes, the plate is gently moved back and forth and from side to side. The microplate was then incubated at 37°C in a humidified atmosphere of 5% CO_2 for 1 h. (Cabaton et al., 2009; Fermentas, 2004)

After incubation with transfection reagents and plasmids, Opti-MEM was removed and replaced by 1 mL/well fresh DMEM medium (w/o DCC-FBS) containing the test substances or the solvent DMSO (max. 0.2%, negative control). E2 10 nM and TCDD 1 nM served as the positive control for ERE- and XRE-mediated luciferase activity respectively. At the end of the 20 h treatment medium was aspirated, the wells rinsed with PBS, and cells lysed using 100 µL/well Reporter Lysis Buffer 1x (Promega). The microplate was then frozen at -80°C for at least 30 min. After thawing attached cells were scraped from the wells and transferred into microtubes. To ensure complete cell lysis cells were submitted to three sequential freezing-thawing cycles in liquid nitrogen and at 37°C. Microtubes were centrifuged (5 min, 10 000xg, room temperature) and the supernatant used for further analysis. Centrifuged cell lysates were stored at -80°C. (Promega, 2006)

For determination of luciferase activity 10 µL of the lysate were pipetted into an opaque white 96-well plate. A volume of 50 µL luciferase assay reagent (Promega) was added to each well. The plate is covered with an adhesive seal and immediately read in a microplate luminometer (TopCountNT, Packard).

The β-galactosidase activity was determined using chlorophenol-red β-D-galactopyranoside (CPRG) (Roche). The cell lysate (10 µL/well) was mixed with 190 µL of the colored yellow dye in a 96-well plate and the chlorophenol red product was measured with a microplate spectrophotometer at 570 nm (MRX Dynex) after 10-15 min. Protein absorbance was measured using 2 µL of the lysate and 198 µL of Bradford reagent 1x according to the Bradford method (see section 4.5.5) on a spectrophotometer at 595 nm (MRX Dynex). (Bradford, 1976). Luciferase activity was normalized against β-galactosidase activity and protein contents, and related to the respective DMSO control.

4.7. GENOTOXICITY

4.7.1. FPG-SENSITIVE COMET ASSAY

4.7.1.1. PRINCIPLE

The comet assay, also known as single-cell gel electrophoresis assay (SCGE assay), was first introduced by Östling and Johanson (1984) and is nowadays one of the standard methods for assessing DNA damage and other DNA alterations at the level of a single cell. Among short-term genotoxicity assays the comet assays is a very simple, sensitive, and inexpensive method, used in many research areas such as human and environmental biomonitoring, DNA repair, and genetic toxicology. Another great advantage is that theoretically any eukaryote cell can be used for genotoxicity testing in the SCGE assay. Moreover, cell lines (proliferating cells) as well as primary cells (non-proliferating cells) can be used. However, non-proliferating cells may be less affected to false positive responses associated with agents that interfere with DNA synthesis. (Tice et al., 2000)

The assay works upon the principle that negatively charged broken DNA migrates in an electric field towards the anode as a result of relaxation of DNA supercoils at the breakage site, whereas undamaged DNA migrates slower and remains within the nucleoid when a current is applied. Intact DNA lacks free ends and the large size of the fragments prevents migration. (Olive and Banath, 2006)
The assay owes its name due to the resulting structures of the DNA from an individual resembling comet (Olive, 1989). The comet head contains the high-molecular-weight DNA and the comet tail contains the leading ends of migrating fragments, which can be measured using special software in order to determine the extent of DNA damage (Olive et al., 1990). For the procedure cells are embedded in agarose on an agarose-precoated microscope slide and are lysed with detergent and high salt removing cell contents leaving the nuclear material. Immobilized cells are treated with alkali buffer to unwind and denature the DNA and are then submitted to electrophoresis, during which the comets are formed. After neutralization the migrating DNA is quantified by staining with a fluorescent intercalating dye and by measuring the intensity of fluorescence with a microscope. (Singh et al., 1988)

Under alkaline conditions increased DNA migration is associated with increased levels of single-strand breaks (SSBs) and double-strand breaks (DSBs), as well as alkali labile sites (ALS) (Tice et al., 2000). ALS are apurinic or apyrimidinic sites, that can be converted into strand breaks. DNA strand breaks may either appear directly as an effect of a DNA-damaging agent or occur as intermediates during nucleotide and base excision repair

processes. (Collins, 2004). In addition to that, also interstrand cross-links can be identified in the comet assay leading to less electrophoretic migration instead of more (Merk and Speit, 1999).

As an additional step the repair enzyme FPG was employed for the detection of oxidative DNA base damage, in particular 8-OH guanine, but also other damaged purines. Strictly taken, the difference of DNA fragmentation introduced following FPG treatment of the cells and the damage that occurred without applying the repair enzyme represents the amount of a specific class of DNA damage which is due to the enzyme's action.

4.7.1.2. COMET SCORING

Comet data are generally collected using image analysis techniques on individual cells. Several software programs are available in order to quantify DNA migration. The simplest method for collecting comet data is based on determining the proportion of cells with altered migration.

Several parameters for image interpretation exist. 'Tail migration' considers the length of migration. Another metric used more frequently is based on the percentage of migrated DNA. 'Tail intensity' is the amount of DNA that moved during electrophoresis. The concept of 'tail moment' (product of tail length and intensity) was introduced by Olive and colleagues (1990) and takes those two effects into account.

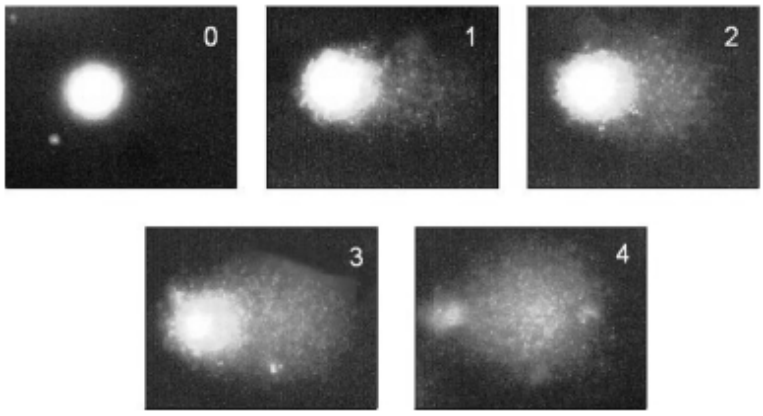

Figure 36: Images of comets (from lymphocytes), representing classes 0-4 as used for visual scoring (according to Collins, 2004).

It is also possible to characterize comets without sophisticated image analysis programs by classifying them into several categories (generally five classes) based on the length of migration and/or the perceived relative proportion of the DNA in the tail (Gedik et al., 1992; Anderson et al., 1994). The human eye can easily be trained to discriminate between different degrees of damage. A numerical value is assigned for each migration class. Figure 36 shows the different kinds of comet categories ranging from 0 (no tail) to 4 (almost all DNA in tail) used for visual scoring. (Collins, 2004)

4.7.1.3. EXPERIMENTAL PROCEDURE

DNA strand breaks were analyzed by the comet assay as described by Valentin-Severin and co-workers (2003). The inclusion of the digestion step with the bacterial enzyme formamidopyrimidine glycosylase (FPG, purchased from A. Collins) was performed according to Schaefer et al. (2006).

For the preparation of agarose-precoated slides 0.5% LMPA (low melting point agarose) and 1.0% NMPA (normal melting point agarose) were heated in the microwave until the agarose dissolved. NMP agarose was kept hot at 80°C in a water bath. Fully frosted slides were dipped into the NMPA solution and the underside was wiped clean. Slides were labeled prior to dipping using a diamond-tipped pen. NMPA-layered slides were air-dried on a flat surface and kept at room temperature until needed. Before starting the experiment the bottle with LMP agarose was equilibrated at 40°C in a water bath.

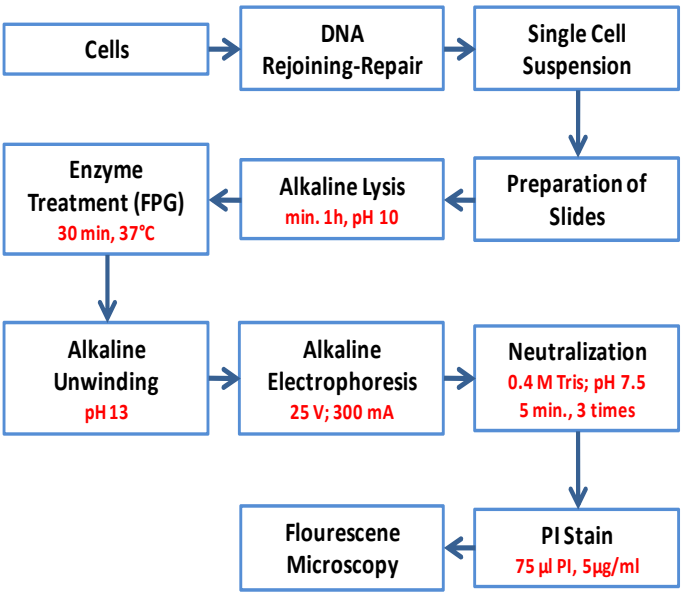

Figure 37: Flowchart of the basic steps of the comet assay (according to Comet Assay Forum, 2009; Tice et al, 2000).

After the treatment of cells in 6-well plates (primary rat hepatocytes or hepatoma cell lines) or 96-well plates (hepatoma cell lines) (see section 4.4.5) cells were rinsed twice with PBS and trypsinated. DMEM (10% FBS) was added (500 µL /well) to stop cell detachment. The cells were gently removed. Using a hemocytometer, cell density was adjusted to about 7 ×10^4 cells per gel and the adequate volume of cell suspension was transferred to a 2.0 mL microtube in a total volume of 1 mL serum-containing DMEM. Cells were centrifuged (5 min, 200 xg) and the pellet was resuspended in PBS (50 µL/slide) and kept on ice to inhibit endogenous damage occurring during sample preparation and repair of the unfixed cells. PBS must be calcium- and magnesium-free to inhibit endonuclease activities. Aliquots of 50 µL of the PBS cell suspension were rapidly mixed with 65 µL of LMPA 0.7% (37°C), and 68 µL of this mixture were pipetted to the coated slide avoiding bubbles and covered with a coverslip. The slides were placed at 4°C for 5 min until the agarose layer hardened.

Coverslips were removed and slides submerged in a coplin jar containing freshly prepared lysis solution (pH 10) and were lysed for at least one hour or overnight at 4°C to liberate DNA. Subsequently, slides were washed three times for 5 min in cold FPG enzyme buffer (1x) at 4°C. After the last washing step slides were put on a slide porter on ice and FPG solution (300x diluted) or enzyme buffer (1x) alone as the control (50 µl/gel and two gels per treatment) was gently pipetted on the slides. Incubation with the FPG enzyme was optimized at 37°C for 30 min. Slides were put on a stand in a water bath. Following FPG treatment coverslips were gently removed and slides were placed horizontally in an electrophoresis chamber that was put on ice. Directly, slides were exposed to alkaline denaturation buffer (pH 13).The high pH allows unwinding of the DNA (20 min), DNA single-strands are formed. Electrophoresis was conducted keeping the electrophoresis solution in the chamber for 20 min at 300 mA (25 mV constant).

Slides were removed from electrophoresis chamber and neutralization was achieved by rinsing 3 times for 5 min with cold neutralization buffer (Tris buffer 0.4 M, pH 7.5). Hence, DNA double-strands are formed again. In addition to that, the washing steps remove alkali which might interfere with the staining step. For conservation of DNA slides were rinsed gently with cold ethanol (96%) and can thus be stored in a box at room temperature until staining.

DNA was stained with 40 µL/ gel of propidium iodide (PI) solution (5 mg/L). Fifty individual comets per slide and two slides per concentration were evaluated under a fluorescence microscope and analyzed using computerized image analysis system Comet IV (Perceptive Instruments). The Olive tail moment (OTM) was chosen to characterise the DNA damage in individual cells.

4.7.2. UNSCHEDULED DNA SYNTHESIS (UDS)

The UDS assay was performed in Prof. Marie-Christine Chagnon's laboratory of Food Toxicology at the University of Burgundy in Dijon, France.

4.7.2.1. PRINCIPLE

A good approach to assess genotoxicity is the indirect measurement of DNA damage by monitoring DNA repair activity. Quantification of Unscheduled DNA synthesis (UDS) indicates DNA repair synthesis in mammalian cells after excision and removal of the part of the DNA strand containing the region of damage induced by a chemical or by physical agents. The assay is based on the incorporation of tritium-labeled thymidine ([3H]-thymidine) into the DNA of mammalian cells which are not undergoing replicative (scheduled) DNA synthesis. The uptake of [3H]-thymidine can be determined by autoradiogra-

phy (AR) or by liquid scintillation counting (LSC) of DNA from treated cells. (OECD-Guideline, 1986; Madle et al., 1994)

UDS detection is highly suitable for mutagenicity testing, since the repair of DNA by excision repair mechanisms (base excision repair and nucleotide excision repair) over the entire mammalian genome is measured (Mitchell et al., 1983).

Routinely, UDS is measured by AR and cells undergoing repair are identified by increases in the number of silver grains overlying the nuclei. In addition to that, AR analysis permits to identify dead and abnormal cells and permits the distinction between grains occurring over the nucleus and over the cytoplasm. (Madle et al., 1994)
In order to discriminate between UDS and normal semi-conservative DNA replication in the LSC-based UDS method, scheduled DNA replication is reduced or inhibited by exposing cultured cells to hydroxyurea (HU) (OECD-Guideline, 1986). HU depletes the pools of dNTP by inactivating ribonucleotide reductase. Thus, the enzyme responsible for the deoxyribonucleotide biosynthesis needed for scheduled DNA synthesis was inhibited. (Skoog and Nordenskjöld, 1971; Thelander and Reichard, 1979) Primary cultures (e.g. rat hepatocytes) as well established cell lines can be used in the assay. In general terms, hepatocytes are recommended for UDS testing, as they exhibit appropriate metabolism, and the liver is often a prime target in rodent bioassays. Permanent cell lines and cells from tissues other than liver may be useful for specific investigations. (Madle et al., 1994)

4.7.2.2. EXPERIMENTAL PROCEDURE

The detection of unscheduled DNA synthesis was performed *in vitro* using the LSC-based method according to the protocol of Valentin-Severin (2002). HepG2 and H4IIE cells were seeded in 96-well plates and rat hepatocytes in 25 cm^2 cell culture flasks (see section 4.4.5). After 16 h treatment time hepatoma cell lines were pre-treated with hydroxyurea (10 mM) in DMEM 0.5% FBS for 1 h in order to inhibit residual scheduled DNA synthesis. Subsequently, test compounds were (re)-added to the cells together with [3H]-thymidine (5 µCi/mL) in the presence of HU for another 4 h. In the case of practically non-proliferating rat hepatocytes, incubation with HU was omitted and simultaneous exposure of cultures to the test chemicals in the presence of [3H]-thymidine was performed. A detailed treatment schedule for UDS assay using cell lines (20 h or 4 h treatment) or rat hepatocytes (20 h treatment) is shown in Figure 38.

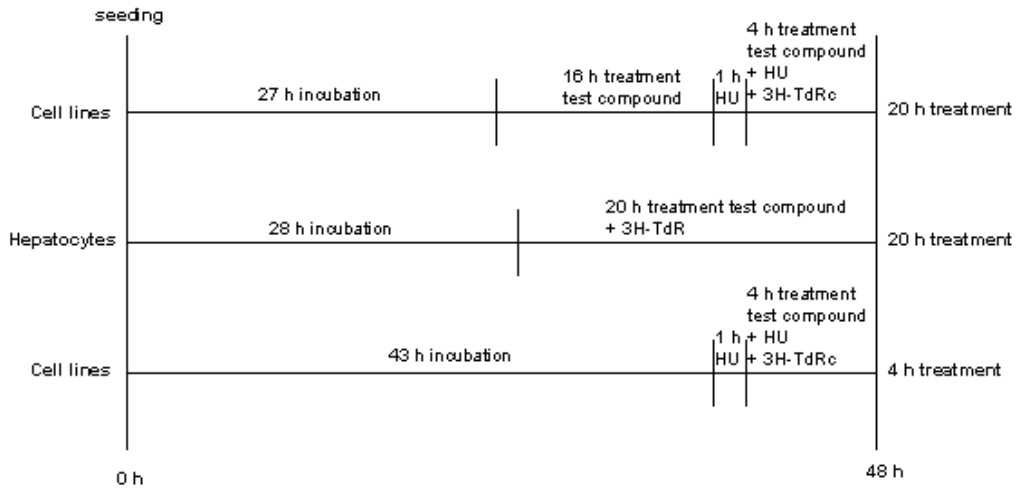

Figure 38: Treatment schedule for UDS assay using cell lines and rat hepatocytes for 20 h or 4 h treatment time with test compounds (according to Valentin et al., 2001).

Treatment with the known mutagens 4-nitroquinoline-N-oxide (NQO), methyl methanesulfonate (MMS), or 2-acetylaminofluorence (2-AAF) for 4 h or 20 h served as the positive controls. At the end of the incubation time cells were washed twice with PBS. Afterwards, the cells were lysed with lysis buffer (100 µL/well, 1 mL/25cm^2 flask) for 10 min at 37°C on a shaker. Cell lysates of cell lines were straightly processed. In contrary to that, hepatocytes were first put at - 20°C overnight, because detached collagene from the flasks rendered lysates too viscous for direct pipetting. Lysed samples (100 µL/well for cell lines, 125 µL/well for hepatocyte) were transferred to a 96-well microplate equipped with GF/C glass filters (Whatman) prewetted with 100 µL/well of cold trichloroacetic acid (TCA, 20%). Another 100 µL/well of TCA was then added in order to optimize precipitation of nucleic acids and proteins on the filter. The mixture of TCA with cell lysates was incubated 10 min and samples were then filtered with the help of a water-jet vacuum pump system (Millipore) and washed twice with cold ethanol (96%, 300 µL/well). The plates were air-dried overnight or put for 1 h at 50 °C in an incubator. For LSC a back seal was glued under the microplate. Scintillator liquid (30 µL/well) was added, the plate covered with a top seal, and the scoring was carried out directly in a microplate scintillation counter (TopCountNT, Packard). The radioactivity on the filter represents the quantity of incorporated radioactive thymidine in the cells. An increase in the incorporation of [3H]-thymidine over control levels (solvent control treated with HU) indicated the induction of UDS. Results were expressed as cpm values. A no-HU control was always performed in parallel when using continuous cell lines in order to assess the inhibition rate of scheduled DNA synthesis. For every treatment and independent experiment at least 8 replicates were prepared.

4.7.3. FPG-SENSITIVE ALKALINE ELUTION TECHNIQUE IN MOUSE HEPATOCYTES

4.7.3.1. PRINCIPLE

Quantification of DNA modifications sensitive to FPG protein from E.coli was carried out following the protocol of the alkaline elution assay according to Kohn et al. (1976) with modifications as described by Pflaum and collegues (1997) and Epe and Hegler (1994). The alkaline elution technique is a very sensitive *in vitro* method to quantify intracellular DNA damage, in particular single-strand breaks, DNA-DNA, and DNA-protein cross-links. In combination with various repair endonucleases such as FPG protein, alkaline elution can be used to quantify steady-state levels of oxidative base modifications in various types of mammalian cells. For this purpose prior to elution, the isolated DNA is incubated with specific repair endonucleases that recognize base modifications and incise DNA at specific sites generating additional single-strand breaks. The detection limit of the alkaline elution assay corresponds to 0.05 lesions per 10^6 base pairs. (Pflaum et al., 1997) Following the experimental procedure cells were lysed on a polycarbonate filter with the help of alkaline lysis buffer containing SDS and Proteinase K. Thereby, cell constituents, cellular proteins, and RNA are washed off the filter retaining double-stranded DNA on it. After washing the DNA in order to get rid of the rests of lysis buffer, incubation with repair endonuclease can be performed. Subsequently, double-stranded DNA is converted into single-strands with elution buffer (pH 12.15), which starts elution. Dependent on the molecule size DNA fragments pass the polycarbonate filter. Short DNA pieces elute more rapidly than big ones, the latter representing less damaged DNA fragments. The eluted DNA content and the amount of DNA retained on the filter is quantified fluorimetrically after neutralization by bisbenzimide (Hoechst 33258). The elution rate is directly proportional to the number of single-strand breaks and alkali-labile lesions of DNA and is calculated accordingly. For calibration, X-rays are used as reference damage, assuming that a dose of 6 Gy generates 1 single-strand break per 106 bp. (Kohn et al., 1976).

4.7.3.2. EXPERIMENTAL PROCEDURE

For each experiment a 25 mL syringe was equipped with a polycarbonate filter. Cell suspension and buffers were pipetted directly on the polycarbonate filter. The solutions were passed through the syringe and filter by means of multichannel pump, and flows into a trash bin. During elution fractions were collected. Polycarbonate filters were carefully filled with distilled H_2O to avoid air bubbles, and washed twice with 2.5 mL of PBS CMF (Ca^{2+}- and Mg^{2+}-free). Filter systems were equilibrated at 4°C in a water bath. Low temperature avoids repair of DNA damage during processing of the samples. A total

number of 0.5 × 10^6 fresh isolated mouse hepatocytes (protocol of isolation of mouse hepatocytes and animal treatment is described in section 4.3.2) were applied to a polycarbonate filter (25 mm diameter, 2 µM pore size). After washing twice with 5 mL PBS CMF the temperature of the water bath was raised to 25°C. Cells were lysed by first pumping 2 mL of lysis solution through the filter at the maximum capacity and then another 5 mL of lysis buffer containing proteinase K (concentration of 0.4 mg/mL) within 90 min. After lysis the temperature was adjusted to 37°C. Subsequent to seven washing step with 25 mL buffer BE_1, the DNA remaining on the filter was incubated with 2 mL of freshly prepared repair endonuclease solution(1 µg/mL FPG protein in BE_1/BSA buffer) for 50 min at 37°C. The incision by the enzyme at sensitive DNA modifications was shown to be completed under these conditions. Quantification of direct strand breaks was determined in parallel in experiments without glycosylase treatment using 2 mL enzyme buffer without BSA. The first mL was pumped through the filter system at maximum capacity. Enzyme residues were rinsed off first with BE_1 buffer (2x 5 mL), then with washing buffer (4 mL). During the washing steps the temperature of the water bath was dropped to 25°C. Alkaline elution buffer (25 mL/filter) was pipetted on the filters and elution was started at 1.9 mL/h for 12 h. Fractions of approximately 3.8 mL were collected every 2 h and 6 fractions were obtained. The supernatant of elution buffer that remained on the filters at the end of elution was pumped through the filter and added to the sixth fraction. Filter and frit were pooled together with the sixth fraction in a Coulter Counter™-tube and incubated under continuous shaking for 2 h at 60°C in a water bath. Therewith, DNA retained on the filters was dissolved. Eluted DNA was neutralized by adding equal amounts (3.8 mL) of phosphate buffer pH 6.0 for 15 min in order to obtain double-stranded DNA. The same volume of phosphate buffer pH 7.2/bisbenzimide (1.5 µM, Hoechst No. 33258) was added and incubated again for 15 min in the dark. Emission intensity of the bisbenzimide-DNA complex of each sample was measured in the fluorimeter (excitation at 360 nm; emission at 450 nm). The blank represents a mixture of elution buffer, phosphate buffer pH 6.0, and phosphate buffer pH 7.2/bisbenzimide (each 3.8 mL). The calculations are based on the fact, that the sum of fluorescence intensities of the single fractions of one sample is proportional to the total amount of DNA of this sample. The amount of DNA of the single fraction in a half-logarithmic scale was displayed in accordance to the time course in a half-logarithmic diagram. The slope of the resulting curve was proportional to the number of single-strand breaks. The numbers of modifications per 10^6 bp were obtained from the slopes of the elution curves.

4.8. STATISTICAL ANALYSIS

Statistical Analysis was performed using Graph Pad Prism Version 4.0. Results were expressed as mean ± standard deviation (SD) from at least three independent experiments. The difference between the control and the treatment or between different treatments was determined using unpaired t-test two-tailed p value attained statistical significance with at least $p \leq 0.05$. The One-way ANOVA with Dunnett's post test was performed with the Alamar Blue assay. Throughout the Results chapter (section 5) only significant effects are assigned one or more asterisks (*$p \leq 0.05$; **$p \leq 0.01$; ***$p \leq 0.001$).

4.9. SOFTWARE

Table 20: Software used for analysis.

Software	**Distributor**
Microsoft Office XP (Excel, Word, Power Point)	Microsoft Corporation
Nanodrop ND-1000, Version 3.1.0	Nanodrop
Ascent Software for Fluoroscan 2.6 FL	Thermo Fisher Scientific
iCycler IQ, Version 3.1	Bio-Rad
Graph Pad Prism, Version 4.00	Graph Pad Software
Comet Assay IV	Perceptive Instruments
ACD/ChemSketch (Freeware), Version 11.02	ACD/Labs

5. RESULTS

5.1. OPTIMIZATION OF CELL CULTURE CONDITIONS IN HEPATOMA CELL LINES

Before starting with experiments and the assessment of CYP 450 induction *in vitro* using hepatoma cell lines and primary rat hepatocytes, optimal cell culture conditions for the different treatments with the estrogen E2 and the dioxin prototype substance TCDD had to be established.

An initial series of experiments was undertaken to determine the appropriate cell culture conditions for CYP 450 expression. Therefore, CYP1A enzyme activities of hepatoma cells grown in Dulbecco's modified Eagle's medium (DMEM) (i.e. standard culture medium for hepatoma cell lines and primary rat hepatocytes in the laboratory) were compared with cells grown in minimum essential medium (MEM). Additionally, the presence of FBS in the media during treatment with the test compounds was considered. Both supplementation with 10% FBS and reduced serum concentrations (0.5% FBS) were utilized. In all cases, media without addition of phenol red were used to prevent interference with effects by the steroid E2. CYP1A activity was measured in intact cultured cells using the EROD assay according to Donato et al. (1993) following protein quantification with the fluorescamine assay as described in the Material and Methods section. Cells were treated with TCDD (1 nM) or E2 (100 nM) over a period of 48 h.

5.1.1. INFLUENCE OF CULTURE MEDIUM AND SERUM SUPPLEMENTATION ON EROD ACTIVITY

5.1.1.1. HEPG2

In order to determine whether CYP1A drug metabolizing enzyme activity is modified by different growth media or by the presence of FBS in the media during treatment with test compounds, different culture conditions were tested.

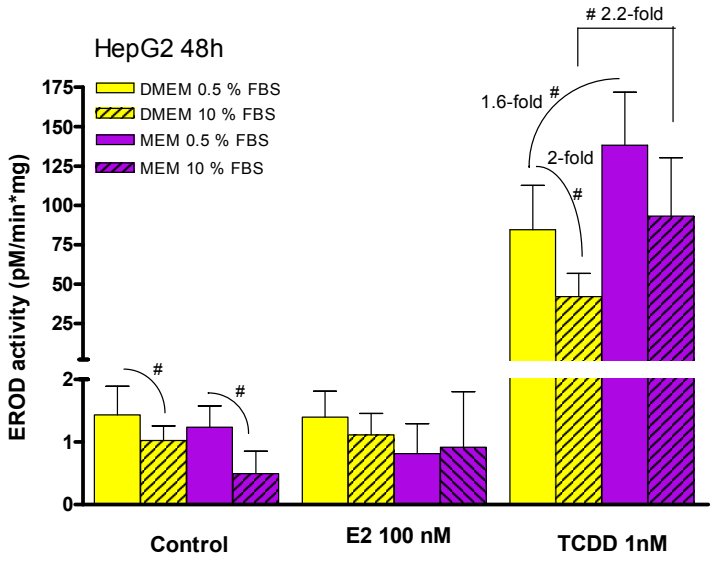

Figure 39: EROD activity measured in HepG2 cells cultured in different media (DMEM and MEM without phenol red) and treated with TCDD and E2 under different serum conditions (0.5% and 10% FBS) for 48 h. DMSO (0.25%) served as the solvent control. Mean ± SD; n ≥ 3. Unpaired t-test, two-tailed p value: statistically different from indicated treatment #p ≤ 0.05.

It can be seen in Figure 39 that HepG2 cells showed higher EROD activities induced by TCDD after 48 h treatment in culture medium with reduced FBS concentration (only 0.5%) compared to 10% FBS. TCDD resulted in a statistically significant 2-fold higher induction in DMEM medium with 0.5% FBS. This effect was only seen as a trend in MEM. Concomitant to induced EROD activities, also basal, i.e. solvent control EROD activities, were significantly higher when cells were cultured for 48 h in 0.5% FBS.

Furthermore, it was tested whether CYP1A enzyme activity could be modified by different growth media. The enzyme activity of cells grown in DMEM was compared with those of cells grown in MEM, i.e. two commonly used culture media for HepG2 cell line. Cells grown in DMEM generally showed lower induced EROD activities, while the cell culture in MEM resulted in significantly higher TCDD-mediated EROD levels (1.6-fold and 2.2-fold) for cells treated either under reduced FBS or high FBS conditions. However, basal enzyme activities were not influenced by the culture media. Estradiol had no effect that could be ascribed either to FBS concentration or to different culture media.

5.1.1.2. H4IIE

The effects of different growth media and FBS supplementation in rat H4IIE cell line are presented in Figure 40. Increased EROD activities following exposure to TCDD 1 nM for 48 h were lower when cultured in DMEM than in MEM at high FBS concentrations, but the effect marginally failed to be statistically confirmed. MEM medium conveyed 1.8-fold higher TCDD-induced EROD activity at reduced FBS concentration, but the experiment was only carried out once. Nevertheless, these results support favorable increasing effects of induced EROD activity levels by MEM. These observations were similar to those in HepG2 cells (see Figure 39). Different media had no effect on basal enzyme activity. Exposure to the solvent or E2 100 nM resulted in significantly higher EROD activities when grown in DMEM at 0.5% FBS compared with the culture medium at 10% FBS supplementation.

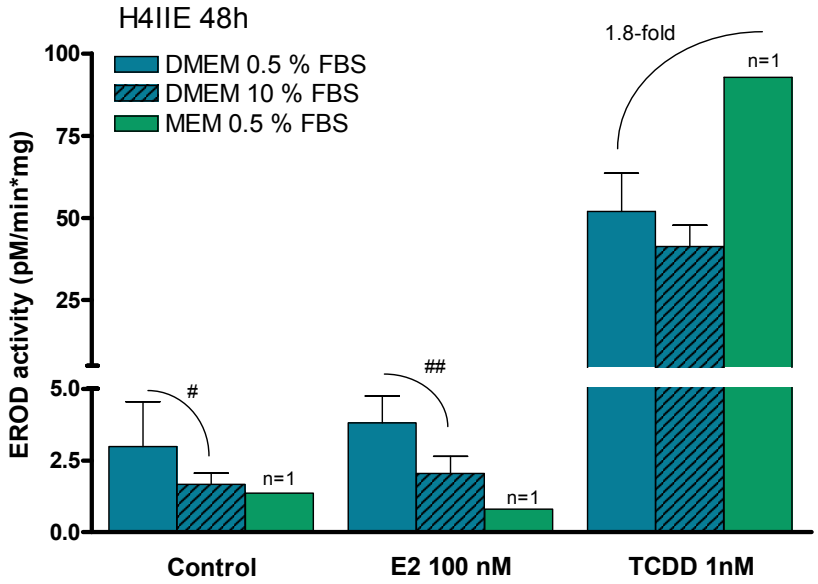

Figure 40: EROD activity measured in H4IIE cells cultured in different media (DMEM or MEM without phenol red) and treated with TCDD or E2 under different serum conditions (0.5% or 10% FBS) for 48 h. DMSO (0.25%) served as the solvent control. Mean ± SD. n ≥ 3 if not indicated otherwise above the bar. Unpaired t-test, two-tailed p value: statistically different from indicated treatment #p ≤ 0.05, ##p ≤ 0.01.

5.1.2. ADOPTION OF OPTIMIZED CELL CULTURE CONDITIONS

EROD activity could be significantly enhanced when cells were treated in MEM medium. However, reduced serum conditions during treatments (0.5%) did not only lead to higher

induced (by TCDD) but also higher basal EROD activities. Different growth media had no influence on basal EROD levels.

Cell cultures in DMEM showed lower induced CYP1A activity. However, for further experiments presented in this work, all treatments with the test compounds were carried out using DMEM as the standard media at 0.5% of FBS. DMEM was kept as the established standard medium for hepatoma cell lines and rat hepatocytes in the laboratory. Exclusively, culture medium without the addition of phenol red was used in order to exclude, that possible estradiol-dependent effects may be overlapped. It was assumed that optimized culture conditions during treatmentsin hepatoma cell lines can be bridged for culturing primary rat hepatocytes.

5.2. CYTOTOXICITY TESTING

In order to determine if the test substances induce a cytotoxic response, the viability of HepG2 and H4IIE cells and rat primary hepatocytes following exposure to TCDD and/or E2 for 20 and 48 h were investigated in initial experiments. Additionally, the effects of the two main estradiol metabolites 2-and 4-hydroxyestradiol on cytotoxicity following 20 h treatment were tested. For this purpose, the resazurin reduction assay, also known as the Alamar Blue assay, was performed aiming to define non-cytotoxic concentrations that can be used for subsequent testing. Cell culture conditions for the treatments were adopted as described in the preceding chapter.

5.2.1. CONCENTRATION-DEPENDENT EFFECTS BY TCDD AFTER 20 H AND 48 H

Figure 41 shows the influence of TCDD on HepG2 cells and primary rat hepatocytes isolated from male rats, which were exposed to concentrations ranging from 0.001 nM to 10 nM for 20 h and 48 h.

In HepG2 cell line there were no concentration-dependent effects observed at 20 h. When considering the standard deviations, cell viability ranged from 87.2% to 91.4% of the solvent control (EtOH 0.1%). At 48 h a significant reduction of cell viability was observed starting at concentrations greater than 0.1 nM. The decrease was most prominent at the highest concentration tested (10 nM: 74.0 ± 5.6%).

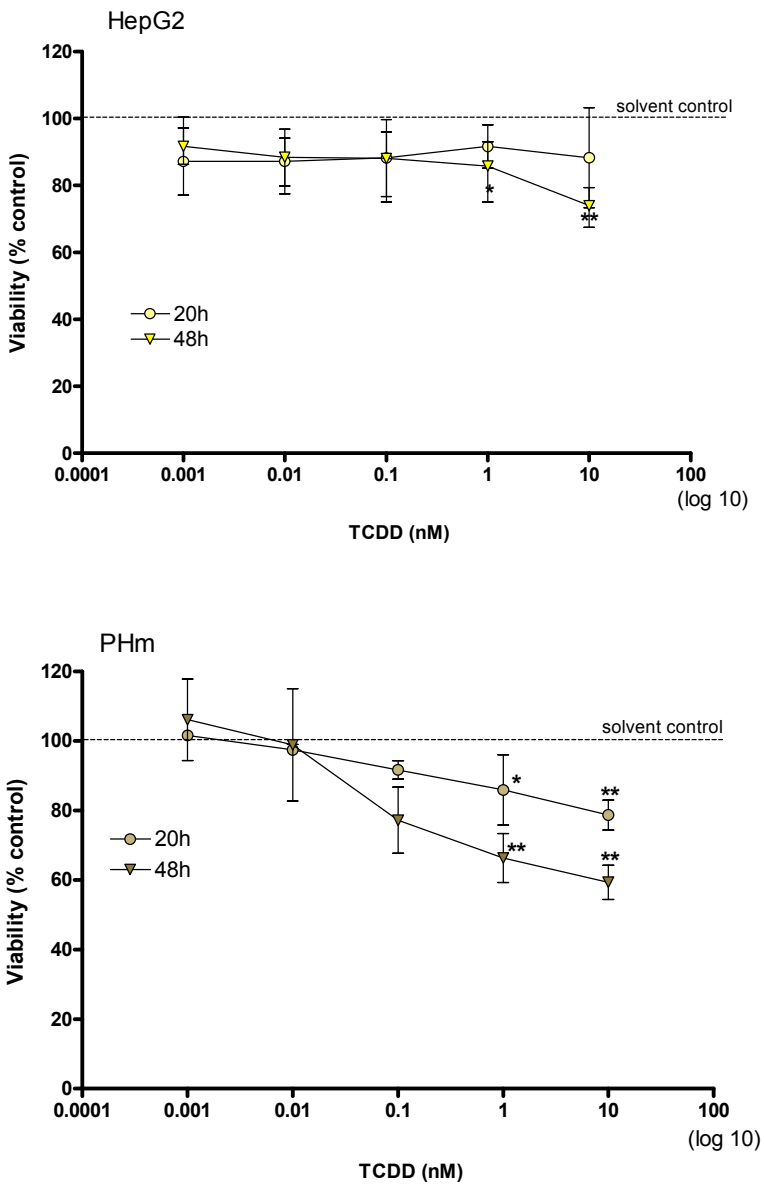

*Figure 41: Cytotoxicity assay (resazurin reduction test) in HepG2 and primary hepatocytes from male (PHm) Wistar rats after exposure to various concentrations of TCDD ranging from 0.001 to 10 nM for 20 h and 48 h. Cells were treated in phenol red-free DMEM culture medium at reduced FBS concentration (0.5%). Results are normalized to the respective solvent control (EtOH 0.1%) which was set at 100%. The horizontal dashed line represents the solvent control level. Mean ± SD; n ≥ 3; One-way ANOVA with Dunnett's post test: significantly different from time-matched solvent control *p ≤ 0.05, **p ≤ 0.01*

At both treatment times, primary hepatocytes from male rats showed a concentration-dependent decrease in the number of viable cells with increasing concentrations starting at 0.1 nM onwards. Treatments with TCDD 1 nM and 10 nM significantly reduced cell viability leading to about 80% of control at the highest concentration at 20 h. This effect was even more prominent after 48 h treatment reaching approximately 60% of control.

Even though treatments with TCDD 1 nM and 10 nM affected cell viability in HepG2 and PHm cells, it never fell below 60% at both treatment times.

5.2.2. CONCENTRATION-DEPENDENT EFFECTS BY E2 AFTER 20 H AND 48 H

Concentration- and time-dependent effects of estradiol were investigated in HepG2 cell line and PHm. Therefore, estradiol was tested at concentrations ranging from 0.01 to 20 µM (Figure 42).

In HepG2 cell line cell viability was not altered by E2 at low concentrations up to 100 nM. A slight decrease was obtained at 1 µM, which was significantly confirmed only at 20 h. At concentrations above 1 µM cell viability further decreased in a concentration-dependent manner. E2 20 µM extensively reduced cell growth to 60.1 ± 26.9% and 39.4 ± 13.5% at 20 h and 48 h respectively indicating a cytotoxic effect, which was more pronounced at the longer treatment time.

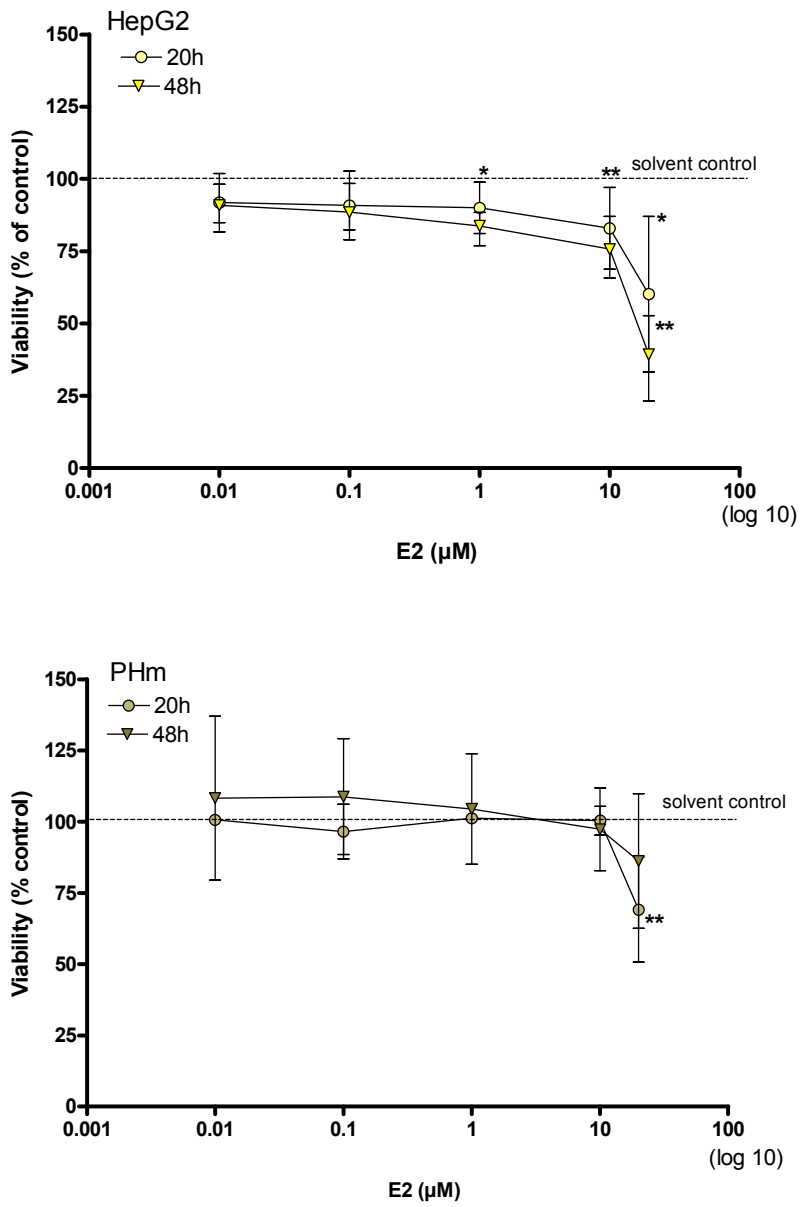

*Figure 42: Cytotoxicity assay (resazurin reduction test) in HepG2 and primary hepatocytes from male (PHm) Wistar rats after exposure to various concentrations of E2 ranging from 0.01 to 20 µM for 20 h and 48 h. Cells were treated in phenol red-free DMEM culture medium at reduced FBS concentration (0.5%). Results were normalized to the respective solvent control (EtOH 0.1%) which was set at 100%. The horizontal dashed line represents the solvent control level. Mean ± SD; n ≥ 3; One-way ANOVA with Dunnett's post test: significantly different from time-matched solvent control *p ≤ 0.05, **p ≤ 0.01.*

Estradiol showed no effect on cell viability in PHm up to a concentration of 10 µM at both treatment times. At the highest concentration tested (20 µM) a considerable reduction in viable cells was observed which was statistically significant at 20 h leading to a 30% decrease. Overall, HepG2 cells were more sensitive to E2 than PHm and the cytotoxic effects at the highest E2 concentration was more pronounced at 48 h.

5.2.3. EFFECTS OF CO-TREATMENTS AFTER 20 H AND 48 H

In the following treatments with TCDD at concentrations of 1and 10 nM as well as with E2 at relatively low concentrations (10 and 100 nM) were chosen and comparative effects on cell viability were investigated in all the four cell models after 20 h and 48 h treatment. Additionally, the combinations of both compounds were tested in order to exclude possible cumulative effects on cell viability (Figure 43 and Figure 44). Treatment with sodium dodecyl sulfate (SDS, 0.1%) served as the positive control and caused the death of all cells.

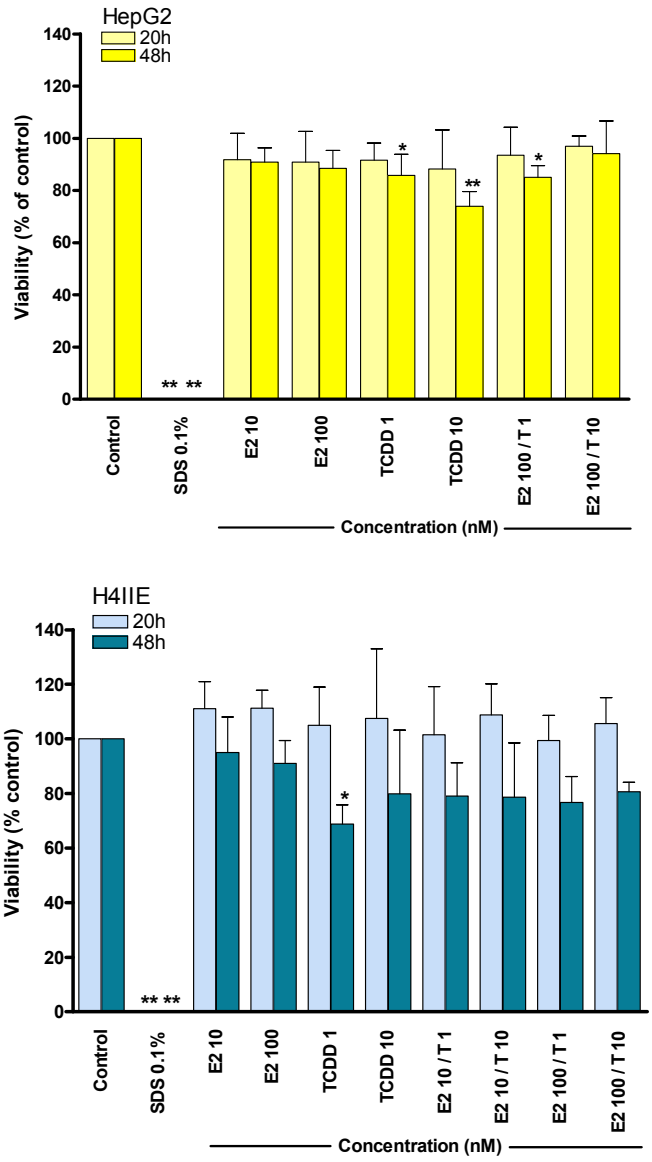

*Figure 43: Cytotoxicity assay (resazurin reduction test) in human and rat hepatoma cell lines (HepG2 and H4IIE) after exposure to TCDD (T) and/or E2 at different concentrations for 20 h and 48 h. Cells were treated in phenol red-free DMEM culture medium at reduced FBS concentration (0.5%). Results were normalized to the respective solvent control (DMSO 0.1% or EtOH 0.1%) which was set at 100%. SDS 0.1% for 20 h and 48 h was used as the positive control. Mean ± SD; n ≥ 3; One-way ANOVA with Dunnett's post test: significantly different from time-matched solvent control *p ≤ 0.05, **p ≤ 0.01.*

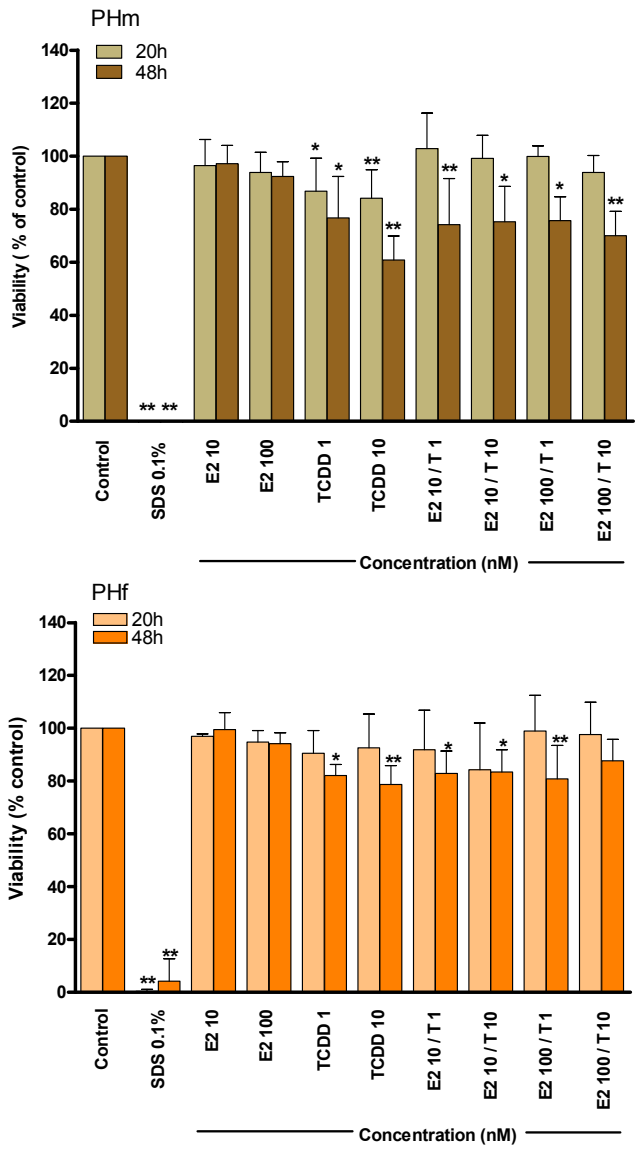

*Figure 44: Cytotoxicity assay (resazurin reduction test) primary hepatocytes from male (PHm) and female (PHf) Wistar rats after exposure to TCDD (T) and/or E2 at different concentrations for 20 h and 48 h. Cells were treated in phenol red-free DMEM culture medium at reduced FBS concentration (0.5%). Results were normalized to the respective solvent control (DMSO 0.1% or EtOH 0.1%) which was set at 100%. SDS 0.1% for 20 h and 48 h was used as the positive control. Mean ± SD; n ≥ 3; One-way ANOVA with Dunnett's post test: significantly different from time-matched solvent control *p ≤ 0.05; **p ≤ 0.01.*

Exposure with E2 and/or TCDD showed no effects on cell viability at 20 h. When the incubation time was more than doubled up to 48 h, TCDD 1 and 10 nM displayed decreased cell viability in all cell models. A decrease of viable cells was observed with TCDD 10 nM in H4IIE cells, but was not significantly confirmed. Thus, except for H4IIE, TCDD 10 nM resulted in prominent significant decreases of cell viability after 48 h. This cytotoxic effect of TCDD 10 nM was strongest in PHm resulting in a reduction of cell viability by approximately 40% compared to solvent control. The other cell models were less responsive reaching however approximately 70to 80% cell viability of the solvent control. Estradiol alone had no effect at 48 h in all cell models. Most of the co-treatments of E2 (10 and 100 nM) with TCDD (1 and 10 nM) showed a decrease in viable cells, that was however

not more severe than effects seen with TCDD alone. Consequently, reduced cell viability seen with the co-treatments can be attributed to treatments with TCDD. For the co-treated cells, the decrease in cell viability was again strongest for PHm, thus the same order of sensitivity as for treatments with TCDD was obtained for the combination of both test substances : PHm>HepG2 = H4IIE = PHf.

Overall, it can be concluded that treatment with TCDD and/or E2 did not affect cell viability after 20 h. After 48 h TCDD resulted in moderate reduction of cell viabililty, which however never fell below 60% of control. The co-treatments did not further enhance the effects seen with TCDD alone. Rat hepatocytes from male rats were the most sensitive cell model.

5.2.4. CONCENTRATION-DEPENDENT EFFECTS BY E2 CATECHOL METABOLITES AFTER 20 H

Hepatoma cell lines and rat hepatocytes isolated from male and female Wistar rat were incubated with either 2- or 4-hydroxyestradiol at concentrations ranging from 0.01 to 10 µM for 20 h. The results on cell viability compared to control in the different cells models are depicted in Figure 45 and Figure 46. It was clearly noted that for both metabolites none of the concentrations tested had an effect different from solvent control viability levels. Experiments with PHm were only performed once. However, it was assumed that in the absence of cytotoxic effects by 2-and 4-OHE2 in at least three independent experiments with the other three cell models, cytotoxicity for the concentration range tested can be excluded.

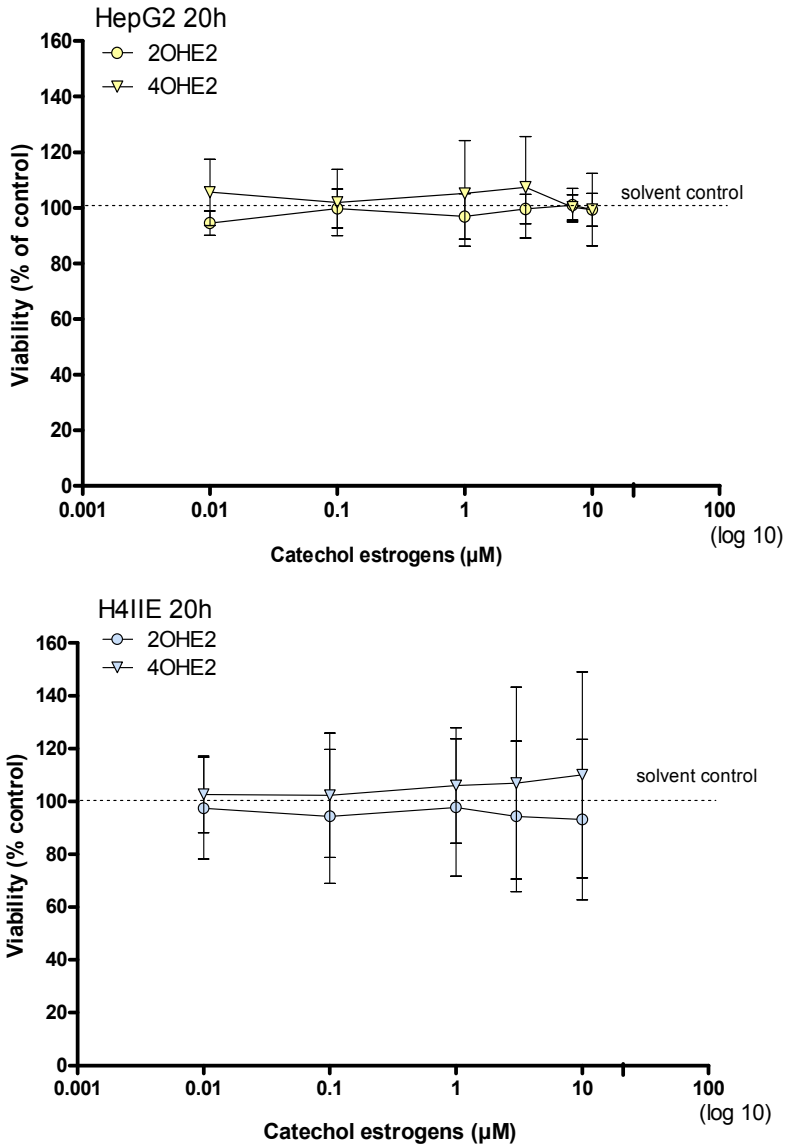

Figure 45: Cytotoxicity assay (resazurin reduction test) in human and rat hepatoma cell lines (HepG2 and H4IIE) after exposure to various concentrations of E2 catechol metabolites 2- and 4-hydroxyestradiol (2- and 4-OHE2) ranging from 0.01 to 10 µM for 20 h. Cells were treated in phenol red-free DMEM culture medium at reduced FBS concentration (0.5%). Results are normalized to the respective solvent control (EtOH 0.1%) which was set at 100%. The horizontal dashed line represents the solvent control level. Means ± SD; n ≥ 3; One-way ANOVA with Dunnett's post test.

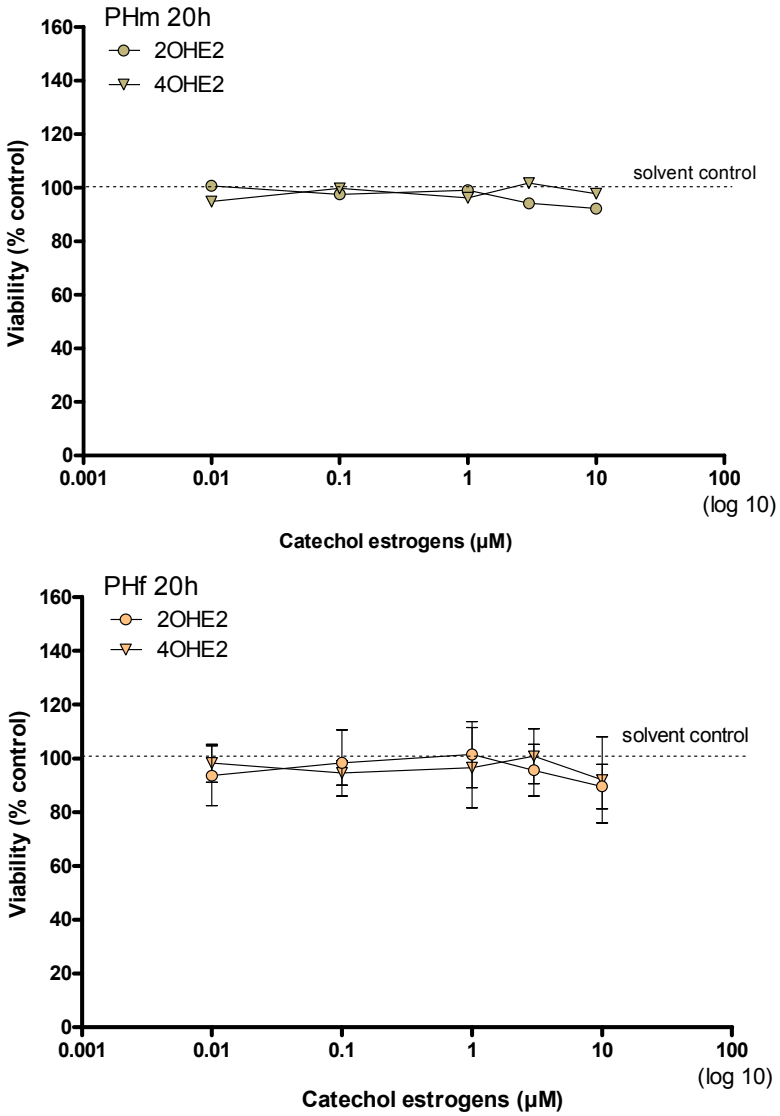

Figure 46: Cytotoxicity assay (resazurin reduction test) in primary hepatocytes from male (PHm) and female (PHf) Wistar rats after exposure to various concentrations of E2 catechol metabolites 2- and 4-hydroxyestradiol (2- and 4-OHE2) ranging from 0.01 to 10 µM for 20 h. Cells were treated in phenol red-free DMEM culture medium at reduced FBS concentration (0.5%). Results are normalized to the respective solvent control (EtOH 0.1%) which was set at 100%. The horizontal dashed line represents the solvent control level. Mean ± SD; n ≥ 3 for PHf and n = 1 for PHm; One-way ANOVA with Dunnett's post test.

5.3. CYP1A1 AND CYP1B1 EXPRESSION

Induction of CYP1A1 and CYP1B1 by TCDD and E2 in the different liver cell models was monitored on mRNA and protein level. Therefore, quantitative (TaqMan) real-time RT PCR method and semi-quantitative Western Blot analysis was used for mRNA and protein expressing respectively.

The possible modulating effects of E2 on TCDD-induced gene expression were investigated by the following co-treatments: E2 10 nM + TCDD (1 and 10 nM) and E2 100 nM + TCDD 1 nM.

5.3.1. BASAL MRNA LEVELS

The levels of CYP1A1 and CYP1B1 mRNA content already present per se in the hepatoma cell lines and rat hepatocytes, i.e. the basal levels, were assessed and calculated as ratios of delta CT values of the solvent control.

Basal CYP1A1 mRNA

Real-time PCR demonstrated that among the four different liver-derived cell models tested, the hepatoma cell lines H4IIE and HepG2 showed the lowest CYP1A1 expression at both treatment times, which were up to 8-fold or one magnitude lower compared to primary rat hepatocytes (Figure 47). At 48 h basal mRNA in HepG2 was even significantly lower than in the rat cell line. Rat hepatocytes from female-rats exhibited highest basal CYP1A1 levels, which were significantly higher than in male-derived hepatocytes at 20 h and 48 h (about 2.8 to 3.8 – fold respectively). No difference in mRNA levels was noticed between the two treatment times except for H4IIE cells, which showed significantly higher basal expression levels after 48 h. Interestingly, expression of ERalpha in transfected HepG2 cell line (HepG2 + ERalpha) led to significantly elevated CYP1A1 basal mRNA levels compared to wild-type HepG2 and reached an even higher level than PHm at 20 h.

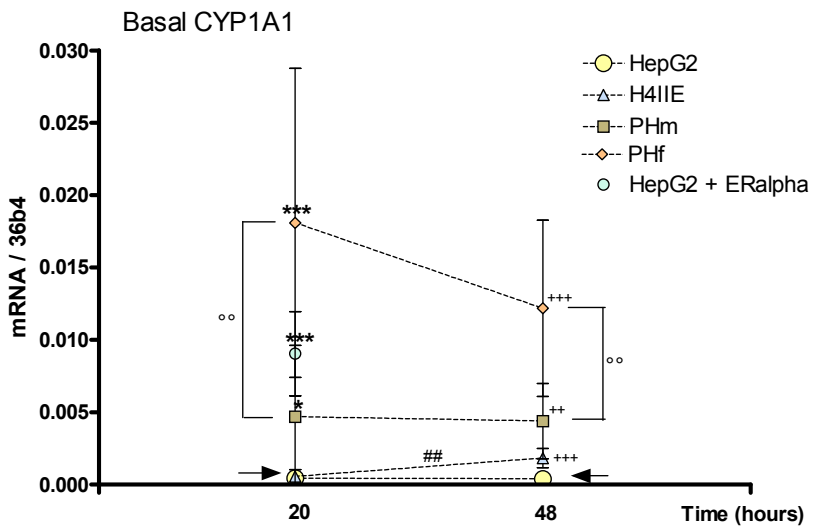

*Figure 47: Real-time RT PCR analysis of basal CYP1A1 mRNA levels in hepatoma cell lines HepG2 and H4IIE and rat hepatocytes from male (PHm) and female (PHf) Wistar rats treated with DMSO (0.25%) over a period of 20 h and 48 h. Transiently transfected HepG2 with ERalpha expression plasmid (HepG2 + ERalpha) were investigated at 20 h. Results were normalized against the housekeeping gene 36B4 and expressed as ratios of delta CT values. Mean ± SD; n ≥ 3; unpaired t-test, two-tailed p value: mRNA expression levels significantly different from time-matched HepG2 control (as indicated by the arrows →) at 20 h (*p ≤ 0.05, ***p ≤ 0.001) or at 48 h ($^{++}$p ≤ 0.01, $^{+++}$p ≤ 0.001); mRNA expression levels significantly different between 20 h and 48 h ## p ≤ 0.01; mRNA expression significantly different between PHm and PHf °°p ≤ 0.01.*

Rank order basal CYP1A1 mRNA	
20 h	*PHf > HepG2+ERalpha > PHm > H4IIE = HepG2*
48 h	*PHf > PHm > H4IIE > HepG2*

Basal CYP1B1 mRNA

Measurable basal levels of CYP1B1 mRNA were observed in all liver cell models (Figure 48). In HepG2 cell line control levels of CYP1B1 mRNA were only achieved using a specific fluorogenic probe for TaqMan real-time RT PCR, which enhanced specificity of the method and allowed detection of trace mRNA products.

HepG2 cell line clearly exhibited the lowest CYP1B1 basal levels, which were significantly up to three magnitudes (480-fold) lower compared to the rat hepatoma cell line and rat primary hepatocytes. Primary rat hepatocytes isolated from female rats showed highest

basal CYP1B1 mRNA amounts but no statistical difference was observed compared to male rat hepatocytes at both treatment times. CYP1B1 expression in H4IIE cell line was comparable to rat hepatocytes and only slightly (1.8- to 3.9-fold) lower at 20 h and 48 h respectively. There was no difference in basal levels between the two treatment times. The presence of ERalpha in HepG2 cells led to significantly higher up to 2-fold CYP1B1 basal levels compared to wild-type HepG2.

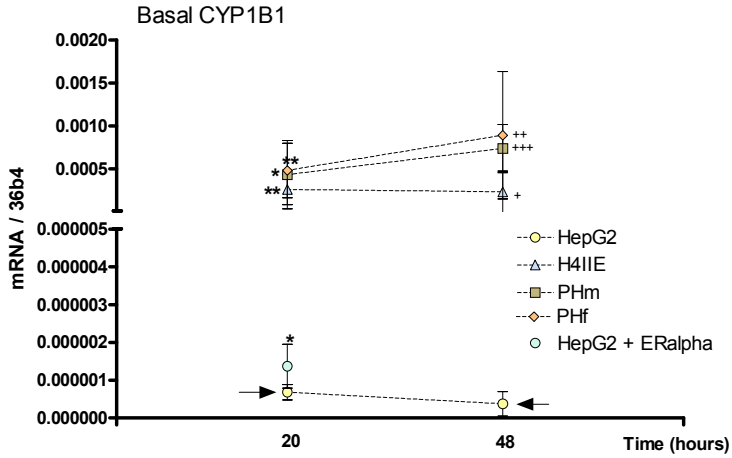

*Figure 48: Real-time RT PCR analysis of basal CYP1B1 mRNA levels in hepatoma cell lines HepG2 and H4IIE and rat hepatocytes from male (PHm) and female (PHf) Wistar rats treated with DMSO (0.25%) over a period of 20 h and 48 h. Transiently transfected HepG2 with ERalpha expression plasmid (HepG2 + ERalpha) were investigated at 20 h. Results were normalized against the housekeeping gene 36B4 and expressed as ratios of delta CT values. Mean ± SD; n ≥ 3; unpaired t-test, two-tailed p value: mRNA expression levels significantly different from time-matched HepG2 control (as indicated by the arrows →) at 20 h (*p ≤ 0.05; **p ≤ 0. 01) or at 48 h ($^{+}$p ≤ 0.05; $^{++}$p ≤ 0.01; $^{+++}$p ≤ 0.001); mRNA expression levels significantly different between 20 h and 48 h: not significant; mRNA expression significantly different between PHm and PHf: not significant.*

Rank order basal CYP1B1 mRNA	
20h	*PHf = PHm>H4IIE>>HepG2+ERalpha > HepG2*
4 h	*PHf = PHm > H4IIE >> HepG2*

Comparison of Basal CYP1A1 and CYP1B1 Expression

Despite the differential expression of basal CYP1A1 and CYP1B1 among the hepatoma cell lines and rat hepatocytes, it was observed that generally basal CYP1A1 levels are considerably higher than basal CYP1B1 mRNA contents, with a difference of several (2 to 3) magnitudes.

5.3.2. CYP1A1 AND CYP1B1 EXPRESSION AFTER EXPOSURE TO TCDD AND/OR E2 IN HEPATOMA CELLS

5.3.2.1. mRNA LEVELS IN HEPG2

Figure 49 displays the analysis of relative CYP1A1 and CYP1B1 gene expression in HepG2 cells. TCDD (1 and 10 nM) extensively induced CYP1A1 mRNA at both treatment times without a concentration-dependent effect (61.91 ± 37.15-fold and 68.48 ± 34.02-fold for 1 nM and 10 nM at 20 h). There was no change observed in mRNA levels following E2 treatment (10 and 100 nM) at the two treatment times. The co-treatment of TCDD 1 nM with E2 100 nM showed the highest relative expression level among the treatments (132.9 ± 64.5-fold). It resulted in a twofold enhanced increase in CYP1A1 mRNA compared to TCDD induction alone at 20 h. However, a high standard deviation was obtained with this treatment at 20 h. The other combinations of TCDD with estradiol had no modulating effect on marked TCDD CYP1A1 mRNA expression at 20 h and 48 h. There were significantly higher TCDD-induced CYP1A1 mRNA levels observed for some of the treatments at the longer treatment time compared to 20 h.

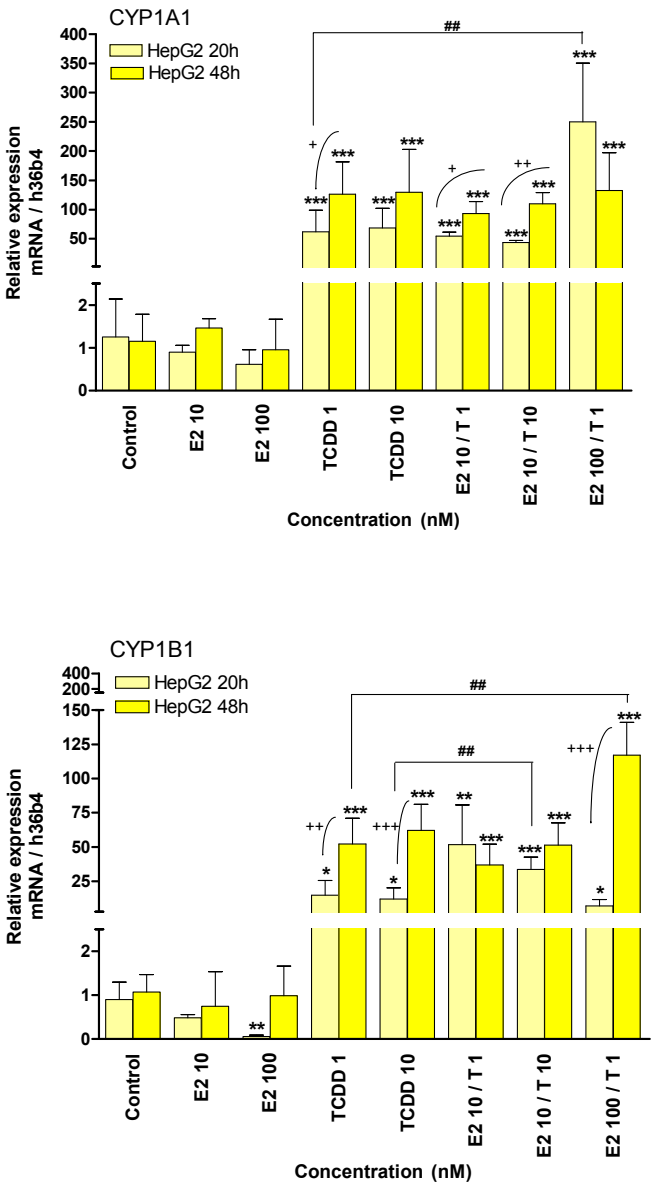

*Figure 49: Real-time RT PCR analysis of HepG2 hepatoma cells on hCYP1A1 and hCYP1B1 (TaqMan) gene expression. Effects of TCDD (T) and/or Estradiol (E2) on mRNA levels were assayed following 20 h and 48 h treatment. CYP450 expression is normalized to 36B4 expression and presented relative to respective solvent control. (DMSO 0.25%). Mean ± SD; n ≥ 3; unpaired t-test, two-tailed p value: mRNA expression levels significantly different from time-matched solvent control *p ≤ 0.05, **p ≤ 0.01, ***p ≤ 0.001; mRNA expression levels significantly different between time-matched treatments ##p ≤ 0.01; mRNA expression levels significantly different between treatment times +p ≤ 0.05, ++p ≤ 0.01, +++p ≤ 0.001.*

As described before in section 5.3.1 HepG2 cells exhibited very low basal levels of CYP1B1 mRNA. Consequently, difficulties were met in detecting CT values following exposure to the solvent control when using standard real-time PCR method with SYBR Green. However, following exposure to TCDD, CYP1B1 CT values could be detected. Measurable basal levels of CYP1B1 mRNA were only obtained with the use of a specific fluorogenic TaqMan probe as described in Materials and Methods (see section 4). Additionally, for hCYP1B1 mRNA real-time amplification cycle number was extended from standard 45 cycles to 50 cycles. The very low basal levels of the gene could also explain the great variances of CT

values seen for solvent control CYP1B mRNA. Thus, induction of CYP1B1 mRNA following TCDD treatment indicates that the gene is completely switched on by the potent dioxin inducer.

Indeed, results of CYP1B1 expression in HepG2 cells (Figure 49) revealed that TCDD significantly induced hCYP1B1 mRNA (e.g. TCDD 1 nM at 20 h: 30.72 ± 26.62-fold). Treatment with E2 alone at the low concentration (10 nM) did not modify CYP1B1 induction compared to solvent control levels. Contrarily to that, the highest E2 concentration of 100 nM caused a significant decrease in CYP1B1 mRNA by 95% at 20 h. After 48 h treatment with E2, CYP1B1 mRNA was at the same level as DMSO control. Two of the co-treatments induced CYP1B1 mRNA above the level observed for TCDD alone. At 20 h the combination of E2 10 nM + TCDD 10 nM significantly exceeded the increase of TCDD single treatment by doubling the fold-induction leading to 33.59 ± 9.01-fold. The highest induction level was obtained by the co-treatment of E2 100 nM + TCDD 1nM at 48 h, which was at 117.1 ± 24.0. This co-treatment also further enhanced the CYP1B1 expression of the single dioxin treatment. The other co-treatments did not show any further inductive effect beyond that of TCDD 1 nM or 10 nM alone. Unfortunately, the treatment of E2 100 nM with the high TCDD concentration was not performed in this test, but could have been useful to investigate a possible concentration-dependent modulating effect of E2 on induction byTCDD.

5.3.2.2. PROTEIN LEVELS IN HEPG2

Immunoreactive CYP1A1 protein was considered to be present if a band at the correct size (56 kDa) was demonstrated.There was no constitutive expression of CYP1A1 protein observed in HepG2 cells (Figure 50). After exposure to TCDD (1 nM and 10 nM) the presence of CYP1A1 protein was clearly observed as a pronounced band leading to a 101.6 ± 34.93 –fold (1 nM, 20 h) induction compared to DMSO control. There exists no difference in protein induction via different TCDD concentrations. E2 alone did not induce CYP1A1 protein. TCDD-induced CYP1A1 protein expression was not increased following exposure to the co-treatments of TCDD with E2 in all the tested combinations. Thus, E2 had no modulating effect on TCDD-induced CYP1A1 protein increase. All the combinations reached about the same induced protein level with no evident difference between the two treatment times.

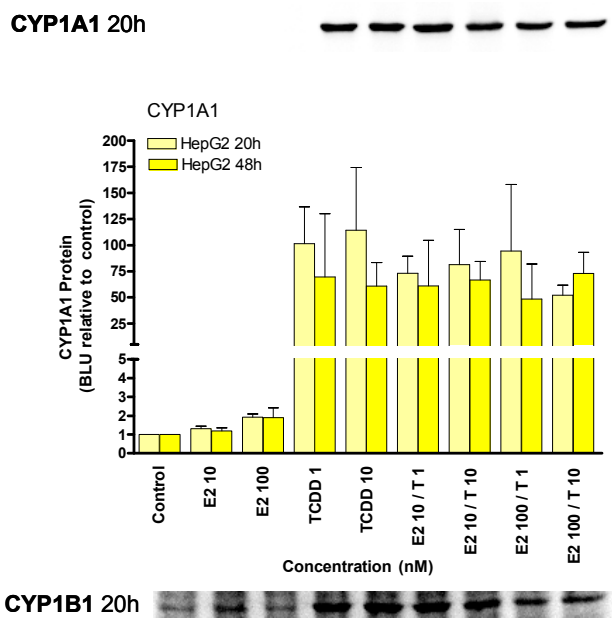

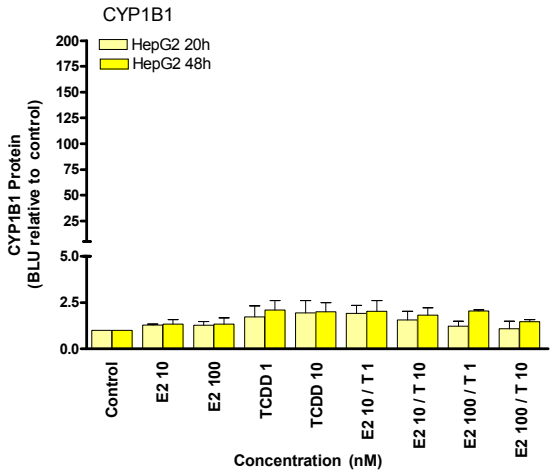

Figure 50: CYP1A1 and CYP1B1 protein levels in HepG2 cell line treated with TCDD (T) and/or E2 for 20 h and 48 h. Representative Western Blots at 20 h with specific protein bands are shown above. Lanes from right to left were loaded with microsomal preparations (30 µg for CYP1A1 and 50 µg for CYP1B1) in the same order as indicated below in the diagram. Densitometric analysis is given in the histogram, representing relative levels of CYP protein found in microsomal samples. Boehringer Light Units (BLUs) were normalized to the solvent control (DMSO 0.25%), which was set at 1. Mean ± SD; n = 3; (n = 2 for CYP1B1 at 48 h)

Some difficulties were met in detection of CYP1B1 protein bands (57 kDa) in HepG2 cells after exposure to TCDD at 20 h and 48 h (Figure 50). CYP1B1 protein in the HepG2 cell line was detectable as a faint product at 20 h. After 48 h CYP1B1 protein was even less evident, therefore results of only two independent experiments could be used for representation of results. In general, it was very difficult to obtain visible bands that could be used for densitometric analysis, even when using 50 µg of loading samples, which was an up to 2.5-fold higher amount than used for detection of CYP1B1 protein bands in the other cell models investigated. Several attempts were undertaken to optimize the conditions of the method. The parameters chosen to improve detection of CYP1B1 protein bands are summarized in Materials and Methods (see section 4).

Despite these time-consuming efforts taken, the Western Blot analysis did not turn out satisfactorily in the course of this work. Nevertheless, a slight induction in protein intensity could be assumed after treatments with TCDD or its combinations with E2. In the densitometric analysis TCDD 1 nM led to a weak induction of about 1.7-fold at 20 h and 2.0-fold at 48 h compared to DMSO control. This evidence could possibly be interpreted as a TCDD-dependent induction of CYP1B1 protein concomitant to similar results found in real-time PCR in HepG2 (see section 5.3.2.1).

5.3.2.3. mRNA LEVELS IN H4IIE

The effects of TCDD and E2 on CYP1A1 transcription in H4IIE cells is presented in Figure 51. TCDD led to an extensive induction of relative CYP1A1 mRNA at both treatment times (1 nM: 163.1 ± 98.7 –fold and 115.3 ± 81.6 –fold at 20 h and 48 h respectively). E2 alone did not modify CYP1A1 mRNA levels compared to control. The co-treatment of TCDD 1 nM + E2 10 nM significantly increased CYP1A1 expression compared to TCDD treatment alone at 20 h, leading to an about 1.8-fold higher mRNA level. The other combinations with estradiol had no additional effect on CYP1A1 induction. Comparisons between the two treatment times showed that dioxin-induced expression levels were significantly higher at 20 h for TCDD 10 nM and the respective co-treatment with E2 10 nM. Slightly higher but not significantly confirmed mRNA levels at 20 h compared to 48 h were also apparent for the other dioxin treatments.

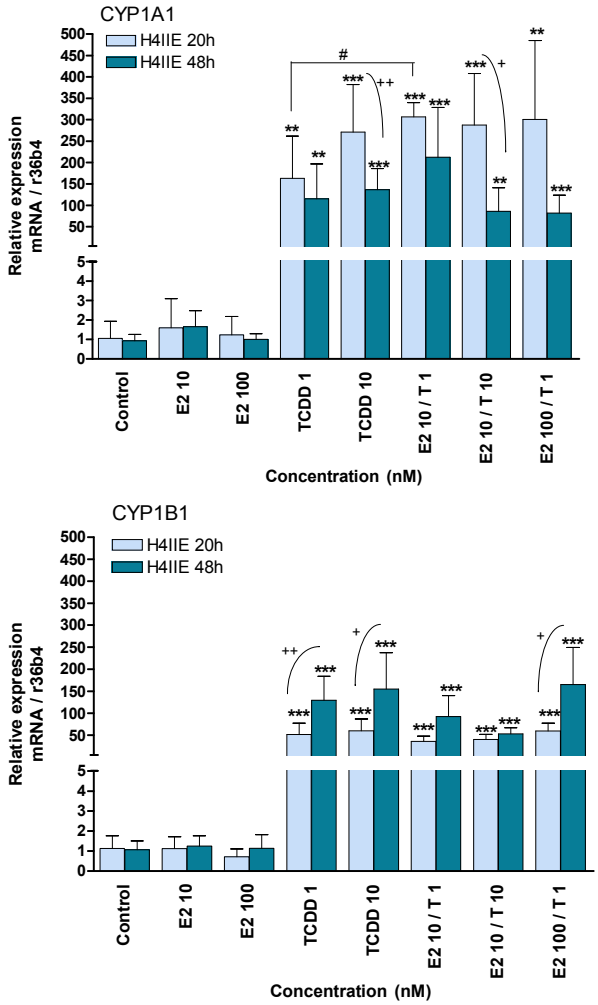

*Figure 51: Real-time RT PCR analysis of H4IIE hepatoma cells on rCYP1A1 and rCYP1B1 gene expression. Effects of TCDD (T) and/or Estradiol (E2) on mRNA levels were assayed following 20 h and 48 h treatment. CYP450 expression is normalized to 36B4 expression and presented relative to respective solvent control (DMSO 0.25%). Mean ± SD; n ≥ 3; unpaired t-test, two-tailed p value: mRNA expression levels significantly different from time-matched solvent control **p ≤ 0.01, ***p ≤ 0.001; mRNA expression levels significantly different between time-matched treatments #p ≤ 0.05; mRNA expression levels significantly different between treatment times +p ≤ 0.05, ++p ≤ 0.01.*

Significant increases in relative CYP1B1 mRNA (Figure 51) were obtained after TCDD treatment at both treatment times with no difference between the two concentrations (1 nM: 51.98 ± 25.39-fold; 10 nM: 60.34 ± 26.94-fold at 20 h). Treatment with E2 alone did not exhibit changes in CYP1B1 mRNA levels different from that of solvent control. The co-treatments of TCDD with estradiol induced gene expression to the same extent as single TCDD treatments. Significantly higher induction levels after 48 h compared to 20 h were observed for the treatments with TCDD alone (1 nM and 10 nM) and the combination of TCDD 1 nM with E2 100 nM.

5.3.2.4. PROTEIN LEVELS IN H4IIE

In H4IIE cells CYP1A1 protein was induced following exposure to TCDD 1 nM leading to a 12-fold induction at 20 h and a more important 81-fold induction at 48 h (Figure 52) without a concentration-dependent effect. E2 treatments did not increase protein levels but a faint protein band similar to DMSO control was detected. Similar to CYP1A1 mRNA

levels, E2 had no modulating effect on TCDD-induced CYP1A1 protein induction. TCDD-mediated induction of CYP1A1 protein expression appeared to be more pronounced at 48 h, assuming a time-dependent increase in CYP1A1 expression.

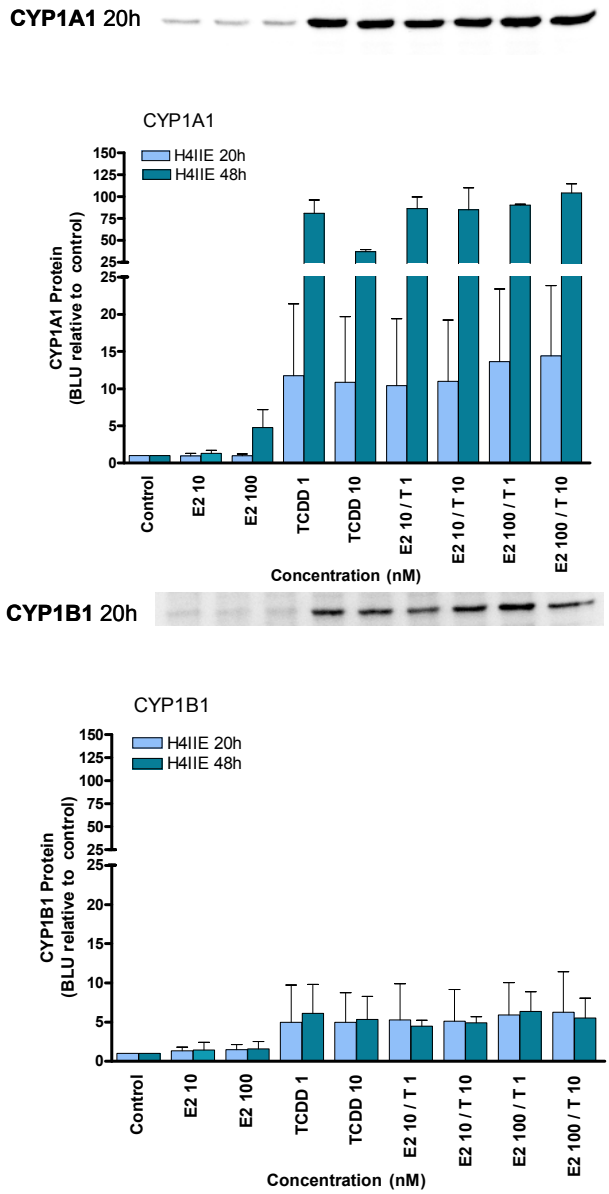

Figure 52: CYP1A1 and CYP1B1 protein levels in H4IIE cell line treated with TCDD (T) and/or E2 for 20 h and 48 h. Representative Western Blots at 20 h with specific protein bands are shown above. Lanes from right to left were loaded with microsomal preparations (30 µg) in the same order as indicated below in the diagram. Densitometric analysis is given in the histogram, representing relative levels of CYP protein found in microsomal samples. Boehringer Light Units (BLUs) were normalized to the solvent control (DMSO 0.25%), which was set at 1. Before hand BLUs of H4IIE treatments were normalized against respective light intensity of rCYP2D1 determined as the loading control after stripping the original blot and reprobing it with the respective antibodies. Mean ± SD; n = 3; (n = 2 for CYP1A1 and the following treatments at 48 h: E2 100 nM, TCDD 1 nM and 10 nM, E2 100 nM/TCDD 1nM, E2 100 nM/TCDD 10 nM).

Loading of the same amount of microsomal preparations (30 µg per lane) showed TCDD-induced CYP1B1 protein. It is evident that TCDD-induced CYP1B1 induction is low and weaker compared to CYP1A1 protein induction in rat H4IIE cell line (Figure 52). Treatment with TCDD 1 nM at 20 h resulted in a 5-fold induction compared to DMSO control and treatment with TCDD 10 nM reached the same protein level. Single E2 treatments did not

show a protein product. Moreover, E2 had no modulating effect on TCDD-induced band intensities. Different treatment times had no influence on CYP1B1 protein production.

5.3.3. CYP1A1 AND CYP1B1 EXPRESSION AFTER EXPOSURE TO TCDD AND/OR E2 IN PRIMARY RAT HEPATOCYTES

5.3.3.1. mRNA LEVELS IN PHM

Following exposure to TCDD for 20 h and 48 h, primary rat hepatocytes from male rats revealed marked increase of CYP1A1 mRNA (1 nM at 20 h: 72.49 ± 43.53–fold;10 nM at 20 h: 72.62 ± 52.29 – fold) compared to control without a concentration pattern (Figure 53). E2-treated rat hepatocytes showed no changes in relative CYP1A1 mRNA expression at both concentrations and treatment times. There was no difference observed between the inductive effect of TCDD alone and the combinations with additional E2, indicating that E2 has no modulating effect on CYP1A1 mRNA in rat primary hepatocytes from male rats. Moreover, dioxin-dependent relative mRNA expression levels were comparable for the two treatment times.

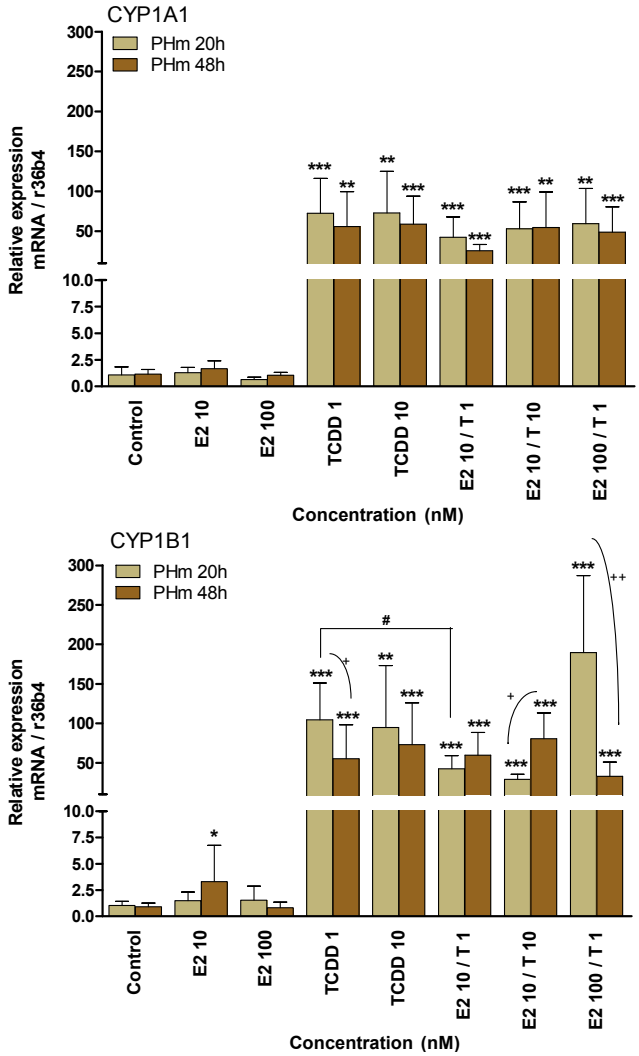

*Figure 53: Real-time RT PCR analysis of primary rat hepatocytes from male Wistar rats (PHm) on rCYP1A1 and rCYP1B1 gene expression. Effects of TCDD (T) and/or Estradiol (E2) on mRNA levels were assayed following 20 h and 48 h treatment. CYP450 expression is normalized to 36B4 expression and presented relative to respective solvent control (DMSO 0.25%). Mean ± SD; n ≥ 3; unpaired t-test, two-tailed p value: mRNA expression levels significantly different from time-matched solvent control *p ≤ 0.05, **p ≤ 0.01, ***p ≤ 0.001; mRNA expression levels significantly different between time-matched treatments #p ≤ 0.05; mRNA expression levels significantly different between treatment times +p ≤ 0.05, ++p ≤ 0.01.*

TCDD also significantly increased CYP1B1 mRNA compared to control (Figure 53). Both concentrations of TCDD reached a similar elevated expression level (1 nM at 20 h: 104.2 ± 47.0-fold). E2 alone had a minor but significant increasing effect on CYP1B1 mRNA, which was only observed at the low concentration following 48 h treatment with a high standard deviation (3.32 ± 3,43 –fold). Co-treatments of TCDD with E2 had no additional increasing effect on TCDD-induced mRNA. Exposure with TCDD 1 nM + E2 10 nM at 20 h even significantly declined CYP1B1 expression level compared to single dioxin treatment, showing a reduction by approximately 60% of the TCDD 1 nM induction.

For thetreatments of TCDD 1 nM and the combination of TCDD 1 nM with E2 100 nM mRNA induction levels were significantly higher at 20 h compared to 48 h, whereas TCDD 10 nM + E2 10 nM –induced gene expression was found to be more pronounced at 48 h. Thus, there was no consistent difference between the two treatment times.

5.3.3.2. PROTEIN LEVELS IN PHM

The presence of induced CYP1A1 protein in primary hepatocytes from male ratsfollowing exposure to TCDD was demonstrated by strong protein bands equivalent to a 75- and 79-fold induction for TCDD 1 and 10 nM respectively at 20 h compared to control (Figure 54). Both TCDD concentrations induced protein levels to the same extent. CYP1A1 protein was not detectable in the absence of the prototype inducer, i.e. treatments with solvent control and E2 (10 nM and 100 nM). The co-treatments with E2 had no modulating effect on TCDD-induced levels. The protein inductions showed no difference between the two treatment times.

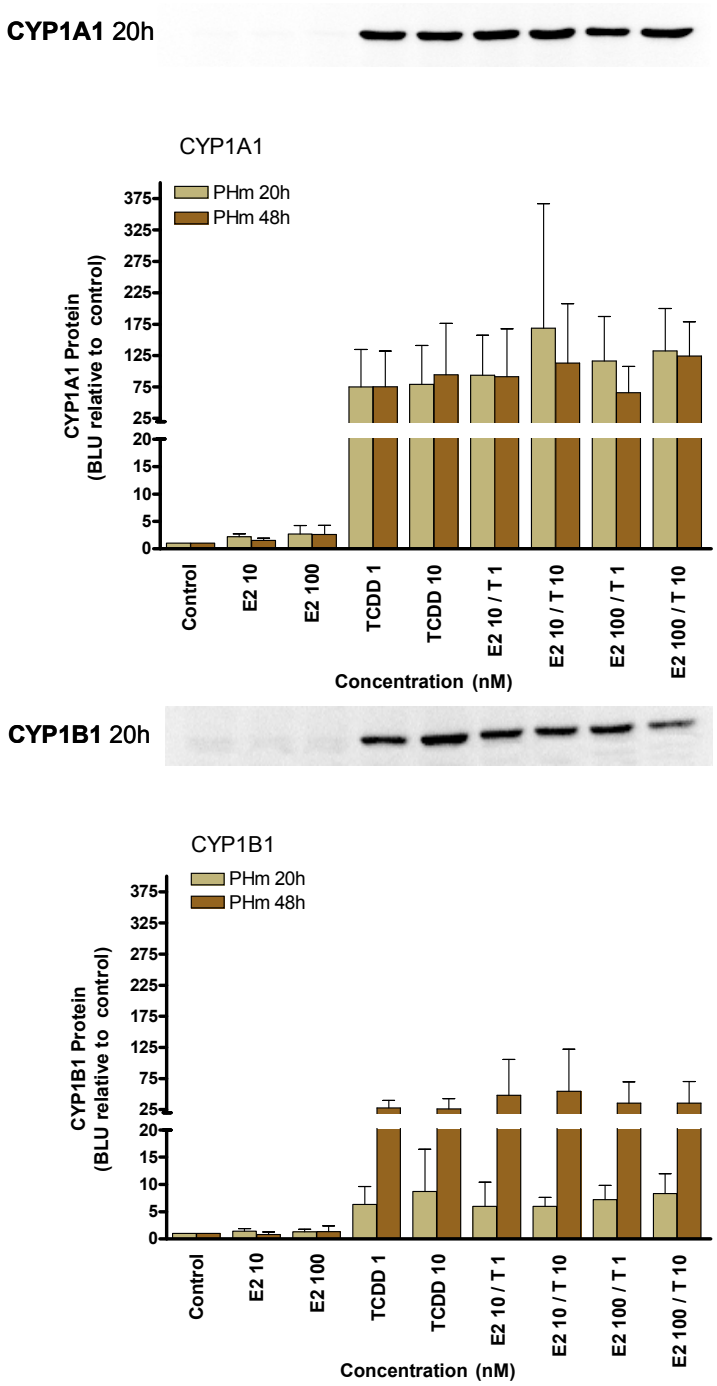

Figure 54: CYP1A1 and CYP1B1 protein in primary rat hepatocytes from male Wistar rats (PHm) treated with TCDD (T) and/or E2 for 20 h and 48 h. Representative Western Blots at 20 h with specific protein bands are shown above. Lanes from right to left were loaded with microsomal preparations (20 µg) in the same order as indicated below in the diagram. Densitometric analysis is given in the histogram, representing relative levels of CYP protein found in microsomal samples. Boehringer Light Units (BLUs) were normalized to of the solvent control (DMSO 0.25%), which was set at 1. Before hand BLUs of PH treatments were normalized against respective light intensity of rCYP2D1 determined as the loading control after stripping the original blot and reprobing it with the respective antibodies. Mean ± SD; n ≥ 3.

TCDD alone also highly induced CYP1B1 protein in male-derived primary rat hepatocytes with no difference between 1 nM and 10 nM (Figure 54). E2 alone did not induce CYP1B1 protein at all. The co-treatments did not lead to any intensifying effects of TCDD-induced CYP1B1 protein induction. A slight trend for higher induced protein levels beyond that of TCDD single treatments could be seen at 48 h for the co-treatments of TCDD with E2

10 nM. Induction levels of these combinations were almost 2-times higher, compared to TCDD alone, i.e. 54.5-fold for TCDD 10 nM + E2 10 nM compared to 26.4-fold for TCDD 10 nM, but high standard deviations were obtained. Protein induction was observed to be more pronounced at 48 h.

5.3.3.3. mRNA LEVELS IN PHF

Primary rat hepatocytes from female rats demonstrated highly increased relative CYP1A1 mRNA levels following exposure to TCDD 1 nM, resulting in a 25.90 ± 11.34–fold induction at 20 h and a 33.18 ± 24.17-fold induction at 48 h (Figure 55). There was no concentration-dependent difference observed in expression levels. Treatments with E2 alone did not change CYP1A1 mRNA compared to the control. Additionally, there was no effect triggered by the co-treatments and different treatment times had no effect on induction levels

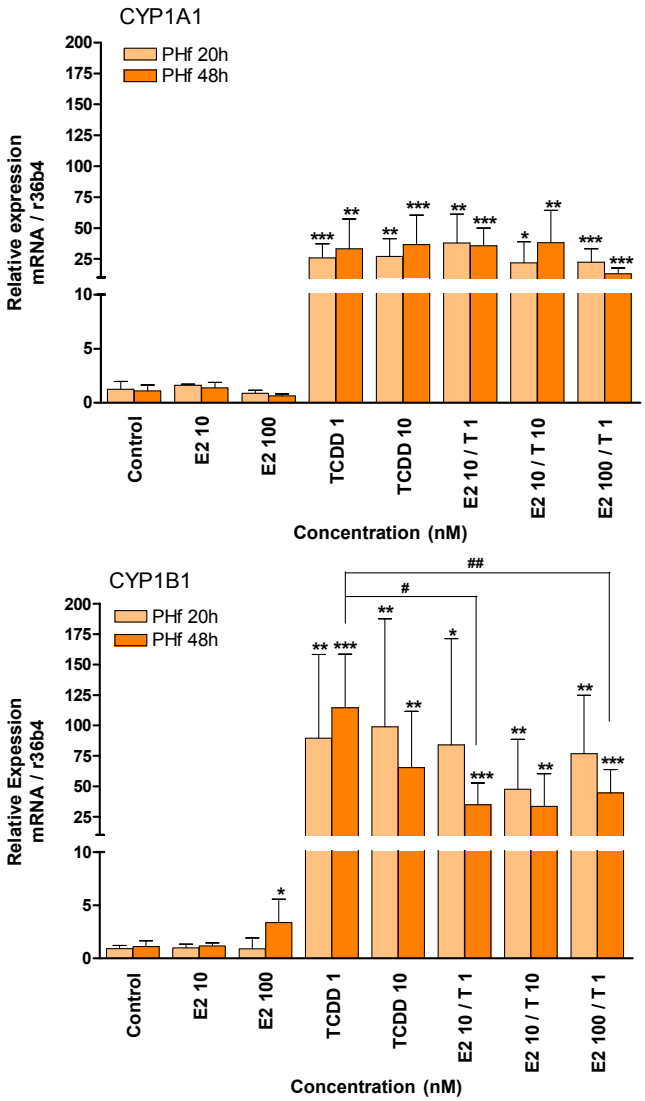

*Figure 55: Real-time RT PCR analysis of primary rat hepatocytes from female Wistar rats (PHf) on rCYP1A1 and rCYP1B1 gene expression. Effects of TCDD (T) and/or Estradiol (E2) on mRNA levels were assayed following 20 h and 48 h treatment. CYP450 expression is normalized to 36B4 expression and presented relative to respective solvent control (DMSO 0.25%). Mean ± SD; n ≥ 3; unpaired t-test, two-tailed p value: mRNA expression levels significantly different from time-matched solvent control *p ≤ 0.05, **p ≤ 0.01, ***p ≤ 0.001; mRNA expression levels significantly different between time-matched treatments #p ≤ 0.05, ##p ≤ 0.01.*

Figure 55 shows that TCDD (1 nM) extensively induced CYP1B1 mRNA in female-derived rat hepatocytes (89.45 ± 68.67-fold at 20 h and 114.5 ± 44.1-fold at 48 h respectively) with no concentration-dependent pattern.

E2 alone led to a small but significant 3.36 ± 2.19-fold increase of CYP1B1 mRNA following exposure to the highest dose of 100 nM and only at 48 h. The co-treatment of TCDD 1 nM + E2 10 nM or E2 100 nM showed a significant decline in CYP1B1 expression by 70% and 60% respectively compared to single TCDD treatment at 48 h. There was no significant difference of effects obtained between the two treatment times.

5.3.3.4. PROTEIN LEVELS IN PHF

In female-derived rat hepatocytes CYP1A1 protein is extensively increased up to 59-fold following exposure to TCDD (1 nM, 20 h) compared to solvent control (Figure 56). The absence of protein bands following treatments with E2 indicated that CYP1A1 protein is not induced by estradiol. There was also no effect observed by the co-treatments. There was a tendency of slightly higher CYP1A1 induced levels (e.g. 112-fold induction for TCDD 1 nM) after 48 h exposure, which was probably due to high standard deviations.

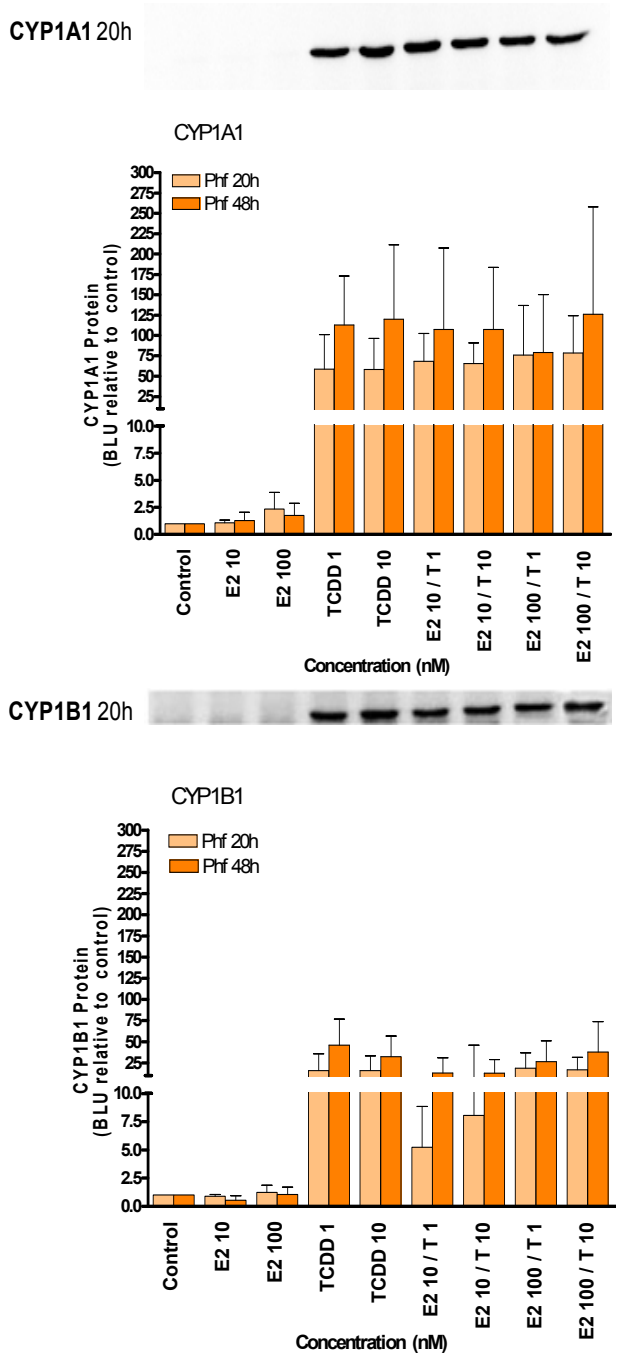

Figure 56: CYP1A1 and CYP1B1 protein in primary rat hepatocytes from female Wistar rats (PHf) treated with TCDD (T) and/or E2 for 20 h and 48 h. Representative Western Blots at 20 h with specific protein bands are shown above. Lanes from right to left were loaded with microsomal preparations (20 µg) in the same order as indicated below in the diagram. Densitometric analysis is given in the histogram representing relative levels of CYP protein found in microsomal samples. Boehringer Light Units (BLUs) were normalized to the solvent control (DMSO 0.25%), which was set at 1. Before hand BLUs of PH treatments were normalized against respective light intensity of rCYP2D1 determined as the loading control after stripping the original blot and reprobing it with the respective antibodies. Mean ± SD; n ≥ 3.

TCDD highly induced CYP1B1 protein after 20 h and 48 h treatment in hepatocytes from female rats, though induction levels were lower than for CYP1A1 (Figure 56). The two TCDD concentrations tested revealed no difference in induction, both leading to about 16-fold induction at 20 h. TCDD at 48 h resulted in higher protein levels, which ranged between 46-fold (1 nM) and 32-fold (1 0nM). There was no protein band detected for

single E2 treatments. Co-treatments with TCDD + E2 did not modify protein induction observed for TCDD incubations. Co-treatments with E2 10 nM at 20 h appeared to be lower compared to inductions with TCDD 1 and 10 nM, resulting in a reduction by 66% for E2 10 nM/TCDD 1 nM at 20 h. Protein levels were slightly more pronounced after 48 h exposure.

5.3.4. CYP1A1 AND CY1B1 MRNA IN ERALPHA-TRANSFECTED HEPG2

The involvement of ERalpha over-expression in CYP1A1 and CYP1B1 mRNA levels following treatments with TCDD and/or E2 for 20 h was investigated in HepG2 cell line transiently transfected with a human ERalpha expression plasmid compared to wild-type, untransfected HepG2 cells (Figure 57).

Unlike higher absolute basal expression levels in ERalpha-transfected HepG2 (see section 5.3.1), relative TCDD–mediated induction of CYP1A1 and CYP1B1 mRNA was similar to untransfected HepG2 cells with no concentration-dependent effect in the presence of ERalpha after 20 h treatment.

E2 alone did not have an influence on CYP1A1 expression levels compared with the solvent control. Additionally, E2 had no modulating effect on TCDD-induced expression. Treatment with the combinations of TCDD with E2 10 nM or 100 nM significantly lowered CYP1A1 mRNA in transfected HepG2 cells. However, the co-treatment of TCDD 1nM + E2 100 nM in wild-type cells exhibited a high standard variation.

Based on statistical analysis of CYP1B1 mRNA induction, there was no difference in response of the prototype dioxin or the co-treatments between wild-type and transfected HepG2. E2 alone did not induce CYP1B1 mRNA in transfected cells. However, a decrease observed in normal HepG2 cells following exposure to E2 could be compensated in the presence of ERalpha. Thus, treatment with E2 resulted in an ERalpha-dependent increase of CYP1B1 mRNA levels to levels comparable with the solvent control.

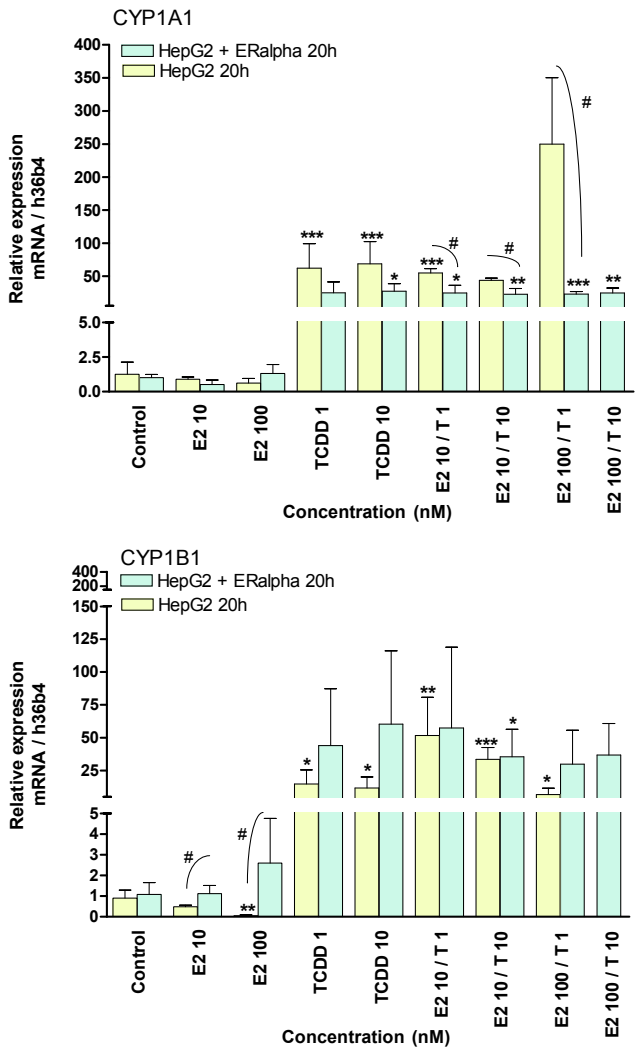

*Figure 57: Real-time RT PCR analysis of transiently transfected HepG2 cell line compared to normal HepG2 cell line on CYP1A1 and CYP1B1 gene expression. Effects of TCDD (T) and/or estradiol (E2) on mRNA levels were assayed following 20 h. Cells were transiently transfected or not with human ERalpha expression plasmid (pRST7-hERα). Co-transfection with ERE-TK-LUC (containing a single copy of vitellogenin-ERE), as well as with pSG5 and pCMVβ-Gal control vectors were performed. CYP expression is normalized against the house keeping gene h36B4 and presented relative to respective time-matched solvent control (DMSO 0.25%).Mean ± SD; n ≥ 3; unpaired t-test, two-tailed p value: mRNA expression levels significantly different from time-matched solvent control: *p ≤ 0.05, **p ≤ 0.01, ***p ≤ 0.001; difference between untransfected and transfected cells: #p ≤ 0.05.*

5.3.5. CYP1A ENZYME ACTIVITY

Altered enzyme function of CYP1A1/2 was evaluated by its enzyme activity. Mixed function oxidases (MFO) activity was performed using the EROD assay according to Donato et al. (1993) as described in Materials and Methods (see section 4). Cells were treated with TCDD 1 nM and/or E2 10 and 100 nM over a period of 48 h.

5.3.5.1. SOLVENT-EFFECTS ON BASAL EROD ACTIVITIES IN HEPATOMA CELL LINES

In order to exclude a possible effect by the solvent DMSO on EROD activity, basal CYP1A1 enzyme activities of untreated cells and DMSO-treated cells were compared in rat und human hepatoma cell lines following 48 h exposure (Figure 58). A final concentration of DMSO 0.25% was chosen representing the maximum concentration used for the treat-

ments conducted in this work. Additionally, the influence of serum concentrations was investigated in parallel, performing treatments in the presence of 0.5% FBS and 10% FBS.

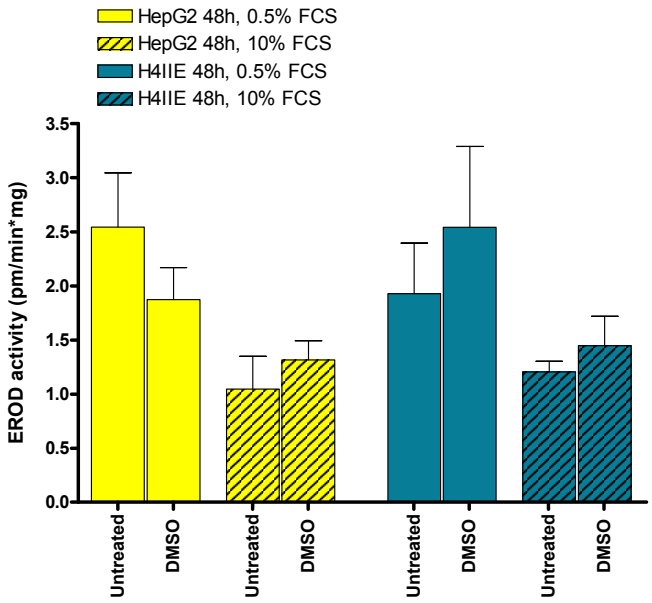

Figure 58. EROD activity measured in HepG2 and H4IIE cells cultured in DMEM without phenol red supplemented with 10% FBS or 0. 5% FBS after 48 h treatment with solvent (DMSO 0.25%) compared to untreated cells. Mean of up to 2 independent experiments with 3 replicates per treatment ± SD.

Results show that there was no influence of DMSO on basal EROD activity in hepatoma cells either under reduced or high serum conditions. EROD activities in the presence of high serum concentrations were lower compared low serum conditions as already observed (see section 5.1).

5.3.5.2. EROD ACTIVITY AFTER EXPOSURE TO TCDD AND/OR E2

Results of the EROD bioassay following 48 h exposure to TCDD and the combination with E2 in the hepatoma cell lines and primary rat hepatocytes from male and female rats from at least three independent experiments are summarized in Figure 59. Basal EROD levels in rat hepatocytes were significantly higher compared to hepatoma cell lines. Solvent control showed an enzyme activity of 1.43 ± 0.46 pM/mg*min in HepG2 which is 9 to 10 times lower than in PHm and PHf. EROD activity was significantly elevated in all tested cells exposed to TCDD alone and to the co-incubation of TCDD with E2. E2 alone was not able to induce CYP1A1 activity compared to control and the co-treatment with TCDD + E2 10 nM or E2 100 nM did not change the effect observed in cells exposed to TCDD alone. Comparison of all cell models revealed that primary hepatocytes from male rats exerted the highest EROD activity. Treatment with TCDD in PHm resulted in 97.8 ± 15.0 pM/mg*min, followed by human HepG2 hepatoma cell line (84.6 ± 28.2 pM/mg*min), whereas primary hepatocytes from female rats and rat H4IIE cell line showed lower levels (68.9 ± 5.6 and 52.0 ± 11.7 pM/mg*min respectively). Thus, the rank order of sensitivity

of the cells towards TCDD in terms of EROD induction was as follows: male rat hepatocytes > HepG2 > female rat hepatocytes > H4IIE.

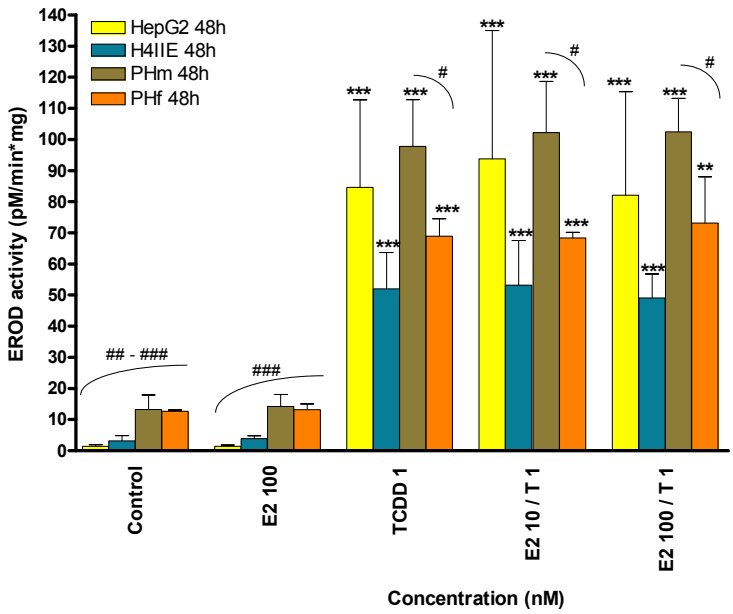

*Figure 59: Effects of TCDD and/or E2 on EROD activity measured in rat and human hepatoma cell lines (HepG2 and H4IIE) and primary rat hepatocytes from male (PHm) and female (PHf) Wistar rats after 48 h treatment in DMEM (0.5% FBS). DMSO (0.25%) served as the solvent control. Mean ± SD; n ≥ 3; unpaired t-test, two-tailed p value: statistically different from control **p ≤ 0.01, ***p ≤ 0.001; treatment statistically different between different cell types #p ≤ 0.05, ##p ≤ 0.01, ###p ≤ 0.001*

Moreover, there was a remarkable gender difference in CYP1A induction between hepatocytes derived from Wistar rats. EROD activity of hepatocytes from male rats was significantly increased compared to hepatocytes from female rats for all the TCDD-treated and co-treated cells. This remarkable difference was not seen for basal EROD levels, i.e. following treatments of DMSO (0.25%) and E2 100 nM. According to the higher basal levels in primary rat hepatocytes compared to hepatoma cell lines, fold-inductions relative to control showed highest induction levels by TCDD in HepG2 cell line followed by H4IIE cell line (see Table 21).

Table 21: Fold-inductions of EROD activity normalized to solvent control (DMSO 0.25%) of results presented in Figure 59.

Fold-inductions of EROD activity					
	Control	E2 100 nM	TCDD 1 nM	E2 10 / T 1	E2 100 / TCDD 1
HepG2	1.00	0.98	59.00	65.41	57.31
H4IIE	1.00	1.22	16.59	16.96	15.64
PHm	1.00	1.07	7.37	7.70	7.72
PHf	1.00	1.05	5.46	5.42	5.79

5.3.6. SUMMARY OF CYP INDUCTION

5.3.6.1. EFFECTS OF TCDD AND/OR E2

In all cell models TCDD was able to induce both CYP1A1 and CYP1B1 levels significantly after 20 h and 48 h treatment. A concentration of TCDD 1 nM was sufficient to lead to remarkable increases that could not be further enhanced by 10 nM.

Estradiol alone 10 nM or 100 nM had no effect on CYP1A1 mRNA and protein levels. In contrast, E2 alone was able to slightly increase CYP1B1 mRNA levels in rat hepatocytes from male and female Wistar rats but only after 48 h exposure. In ERalpha-transfected HepG2 cells E2 alone had no influence on CYP1B1 mRNA compared with solvent control. However, a slight decrease of CYP1B1 observed in wild-type cells following treatment with E2 re-increased to control levels in the presence of ERalpha.

Generally, co-treatments with E2 nM did not modulate TCDD-induced effects on CYP1A1 and CYP1B1 expression or CYP1A enzyme activity (after 48 h) Nevertheless, single occurrences of co-treatments showing enhancing effectson TCDD-mediated induction were found at the transcript level in HepG2 and H4IIE cells. In rat hepatocytes from both sexes decreased CYP1B1 mRNA were observed for some of the co-treatments compared with TCDD-mediated expression. Over-expression of ERalpha did not affect CYP induction levels by treatments with TCDD or the combination of TCDD with E2 in transfected HepG2.

5.3.6.2. COMPARISON OF TCDD-MEDIATED INDUCTION

Among the different cell models, rat H4IIE cell line showed the highest increase in CYP1A1 mRNA induction by TCDD at 20 h but the lowest CYP1A1 protein induction. TCDD-induced CYP1A1 mRNA levels were lowest in rat hepatocytes from female rats, which were about 2 to 2.5 times lower compared with male-derived hepatocytes and HepG2 cell line. TCDD-induced CYP1A1 protein levels were highest in HepG2 cells followed by the rat primary hepatocytes and rat hepatoma cell line.

Rat and human hepatoma cell lines showed low CYP1B1 mRNA induction by TCDD which correlated well with protein levels. TCDD-mediated CYP1B1 mRNA induction was much more pronounced in rat hepatocytes. Compared with high CYP1B1 mRNA induction levels in rat hepatocytes, their corresponding protein levels were relatively low. Nevertheless, female-derived hepatocytes showed highest CYP1B1 protein induction of all tested cell models and at both treatment times. CYP1B1 protein levels of male-isolated rat hepatocytes increased to the same level as in PHf but only after 48 h.

Generally TCDD-mediated CYP1A1 induction was higher than CYP1B1 induction in hepatoma cell lines.

5.3.6.3. COMPARISON OF THE TWO TREATMENT TIMES

Regarding the two treatment times, a slight trend towards more pronounced CYP expression levels at 48 h was not consistent, neither among treatments nor between transcription and translation levels. HepG2 showed higher mRNA expression levels for some but not all dioxin treatments at 48 h. This effect was not subsequently reflected in protein levels. H4IIE cells showed higher TCDD-induced CYP1A1 mRNA levels at 20 h, whereas protein levels were more pronounced at 48 h. In turn, induced CYP1B1 mRNA levels were higher at 48 h in H4IIE, which was not reflected in respective protein levels. In rat hepatocytes there was no consistent difference in expression levels noted between the two treatment times. Higher CYP1B1 protein levels were found in male rat hepatocytes at 48 h. In female rat hepatocytes, slightly higher TCDD-induced CYP1A1 and CYP1B1 protein could be assumed at the longer treatment time.

5.4. EXPRESSION OF NUCLEAR RECEPTORS

5.4.1. BASAL AHR MRNA LEVELS

The different cell models showed marked differential expression of the Ah receptor mRNA at basal levels (Figure 60). At both treatment times basal AhR mRNA levels were highest in PHm, which were significantly higher than in female-derived cells (up to 12-fold at 48 h). H4IIE cells expressed the lowest basal AhR mRNA, which was significantly different from HepG2 cell line. There was no difference in steady state AhR mRNA in HepG2 with or without transient expression of ERalpha. Different treatment times had no influence on AhR expression levels.

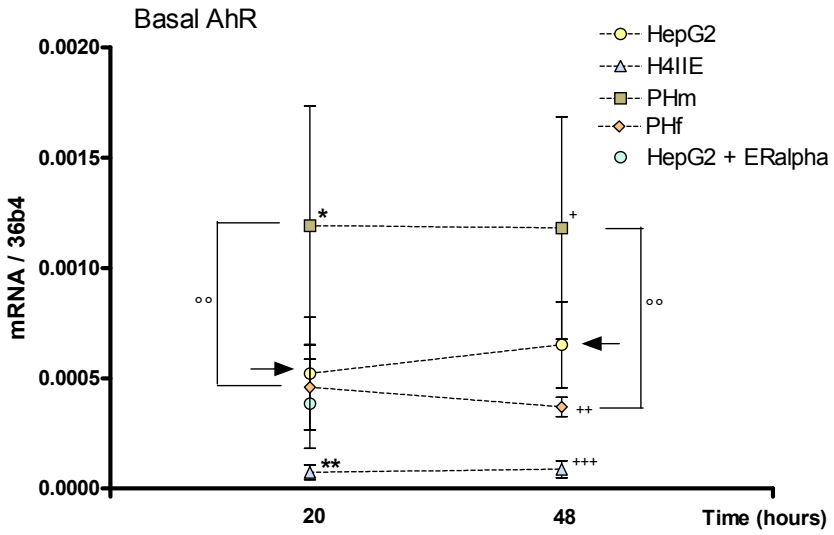

*Figure 60: Real-time RT PCR analysis of basal Ah receptor mRNA levels in hepatoma cell lines HepG2 and H4IIE and rat hepatocytes from male (PHm) and female (PHf) Wistar rats treated with DMSO (0.25%) over a period of 20 h and 48 h. Transiently transfected HepG2 with ERalpha expression plasmid (HepG2 + ERalpha) were investigated at 20 h. Results were normalized against the housekeeping gene 36B4 and expressed as ratios of delta ct values. Mean ± SD; n ≥ 3; unpaired t-test, two-tailed p value: mRNA expression levels significantly different from HepG2 control at 20 h (*p ≤ 0.05, **p ≤ 0.01) or at 48 h ($^{++}$p ≤ 0.01, $^{+++}$p ≤ 0.001); mRNA expression levels significantly different between 20 h and 48 h: not significant; mRNA expression significantly different between PHm and PHf °°p ≤ 0.01.*

Rank order basal AhR mRNA	
20 h	*PHm > HepG2 = HepG2 + ERalpha = PHf >H4IIE*
48 h	*PHm > HepG2 > PHf > H4IIE*

5.4.2. AhR mRNA Expression after Exposure to TCDD and /or E2

Quantitative Real-time RT PCR using a fluorogenic TaqMan probe demonstrated AhR mRNA expression in the two hepatoma cells line as well as in primary rat hepatocytes from male and female Wistar rats at both basal levels and following exposure to the test substances TCDD and/or E2 (Figure 61 and Figure 62). There were no significant changes in AhR mRNA obtained in HepG2 cells and in primary rat hepatocyte cultures following treatments for 20 h and 48 h. Rat hepatoma cells significantly induced AhR mRNA following exposure to TCDD 1 nM and 10 nM (2.81 ± 1.17–fold and 3.87 ± 1.56– fold respectively) and the co-treatments of TCDD with E2 (e.g. TCDD 1nM/ E2 10 nM: 3.57 ± 0.95). These inductions were only detected after 48 h with no difference in expression pattern between the treatments and different concentrations. Furthermore, a small but significant

increase was also observed for E2 alone (10 nM) in the rat hepatoma cells at 48 h, resulting in a 2.04 ± 0.18-fold expression.

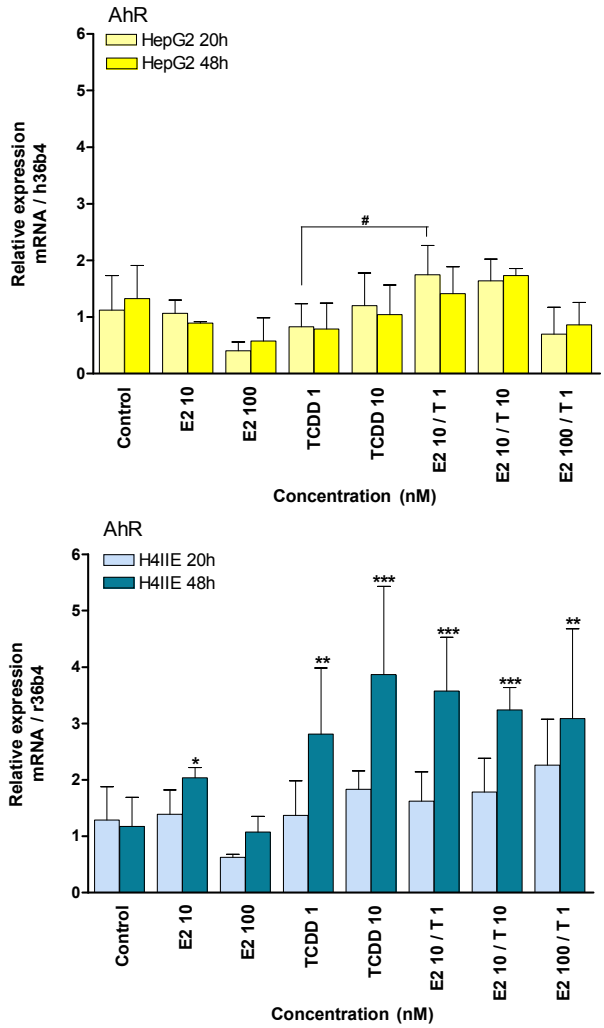

*Figure 61: TaqMan real-time RT PCR analysis of rat and human hepatoma cells HepG2 and H4IIE on AhR gene expression. Effects of TCDD (T) and/or Estradiol (E2) on mRNA levels were assayed following 20 h and 48 h treatment. AhR expression is normalized to 36B4 expression and presented relative to respective solvent control (DMSO 0.25%). Mean ± SD; n ≥ 3; unpaired t-test, two-tailed p value: mRNA expression levels significantly different from time-matched solvent control *p ≤ 0.05, **p ≤ 0.01, ***p ≤ 0.001; mRNA expression levels significantly different between time-matched treatments #p ≤ 0.05.*

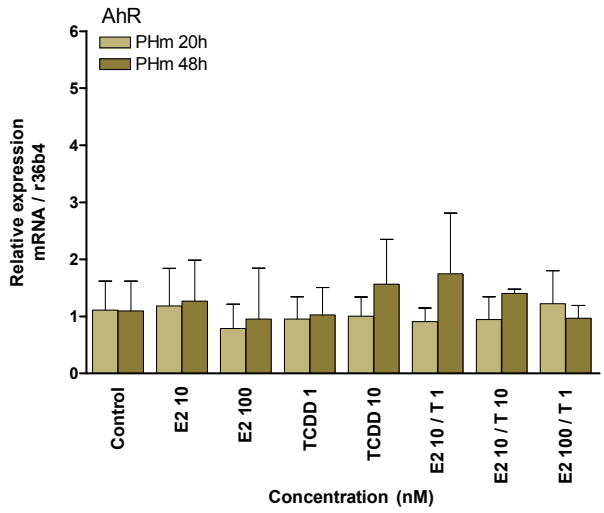

*Figure 62: TaqMan real-time RT PCR analysis of primary hepatocytes from male (PHm) and female (PHf) Wistar rats on AhR gene expression. Effects of TCDD (T) and/or Estradiol (E2) on mRNA levels were assayed following 20 h and 48 h treatment. AhR expression is normalized to 36B4 expression and presented relative to respective solvent control (DMSO 0.25%). Mean ± SD; n ≥ 3; unpaired t-test, two-tailed p value: mRNA expression levels significantly different from time-matched solvent control *p ≤ 0.05*

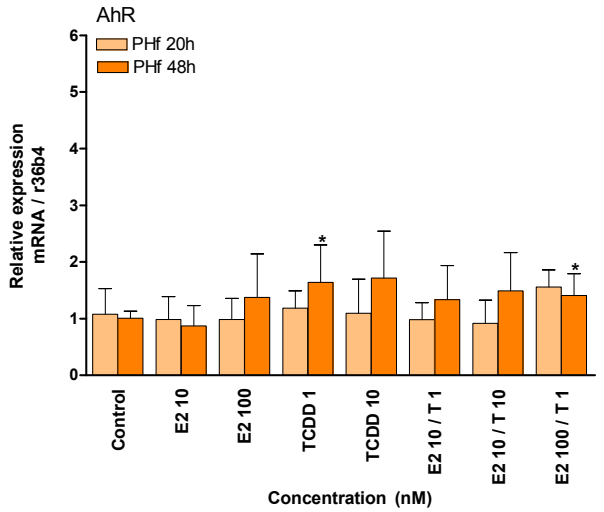

Primary hepatocytes from female rats showed slightly but significantly increased AhR mRNA levels following exposure to TCDD 1 nM and the co-treatment of TCDD 1 nM + E2 100 nM at the 48 h time point.

In ERalpha-transfected HepG2 cellsAhR mRNA was slightly but significantly elevated after exposure to TCDD 10 nM (2.1 ± 0.5-fold) and the co-treatment of TCDD 10 nM + E2 10 nM (Figure 63). Compared to wild-type HepG2 cells at 20 h, relative AhR mRNA levels were significantly increased after E2 100 nM or TCDD 10 nM treatments in the presence of over-expressed ERalpha.

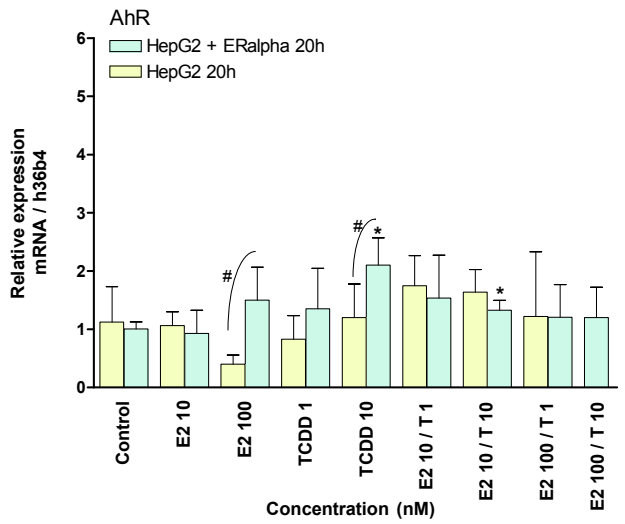

*Figure 63: Real-time RT PCR analysis of transiently transfected HepG2 cell line compared to normal HepG2 cell line on AhR gene expression. Effects of TCDD (T) and/or Estradiol (E2) on mRNA levels were assayed following 20 h. Cells were transiently transfected or not with human ERalpha expression plasmid (pRST7-hERα). Co-transfection with ERE-TK-LUC (containing a single copy of vitellogenin-ERE), as well as pSG5 and pCMVβ-Gal control vectors were performed. AhR expression is normalized against the house keeping gene h36B4 and presented relative to respective time-matched solvent control (DMSO 0.25%). Mean ± SD; n ≥ 3; unpaired t-test, two-tailed p value: mRNA expression levels significantly different from time-matched solvent control: *p ≤ 0.05; difference between untransfected and transfected cells: #p ≤ 0.05.*

5.4.3. BASAL ERALPHA MRNA LEVELS

ERalpha mRNA was not detectable in hepatoma cell lines usingTaqMan Real-time RT PCR, even after extension of cycle numbers in the temperature protocol or increase of amount of cDNA template as described in section 4.6.2.4. Contrarily to hepatoma cell lines, low measurable basal levels of ERalpha mRNA were detected in rat hepatocytes from male and female Wistar rats as presented in Figure 64. There was no sex difference observed, and treatment time had no influence either. Transient transfection of ERalpha in HepG2 cell line showed high basal ERalpha mRNA levels which were more than 500-fold higher compared to rat hepatocytes. There was a difference in ERalpha contents of three orders of magnitude.

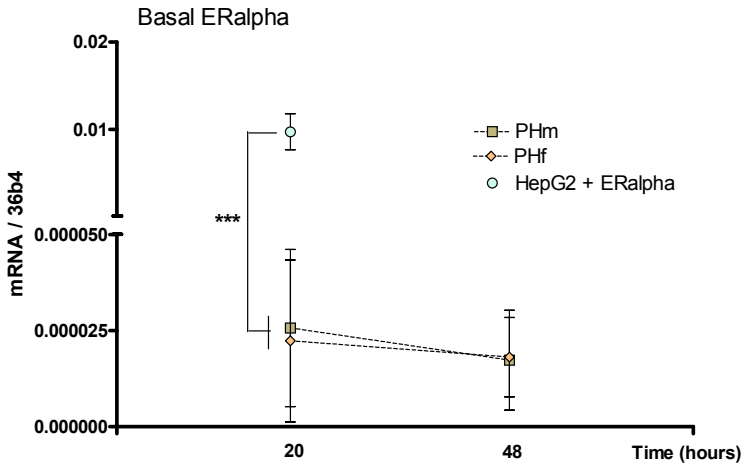

*Figure 64: Real-time RT PCR analysis of basal Estrogen receptor alpha mRNA levels in hepatoma cell lines HepG2 and H4IIE and rat hepatocytes from male (PHm) and female (PHf) Wistar rats treated with DMSO (0.25%) over a period of 20 h and 48 h. Transiently transfected HepG2 with ERalpha expression plasmid (HepG2 + ERalpha) were investigated at 20 h. Results were normalized against the housekeeping gene 36B4 and expressed as ratios of delta ct values. There was no mRNA detected for HepG2 and H4IIE Mean ± SD; n ≥ 3; unpaired t-test, two-tailed p value: mRNA expression levels significantly different from HepG2_ERalpha control at 20 h ***p ≤ 0.001; mRNA expression levels significantly different between 20 h and 48 h: not significant; mRNA expression significantly different between PHm and PHf: not significant.*

5.4.4. ERALPHA EXPRESSION AFTER EXPOSURE TO TCDD AND/ OR E2

5.4.4.1. MRNA LEVELS

ERalpha mRNA levels were not affected by the treatments in male-derived hepatocytes after 20 h and 48 h (see Figure 65). Female-derived hepatocytes showed decreased relative ERalpha mRNA levels following treatment with E2 10 nM and the co-treatment of E2 10 nM/TCDD 1 nM at 20 h. Moreover, ERalpha mRNA levels were also decreased following exposure E2 100 nM, TCDD 1nM and the co-treatments of E2 10 nM and TCDD 1nM/10 nM at 48 h. All in all, there is a tendency of decreased ERalpha mRNA levels in female-derived rat hepatocyte culture which was mainly mediated by single treatment with E2 10 nM or the respective co-treatments with E2 10 nM.

. Over-expression of ERalpha in transfected HepG2 cells was not affected by treatments with TCDD and/or E2 at the indicated concentrations at 20 h.

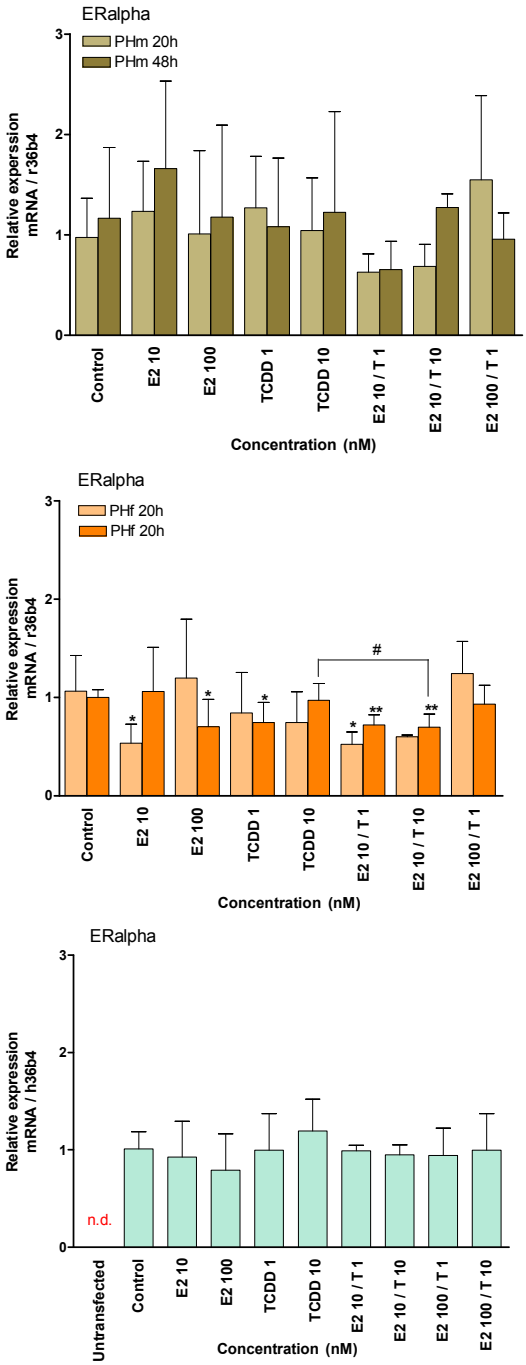

*Figure 65: TaqMan real-time RT PCR analysis of primary hepatocytes from male (PHm) and female (PHf) Wistar rats and ERalpha-transfected HepG2 cells on ERalpha gene expression. Effects of TCDD (T) and/or Estradiol (E2) on mRNA levels were assayed following 20 h or 48 h treatment. ERalpha expression is normalized to 36B4 expression and presented relative to respective solvent control (DMSO 0.25%). Mean ± SD; n ≥ 3; unpaired t-test, two-tailed p-value: mRNA expression levels significantly different from time-matched solvent control *p ≤ 0.05; **p ≤ 0.01; mRNA expression levels significantly different between time-matched treatments #p ≤ 0.05, n.d.: not detected.*

5.4.4.2. PROTEIN LEVELS

ERalpha protein (68 kDa) could be detected in primary rat hepatocytes at both treatment times as a faint band (see Figure 66). The treatments of TCDD and or/E2 had no effect on nuclear receptor levels.

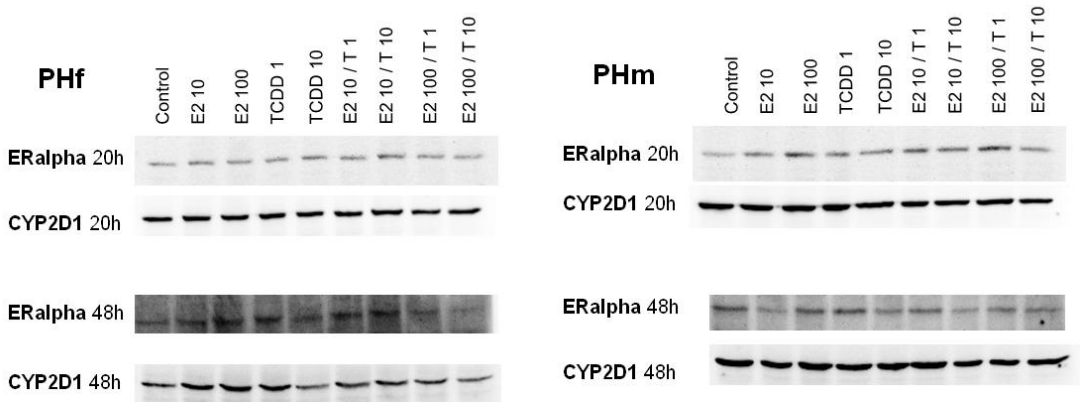

Figure 66: Representative Western Blots of ERalpha protein levels in primary rat hepatocytes from male (PHm) and female (PHf) Wistar rats treated with TCDD (T) and/or E2 for 20 h or 48 h at the indicated nanomolar concentrations. Time-matched PHm and PHf samples were handled simultaneously throughout the whole procedure of SDS-PAGE, immunoblotting and chemiluminescent detection and thus can be compared directly. Lanes from right to left were loaded with respective homogenate samples (50 µg/lane) as outlined. DMSO (0.25%) served as the solvent control. After detection of ERalpha immunoreactive protein, the membrane was stripped and reprobed with CYP2D1 antibodies as the control protein.

5.5. EFFECTS OF ERALPHA ON XRE- AND ERE-DEPENDENT TRANSCRIPTIONAL ACTIVITY IN HEPG2

The transactivation functions of estrogen receptor alpha on ER- and AhR-regulated target genes were investigated in HepG2 cell line.

HepG2 cells were transiently co-transfected with a luciferase transporter under the regulation of the human vitellogenin (ERE-TK-LUC) and co-transfected or not with a human ERalpha expression plasmid (see Figure 67). Treatment with E2 10 nM for 20 h resulted in a remarkable induction of reporter gene activity up to 84-fold above solvent control activity. When cells were co-treated with E2 10 nM and TCDD 1 nM, hormone-induced ERE-mediated activity was significantly decreased to about half the activity of E2 alone (42-fold). TCDD alone did not activate ERE-mediated transcription. The estrogenic action of E2 and the co-treatment was blocked by the pure estrogen antagonist ZK 191 703 (1 µM, simultaneously added) and resulted in luciferase activity similar to that of solvent control. In contrast, a known AhR antagonist, 8-methoxypsoralen (50 µM, simultaneously added) to the test compounds did not affect ERE-dependent induction. Mono (ERE-TK-LUC)-transfected HepG2 cells still resulted in a slight induction of reporter gene activity upon E2 treatment, which could be dropped down using the pure anti-estrogen ZK 191 703. However, co-treatment of E2 10 nM with TCDD 1 M had no effect in the absence of con-

stitutively expressed ERalpha. Basal levels of ERE-mediated activity were not influenced by transfection of ERalpha or solvent treatment.

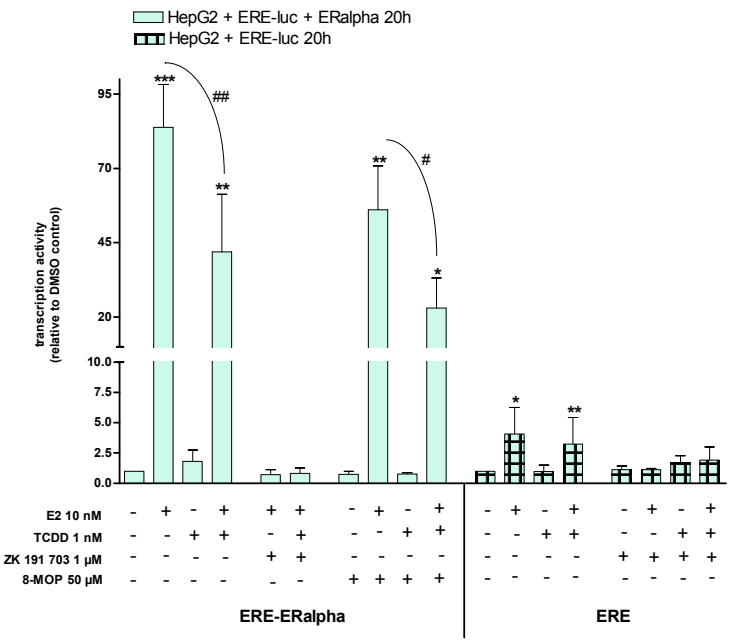

*Figure 67: Effect of ERalpha on ER-mediated transcription. HepG2 cells were transiently transfected with ERE-TK-LUC reporter gene (containing a single copy of vitellogenin-ERE) and co-transfected or not with human ERalpha expression plasmid (pRST7-hERalpha). Cells were treated with vehicle control (DMSO 0.2% max.), TCDD (1 nM) and/or E2 (10 nM) or co-treated with ZK 191 703 (1 µM) or 8-methoxypsoralen (MOP, 50 µM in the dark) for 20 h as indicated (+/-). Cells were transiently co-transfected with pSG5 and pCMVβ-Gal control vectors. Luciferase activity was normalized against β-galactosidase activity and protein contents and related to respective DMSO control. Mean ± SD; n ≥ 3; unpaired t-test, two-tailed p value: significantly different from respective solvent control: *p ≤ 0.05, **p ≤ 0.01, ***p ≤ 0.001; significantly different between treatments: #p ≤ 0.05, ##p ≤ 0.01*

When HepG2 cells were co-transfected with a XRE-luciferase reporter gene encoding for the rat CYP1A1 in combination with ERalpha expression plasmid, TCDD 1 nM (20 h) induced the reporter gene activity 9-fold above solvent control (see Figure 68). Co-treatment of TCDD 1 nM with 10 nM E2 significantly enhanced TCDD-mediated transcriptional activity via AhR resulting in an up to 16-fold increase. Though TCDD effectively activated transcription through XRE, E2 alone did not. In the presence of the anti-estrogen ZK 191 703, the XRE-driven increase by TCDD 1 nM was still observed (7-fold), but the co-treatment resulted in about the same increase (8-fold) as that of TCDD alone**.** The AhR-mediated action was inhibited by the AhR antagonist 8-MOP. In mono (XRE-LUC)-transfection experiments without exogenous receptor ERalpha, TCDD stimulated (12-fold) XRE-mediated transcription, but the co-treatment of both TCDD+E2 did not enhance this activation. There was no statistical difference obtained between TCDD-induced luciferase activity in the presence of the ER antagonist or in the absence of transfected ERalpha, alike for the increase by the co-treatments. Basal levels of XRE-mediated activity were not influenced by transfection of ERalpha or solvent treatment.

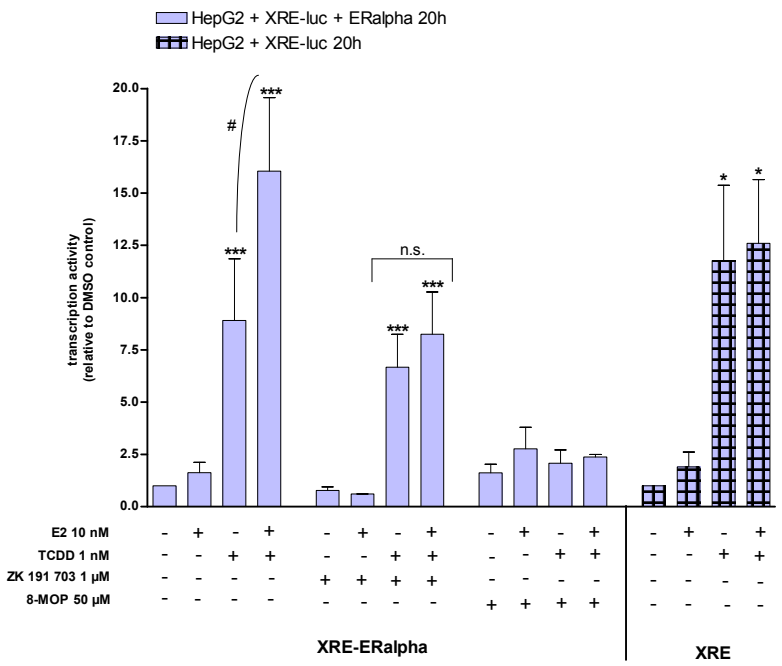

*Figure 68: Effect of ERalpha on AhR-mediated transcription. HepG2 cells were transiently transfected with pGL3-XRE reporter gene (containing a fragment of the rat CYP1A1 gene including 2x XREs) and co-transfected or not with human ERalpha expression plasmid (pRST7-hERalpha). Cells were treated with the vehicle control (DMSO 0.2% max.), TCDD (1 nM) and/or E2 (10 nM) or co-treated with ZK 191 703 (1 µM) or 8-methoxypsoralen (MOP, 50 µM in the dark) for 20 h as indicated (+/-). Cells were transiently co-transfected with pSG5 and pCMVβ-Gal control vectors. Luciferase activity was normalized against β-galactosidase activity and protein contents and related to respective DMSO control. Mean ± SD; n ≥ 3; unpaired t-test, two-tailed p value: significantly different from respective solvent control: *p ≤ 0.05, **p ≤ 0.01, ***p ≤ 0.001; significantly different between treatments: #p ≤ 0.05, n.s.: non-significant.*

5.6. CELLULAR ROS LEVEL

In order to evaluate the formation of ROS in the different cell models, the H_2DCFDA fluorescence assay was performed in cracked cells in the presence of NADPH. For this purpose, cells were treated over a period of 20 or 48 h with TCDD (1 and 10 nM) and /or E2 (10 and 100 nM).

5.6.1. BASAL ROS LEVELS

Distinct basal levels in ROS formation were observed between hepatoma cell lines and rat hepatocytes. Rat hepatocytes from male and female rats showed a similar response and

exerted significantly higher ROS levels than rat and human hepatoma cell lines in DMSO (0.1%)-treated cells at 20 h and 48 h (Figure 69). Basal levels of ROS formation were in the same range for rat and human hepatoma cell line. Treatment with ethanol showed a similar ROS formation pattern as DMSO. Even though the experimentswith ethanol were not performed three times in H4IIE and rat hepatocytes from male rats it is however suggested that ethanol has no effect on basal ROS levels different from DMSO.

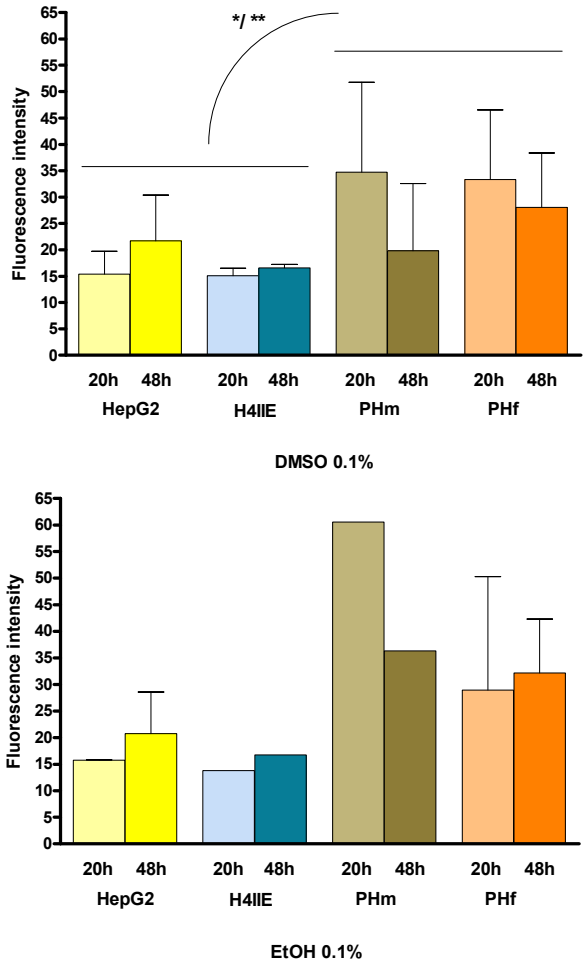

Figure 69: Basal cellular ROS measured as oxidation of H_2DCF in 0.1% solvent–treated (DMSO, EtOH) hepatoma cell lines HepG2 and H4IIE for 20 h and 48 h. Results are presented as fluorescence intensities proportional to dichlorofluo-rescein (DCF) formation. NADPH was added just prior to the reaction. Mean ± SD for experiments $n \geq 3$; $n = 1$ for incubation with EtOH 0.1% in H4IIE, PHm, and HepG2 (20 h); unpaired t-test, two-tailed p value: statistical significance $*p \leq 0.05$, $**p \leq 0.01$.

5.6.2. RELATIVE ROS LEVELS AFTER EXPOSURE TO TCDD AND/OR E2

5.6.2.1. ROS FORMATION IN HEPATOMA CELL LINES

The effects of TCDD and/or E2 on cellular ROS levels in hepatoma cell lines HepG2 and H4IIE following 20 h or 48 h treatment are shown in Figure 70.

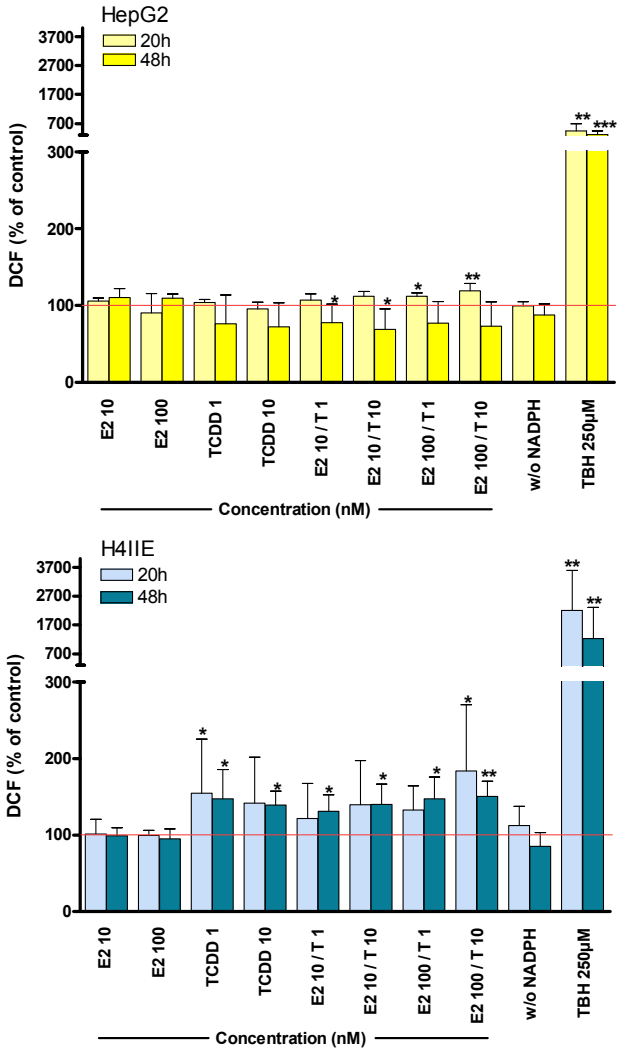

*Figure 70: Formation of cellular ROS measured as oxidation of H_2DCF in hepatoma cell lines HepG2 and H4IIE exposed to TCDD (T) and/or E2 for 20 h and 48 h. Results are normalized to the solvent control (DMSO 0.1%) and presented in percent of dichlorofluorescein (DCF) formation related to an external calibration curve. The horizontal red-colored line represents the solvent control level set at 100%. Tert-butylhydroxyde (TBH) served as the positive control and was initially added to the well of cracked untreated cells just before starting the incubation with the fluorescent dye. NADPH-independent ROS formation (w/o NADPH) was also monitored. Mean ± SD; n ≥ 3; unpaired t-test, two-tailed p value: statistically different from solvent control: *p ≤ 0.05, **p ≤ 0.01, ***p ≤ 0.001.*

In human HepG2 cells neither TCDD nor E2 alone induced ROS formation after 20 h treatment. Only the co-treatments of TCDD with E2 100 nM slightly but significantly enhanced formation of ROS, leading to 112.1 ± 4.5% forE2 100 nM/TCDD 1 nM and 119.5 ± 9.1% for E2 100 nM/TCDD 10 nM. After 48 h, no elevation in the cellular ROS status was observed. There was a trend towards decreased ROS levels compared to con-

trol, which was significantly decreased for the co-treatments of TCDD (both concentrations) + E2 10 nM by up to 31% (E2/TCDD 10 nM: 68.8 ± 27.1%).

In rat H4IIE cells at 20 h TCDD 1 nM and the combination of TCDD 10 nM + E2 100 nM significantly induced ROS formation, resulting in an up to 1.83-fold increase (Figure 70). E2 alone showed no effect. Prolonged treatment time (48 h) further enhanced the oxidative stress response by TCDD. Statistically significant elevated ROS levels were achieved for all the treatments or co-treatments with TCDD without a concentration-dependent effect. TCDD 10 nM led to induced oxidative stress of 139.4 ± 18.2% and the highest ROS level was obtained by the respective co-treatment TCDD 10 nM + E2 100 nM (150.9 ± 19.93%). However, co-treatment effects did not statistically differ from single TCDD treatments. There was no statistical difference obtained between the two treatment times.

Tert-butyl hydroperoxide (TBH, 250 µM), used as the positive control, was efficient to extensively and significantly increase ROS formation in hepatoma cell lines which was approximately 5-fold more prominent in H4IIE (2210 ± 1379%) cells than in HepG2 (448.8 ± 248.2%) at 20 h. Different exposure time had no effect on the response. Generally, TBH-induced alterations were about 4- (HepG2) to 12-fold (H4IIE) more effective in inducing ROS than the test substances, suggesting that HepG2 cells are less sensitive. NADPH-independent ROS formation did not differ from control levels at both treatment times and for both cell lines.

5.6.2.2. ROS FORMATION IN ERALPHA-TRANSFECTED HEPG2

ROS formation following treatment with TCDD 1 nM and/or E2 10 nM for 20 h was also determined in the presence of over-expressedERalpha, which was transiently transfected into HepG2 cells (Figure 71). Control levels of basal ROS formation were not modified as a consequence of ERalpha transfection. Additionally, no effect was observed following treatments with TCDD 1 nM and the co-treatments with E2 10 nM in HepG2+ERalpha. Solely E2 10 nM resulted in a slight significant decrease of ROS level compared to control.

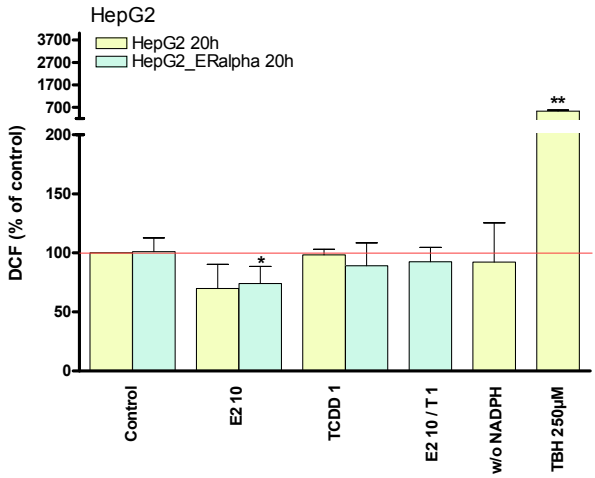

*Figure 71: Formation of cellular ROS measured as oxidation of H_2DCF in HepG2 cell line. Cells were transiently transfected or not with human ERalpha expression plasmid (pRST7-hERalpha) and exposed to TCDD (T) and/or E2 for 20 h. Co-transfections with ERE-TK-LUC (containing a single copy of vitellogenin-ERE), as well as pSG5 and pCMVβ-Gal control vectors were performed. Results are normalized to the untransfected solvent control (DMSO 0.1%) and presented in percent of dichlorofluorescein (DCF) formation related to an external calibration curve. The horizontal red-colored line represents the untransfected solvent control level. Tert-butylhydroxyde (TBH) served as the positive control and was initially added to the well of cracked untreated cells just before starting the incubation with the fluorescent dye. NADPH-independent ROS formation (w/o NADPH) was also monitored. Mean ± SD; n = 3; unpaired t-test, two-tailed p value: statistically different from respective solvent control: *p ≤ 0.05; difference between untransfected and transfected cells: not significant.*

5.6.2.3. ROS FORMATION IN PRIMARY RAT HEPATOCYTES

The production of ROS following treatments of TCDD and/or E2 in primary rat hepatocytes derived from both sexes after 20 h and 48 h exposure are presented in Figure 72.

Neither TCDD nor E2, or the combinations of both compounds at the tested concentrations were able to modify ROS formation after 20 h in primary hepatocytes from male rats. After 48 h incubation E2 alone at the high concentration (100 nM; 140.3 ± 31.8%) and the co-treatment of E2 100 nM with TCDD 1 nM (125.5 ± 13.1%) were able to significantly increase ROS production.

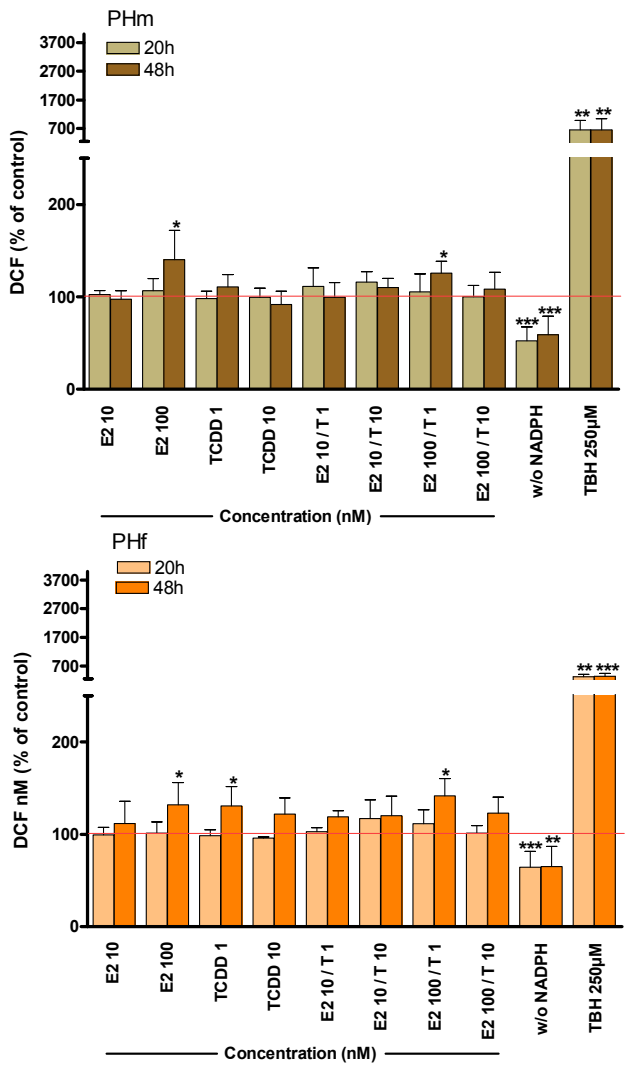

*Figure 72: Formation of cellular ROS measured as oxidation of H2DCF in primary rat hepatocytes from male (PHm) and female (PHf) Wistar rats exposed to TCDD (T) and/or E2 for 20 h and 48 h. Results are normalized to the solvent control (DMSO 0.1%) and presented in percent of dichlorofluorescein (DCF) formation related to an external calibration curve. The horizontal red-colored line represents the solvent control level set at 100%. Tert-butylhydroxyde (TBH) served as the positive control and was initially added to the well of cracked untreated cells just before starting the incubation with the fluorescent dye. NADPH-independent ROS formation (w/o NADPH) was also monitored. Mean ± SD; n ≥ 3; unpaired t-test, two-tailed p value: statistically different from solvent control: *p ≤ 0.05, **p ≤ 0.01, ***p ≤ 0.001.*

For female-derived rat hepatocytes the situation was similar. Only at the longer treatment time of 48 h, ROS formation was significantly enhanced following exposure to E2 100 nM (131.9 ± 24.1%) or TCDD 1 nM (130.8 ± 20.9%). The combination of both compounds also resulted in an increase (E2 100/TCDD 1: 141.8 ± 18.6%) which reached the same level as the single compound treatments.

TBH-induced ROS production resulted in an about 6.5-fold increase in hepatocytes from male rats. Its ROS formation was approximately 2 times higher in PHm (653 ± 329%) than in PHf (324 ± 87%) at 20 h. Similar results were obtained after treatment over 48 h. NADPH-independent formation of ROS was significantly decreased in rat hepatocytes derived from both sexes, i.e. by up to 25-47% in PHf and PHm respectively.

5.6.3. EFFECTS OF CYP1 INHIBITION ON ROS FORMATION

The interaction of the furocoumarin 8-methoxypsoralen (8-MOP) on ROS formation was investigated in hepatoma cells and rat primary hepatocytes. 8-MOP is known to be a potent inhibitor of CYP1A1 activity. Cell treatment conditions for the inhibitor were adapted according to Baumgart and co-authors (2005). Cells were treated simultaneously with the test substances TCDD and/or E2 in the presence 8-MOP (50 µM) over a period of 20 h and 48 h under exclusion of light. ROS formation was monitored in the H_2DCFDA fluorescence assay.

5.6.3.1. ROS FORMATION IN 8-MOP-TREATED HEPG2

In general, no alterations of ROS levels were observed in HepG2 cells with and without treatment with the CYP1 inhibitor 8-MOP at 20 h and 48 h (see Figure 73). The slightly induced ROS formation by the co-treatment of E2 10 nM/TCDD 10 nM seen at 20 h was significantly decreased by 8-MOP. A slight but significant decrease by 8-MOP was also observed for the co-treatment of E2 10 nM/TCDD 1 nM.

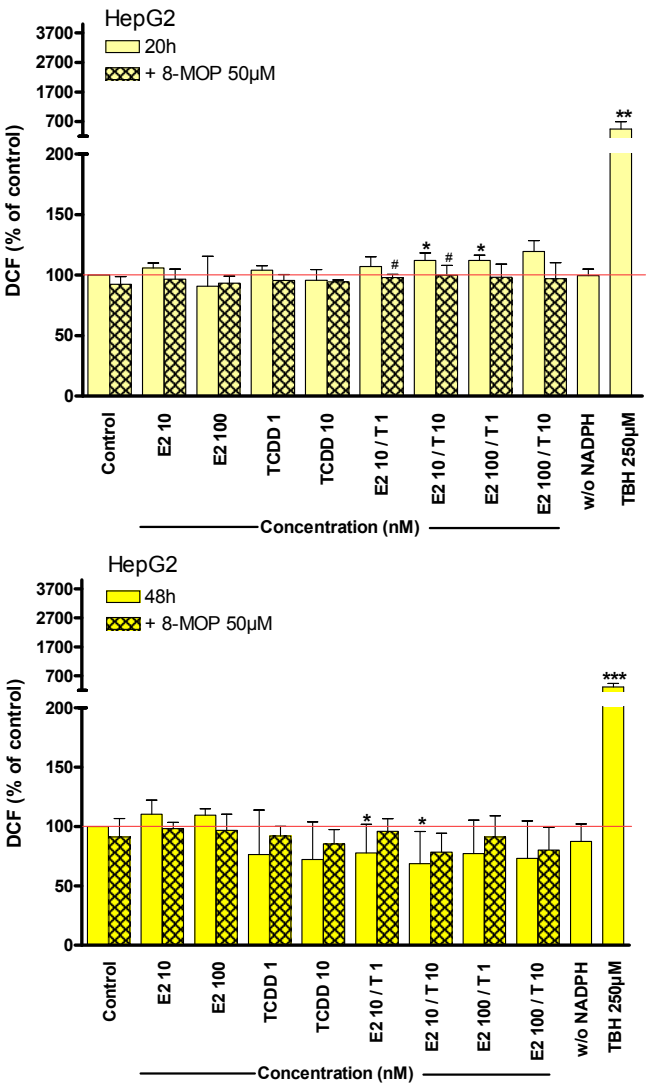

*Figure 73: Formation of cellular ROS measured as oxidation of H_2DCF in human hepatoma cell line HepG2 exposed to TCDD (T) and/or E2 for 20 h and 48 h in the absence or presence of 8-methoxypsoralen (8-MOP, 50 µM). Results are normalized to the solvent control without 8-MOP (DMSO 0.1%) and presented in percent of dichlorofluorescein (DCF) formation related to an external calibration curve. The horizontal red-colored line represents the solvent control level set at 100%. Tert-butylhydroxyde (TBH) served as the positive control and was initially added to the well of cracked untreated cells just before starting the incubation with the fluorescent dye. NADPH-independent ROS formation (w/o NADPH) was also monitored. Mean ± SD; n ≥ 3; unpaired t-test, two-tailed p value: statistically different from solvent control: *p ≤ 0.05, **p ≤ 0.01, ***p ≤ 0.001; significantly different from respective treatment with 8-MOP: #p ≤ 0.05*

5.6.3.2. ROS FORMATION IN 8-MOP-TREATED H4IIE

In a more general term, all incubations with 8-MOP decreased ROS levels in H4IIE cell line to a level of about 60-70% of solvent control without 8-MOP at 20 h and 48 h (Figure 74). The different treatments had no impact on 8-MOP-mediated ROS levels.

Thus, all TCDD-mediated induced ROS levels at both treatment times were reduced to basal ROS levels for 8-MOP treatment.

Since ROS induction in H4IIE was more pronounced following 48 h treatments with TCDD or the co-treatments, the 8-MOP-dependent decrase was statistically significant for nearly all the treatments that showed a significant increase in the absence of 8-MOP.

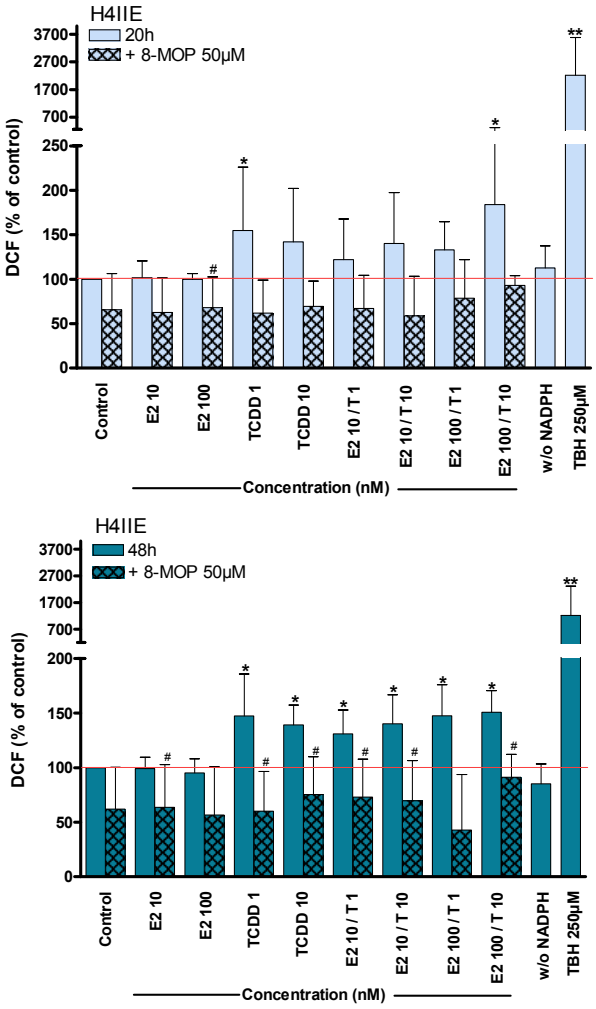

*Figure 74: Formation of cellular ROS measured as oxidation of H_2DCF in rat hepatoma cell line H4IIE exposed to TCDD (T) and/or E2 for 20 h and 48 h in the absence or presence of 8-methoxypsoralen (8-MOP, 50 µM). Results are normalized to the solvent control without 8-MOP (DMSO 0.1%) and presented in percent of dichlorofluorescein (DCF) formation related to an external calibration curve. Control level (100%) is indicated as a red line. Tert-butylhydroxyde (TBH) served as the positive control and was initially added to the well of cracked untreated cells just before starting the incubation with the fluorescent dye. NADPH-independent ROS formation (w/o NADPH) was also monitored. Mean ± SD; n ≥ 3; unpaired t-test, two-tailed p value: statistically different from solvent control: *p ≤ 0.05, **p ≤ 0.01, ***p ≤ 0.001; significantly different from respective treatment with 8-MOP: #p ≤ 0.05*

For example, ROS induction evoked by TCDD 1nM after 48 h (147.5 ± 38.4%) was completely diminished down to 60.18 ± 36.44% in the presence of 8-MOP. These observations indicated that TCDD-induced oxidative stress was prevented by applying a potent inhibitor of CYP1A activity.

5.6.3.3. ROS FORMATION IN 8-MOP-TREATED RAT HEPATOCYTES FROM MALES

Modulation of 8-MOP on cellular ROS level in primary rat hepatocytes are summarized in Figure 75 and Figure 76. In male-derived rat hepatocytes after 20 h, 8-MOP was able to significantly decrease basal ROS levels about one third down to 70.47 ± 4.39% solvent control without 8-MOP (DMSO 0.1%). The different treatments in the presence of 8-MOP caused no effect compared to 8-MOP control.

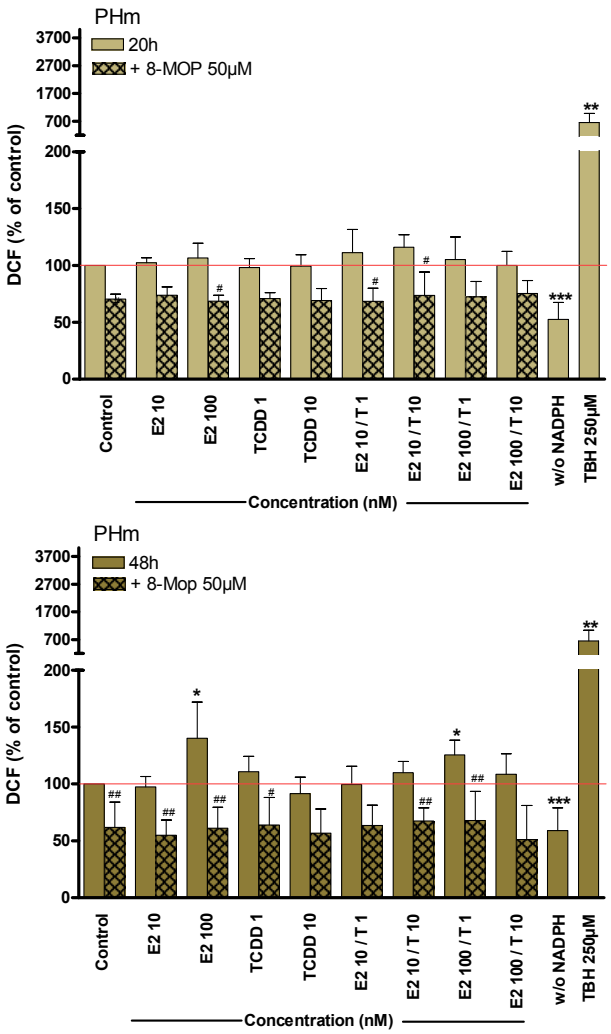

*Figure 75: Formation of cellular ROS measured as oxidation of H_2DCF in primary hepatocytes from male Wistar rats (PHm) exposed to TCDD (T) and/or E2 for 20 h and 48 h in the absence or presence of 8-methoxypsoralen (8-MOP, 50 µM); Results are normalized to the solvent control without 8-MOP (DMSO 0.1%) and presented in percent of dichlorofluorescein (DCF) formation related to an external calibration curve. Control level (100%) is indicated as a red line. Tert-butylhydroxyde (TBH) served as the positive control and was initially added to the well of cracked untreated cells just before starting the incubation with the fluorescent dye. NADPH-independent ROS formation (w/o NADPH) was also monitored. Mean ± SD; n ≥ 3; unpaired t-test, two-tailed p-value: statistically different from solvent control: *p ≤ 0.05, **p ≤ 0.01, ***p ≤ 0.001; significantly different from respective treatment with 8-MOP: #p ≤ 0.05, ##p ≤ 0.01*

At the longer treatment time the reduction of basal ROS formation triggered by 8-MOP was slightly more pronounced compared to 20 h, leading to 8 decrease by about 40% compared to normal solvent control (without 8-MOP).

The CYP1A inhibitor was able to significantly diminish the induced ROS production by E2 100 nM (140.3 ± 31.76%) and the co-treatment of E2 100 nM / TCDD 1nM

(125.5 ± 13.11%) resulting in 61.13% and 67.83% respectively. Thus, the CYP1A inhibitor prevents E2 and TCDD from ROS formation normally seen after treatment over 48 h in PHm.

5.6.3.4. ROS FORMATION IN 8-MOP-TREATED RAT HEPATOCYTES FROM FEMALES

In primary rat hepatocytes from female rats (Figure 76) there was no difference in the presence or absence of 8-MOP on basal ROS levels at both treatment times. Additionally, the treatments in the presence of 8-MOPdid not change basal ROS formation. However, ROS-inducing effects by several treatments with E2 100 nM and/or TCDD 1 nM after 48 h were decreased in the presence of 8-MOP. For example, the effect of ROS induction seen with TCDD 1nM was significantly reduced to 80.37 ± 3.61% when the inhibitor was added.

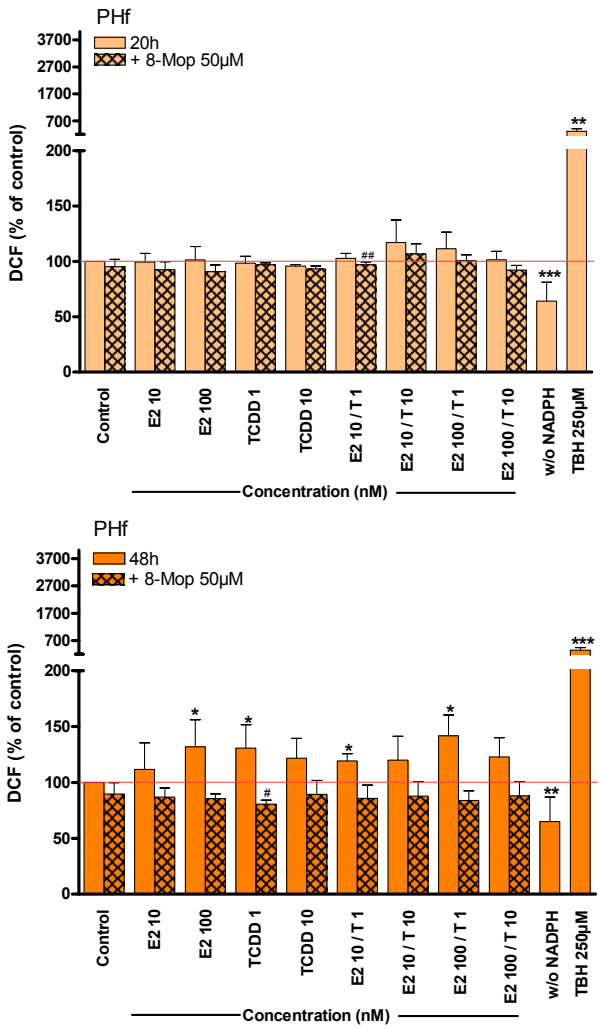

*Figure 76: Formation of cellular ROS measured as oxidation of H_2DCF in primary hepatocytes from female Wistar rats (PHf) exposed to TCDD (T) and/or E2 for 20 h and 48 h in the absence or presence of 8-methoxypsoralen (8-MOP, 50 µM); Results are normalized to the solvent control without 8-MOP (DMSO 0.1%) and presented in percent of dichlorofluorescein (DCF) formation related to an external calibration curve. Control level (100%) is indicated as a red line. Tert-butylhydroxyde (TBH) served as the positive control and was initially added to the well of cracked untreated cells just before starting the incubation with the fluorescent dye. NADPH-independent ROS formation (w/o NADPH) was also monitored. Mean ± SD; n ≥ 3; unpaired t-test, two-tailed p value: statistically different from solvent control: *p ≤ 0.05, **p ≤ 0.01, ***p ≤ 0.001; significantly different from respective treatment with 8-MOP: #p ≤ 0.05, ##p ≤ 0.01*

5.7. DEFENSE MECHANISMS AGAINST OXIDATIVE STRESS

5.7.1. CELLULAR GSH AND GSSG LEVELS

The antioxidant status of the cells was assessed by its intracellular glutathione levels. Total GSH (tGSH) and oxidized GSH (GSSG) were determined following treatment of TCDD and/or E2 at 20 h in hepatoma cells and rat hepatocytes using the method of reduction of 5,5'-dithiobis-2-nitrobenzoic acid (DTNB) by NADPH. Menadione (MD), a known redox cycler, served as a reference substance for the induction of oxidative stress.

5.7.1.1. SOLVENT-EFFECTS ON BASAL TGSH LEVELS

In initial experiments, influence of two solvents ethanol and DMSO on basal total glutathione (tGSH) was investigated in hepatoma cells and rat hepatocytes. The effects of EtOH at a final concentration of 0.1% and of DMSO at 0.25%, representing the respective maximum final concentrations used in experiments, were compared with untreated cells. Absolute basal tGSH levels of hepatoma cell lines and rat hepatocytes after 20 h showed no significant difference between the solvent-treated and untreated cells (Table 22). Thus, both EtOH and DMSO can be used as the solvent control for tGSH measurements. Concomitant to comet assay experiments (see section 5.8.1), test substances were dissolved in EtOH and treated at a final concentration of 0.1%.

Table 22: Influence of different solvents on basal tGSH levels in hepatoma cell lines and primary rat hepatocytes from male (PHm) and female (PHf) Wistar rats. Cells were treated with EtOH (0.1%) or DMSO (0.25%) or kept in normal DMEM culture medium (0.5% FBS) over a period of 20 h. Total GSH levels are determined as a reduction of 5,5'-dithiobis-2-nitrobenzoic acid (DTNB) by NADPH and expressed in µM per mg protein. Mean ± SD; n ≥ 3.

	tGSH (µM/mg)		
	Untreated	**EtOH (0.1%)**	**DMSO (0.25%)**
HepG2	40.30 ±13.9	49.05 ± 24.4	40.97 ± 19.2
H4IIE	72.83 ± 40.5	72.65 ± 26.2	59.29 ± 17.5
PHm	75.83 ± 18.5	60.07 ± 28.4	65.31 ± 38.6
PHf	35.18 ± 4.5	49.88 ± 25.3	62.79 ± 23.3

5.7.1.2. GSH STATUS

In order to evaluate the contribution of GSH in percent of tGSH contents, the GSH status is presented. Table 23 summarizes the GSH status of control cells, which gives an impression of the balance between the oxidized and reduced form of glutathione. GSH status ranged between approximately 80 – 93% in the cell models, indicating that the majority of GSH is present in the reduced form. Highest GSH status was found in male-derived primary rat hepatocytes, exerting more than 92.8% of the reduced glutathione form. In rat hepatocytes from female rats GSH status was slightly below 80%. However, no statistical difference in the GSH status was observed between hepatoma cell lines and rat hepatocytes.

Table 23: GSH status in % of control (EtOH 0.1%) in hepatoma cell lines and rat primary hepatocytes at 20 h. Mean ± SD; n ≥ 3.

	Hepatoma Cell Line		**Primary Rat Hepatocytes**	
	HepG2	**H4IIE**	**PHm**	**PHf**
GSH Status (Solvent Control)	87.5 ± 7.3%	85.9 ± 4.6%	92.8 ± 1.2%	78.8 ± 13.1%

5.7.1.3. tGSH LEVELS IN HEPATOMA CELL LINES

In human HepG2 cells (Figure 77) tGSH levels showed a tendency of increase following treatments with TCDD (1 and 10 nM) and the co-treatments with E2 (10 and 100 nM). The co-incubation of TCDD 1 nM + E2 10 nM resulted in a significant elevation of tGSH compared to solvent control (160.8 ± 25.0%). E2 alone did not cause any visible changes in tGSH levels. The trend for an increase in tGSH appeared to correlate with significantly elevated reduced GSH but not GSSG levels. Menadione (3 µM and 10 µM) decreased tGSH levels, even if the drop of tGSH marginally failed to be statistically confirmed.

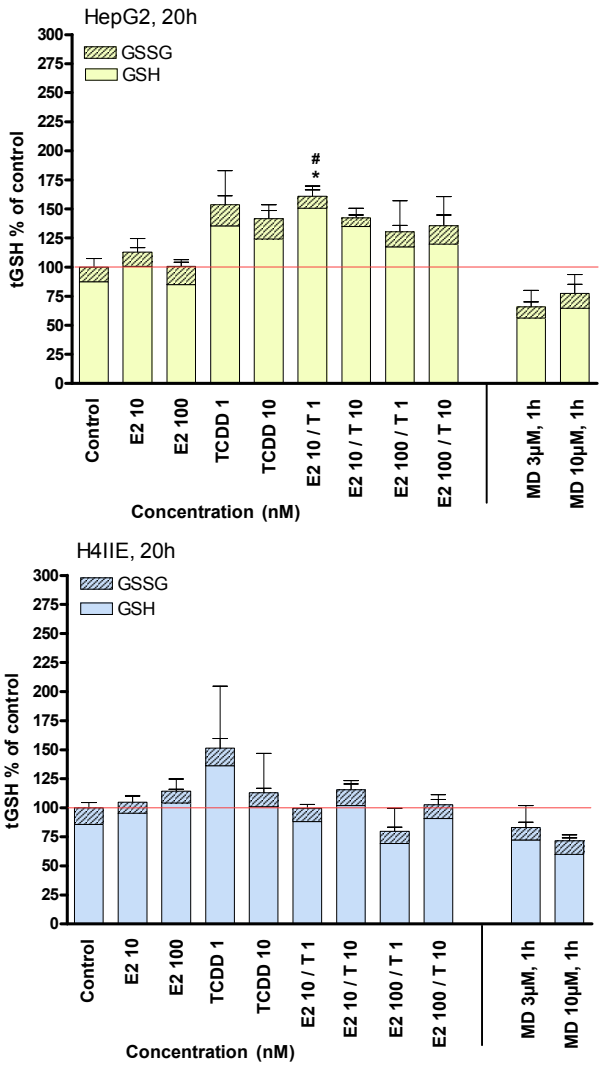

Figure 77: Modulation of cellular total glutathione (tGSH) in hepatoma cell lines (HepG2 and H4IIE) after 20 h incubation with TCDD (T) and/or E2. Total GSH content was determined photometrically as formation of 5-thio-2-nitrobenzoate (TNB). Results are expressed as tGSH (µM/ mg protein) in % of solvent control (EtOH 0.1%). Compartments of GSH and GSSG are documented in the histogram respectively.
*Mean± SD; n ≥ 3; unpaired t-test, two-tailed p value: tGSH (*), GSH (#), or GSSG (+) significantly different from solvent control *, #p ≤ 0.05; menadione (MD) treatment for 1 h was used to monitor tGSH alteration of a redox cycler.*

In the rat hepatoma cell line H4IIE, tGSH levels were not statistically different from control by the different treatments (Figure 77). However, a slight increase of intracellular

tGSH levels was observed following exposure to TCDD 1 nM and the co-treatment of TCDD 10 nM + E2 10 nM, but high standard deviations were obtained. Similar to HepG2 cell line, menadione at concentrations of 3 and 10 µM decreased tGSH fraction after 1 h treatment, suggesting consumption of the GSH pool as a result of an important oxidative stress response. Concentrations of MD greater than 10 µM were cytotoxic in both hepatoma cell lines as confirmed visually under the light microscope.

5.7.1.4. tGSH LEVELS IN PRIMARY RAT HEPATOCYTES

Male-derived rat primary hepatocytes showed no statistically significant difference in GSH levels following exposure to TCDD and/or E2 (Figure 77). However, a trend for a slight increase subsequent to treatments with E2 or TCDD alone and co-treatments with the low E2 concentration of 10 nM was observed. Treatment with E2 10 nM reached a tGSH level of 191.2 ± 50.9% and E2 10nM/TCDD 1nM resulted in 199.3 ± 103.9%, but high standard deviations were obtained. This alteration was accompanied by a non-significant increase of the fractions of both redox partners, GSH as well GSSG. Menadione tested at the highest concentration (20 µM) led to a decrease in tGSH, which was not statistically confirmed.

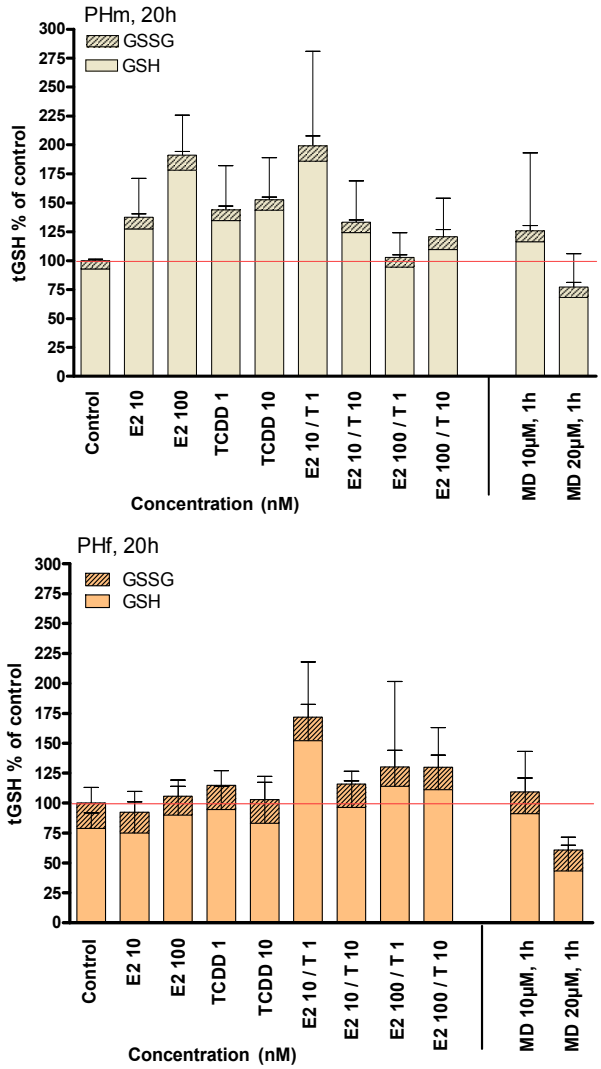

Figure 78: Modulation of cellular total glutathione (tGSH) in primary rat hepatocytes from male (PHm) and female (PHf) Wistar rats after 20 h incubation with TCDD (T) and/or E2. Total GSH content was determined photometrically as formation of 5-thio-2-nitrobenzoate (TNB). Results are expressed as tGSH (µM/mg protein) in % of solvent control (EtOH 0.1%). Compartments of GSH and GSSG are documented in the histogram respectively. Mean ± SD; n ≥ 3; unpaired t-test, two-tailed p value: not significantly different from solvent control; menadione (MD) treatment for 1 h was used to monitor tGSH alteration of a redox cycler.

Likewise, in female-derived rat hepatocytes tGSH levels were not affected by treatments with E2 and/or TCDD at 20 h (Figure 77). The only hint for an elevation was observed following exposure to the co-treatment E2 10 nM + TCDD 1 nM (171.8 ± 72.02%). The redox cycler menadione (20 µM) induced a tGSH decrease, which failed to be a statistically significant effect.

5.7.2. COMT EXPRESSION

The possible involvement of COMT was examined by detection of mRNA levels.

5.7.2.1. BASAL LEVELS OF COMT MRNA

All hepatoma cell lines and primary rat hepatocytes of both sexes proved to have measurable basal COMT mRNA after 20 h and 48 h (Figure 79).

Basal COMT mRNA levels were significantly lower in hepatoma cells compared to rat hepatocytes at 20 h (decrease by 3.2-fold). At 48 h, expression levels were lowest for HepG2. H4IIE cells showed a significant increase in COMT expression at 48 h, which reached comparable basal COMT mRNA levels as for rat hepatocytes. Except for H4IIE cells, basal mRNA levels of the other cell models were significantly lowered at 48 h toabout half the level compared to 20 h. There was no sex difference in basal expression levels detected for rat hepatocytes. Additionally, the presence of ERalpha in transfected HepG2 cells, which was examined at 20 h, had no remarkable influence on basal levels of the estradiol-methylating enzyme, though a slight but not significant increase was assumed.

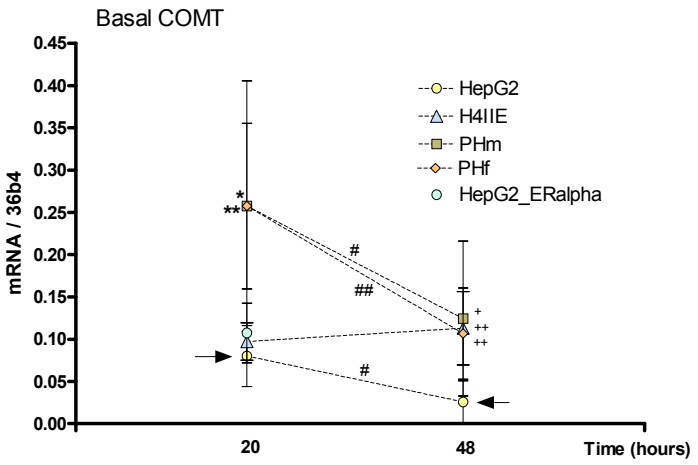

*Figure 79: Real-time RT PCR analysis of absolute basal COMT mRNA levels in hepatoma cell lines (HepG2 and H4IIE) and rat hepatocytes from male (PHm) and female (PHf) Wistar rats treated with DMSO (0.25%) over a period of 20 h 48 h. HepG2 transiently transfected with ERalpha expression plasmid (HepG2+ ERalpha) were investigated at 20 h. Results were normalized against the housekeeping gene 36B4 and expressed as ratios of delta ct values. Mean ± SD; n ≥ 3; unpaired t-test, two-tailed p value: mRNA expression levels significantly different from time-matched HepG2 control (as indicated by the arrow →) at 20 h (*p ≤ 0.05; **p ≤ 0.01) or at 48 h ($^{+}$p ≤ 0.05; $^{++}$p ≤ 0.01); mRNA expression levels significantly different between 20 h and 48 h: # p ≤ 0.01; ## p ≤ 0.01; mRNA expression significantly different between PHm and PHf : not significant*

Rank order of basal COMT mRNA	
20 h	*PHf = PHm >> HepG2_Eralpha = H4IIE = HepG2*
48 h	*PHf = PHm = H4IIE >> HepG2*

5.7.2.2. COMT mRNA after Exposure to TCDD and/or E2 in Hepatoma Cell Lines

Real-time RT PCR demonstrated hCOMT mRNA expression in human HepG2 cell line examined at both basal levels and following exposure to TCDD and/or E2 at two different treatment times (Figure 80).

Treatment with TCDD at 20 h showed a significant decrease in relative COMT gene expression, which was even more important at the higher concentration tested (TCDD 10 nM: 0.38 ± 0.31 –fold). Exposure to E2 alone also showed a significant about 8-fold decline in COMT mRNA, which was only observed at the high E2 concentration of 100 nM. With regard to the co-treatments, expression levels of E2 100 nM + TCDD 1 nM also significantly dropped down COMT mRNA expression levels compared to DMSO control but to a lesser extent than for E2 100 nM alone.

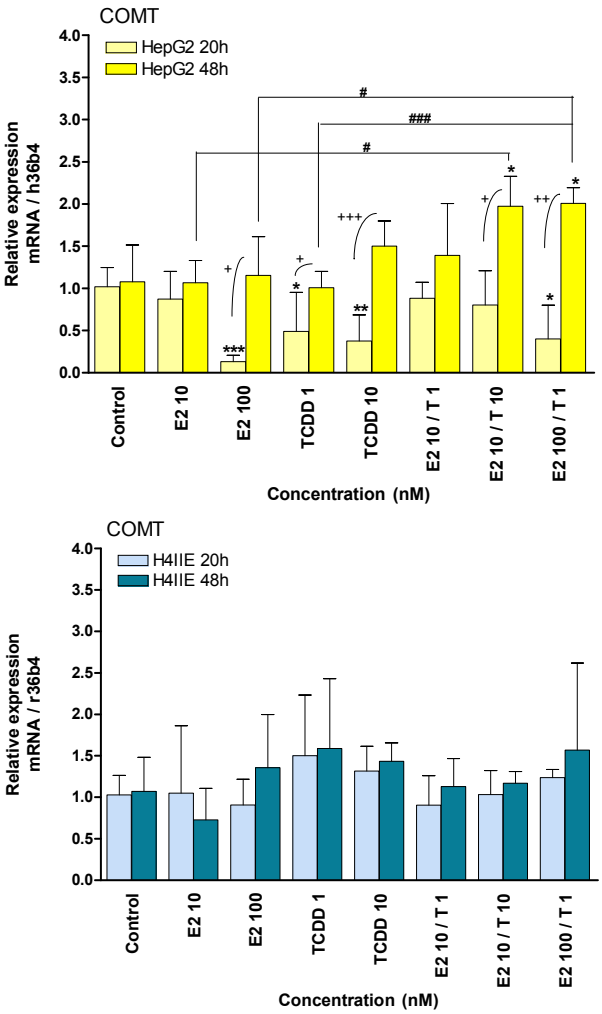

*Figure 80: Real-time RT PCR analysis of human and rat hepatoma cell lines HepG2 and H4IIE on COMT gene expression. Effects of TCDD (T) and/or Estradiol (E2) on mRNA levels were assayed following 20 h and 48 h treatment. COMT expression is normalized to 36B4 expression and presented relative to time-matched solvent control (DMSO 0.25%). Mean ± SD; n ≥ 3; unpaired t-test, two-tailed p value: mRNA expression levels significantly different from time-matched solvent control *p ≤ 0.05, **p ≤ 0.01, ***p ≤ 0.001, mRNA expression levels significantly different between time-matched treatments #p ≤ 0.05, ###p ≤ 0.001; mRNA expression levels significantly different between treatment times +p ≤ 0.05, ++p ≤ 0.01, +++p ≤ 0.001.*

After 48 h exposure, there was no decrease of relative COMT mRNA observed whatever the treatment. Contrarily to that, there was a tendency of increased mRNA. This increase was statistically significant following exposure to the co-treatments of TCDD 10 nM + E2 10 nM (1.97 ± 0.35-fold) TCDD 1 nM + E2 100 nM (2.00 ± 0.19), nearly doubling the COMT mRNA levels compared to control. COMT mRNA levels in HepG2 cell clearly showed a difference of response between the two treatment times. Whereas decreased expression levels were observed for E2, TCDD, and some of the co-treatments at 20 h, treatment-mediated increased expression was found at 48 h.

In H4IIE cells at 20 h and 48 h, there was no difference of COMT expression observed between DMSO control and treatments with E2, TCDD, or the respective combinations of both substances (Figure 80).

5.7.2.3. COMT mRNA after Exposure to TCDD and/or E2 in Primary Rat Hepatocytes

Relative COMT gene expression levels in cultured hepatocytes from male and female Wistar rats are presented in Figure 81. In hepatocytes from male rats exposure to TCDD and/or E2 displayed similar levels of COMT mRNA as DMSO control at 20 h. After 48 h incubation TCDD 10 nM resulted in a significant about 2-fold increase of COMT mRNA (1.94 ± 0.70–fold). Likewise, E2-treated hepatocytes significantly induced COMT gene expression, but only at the lower concentration of 10 nM (2.23 ± 1.13-fold). Consistent with the increase observed for these single treatments, the combination of both compounds E2 10 nM + TCDD 10 nM showed significantly elevated COMT mRNA levels (2.10 ± 0.63-fold), which did however not further enhance the effect of the test substances alone.

In female-derived rat hepatocytes relative COMT expression was significantly declined by a quarter (0.75 ± 0.29-fold) following treatments with TCDD 1 nM and 10 nM for 20 h. There was no significant difference observed for the other treatments with E2 alone or the co-treatments. Similarly, at 48 h the only significant effect was a decrease by TCDD 10 nM (0.66 ± 0.26-fold). A slight trend for decreased levels of COMT mRNA could be anticipated for the co-treatments at 48 h, which was however not statistically confirmed. There were no differences in relative expression levels observed between effects at the two treatment times.

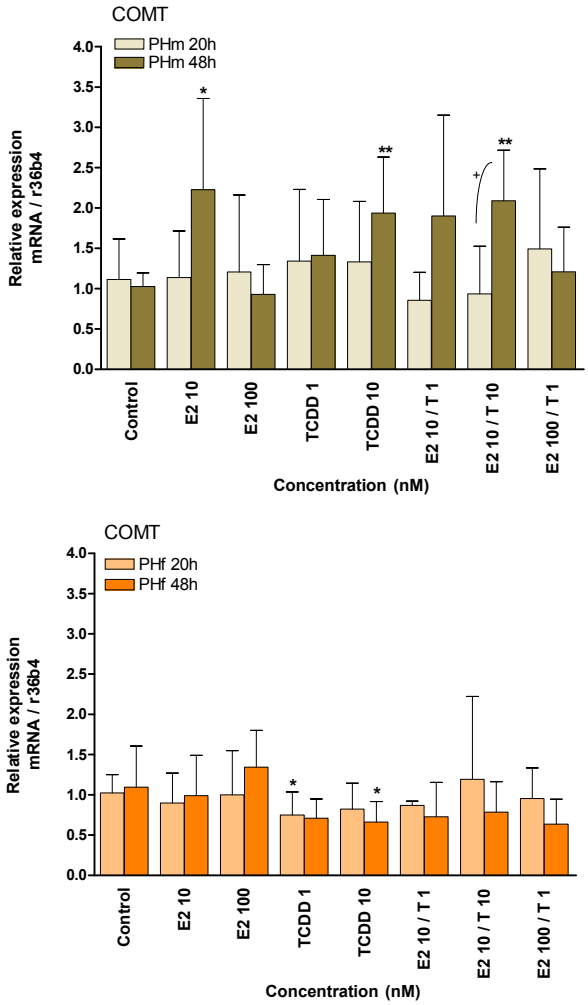

*Figure 81: Real-time RT PCR analysis of primary hepatocytes from male (PHm) and female (PHf) Wistar rats on rCOMT gene expression. Effects of TCDD (T) and/or Estradiol (E2) on mRNA levels were assayed following 20 h and 48 h treatment. COMT expression is normalized to r36B4 expression and presented relative to respective solvent control (DMSO 0.25%). Mean ± SD; n ≥ 3; unpaired t-test, two-tailed p value: mRNA expression levels significantly different from time-matched solvent control *p ≤ 0.05, **p ≤ 0.01; mRNA expression levels significantly different between treatment times $^{+}$p ≤ 0.05.*

5.7.2.4. COMT mRNA after Exposure to TCDD and/or E2 in ERalpha-Transfected HepG2

COMT mRNA levels were also monitored after transient transfection of an ERalpha expression plasmid in HepG2 cell line following 20 treatment and were compared with effects of wild-type HepG2 cell line (Figure 82).

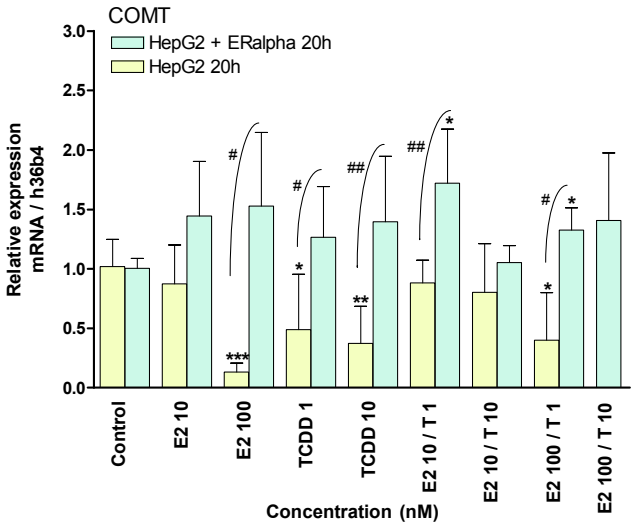

*Figure 82: Real-time RT PCR analysis of transiently transfected HepG2 cell line compared to normal HepG2 cell line in COMT gene expression. Effects of TCDD (T) and/or Estradiol (E2) on mRNA levels were assayed following 20 h. Cells were transiently transfected or not with human ERalpha expression plasmid (pRST7-hERα). Co-transfection with ERE-TK-LUC (containing a single copy of vitellogenin-ERE), as well as pSG5 and pCMVβ-Gal control vectors were performed. COMT expression is normalized to h36B4 expression and presented relative to respective time-matched solvent control (DMSO 0.25%).Mean ± SD; n ≥ 3; unpaired t-test, two-tailed p value: mRNA expression levels significantly different from time-matched solvent control: *p ≤ 0.05, **p ≤ 0.01, ***p ≤ 0.001; difference between untransfected and transfected cells: #p ≤ 0.05, ##p ≤ 0.01.*

In transfected cells there was no influence on COMT mRNA levels after exposure to TCDD (1 and 10 nM) and E2 (10 and 100 nM), though a slight increase was noted. The co-treatments of E2 at both concentrations with TCDD 1 nM demonstrated significantly enhanced COMT mRNA in ERalpha-transfected HepG2 cells. In general, the decreasing effects of COMT mRNA levels, that were observed for wild-type HepG2 cell line at 20 h (see section 5.7.2.2), were overcome by rather increased COMT mRNA levels in the presence of over-expressed ERalpha. This difference in response between transfected and untransfected HepG2 cells was statistically significant for most of the treatments.

5.8. GENOTOXICITY TESTING

The genotoxic potential of TCDD as well as estradiol and its metabolites in the liver cell models was investigated by means of two genotoxicity assays, which are also commonly used in standard genotoxicity testing. First, DNA damage was monitored directly by detecting DNA strand break formation with the comet assay. Secondly, DNA damage was determined indirectly by measuring DNA repair with the Unscheduled DNA synthesis (UDS) assay. The specificity of the comet assay was increased by formamidopyrimidine DNA glycosylase (FPG). The bacterial repair enzyme initiates the base excision repair of 8-oxo-G and other related purine modifications, thus additionally forms DNA strand breaks which are mainly indicative of oxidative DNA damage.

5.8.1. FPG-SENSITIVE DNA DAMAGE IN THE COMET ASSAY

The impact of exposure to E2 (10 and 100 nM), TCDD (1 and 10 nM), and the combination of both compounds for 20 h on DNA strand break formation was investigated in hepatoma cell lines and rat primary hepatocytes. Additionally, the direct effects of the two main estradiol metabolites 2-and 4- hydroxyestradiol (2- and 4-OHE2, 10 nM – 10 µM) were assessed in the comet assay after 20 h treatment. Effects on DNA damage were investigated with and without addition of FPG.

During initial experiments carried out to optimize FPG treatment for the different cell models the commonly used solvent DMSO at final concentrations as low as 0.1% was found to still cause remarkable DNA fragmentation. Consequently, DMSO could not be used as an adequate negative control representing comets that fit into scoring class 0 or 1. For this reason, test compounds were solved in ethanol. EtOH 0.1% did not cause FPG-sensitive DNA damage neither in hepatoma cell lines nor in primary rat hepatocytes.

5.8.1.1. EFFECTS OF TCDD AND/OR E2 IN HEPATOMA CELL LINES

The potential effects of TCDD and/or E2 on DNA damage with or without FPG application in HepG2 cells are presented in Figure 83. Under normal alkaline assay conditions, i.e. without the use of FPG treatment, solvent control cells (EtOH 0.1%) resulted in very low OTM values lower than 1 (0.59 ± 0.33) representing comets of class 0 score. In the absence of FPG, neither TCDD or E2 alone nor the co-treatments resulted in DNA fragmentation. OTM levels never exceeded a value 2 for all the treatments and no DNA damage was manifested after visual observation of the DNA in the microscope. The positive con-

trols MMS 50 µM (20 h) and menadione (MD, 10 µM, 1 h)significantly increased DNA strand break formation (OTM MMS: 22.62 ± 18.11) to the same extent.

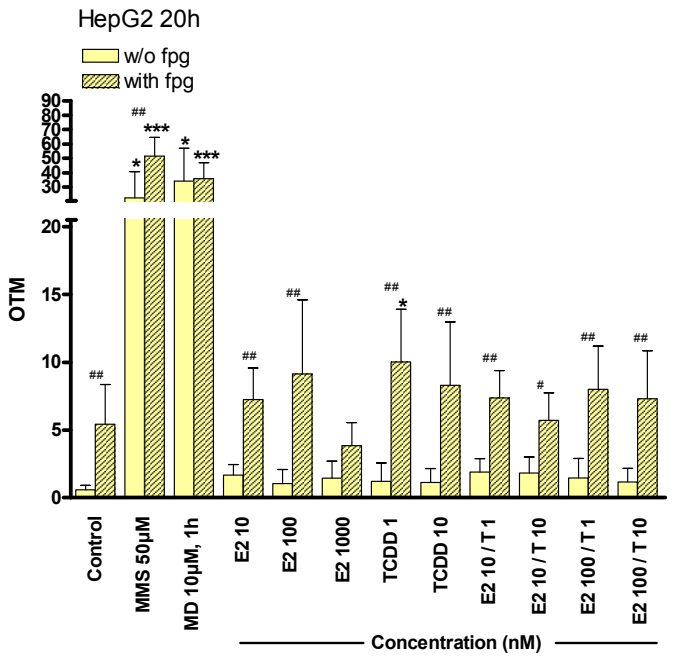

*Figure 83: DNA damage (comet assay) in HepG2 cell line exposed to TCDD (T) and/or E2 for 20 h in the absence (w/o) or presence of FPG repair enzyme. Results are presented as olive tail moments (OTMs) for treatments with and w/o FPG. EtOH (0.1%) represents the negative control. Treatments with MMS (50 µM, 20 h) and menadione (MD, 10 µM, 1 h) served as the positive controls. Mean ± SD; n ≥ 4; unpaired t-test, two-tailed p value: significantly different from solvent control *p ≤ 0.05, **p ≤ 0.01, ***p ≤ 0.001; significant difference between treatment with and without FPG #p ≤ 0.05, ##p ≤ 0.01.*

After FPG digestion, basal levels of DNA damage were significantly increased compared to cells treated with the enzyme buffer. OTM levels of solvent control were 12-fold higher in the presence of the specific repair glycosylase, reaching an OTM value of 5.41 ± 2.94. TCDD 1 nM significantly increased OTM levels (10.02 ± 3.89) compared to FPG-treated control cells. TCDD 10 nM did not lead to significantly elevated FPG-sensitive DNA damage. Likewise, E2 alone or the combinations of E2 with the dioxin compound had no effect on FPG-sensitive strand breaks compared to FPG-control. The remarkable damaging effect of MMS seen already under normal alkaline conditions were doubled following FPG protein application (OTM: 51.47 ± 13.07). Menadione (10 µM, 1 h) led to extensive DNA fragmentation, which was nevertheless not dependent on the use of the FPG enzyme.

Results for the rat hepatoma cell line are shown in Figure 84. H4IIE cells did not show any DNA-damaging effects by E2 and/or TCDD after 20 h in the alkaline version of the comet assay. All treatments showed low OTM levels comparable with solvent control (0.53 ± 0.09) and comets were categorized into class 0 (no tail) by microscopic observation. Treatment with MMS 70 µM for 20 h and menadione 15 µM for 1 h extensively increased DNA damage (OTMs: 13.40 ± 1.82 and 32.24 ± 24.03 respectively). This induction was about 2.5-fold more induced for menadione compared to MMS.

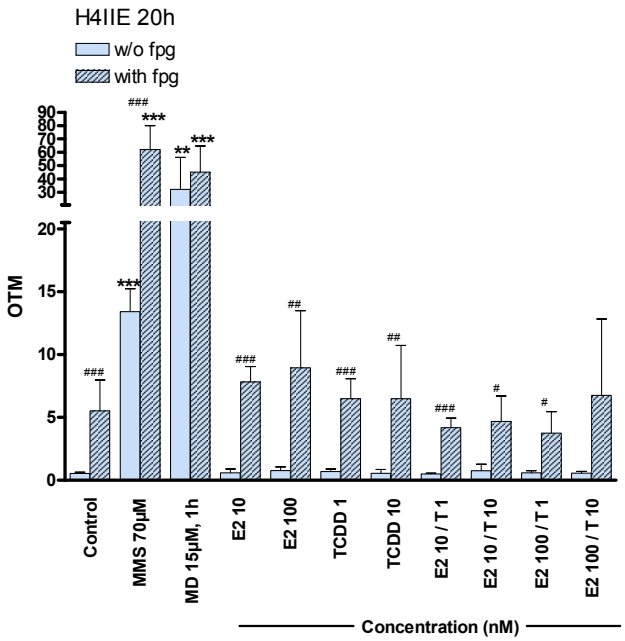

*Figure 84: DNA damage (comet assay) in H4IIE cell line exposed to TCDD (T) and/or E2 for 20 h in the absence (w/o) or presence of FPG repair enzyme. Results are presented as olive tail moments (OTMs) for treatments with and w/o FPG. EtOH (0.1%) represents the negative control. Treatments with MMS (70 µM, 20 h) and menadione (MD, 15 µM, 1 h) served as the positive controls. Mean ± SD; n ≥ 4; unpaired t-test, two-tailed p value: significantly different from solvent control **p ≤ 0.01, ***p ≤ 0.001; significant difference between treatment with and without FPG #p ≤ 0.05, ##p ≤ 0.01, ###p ≤ 0.001.*

Enzyme-linked comet assay enhanced basal induction levels significantly about 11-fold (OTM EtOH 0.1%: 5.52 ± 2.44). However, none of the treatments with TCDD and/or E2 resulted in a significantly enhanced level of FPG-dependent DNA damage compared to respective FPG-control. The positive control MMS 70 µM clearly induced DNA damage which was about 4.6-fold further enhanced by FPG (61.99 ± 17.92) compared to normal strand break induction. DNA-damaging effect of menadione was not more pronounced with FPG (OTM: 45.08 ± 19.55).

5.8.1.2. EFFECTS OF TCDD AND/OR E2 IN HEPATOCYTES FROM MALE AND FEMALE RATS

OTMs of male-derived primary rat hepatocytes (PHm), used as a measure of DNA damage in the comet assay with and without detection of FPG-sensitive sites, are summarized in Figure 85. In the normal alkaline comet assay the response was similar to hepatoma cell lines. Treatment with TCDD, E2, or the co-treatments for 20 h failed to induce DNA strand-breaks. Tail moment values were relatively low ranging between 0.4 and 1.5 (e.g. OTM solvent control: 0.41 ± 0.32). The positive controls MMS (70 µM, 20 h) and Menadione (20 µM, 1 h) significantly induced DNA damage.

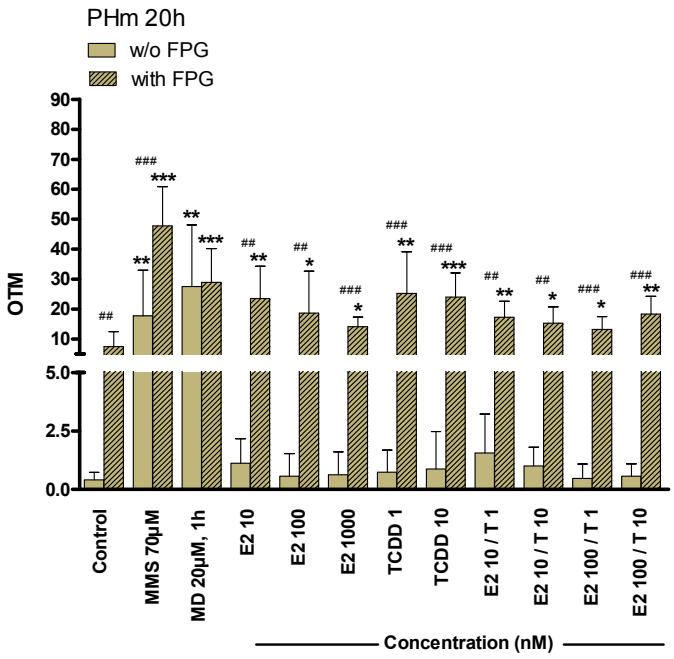

*Figure 85: DNA damage (comet assay) in rat primary hepatocytes from male Wistar rats (PHm) exposed to TCDD and/or E2 for 20 h in the absence (w/o) or presence of FPG repair enzyme. Results are presented as olive tail moments (OTMs) for treatments with and w/o FPG. EtOH (0.1%) represents the negative control. Treatments with MMS (70 µM, 20 h) and menadione (20 µM, 1 h) served as the positive controls. Mean ± SD; n ≥ 4; unpaired t-test, two-tailed p value: significantly different from solvent control *p ≤ 0.05, **p ≤ 0.01, ***p ≤ 0.001; significant difference between treatment with and without FPG #p ≤ 0.01, ###p ≤ 0.001.*

Application of the bacterial repair enzyme FPG significantly enhanced basal levels of DNA fragmentation resulting in OTM levels of 7.48 ± 5.01 for solvent control cells. The obtained increase by FPG did however not result in severe DNA damage for negative controls. TCDD (1 and 10 nM) significantly enhanced DNA strand-break formation compared to FPG-control without a concentration-dependent effect. Likewise, exposure to E2 led to a statistically significant increase in DNA migration (OTM E2 10 nM: 23.53 ± 10.72). The extent of DNA damage was comparable among the different E2 concentrations up to 1 µM. The co-treatments did not modulate the damaging effects observed for single treatments with TCDD or E2. Via the action of FPG MMS-induced DNA migration could be further enhanced about 2.6-fold (OTM FPG: 47.78 ± 13.13). The use of FPG had no influence on menadione-mediated DNA damage (OTM: 28.88 ± 11.34). Strand break formation of menadione, TCDD, E2, or the co-treatments was comparable after application of FPG.

Detection of DNA strand breaks with and without the lesion-specific FPG enzyme in primary rat hepatocytes from female Wistar rats (PHf) showed similar results to those observed for male-derived rat hepatocytes (Figure 86). There was no DNA damage found with TCDD, E2 or the co-treatments in the alkaline comet assay; OTM levels remained low (OTM negative control: 0.37 ± 0.55). For treatments with E2 10 nM or respective co-treatments slightly elevated OTM levels were found, which were even statistically significant for the co-treatment of E2 10 nM with TCDD 1 nM (2.51 ± 2.93). However, standard deviations for these treatments were high and the observed increase did not reflect a

DNA-damaging effect. The positive controls MMS 70 µM and menadione 10 µM (1 h) exerted strong DNA-damaging effects (OTM MMS: 20.60 ± 17.05).

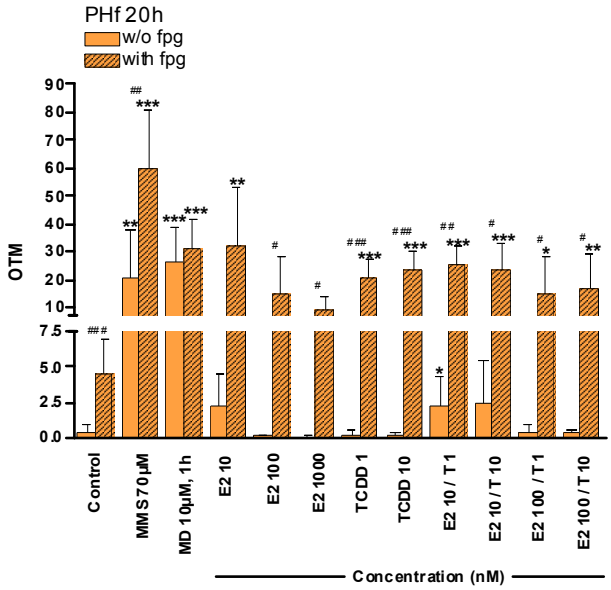

*Figure 86: DNA damage (comet assay) in rat primary hepatocytes from female Wistar rats (PHf) exposed to TCDD (T) and/or E2 for 20 h in the absence (w/o) or presence of FPG repair enzyme. Results are presented as olive tail moments (OTMs) for treatments with and w/o FPG. EtOH (0.1%) represents the negative control. Treatments with MMS (70 µM, 20 h) and menadione (10 µM, 1 h) served as the positive controls. Mean ± SD; n ≥ 4; unpaired t-test, two-tailed p value: significantly different from solvent control *p ≤ 0.05, **p ≤ 0.01, ***p ≤ 0.001; significant difference between treatment with and without FPG #p ≤ 0.05, ##p ≤ 0.01, ###p ≤ 0.001.*

Modification of the comet assay with FPG increased basal OTM levels significantly (OTM FPG-control: 4.58 ± 2.43). Female-derived hepatocytes showed clear induction of DNA migration by TCDD and E2 treatments. TCDD significantly increased DNA strand break formation with no difference between the concentrations used (OTM 1 nM: 20.88 ± 6.42). E2 10 nM showed the highest increase in OTM level which was about 7-fold elevated compared to FPG-control, but high standard deviations were obtained (OTM: 32.18 ± 21.15). There was a trend towards a concentration-dependent decrease in OTM levels with increasing E2 concentrations up to 1 µM. E2 at concentrations above 10 nM did not significantly induce FPG-sensitive strand break formation. The co-incubations of TCDD with E2 highly significantly increased DNA fragmentation compared to control but did not modulate the effects of the single treatments.

The strongest damaging effects in PHf were obtained with MMS (70 µM) which was about 3-fold further enhanced following FPG treatment (OTM: 59.56 ± 21.16). Exposure to menadione (10 µM, 1 h) displayed a prominent DNA-damaging effect which was irrespective of FPG application. The menadione-dependent significant increase reached the same OTM levels as E2 10 nM, TCDD, and the co-treatments. OTM levels following FPG application were significantly higher than in the absence of the specific repair enzyme with the exception of treatments with menadione.

5.8.1.3. EFFECTS OF E2 METABOLITES IN HEPATOMA CELL LINES

The effects of direct treatment with the two main E2 metabolites 2- and 4- hydroxyestradiol after 20 h treatment in HepG2 cell line with or without FPG digestion are presented in Figure 87. Under normal alkaline comet assay conditions the OTM of the negative control (EtOH 0.1%, without FPG) was very low at 0.98 ± 0.82. For none of the two E2–catechols at the tested concentrations ranging from 0.01 to 10 µM a statistical difference was observed compared to solvent control.

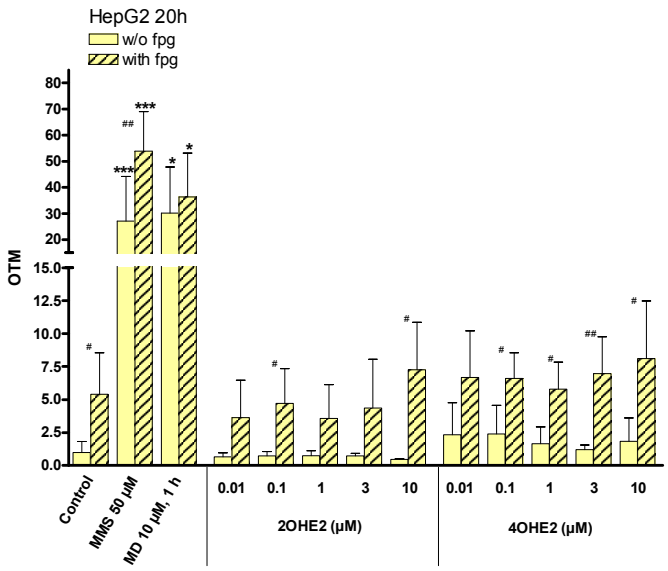

*Figure 87: DNA damage (comet assay) in human hepatoma cell line HepG2 exposed to the main E2- metabolites, 2-hydroxyestradiol (2-OHE2) and 4-hydroxyestradiol (4-OHE2) at concentrations ranging from 10nM to 10 µM for 20 h in the absence (w/o) or presence of FPG repair enzyme. Results are presented as olive tail moments (OTMs) for treatments with and w/o FPG. EtOH (0.1%) represents the solvent control. Treatments with MMS (50 µM, 20 h) and menadione (MD 10 µM, 1 h) served as the positive controls. Mean ± SD; n ≥ 3; unpaired t-test, two-tailed p value: significantly different from solvent control *p ≤ 0.05, **p ≤ 0.01, ***p ≤ 0.001; significant difference between treatment with and without FPG #p ≤ 0.05, ##p ≤ 0.01.*

Following application of FPG, formation of basal strand breaks was generally significantly elevated compared to the treatments without FPG. Both catechol estrogens did not lead to significant inductions of DNA migration. As already seen earlier in the comet assay experiments with HepG2, both positive controls gave rise to significant DNA strand break induction with and without FPG.

The results in rat H4IIE cell line subsequent to exposure to E2 catechols are displayed in Figure 88. 2-and 4-hydroxyestradiol had no effect on OTM levels compared to control. Following treatment with repair enzyme, the extent of basal DNA strand breaks was significantly enhanced. Solvent control led to OTM levels of 5.05 ± 2.46, which was about 6.7-fold elevated compared to control without FPG. No DNA damage was detected in cells treated with 2-OHE2 and 4-OHE2 for 20 h with or without FPG. The highest OTM level was found for 4-OHE2 3 µM (8.37 ± 4.57). There was neither a concentration-dependent effect nor a clear difference between the 2-hydroxylated and the 4-hydroxylated isomers observed.

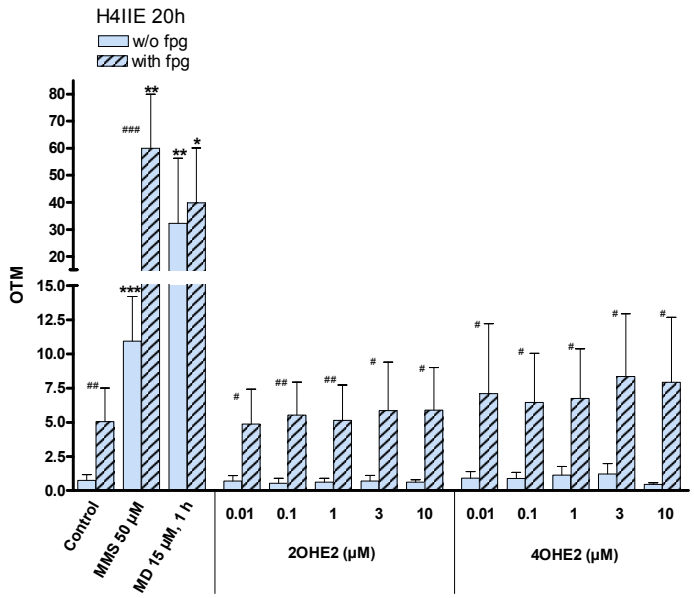

*Figure 88: DNA damage (comet assay) in rat hepatoma cell line H4IIE exposed to the main E2- metabolites, 2-hydroxyestradiol (2-OHE2) and 4-hydroxyestradiol (4-OHE2) at concentrations ranging from 10nM to 10 µM for 20 h in the absence (w/o) or presence of FPG repair enzyme. Results are presented as olive tail moments (OTMs) for treatments with and w/o FPG. EtOH (0.1%) represents the solvent control. Treatments with MMS (50 µM, 20 h) and menadione (MD 10 µM, 1 h) served as the positive controls. Mean ± SD; n ≥ 3; unpaired t-test, two-tailed p value: significantly different from solvent control *p ≤ 0.05, **p ≤ 0.01, ***p ≤ 0.001; significant difference between treatment with and without FPG #p ≤ 0.05, ##p ≤ 0.01, ###p ≤ 0.001.*

5.8.1.4. EFFECTS OF E2-METABOLITES IN HEPATOCYTES FROM MALE AND FEMALE RATS

In primary rat hepatocytes it was interesting to see whether the FPG-sensitive DNA damage produced by E2 itself in the comet assay (see section 5.8.1.2) could be attributed to the main E2 metabolites.

Effects in rat hepatocytes from male Wistar rats following 20 h exposure to 4-OHE2 and 2-OHE2 (Figure 89) revealed that under normal alkaline comet assay conditions (without FPG) the hydroxylated estradiol forms were not able to induce DNA strand breaks. Basal OTM levels without FPG were very low and could be significantly enhanced following FPG application without causing manifested DNA damage. In contrast to that, the catechols 2-OHE2 and 4-OHE2 were able to induce FPG-sensitive DNA strand break formation.

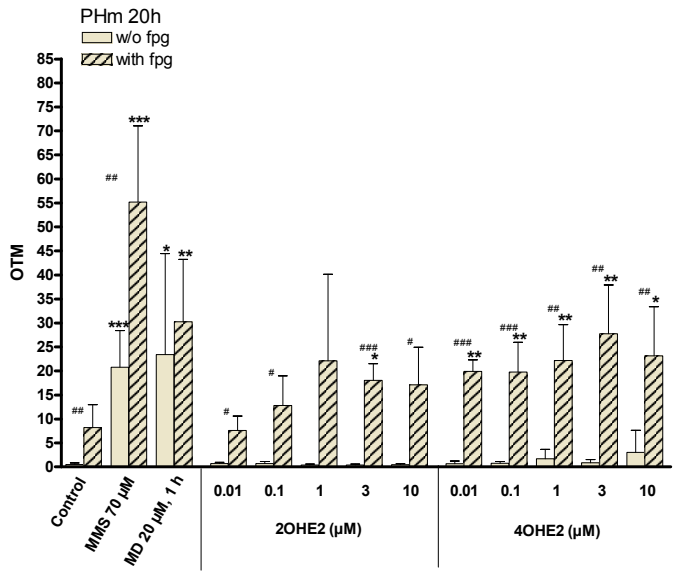

*Figure 89: DNA damage (comet assay) in primary rat hepatocytes from male Wistar rats (PHm) exposed to the main E2- metabolites, 2-hydroxyestradiol (2-OHE2) and 4-hydroxyestradiol (4-OHE2) at concentrations ranging from 10 nM to 10 µM for 20 h in the absence (w/o) or presence of FPG repair enzyme. Results are presented as olive tail moments (OTMs) for treatments with and w/o FPG. EtOH (0.1%) represents the solvent control. Treatments with MMS (70 µM, 20 h) and menadione (20 µM, 1 h) served as the positive controls. Mean ± SD; n ≥ 3-4; unpaired t-test, two-tailed p value: significantly different from solvent control *p ≤ 0.05,**p ≤ 0.01,***p ≤ 0.001; significant difference between treatment with and without FPG #p ≤ 0.05, ,##p ≤ 0.01, ###p ≤ 0.001.*

A significant DNA-damaging effect was obtained with 2-OHE2 starting at a concentration of 3 µM (OTM: 18.03 ± 3.47). 2-OHE2 1 µM also yielded a high OTM (22.12 ± 18.03) but with a remarkable standard deviation. The 4-hydroxylated E2 metabolite appeared to be more potent than the 2-OHE2 as significant effects were observed at all concentrations even at the low doses. However, there was no statistical difference in induced OTM levels between the two isomers at the same concentration levels. The considered more active metabolite 4-OHE2 did not cause a concentration-dependent induction. The strongest increase in FPG-sensitive DNA migration was caused by 4-OHE2 3 µM (27.74 ± 10.19), being about 3-fold elevated compared to FPG-control. Significant FPG-dependent DNA-damaging effects seen in PHm were comparable with OTM levels of MMS 70 µM without FPG (20.79 ± 7.61).

In female-derived rat hepatocytes the catechol metabolites showed effects only after FPG-treatment (Figure 90). Both catechol metabolites induced FPG-sensitive DNA damage already at the low concentrations of 10 nM and 100 nM (OTM 2-OHE2 and 4-OHE2 10nM: 17.90 ± 9.67 and 14.43 ± 6.97 respectively), representing a 3-fold induction compared to FPG-control. There was no concentration-dependent increase in DNA strand break formation. Thus, DNA-damaging OTM levels at the higher concentrations reached the same OTM level. (e.g. 2-OHE2 10 µM:19.74 ± 9.00). Additionally, there was no difference in reactivity towards DNA strand break formation observed between 2-and 4-OHE2.

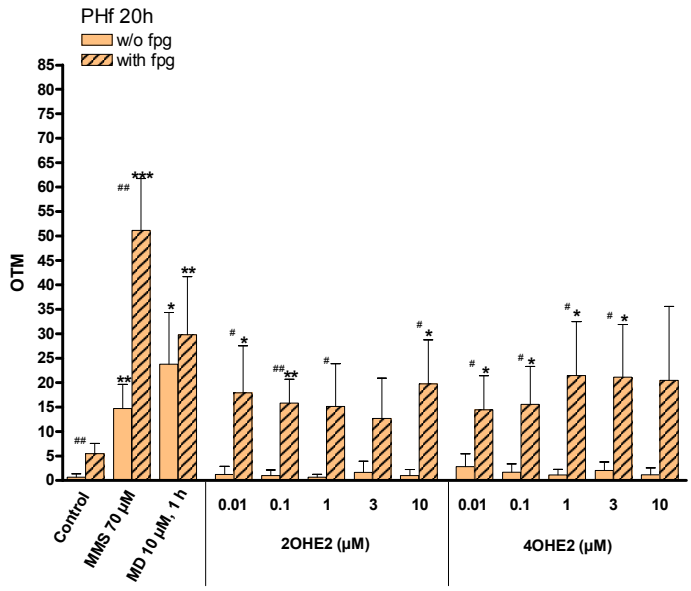

*Figure 90: DNA damage (comet assay) in primary rat hepatocytes from male Wistar rats (PHm) exposed to the main E2- metabolites, 2-hydroxyestradiol (2-OHE2) and 4-hydroxyestradiol (4-OHE2) at concentrations ranging from 10nM to 10 µM for 20 h in the absence (w/o) or presence of FPG repair enzyme. Results are presented as olive tail moments (OTMs) for treatments with and w/o FPG. EtOH (0.1%) represents the solvent control. Treatments with MMS (70 µM, 20 h) and menadione (20 µM, 1 h) served as the positive controls. Mean ± SD; n ≥ 3; unpaired t-test, two-tailed p value: significantly different from solvent control *p ≤ 0.05, **p ≤ 0.01, ***p ≤ 0.001; significant difference between treatment with and without FPG #p ≤ 0.05, ##p ≤ 0.01, ###p ≤ 0.001.*

5.8.1.5. COMPARISON OF E2 AND E2 METABOLITES

In the following, the effects of E2 and 2-and 4-OHE2 on DNA damage at the same concentrations (10 and 100 nM) in the comet assay with FPG were compared.

As described before, in hepatoma cell lines E2 and its metabolites were unable to induce DNA fragmentation in the comet assay with and without FPG. Consequently, in the absence of FPG no significant difference was observed between effects of DNA migration by E2 or 2-and 4-OHE2 at the concentrations of 10 nM and 100 nM respectively. However, with FPG 2-OHE2 (10nM) resulted in a significant reduction compared to the parent compound (E2 10nM) in HepG2, and a similar yet not significant trend was also observed at 10 nM in H4IIE cells.

In order to assess whether E2 damaging effect in FPG-sensitive comet assay in primary hepatocytes from male and female rats can be ascribed specifically to one of the two

metabolites, treatments with E2, 2-and 4-OHE2 at the low concentration of 10 and 100nM for 20 h are assorted in Figure 91.

In male primary hepatocytes E2-induced DNA strand breaks (10 nM) reached about the same OTM levels than 4-hydroxyestrol 10 nM, whereas the 2-hydroxylated metabolite resulted in significantly reduced DNA fragmentation compared to E2. At the high concentration (100 nM) the difference between treatments with E2 and 2OHE was no longer evident. In female-derived primary rat hepatocytes there was no clear difference in response seen between E2 and its two major metabolites.

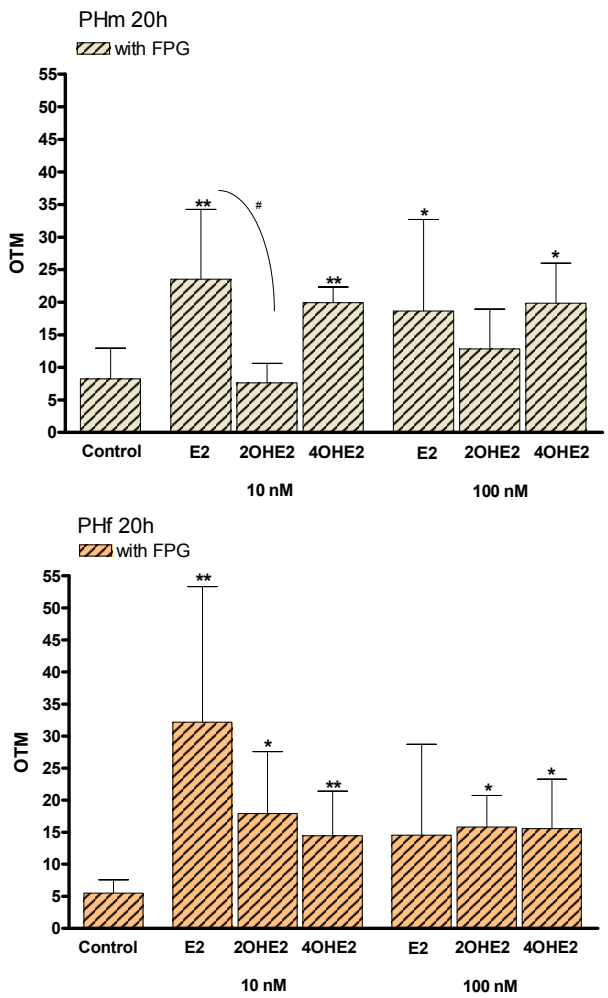

*Figure 91: Overview of FPG-sensitive DNA-damaging effects (comet assay) in rat primary hepatocytes from male (PHm) and female (PHf) Wistar rats exposed to E2 and the main E2- metabolites, 2-hydroxyestradiol and 4-hydroxyestradiol (2-OHE2 and 4-OHE2) at 10 nM and 100 nM for 20 h. Results are presented as olive tail moments (OTMs) for treatments with FPG digestion. EtOH (0.1%) represents the negative control. Mean ± SD; n ≥ 3; unpaired t-test, two-tailed p value: significantly different from solvent control *p ≤ 0.05, **p ≤ 0.01; significantly different between treatments #p ≤ 0.05.*

5.8.2. SUMMARY OF FPG-SENSITIVE COMET ASSAY

The effects of the treatments with TCDD and/or E2 or with E2 metabolites for 20 h in all the four cell models are compiled in Table 24 and Table 25. Since in the absence of FPG no DNA strand break induction was observed only FPG-sensitive effects on DNA damage

are listed. The absolute mean OTM levels and significant effects compared to the respective solvent control in hepatoma cell lines and primary rat hepatocytes isolated from both sexes are highlighted.

There was no E2- or TCDD-mediated increase in oxidative DNA damage observed in hepatoma cell lines (Table 24). In HepG2 cells TCDD 1°nM resulteded in a statistically significant effect, but the increase was of minor relevance because no DNA damage was manifested.

Primary rat hepatocytes from both male and female Wistar rats (Table 24) resulted in pronounced FPG-sensitive strand break formation following single treatments of the test compounds. The co-treatments did not further enhance this effect. There was no concentration-dependent difference in DNA damage after exposure to TCDD. The increase by E2 reached the same OTM level as by TCDD alone. The strongest DNA-damaging effect was observed following exposure to E2 10 nM in PHf, which was almost 7-fold higher than FPG-control.However, standard deviations were very high for both PHm and PHf and a tendency of a concentration-dependent decrease was obtained with increasing E2 concentrations.

*Table 24: Overview of genotoxic effects by TCDD (T) and/or estradiol (E2) after 20 h treatment in hepatoma cell lines and rat primary hepatocytes from male (PHm) and female (PHf) Wistar rats as determined in the alkaline comet assay following application of the repair enzyme FPG. Mean absolute olive tail moment values (OTM) of at least 3 independent experiments are shown. Control levels are presented for the solvent control (C, EtOH 0.1%) and the positive controls (MMS 50-70 µM, 20 h; menadione (MD) 10-20 µM, 1 h). Red up arrows stand for a significant induction compared to solvent control. Significantly different from respective solvent control *p ≤ 0.05, **p ≤ 0.01, ***p ≤ 0.001; significantly different between different E2 and TCDD treatments: not significant.*

	FGP-sensitive DNA strand breaks (OTM level)										
	Controls										
	C	**MMS**	**MD**	**TCDD 1**	**TCDD 10**	**E2 10**	**E2 100**	**E2 10/ T1**	**E2 10/ T0**	**E2 100/ T1**	**E2 100/ T 10**
Hepatoma cell lines											
HepG2	5.4	51.5 ↑ ***	34.3 ↑ ***	10.02 ↑ *	8.3	7.2	9.1	7.4	5.7	8.0	7.3
H4IIE	5.5	62.0 ↑ ***	45.1 ↑ ***	6.5	6.5	7.8	8.9	4.2	4.7	3.7	6.7
Primary rat hepatocytes											
PHm	7.5	47.8 ↑ ***	28.9 ↑ ***	25.2 ↑ **	24.0 ↑ ***	23.5 ↑ **	18.6 ↑ *	17.2 ↑ **	15.3 ↑ *	13.2 ↑ *	18.3 ↑ **
PHf	4.6	59.6 ↑ ***	31.1 ↑ ***	20.9 ↑ ***	23.7 ↑ ***	32.2 ↑ **	14.5	25.7 ↑ ***	23.7 ↑ ***	15.2 ↑ *	17.2 ↑ **

None of the tested cell models showed induction of DNA fragmentation by the two main E2 metabolites (2-OHE2 and 4-OHE2) in the normal alkaline comet assay after 20 h treatment. The effects of E2 metabolites on FPG-dependent DNA migration are depicted in Table 25.

*Table 25: Overview of genotoxic effects by E2 catechol metabolites 2- and 4-hydroxyestradiol (2- and 4-OHE2) after 20 h treatment in hepatoma cell lines and rat primary hepatocytes from male (PHm) and female (PHf) Wistar rats as determined in the alkaline comet assay following application of the repair enzyme FPG. Mean absolute olive tail moment values (OTM) of at least 3 independent experiments are shown. Control levels are presented for the solvent control (C, EtOH 0.1%) and the positive controls (MMS 50-70 µM, 20 h; menadione (MD) 10-20 µM, 1 h). Red up arrows stand for a significant induction compared to solvent control. Significantly different from respective solvent control *p ≤ 0.05, **p ≤ 0.01, ***p ≤ 0.001; significantly different between different treatments with 2- and 4-OHE2: not significant.*

	FGP-sensitive DNA strand breaks (OTM level)												
	Controls			**2OHE2 (µM)**					**4OHE2 (µM)**				
	C	**MMS**	**MD (1 h)**	**0.01**	**0.1**	**1**	**3**	**10**	**0.01**	**0.1**	**1**	**3**	**10**
Hepatoma cell lines													
HepG2	5.4	53.9 ↑ ***	36.3 ↑ *	3.6	4.7	3.6	4.4	7.3	6.7	6.6	5.8	7.0	8.1
H4IIE	5.1	60.0 ↑ **	39.9 ↑ *	4.9	5.5	5.1	5.9	5.9	7.1	6.4	6.7	8.4	7.9
Primary rat hepatocytes													
PHm	8.2	55.2 ↑ ***	30.2 ↑ **	7.6	12.8	22.1	18.0 ↑ *	17.1	19.9 ↑ **	19.8 ↑ **	22.2 ↑ **	27.7 ↑ **	23.2 ↑ *
PHf	5.5	51.2 ↑ ***	29.8 ↑ **	17.9 ↑ *	15.8 ↑ **	15.1	12.7	19.7 ↑ *	14.4 ↑ *	15.6 ↑ *	21.4 ↑ *	21.2 ↑ *	20.5

Both catechol estrogens clearly showed genotoxic activity only in primary rat hepatocytes. In male-derived hepatocytes, 4-OHE2 was more responsive to DNA fragmentation than the 2-hydroxylated isomer. 2-OHE2 only exhibited DNA damage at concentrations of 3 µM and above. Compared to PHm, female-derived hepatocytes were more sensitive to DNA damage induced by 2-OHE2, which enhanced DNA migration already at the low concentrations of 10 and 100 nM. However, comparison of absolute mean OTM values

demonstrated no significant sex-specific difference in response by 2-and 4-OHE in rat hepatocytes.

The positive controls MMS (50-70 µM, 20 h) highly damaged DNA to the same extent for the different cell models leading up to 10-fold inductions (see Table 24 and Table 25). Male-derived rat hepatocytes and H4IIE cells were less sensitive towards menadione treatment for 1 h, because a higher concentration was needed (15 µM) compared to HepG2 and PHf (10 µM) to obtain the same level of DNA damage.

5.8.3. DNA REPAIR IN THE UDS ASSAY

The identification of induced DNA repair activity by the test substances TCDD and/or E2 in the different liver cell models after 4 h (HepG2) or 20 h (all cell models) exposure was measured by the Unscheduled DNA synthesis (UDS) assay *in vitro*. The UDS test is based on the incorporation of the radiolabelled nucleoside [3H]-thymidine into the DNA of cells that are not undergoing scheduled (i.e. S-phase) DNA synthesis. The existence and degree of DNA damage is inferred from an increase in [3H]-thymidine incorporation into the DNA compared to untreated cells and was quantified by applying liquid scintillation counting (LSC) as described by Naji-ali et al. (1994) and Valentin-Séverin (2002). Hepatoma cell lines were additionally incubated with hydroxyurea (HU) to minimize residual replicative DNA synthesis as described in the experimental protocol (see section 4.7).

5.8.3.1. BACKGROUND LEVELS OF DNA REPAIR ACTIVITY

DNA repair background levels varied a lot among the different liver cell models and are presented in Table 26.

Table 26: Background levels of DNA repair activity (UDS assay) in hydroxyurea-treated hepatoma cell lines and primary rat hepatocytes from male and female Wistar rats (PHm and PHf). Control levels (DMSO 0.1%, 20 h) are expressed in cpm.

UDS	**Hepatoma cell line**		**Primary rat hepatocytes**	
	HepG2	**H4IIE**	**PHm**	**PHf**
Background levels (cpm)	1543 ± 104	328 ± 90	5470 ± 3373	9665 ± 415

Highest background levels were obtained in female-derived hepatocytes, which were about 1.8-fold higher than in male-derived hepatocytes, though standard variations in PHm were very high. Hydroxyurea-inhibited replicative DNA synthesis in hepatoma cell

lines led to lowest background levels in H4IIE cells, which were about 4.7-fold lower than in HepG2 cells.

5.8.3.2. DNA REPAIR ACTIVITY AFTER EXPOSURE TO TCDD AND/OR E2 IN HEPATOMA CELL LINES

Liquid Scintillation counting measurements of the level of [3H]-thymidine uptake by HepG2 under conditions that inhibit scheduled DNA synthesis are demonstrated in the presence of TCDD and/or E2 at the indicated concentrations after 4 h and 20 h treatment (Figure 92).

Following 4 h exposure, control cells without HU supplementation resulted in excessive [3H-thymidine uptake (16079 ± 1203 cpm). Treatment of solvent control with HU caused measurable but considerably lower radionucleotide-incorporation (1394 ± 105 cpm). Inhibition of replicative DNA synthesis by hydroxyurea was efficient, blocking approximately 91% of the [3H]-thymidine uptake. None of the treatments with TCDD and/or E2 tested showed a significant difference in radionucleotide incorporation compared to HU-solvent control. Treatment with the positive control 4-nitroquinoline N-oxide (NQO) yielded a statistically significant increase of the UDS response (2512 ± 221), which was about 1.8-fold higher than background levels of HU-control. Thus, NQO 2 µM was used as a positive control for 4 h in the HepG2 cell line.

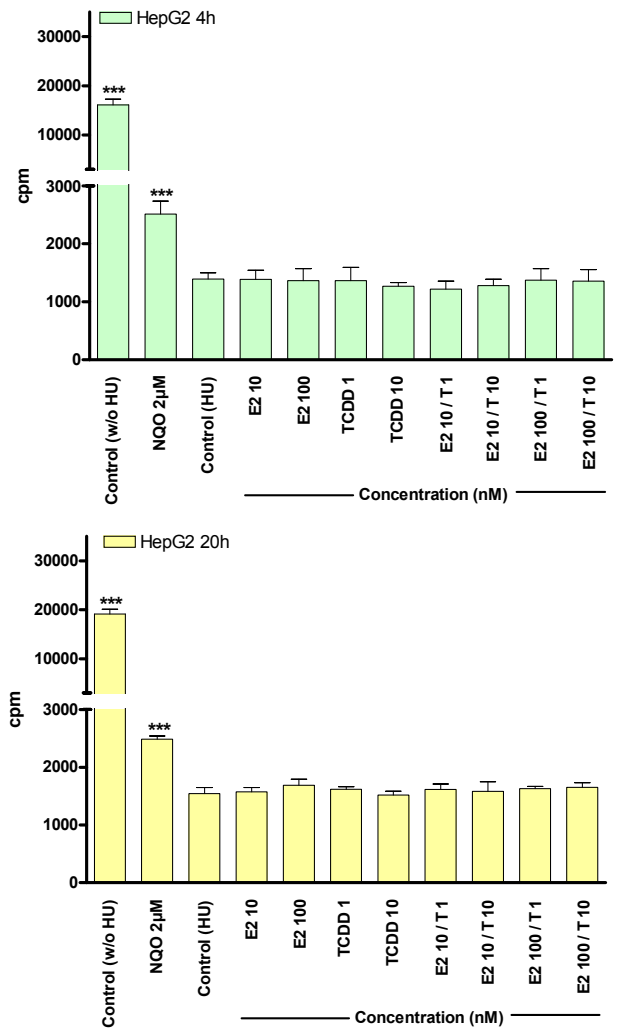

*Figure 92: [3H]-thymidine incorporation (UDS assay) into HepG2 cells following exposure to TCDD (T) and/or E2, for 4 h and 20 h supplemented with hydroxyurea (HU, 10 mM, 1 h). Results are presented as counts per minute (cpm). Ethanol (0.1%) supplemented with hydroxyurea (HU, 10 mM, 1 h) represents the negative control (Control HU) for unscheduled DNA synthesis. EtOH (0.1%) without hydroxyurea (Control w/o HU) represents incorporation of unscheduled and replicative DNA synthesis. Treatment with 4-nitroquinoline-N-oxide (NQO) was used as the positive control. Mean ± SD; n = 3; unpaired t-test, two-tailed p value: significantly different from solvent control with HU ***p ≤ 0.001.*

After 20 h treatment UDS activity in HepG2 response was similar. Solvent-treated cells supplemented with HU showed [3H]-thymidine uptake at a level of 1543 ± 104 cpm, which corresponded to an inhibition of replicative DNA synthesis by approximately 92%. This enabled to adequately monitor possible DNA repair. Even after prolongated treatment time, neither TCDD or E2 nor their combinations were able to induce DNA repair in HepG2 cells. The positive control NQO 2 µM resulted in a significant 1.6-fold increase of UDS activity compared to HU control. The results at both treatment times clearly showed that DNA repair is not enhanced in human HepG2 cell line when treated with TCDD and/or E2 whatever the concentration used suggesting the absence of unscheduled DNA synthesis.

In H4IIE cell line a series of optimizationexperiments were undertaken to determine UDS repair activity (Figure 93). Dose-response relationships for two known mutagens, namely

NQO and MMS, were examined to check the most appropriate positive control for H4IIE in the UDS assay.

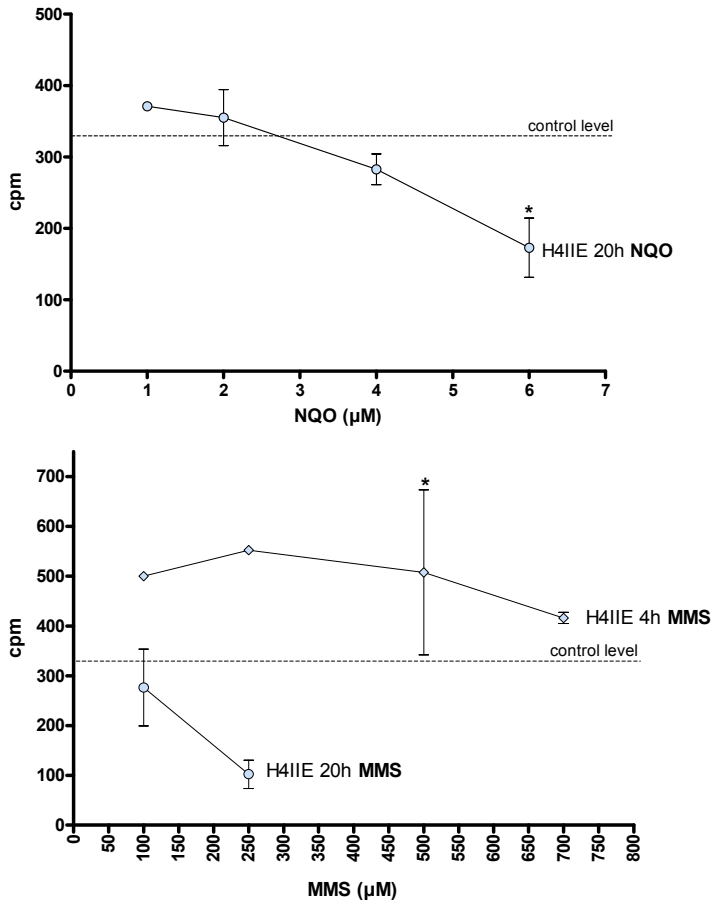

*Figure 93: [3H]-thymidine incorporation (UDS assay) into H4IIE cells following exposure to known mutagens, 4-nitroquinoline-N-oxide (NQO) and methyl methanesulfonate (MMS) at various concentrations in the presence of hydroxyurea (HU, 10 mM. 1 h) for 4 h or 20 h as indicated. Results are presented as counts per minute (cpm). DMSO (0.1%) supplemented with 10 mM hydroxyurea (HU) represents the negative control for unscheduled DNA synthesis. The dashed line displays the level of solvent control cells with HU. Mean ± SD; n ≥ 2, n = 1 when error bars are missing; unpaired t-test, two-tailed p value: significantly different from solvent control *p ≤ 0.05.*

Highest UDS activity was observed in the presence of MMS 250–500 µM after 4 h exposure, which was up to 1.7-fold increased compared to control with HU. A concentration-dependent increase was missing. At the highest dose of MMS 700 µM (4 h) the UDS response slightly decreased, possibly indicating cytotoxicity. Following 20 h treatment, the low MMS concentration (100 µM) did not modify UDS activity, whereas the highest concentration tested (250 µM) yielded a depression of the UDS response, hinting at cytotoxic effects. Treatment with NQO 1-4 µM for 20 h did not induce UDS activity in H4IIE cells. At the highest concentration of NQO 6 µM UDS response was significantly diminished. Microscopic observations confirmed that the cell layer was slightly affected at the highest concentrations for both compounds. Consequently, MMS 100-500 µM at 4 h can be used as an appropriate positive control for the LSC-based method in H4IIE cells.

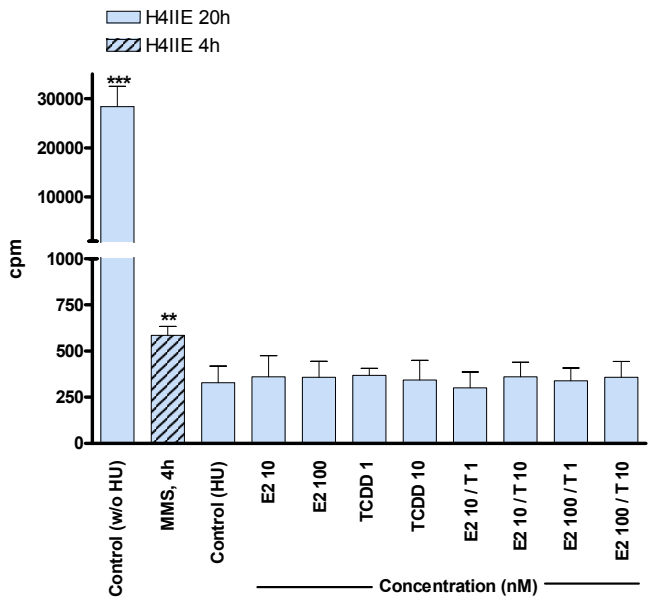

*Figure 94: [3H]-thymidine incorporation (UDS assay) into H4IIE cells following exposure to TCDD (T) and/or E2 for 20 h in the presence of hydroxyurea (HU, 10 mM, 1 h). Results are presented as counts per minute (cpm). DMSO (0.1%) supplemented with HU (10 mM, 1 h) represents the negative control (Control HU) for unscheduled DNA synthesis. DMSO (0.1%) without hydroxyurea (Control w/o HU) represents incorporation of unscheduled and replicative DNA synthesis. Three experiments using either treatment with MMS 250 µM or 500 µM after 4 h exposure were exploited as the positive control. Mean ± SD; n ≥ 3; unpaired t-test, two-tailed p value: significantly different from solvent control with HU **p ≤ 0.01, ***p ≤ 0.001.*

Results of the DNA repair assay in rat H4IIE cell line after 20 h treatment with TCDD and/or E2 are presented in Figure 94. The highest UDS increase was demonstrated in control cells without addition of HU (28373 ± 4182 cpm). Supplementation with HU led to a low radionucleoside-uptake in HU-control (329 ± 90 cpm) resulting in about 98.8% inhibition of replicative DNA repair.There occured no DNA repair induction following treatment with TCDD, E2, or respective combinations for 20 h. The chosen positive control MMS 250 or 500 µM after 4 h treatment resulted in a significant about two-fold higher [3H]-thymidine uptake (545 ± 89 cpm) compared to the negative control with HU.

5.8.3.3. DNA REPAIR ACTIVITY AFTER EXPOSURE TO TCDD AND/OR E2 IN PRIMARY RAT HEPATOCYTES

The optimization experiments for the use of a positive control in male rat hepatocytes are shown in Figure 95. For this purpose, three different potential mutagens, MMS, NQO, and 2-acetylaminofluorene (2-AAF) were tested at various concentrations for 4 h or 20 h.

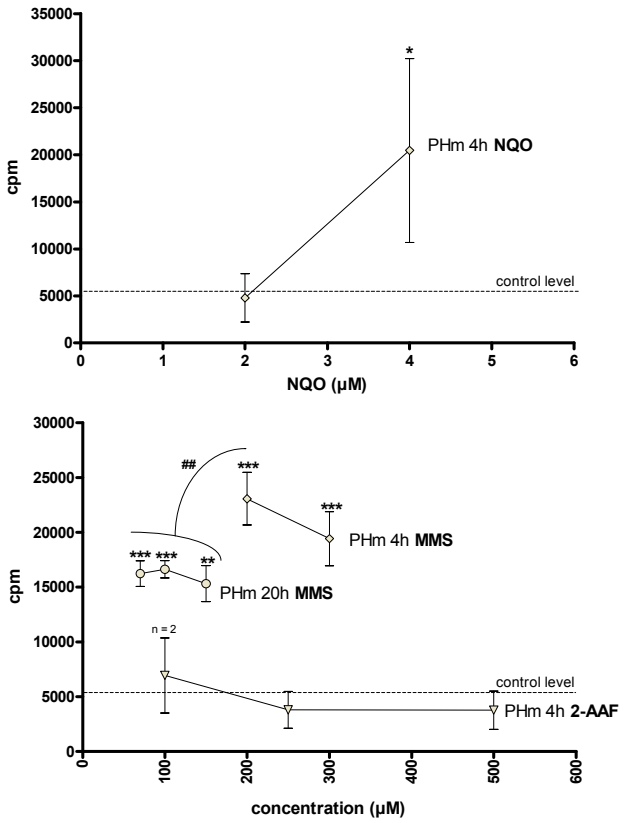

*Figure 95: [3H]-thymidine incorporation (UDS assay) into primary rat hepatocytes from male (PHm) Wistar rats following exposure to known mutagens, 4-nitroquinoline-N-oxide (NQO), methyl methanesulfonate (MMS), and 2-acetylaminofluorene (2-AAF) at various concentrations for 4 h or 20 h as indicated. Results are presented as counts per minute (cpm). DMSO (0.1%) represents the negative control for unscheduled DNA synthesis. The dashed line displays the level of solvent control cells. Mean ± SD; n = 3-4 if not indicated otherwise above the error bars; unpaired t-test, two-tailed p value: significantly different from solvent control *p ≤ 0.05, **p ≤ 0.01, ***p ≤ 0.001; significantly different from indicated treatment ## p ≤ 0.01.*

Despite of great variations, NQO resulted in a significant 3.7-fold induction compared to background levels at the highest concentration tested (4 µM). MMS tested after 4 h (200 and 300 µM) and 20 h treatment (70, 100, 150 µM) significantly increased [3H]-thymidine incorporation. MMS 200 µM (4 h) reached the maximum UDS activity and resulted in a 4.2-fold increase above HU-control (23070 ± 2407 cpm). However, there was no significant difference between the different MMS concentrations. Following 20 h incubation, MMS showed a clear positive response (about 3.0-fold induction), which was significantly lower than the induction achieved by MMS 200 µM after 4 h, but there was no concentration-dependent effect. 2-Acetylaminofluorene did not increase [3H]-thymidine incorporation in male rat hepatocytes at all the concentrations tested after 4 h (100, 250, 500 µM). The highest concentration tested, 2-AAF 500 µM, represented the limit concentration with respect to solubility in DMSO (0.1%).

Tritium-labeled thyimidine uptake into the DNA of male rat-hepatocytes following exposure to TCDD and/or E2 for 20 h is shown in Figure 96.

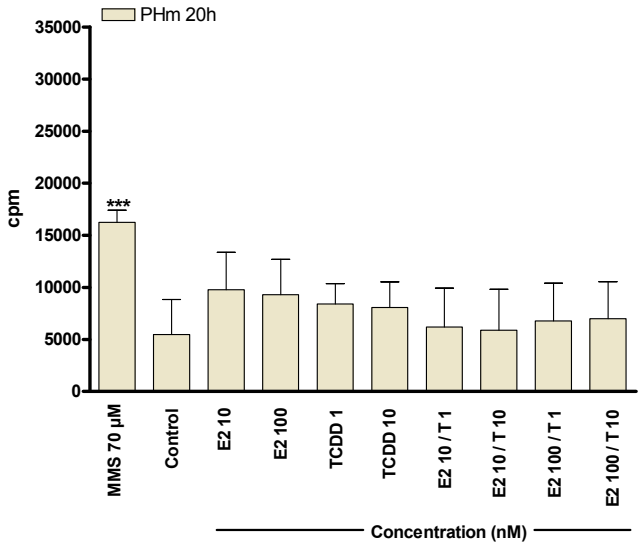

*Figure 96: [3H]-thymidine incorporation (UDS assay) into primary rat hepatocytes from male (PHm) Wistar rats following exposure to TCDD (T) and/or E2 for 20 h. Results are presented as counts per minute (cpm). DMSO (0.1%) represents the negative control. Treatment with MMS 70 µM served as the positive control. Mean ± SD; n = 4; unpaired t-test, two-tailed p value: significantly different from solvent control ***p ≤ 0.001.*

Background levels of unscheduled DNA synthesis were relatively high in primary rat hepatocytes. Solvent control levels from male-derived hepatocytes yielded 5470 ± 3373 cpm. There was no significant difference in DNA repair action observed for all the TCDD and/or E2 treatments compared to solvent control. A tendency to induce DNA repair activity could be demonstrated for single exposure withE2 10 and 100 nM (about 1.7–1.8 fold) or with TCDD 1 and 10 nM (1.5-fold). However, these effects were not statistically significant due to high standard variations. The alkylating agent MMS 70 µM resulted in a highly significant positive response of UDS induction at 20 h (3-fold increase). The testing of several potential positive compounds for the LSC-based UDS assay in primary rat hepatocytes from female rats is compiled in Figure 97. None of the tested positive controls, MMS, NQO, and 2-AAF, showed a positive response under the exact conditions and at the same concentrations that were used for PHm (see Figure 95). DNA repair activity was even significantly lowered for most of the treatments performed. 2-AAFsignificantly diminished UDS activity with increasing concentrations to about half of the solvent control level. Possible cytotoxic effects on adherent cell monolayer cultures were at least not observed under the light microscope. Treatments with 2-AAF and NQO were not performed after 20 h. Consequently, there was no appropriate positive control, which could be exploited in female rat hepatocytes in the course of these experiments.

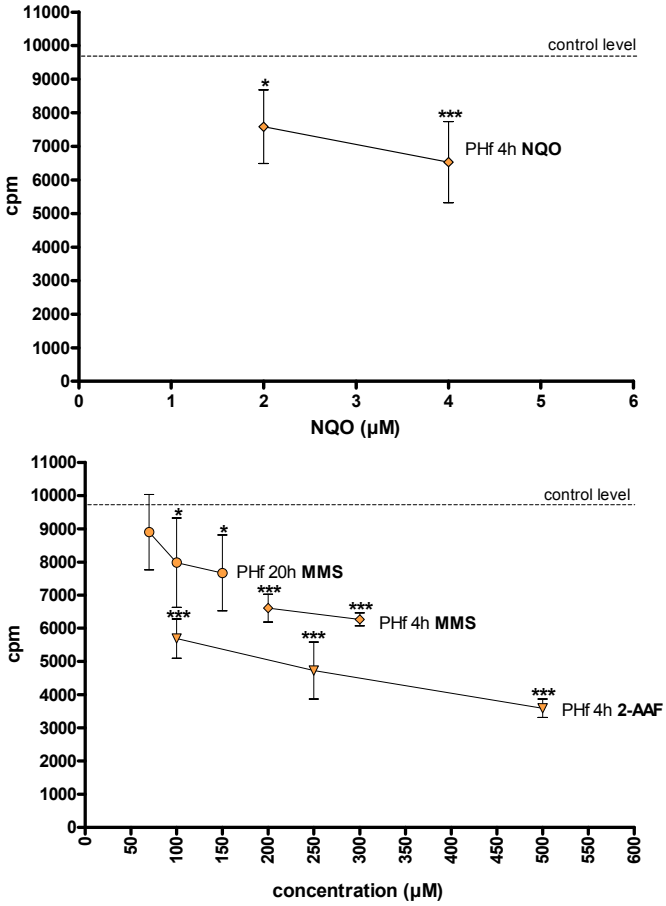

*Figure 97: [3H]-thymidine incorporation (UDS assay) into primary rat hepatocytes from female (PHf) Wistar rats following exposure to known mutagens, 4-nitroquinoline-N-oxide (NQO), methyl methanesulfonate (MMS), and 2-acetylaminofluorene (2-AAF) at various concentrations for 4 h or 20 h as indicated. Results are presented as counts per minute (cpm). DMSO (0.1%) represents the negative control for unscheduled DNA synthesis. The dashed line displays the level of solvent control cells. Mean ± SD; n = 3-4; unpaired t-test, two-tailed p value: significantly different from solvent control *p ≤ 0.05, ***p ≤ 0.001.*

The effects of TCDD and/or E2 in female rat hepatocytes are shown inFigure 98. UDS activity in PHf exerted high background levels for the solvent control. TCDD did not modify DNA repair activity compared to control. Contrary to that, exposure to E2 10 nM and 100 nM resulted in a statistically significant increase (1.3-fold) in [3H]-thimidine incorporation compared to solvent control. There was no concentration-dependent effect observed and the co-treatments showed no effect either. However, the interpretation of these results is difficult because of the lack of a positive control in the LSC-based UDS assay in female rat hepatocytes.

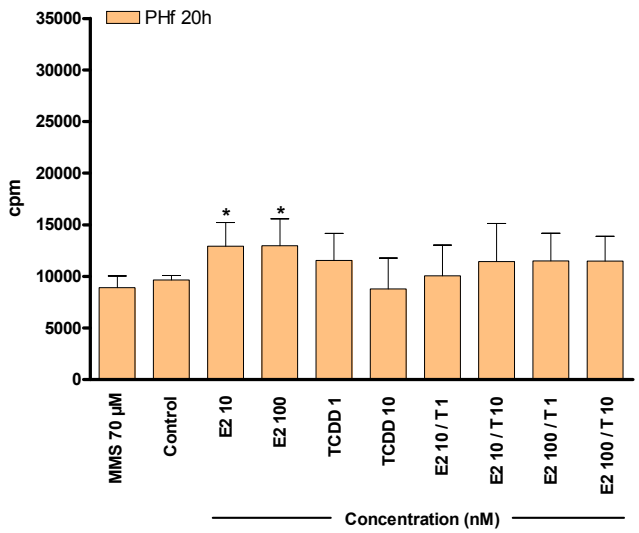

*Figure 98: [3H]-thymidine incorporation (UDS assay) into primary rat hepatocytes from female (PHf) Wistar rats following exposure to TCDD (T) and/or E2 for 20 h. Results are presented as counts per minute (cpm). DMSO (0.1%) represents the negative control. Treatment with MMS 70 µM served as the positive control.. Mean ± SD; n = 4; unpaired t-test, two-tailed p value: significantly different from solvent control *p ≤ 0.05, ***p ≤ 0.001.*

5.8.3.4. SUMMARY OF GENOTOXICITY TESTING

The effects of TCDD and estradiol in the comet assay (normal alkaline conditions and application of FPG) as well as the UDS DNA repair assay of the liver cell models are summarized in Table 27. Since there were no significant concentration-dependent effects observed, the treatments with E2 10 nM, TCDD 1 nM, and the respective co-treatment were chosen as the representative treatments.

In the normal alkaline comet assay (without FPG), neither E2 nor TCDD or the co-treatments were able to induce DNA strand breaks in all the liver cell models tested. In the presence of the FPG protein basal DNA migration was enhanced significantly compared to OTM control levels without FPG. There was no induction of FPG-sensitive DNA damage observed in HepG2 cells and H4IIE cells by E2, TCCD, or the combinations, except for TCDD 1 nM in HepG2. Single treatments with TCDD or E2 induced repair enzyme-specific DNA fragmentation only in rat hepatocytes. The co-treatments enhanced DNA migration to the same extent as the single treatments. The highest DNA damage relative to FPG-solvent control was observed after exposure to E2 10 nM (7.0-fold) in female-derived hepatocytes, which was about 2 times more pronounced compared to male-derived hepatocytes. However, there was no significant sex difference obtained.

Detection of DNA repair activity using the LSC-based UDS assay showed no effects by the treatments in rat and human hepatoma cell lines. Rat primary hepatocytes did not result

in clear DNA repair induction following treatments of the test compounds for 20 h. In PHm there was a minimal tendency of an increasing effect observed by TCDD or E2 single treatments, which was not statistically significant. Cultured female rat hepatocytes showed a small but significant increase in DNA repair activity following exposure to E2 10 nM and 100 nM. However, as there was no adequate positive response obtained in PHf in the UDS assay, the interpretation of the marginal significant response by E2 is difficult.

*Table 27: Overview of genotoxic effects by TCDD (1 nM) and/or E2 (10 nM) after 20 h treatment in hepatoma cell lines and rat primary hepatocytes from male (PHm) and female (PHf) Wistar rats in the alkaline comet assay (with and without FPG) and in the UDS DNA repair assay. Fold inductions compared to respective solvent controls are indicated in the table. Red up arrows stand for a significant induction, the size of the arrow reflects the importance of the damaging effect; (—) indicates no effect compared to solvent control; significantly different from respective solvent control *p ≤ 0.05,**p ≤ 0.01,***p ≤ 0.001.*

	Fold-inductions relative to control				
		Hepatoma cell line		**Primary rat hepatocytes**	
	Treatment (nM)	**HepG2**	**H4IIE**	**PHm**	**PHf**
comet assay (without FPG)	E2 10	—	—	—	—
	TCDD 1	—	—	—	—
	Co	—	—	—	—
comet assay (with FPG)	E2 10	—	—	3.1x ↑**	7.0x ↑**
	TCDD 1	1.9x ↑*	—	3.4x ↑**	4.6x ↑***
	Co	—	—	2.3x ↑**	5.6x ↑***
UDS (LSC)	E2 10	—	—	1.8x	1.3x ↑*
	TCDD 1	—	—	1.5x	—
	Co	—	—	—	—

5.9. FPG-SENSITIVE DNA MODIFICATIONS IN TCDD-TREATED REPAIR-DEFICIENT MICE

The alkaline elution technique was used to quantify the basal levels of FPG-sensitive modifications in the chromosomal DNA of cells isolated from liver of wild-type versus homozygous OGG1$^{-/-}$/csb$^{mut/mut}$ mice 96 h after a single administration of TCDD (i.p., 1 µg/kg bw). The experiments were carried out in cooperation with the Institute of Pharmacy of Prof. Bernd Epe's working group (University of Mainz, Germany), who also kindly provided the knockout animals. Knockout and wild-type mice were aged between 3 and 7 months. The viability of the isolated hepatocytes ranged between 58-88%, which was in the acceptable range according to former experiments performed in the lab. Two animals had to be excluded from the measurements (one ko animal of the TCDD-treated group and one wt animal of the vehicle control group) because of problems during isolation of hepatocytes.

Steady-state (background) levels of FPG-sensitive modifications in hepatocytes of OGG1$^{-/-}$/csb$^{mut/mut}$ knockout mice (0.66 modifications/10^6 bp) were 2.0-fold higher than in wild-type mice (see Figure 99). Likewise, the occurrence of single-strand breaks was also 2.0-fold more elevated in repair-deficient mice (0.10 modifications/10^6 bp) than in wt animals. Thus, DNA modifications were increased to the same extent in OGG1$^{-/-}$/csb$^{mut/mut}$ compared to wild-type mice. However, FPG-sensitive DNA modifications were significantly increased in both knockout mice (about 6-fold) and wild-type animals (about 3-fold) compared to the FPG-independent single-strand break levels. There was no significant difference between the treatment with TCDD and the vehicle control.

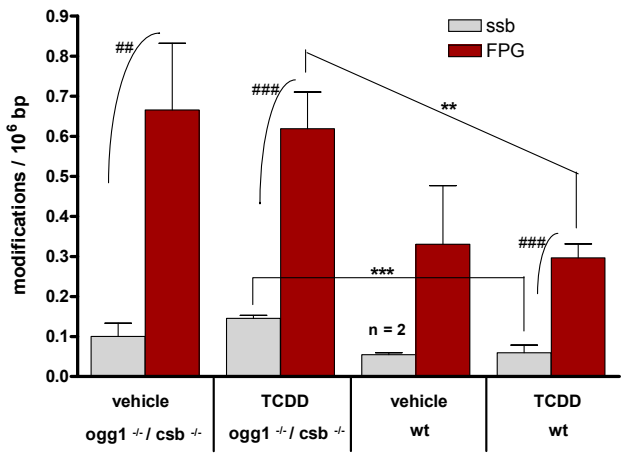

Figure 99: FPG-sensitive DNA modifications (FPG) and single-strand breaks (SSB) in hepatocytes isolated from OGG1$^{-/-}$/csb$^{mut/mut}$ mice and wild-type (wt) animals treated once with TCDD (1 µg/kg bw) and vehicle control (DMSO 0.5%) in corn oil for 96 h. Mean ± SD; n = 3 if not indicated otherwise. Unpaired t-test, two-tailed p value: FPG modifications significantly different from SSB $^{##}p \leq 0.01$, $^{###}p \leq 0.001$. ko mice significantly different from wt-mice $^{**}p \leq 0.01$, $^{***}p \leq 0.001$.

As DNA modifications can be dependent on the quality of the hepatocytes, the correlation between steady-state levels of FPG-sensitive modifications and the viability of the isolated hepatocytes determined by trypan blue exclusion is demonstrated (Figure 100). Generally hepatocyte viability of the animals was higher than 70%. Especially in the wild-type animals, cell viability was about or above 80% (80-88%), whereas in the knockout mice only one animal reached a level of 81%. Hepatocyte viability of the other knockout mice ranged between 58-76%. This relatively reduced viability compared to the wild-type animals might be associated with higher background levels particularly observed for FPG-independent DNA strand breaks. The increase in single-strand breaks is an artifact caused by variable cellular damage during the isolation procedure. Hence, relatively reduced hepatocyte viability in TCDD-treated knockout mice, where 2 out of 3 animals had viability even below 70%, might be responsible for the significant increase in SSB compared to wt mice (compare Figure 99).

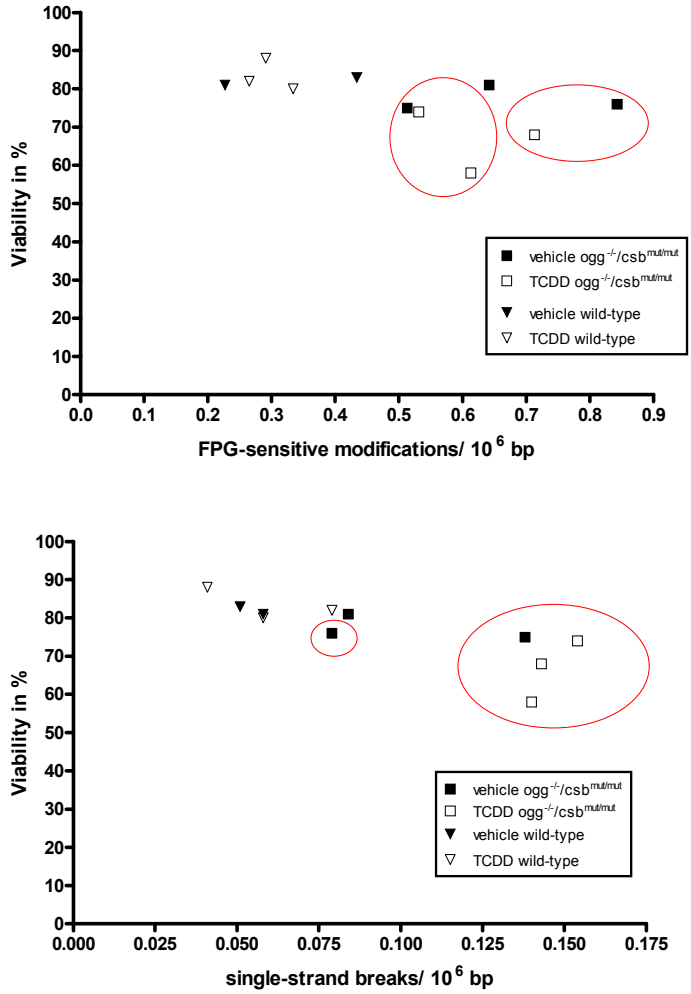

Figure 100: Correlation of the levels of FPG-sensitive modifications (upper diagram) and single-strand breaks (lower diagram) in primary hepatocytes isolated from OGG1$^{-/-}$/csb$^{mut/mut}$ knockout mice and wild-type animals treated once with TCDD and vehicle control (DMSO 0.5% in corn oil) with the viability of the hepatocytes as determined by trypan blue exclusion. Animals with hepatocyte cell viability below 80% are encircled (red line).

All in all, the experiment demonstrated an accumulation of oxidative DNA modifications detected in isolated hepatocytes from OGG1$^{-/-}$/csb$^{mut/mut}$ knockout mice, whereas treatment with TCDD over 96 h did not increase the level of FPG-sensitive DNA modifications. Increased levels of single-strand breaks in knockout mice were in accordance with reduced hepatocyte viability and were rather an artifact caused during isolation procedure.

6. DISCUSSION

6.1. OPTIMIZATION OF CELL CULTURE PARAMETERS

6.1.1. CELL CULTURE MEDIUM AND SERUM SUPPLEMENTATION

The choice of appropriate cell culture medium is essential when investigating enzyme activities and expressions *in vitro*. During this study, different liver cell models, permanent hepatoma cell lines and freshly isolated rat hepatocytes, known to retain endogenous bioactivation and detoxification capacities (Phase 1 and Phase 2 metabolizing enzymes), were used for the investigation of CYP enzyme expression and genotoxicity testing.

The HepG2 hepatoma cell line is a widely used advantageous human-derived permanent cell line, which resembles liver parenchymal cells and expresses a spectrum of certain Phase 1 and Phase 2 metabolizing enzymes (Knasmüller, 1998; Knowles et al., 1980; Sassa et al., 1987; Diamond et al., 1980). However, it has been well documented that drug metabolizing enzymes are unstable and vary greatly in cultured cells. Primary hepatocyte cultures from humans and rodents have been improved over the years, but they lose their drug metabolizing capacity during isolation procedure (Bissel and Guzelian, 1980) or rapidly during the first days if maintained in monolayer culture (Butterworth et al., 1989; Grant et al., 1985). After 24 h in culture about 50% of the aryl hydrocarbon hydroxylase (AHH) activities were lost in rat hepatocytes from Fischer rats, but still high enzyme activities were conserved (Croci and Williams, 1981). Likewise, in cell lines such as HepG2 changes of enzyme activities during one growth period after passaging was reported (Doostdar et al., 1990). Cultured hepatocytes are usually allowed to attach as a monolayer on collagen-coated dishes in order to differentiate. Hepatocytes cultured in a sandwich culture between two layers of gelled extracellular matrix proteins not only prolonged the time of culture but also maintained the cell-specific functions up to several weeks (Tuschl and Müller, 2006).

A number of reports suggest that drug metabolizing enzyme activities depend on the standard culture medium used and the amount of serum addition (Doostdar et al., 1988;

Nakama, 1999; Tuschl and Mueller, 2006). With regard to media, particularly CYP activities and to a lesser extent the activities of the conjugating enzymes UDPGT and GST, were shown to be affected by the use of different available standard media (Doostdar et al., 1988). The lowest MFO activities were obtained in cells grown in DMEM medium, whereas cultures in MEM medium increased EROD, methoxyresorufin *O*-dealkylase (MROD), benzyloxyresorufin *O*-debenzylase (BROD), and pentoxyresorufin *O*-dealkylase (PROD) activities considerably after 7 days in culture (Doostdar, 1988). This was consistent with EROD results in H4IIE and HepG2 cells in the present work, which revealed that culturing in MEM medium was favorable towards increasing induced-EROD levels compared with DMEM. It has to be noted that MEM is also recommended as the appropriate medium for the hepatoma cell lines HepG2 and H4IIE according to the supplier (Health Protection Agency, 2009). Furthermore, MEM is known to be the most effective medium for maintaining CYP contents of cultured rat hepatocytes (Grant et al., 1985). Still, despite the favorable effects of the MEM medium, DMEM medium was kept for the experiments in the present work since it has constituted the well-established standard medium for hepatoma cell lines and primary rat hepatocyte cultures in the laboratory over years.

In addition, medium supplementation, i.e. the addition or omission of serum or specified hormone mixtures has great influence on the morphological development and cell survival of hepatoma cells and hepatocytes in culture. It is well known that serum supplementation enhances the surface attachment of hepatocytes and stimulates cell growth (Williams et al., 1977). Serum added to cell culture medium contains various components such as growth factors, hormones, adhesion molecules, cytokines, amino acids, and vitamins, which exert growth promoting effects for the *in vitro* cultures (Schmitz, 2009). Therefore, cells were seeded in serum-containing medium (10% FBS) for attachment and during the first 24 h of culture before treatment. Nevertheless, reduced serum or serum-free culture was shown to be most applicable for long-term treatments and maintenance of Phase 1 enzyme-inducing potential such as CYP in rat hepatocytes monolayer culture (Tuschl and Müller, 2006). It was also demonstrated that the induction of EROD activity by 3-methylcholanthrene (MC) in HepG2 cells cultured in serum-free medium was about twice as high as in cells cultured in serum-supplemented medium (Nakama et al. 1995). Likewise, in the present work reduced serum conditions (0.5% FBS) during the treatment time did not only lead to higher induced (by TCDD) but also higher basal EROD activities. Thus, reduced FBS serum concentrations (0.5% FBS) were used during the treatments. Additionally, phenol red-free medium was chosen for continuous cell culturing throughout the present work. Usually, phenol red is used as a pH indicator in cell culture media, but it bears a structural resemblance to some non-steroidal estrogens. It exhibits signifi-

cant estrogenic activity at the concentrations at which it is present in culture media. Moreover, it stimulates cell proliferation in ERalpha-containing cells. (Berthois et al., 1986). Generally, it is difficult to evaluate the effects of E2 on cellular metabolism in the presence of serum and phenol red since both factors reduce the degree to which exogenous E2 is able to stimulate responses. For example, different sera containing different amounts of E2 were able to modulate ERalpha expression and inducibility of CYP1A1 and CYP1B1 expression (Spink et al., 2003).

Taken together, medium composition and serum supplementation have great influence on the drug metabolizing activities, which has to be taken into account when comparing characterizing gene expression profiles or enzyme activities between different cell models.

6.1.2. CYTOTOXICITY

Under the optimized culture conditions there were no effects on cell viability observed by the concentrations of TCDD, E2, or the respective co-treatments used in the present study. Likewise, the 2-OHE2 and 4-OHE2 metabolites did not show any cytotoxic effects at the concentrations applied in the comet assay. Thus, based on the results in the Alamar Blue Assay it can be excluded that effects observed in the experiments were due to a cytotoxic effect.

6.2. CYP1A1 AND CYP1B1 EXPRESSION

One proposed mechanism of AhR/ER cross talk is the enhanced metabolism of E2 by TCDD-mediated induction of CYP1A1 and CYP1B1 (Safe and Wormke, 2003) (Figure 101, mechanism 1). Both enzymes are implicated in the activation of E2, and the resulting catechol estradiol metabolites may undergo redox cycling, thus producing ROS and DNA damage (Spink et al., 1990 and 1994).

TCDD, the prototype substance for CYP1A1 induction via the AhR signaling pathway (Whitlock, 1996), highly induced CYP1A1 mRNA, protein, and EROD activity in human HepG2 and rat H4IE hepatoma cell lines, as well as in primary hepatocytes from male and female rats. There was no concentration-dependent effect observed, suggesting that TCDD 1 nM was sufficient to maximize the effect. TCDD is known to be a high affinity AhR agonist in the nanomolar range (Denison and Nagy, 2003). Estradiol 10 and 100 nM did not change CYP1A1 expression at all detection levels (transcription, translation, and activity) in none of the liver cell models tested in the present study. Likewise, E2 did not mod-

ulate TCDD-induced CYP1A1 during co-treatments. The observed low basal expression of CYP1B1 and therefore potentially high magnitude of induction by TCDD can be relevant for E2 metabolism. CYP1B1 has a crucial role for the specificity of the production of the more reactive and genotoxic E2 metabolite 4-OHE2 (Lee et al., 2003; Shou et al., 1997). Basal and induced CYP1B1 expression levels were higher in primary rat hepatocytes than in hepatoma cell lines. Additionally, even E2 was able to slightly induce CYP1B1 mRNA in rat hepatocytes, suggesting an important role for this enzyme.

6.2.1. BASAL CYP EXPRESSION LEVELS

In the present work CYP1A1 and CYP1B1 were constitutively detected at the transcript level in all liver cell models. Generally, basal CYP1B1 mRNA was found to be considerably lower expressed compared to CYP1A1 mRNA. In extrahepatic tissues the major PAH-inducible CYP, CYP1A1, is normally not expressed constitutively, whereas CYP1A1 mRNA and protein can be detected in human liver with highest levels in hepatocytes and in the lung (McLemore et al., 1990; McKinnon et al., 1991). Contrarily, CYP1B1 expression is very low in normal human tissues. CYP1B1 is mainly expressed constitutively in extrahepatocellular (hormone-dependent) organs including the adrenal glands, ovaries, prostate, but also kidney and lung. However, it is inducible by PAHs in the liver. (Shimada et al. 1996)

Significantly higher basal CYP1A1 and CYP1B1 mRNA levels and CYP1A activity were observed in rat primary hepatocytes compared with hepatoma cells. This was consistent with a general finding that activity and expression of Phase 1 enzymes, especially CYPs, were demonstrated to be extremely low in HepG2 cells compared to primary hepatocytes (Wilkening et al., 2003; Wilkening and Bader, 2003). However, the lower endogenous metabolic activities in HepG2 or H4IIE cell line may be either due to original transformation of the hepatocytes to tumor cells or perhaps also in part be a result of inappropriate culture conditions (Doostdar et al., 1988) (see section 6.1). It was reported that rat hepatocytes showed a similar pattern of Phase 1 and Phase 2 enzymatic activities compared to intact rat liver (Croci and Williams, 1981). Thus, human and rat primary hepatocytes are considered to reflect the natural metabolism in the liver more closely than hepatoma cell lines (Croci and Williams, 1981; Wilkening et al., 2003).

Among the different liver cell models, HepG2 showed extremely low basal CYP1B1 levels. Detection of CYP1B1 was difficult in this cell line. However, structural genes for CYP1A1 as well as CYP1B1 have been described to be present in HepG2 cell line (Kress and Greenlee, 1997). Measurable basal levels of CYP1B1 mRNA were only obtained in HepG2 when a specifically designed TaqMan probe was applied during real-time RT PCR. Moreover, a

RNA extraction method resulting in purified mRNA was chosen to improve RNA quality. The high CT values obtained for solvent-treated HepG2 cells revealed that only traces of CYP1B1 mRNA were detected, which could also explain the high standard deviations.

Transient transfection of ERalpha in HepG2 cells led to a significant increase in absolute basal CYP1A1 and CYP1B1 mRNA levels compared to wild-type HepG2 cells, suggesting a role for ERalpha in the modulation of CYP status. Similar results of increased CYP1A1 mRNA were observed after over-expression of ERalpha in T47D human breast cancer cells (Matthews et al., 2007). The endogenous expression of ERalpha in the primary rat hepatocytes may correlate with higher basal CYP levels compared with ERalpha-negative hepatoma cells (see section 6.5 mRNA).

In the present work CYP1A1 basal levels were found to be considerably higher than CYP1B1 basal mRNA levels, whereas no constitutive protein expression was detected. Similarly, in the liver of female Sprague Dawley rats measurable basal CYP1B1 and CYP1A mRNA levels were detectable using real-time RT PCR, though CYP1B1 basal levels were considerably lower and in contrast to CYP1A1 protein, no CYP1B1 protein was detected in the control animals (Tritscher et al., 1996).

6.2.2. EFFECTS OF TCDD AND/OR E2 TREATMENT

6.2.2.1. CYP1A1 AND CYP1B1 EXPRESSION IN HEPG2

In spite of low basal mRNA levels HepG2cells highly induced CYP1A1 mRNA, protein, and activity after TCDD treatment, being almost as efficient as rat hepatocytes. Previously performed experiments already showed considerably increased CYP1A1 protein or mRNA levels (Northern Blot analysis) in TCDD-treated (1 and 10 nM, 48 h; 2 nM, 20 h) HepG2 cells but not in control cells (Zeiger et al., 2001; Knerr et al., 2006).

E2 alone was not able to change CYP1A1 levels and did not modulate TCDD-induced expression levels. Likewise, Coumoul and co-workers (2001) demonstrated that E2 10 nM did not modify TCDD-induced mRNA levels after 24 h incubation as detected by Northern Blot analysis. However, in their study E2 was able to decrease TCDD-induced EROD activity after, suggesting a post-transcriptional effect (Coumoul et al., 2001). (EROD results see section 6.3)

HepG2 cells showed extremely low basal CYP1B1 mRNA, but TCDD clearly induced CYP1B1 levels. Surprisingly, after 20 h treatment E2 alone dose-dependently decreased CYP1B1 mRNA resulting in a significant decrease at the highest E2 concentration of 100 nM. Two of the co-treatments with E2 10 nM and 100 nM were able to enhance TCDD-induced CYP1B1 mRNA level, but without a time- and dose-related effect. Very low

CYP1B1 mRNA correlated with weak immunoreactive CYP1B1 protein bands. A minimal induction by TCDD and the co-treatments could possibly be interpreted as a TCDD-dependent induction of CYP1B1 protein.

Reports of of CYP1B1 expressionin the HepG2 cell line are inconclusive. Very often CYP1B1 mRNA was not detected in both control and dioxin-treated HepG2 cells using RNA hybridization analysis. In several independent studies basal levels of CYP1A1 and CYP1B1 mRNA could not be detected in HepG2 using Northern Blot analysis, but TCDD increased levels of CYP1A1 but not CYP1B1 mRNA (Coumoul et al., 2001; Kress and Greenlee, 1997; Spink et al., 1994). Additionally, the expression pattern of CYP1A1 and CYP1B1 protein reflected the expression of the respective mRNAs in TCDD-treated (10 nM, 24 h) cells (Kress and Greenlee, 1997). Using RT-PCR method, CYP1B1 mRNA was sometimes found to be constitutively expressed and inducible by TCDD in HepG2 cells (Li et al., 1998; Lekas et al., 2000), while others were not able to detect basal CYP1B1 mRNA levels (McFadyen et al., 2003). Spencer and co-workers (1999) found a clear dose-dependent CYP1B1 mRNA induction in HepG2 exposed to TCDD (0.1 – 10 nM, 72 h) using classic RT-PCR. However, the levels of CYP1B1 expression were stated to be much lower in HepG2 cells than in human breast cancer MCF-7 cells, the latter are well known to express CYP1B1 (Spencer et al., 1999). With the use of the nowadays commonly used very sensitive real-time RT PCR method basal and AhR ligand-induced CYP1B1 mRNA levels were detected after treatment with the low affinity AhR ligand 3-MC (McFadyen et al., 2003). Taken together, the failure of the expression of CYP1B1 in HepG2 cell line often described in the literature was rather due to the low sensitivity of the method used. It is suggested that CYP1B1 expression is very low in HepG2 and probably below the level of detection for Northern Blot analysis. The more sensitive method of real-time RT PCR was found to be more appropriate to detect such trace mRNA levels. Other reasons for the inconsistency in the published results may be differences in the quality of purified mRNA (extraction method) or different cell culture conditions.

Several studies focusing on differences in CYP1A1 and CYP1B1 expression have been performed with HepG2 cell line in comparison with ER-positive MCF-7 breast cancer cells. Basal and induced levels of both genes were only detected in MCF-7 cell, but TCDD increased CYP1A1 mRNA but not CYP1B1 in HepG2 (Coumoul et al., 2001). Significant levels of basal CYP1B1 mRNA and dose-dependent induction of CYP1B1 mRNA by TCDD can easily be detected in MCF-7 by Northern blot analysis (Hayes et al., 1996). Using real-time RT PCR analysis, the breast cancer cell line showed higher basal and 3-MC-induced CYP1B1 mRNA levels than HepG2 cells, which was also reflected in Western Blot analysis, since CYP1B1 protein could only be detected in 3-MC-treated MCF-7 but not in HepG2

cells (McFadyen et al., 2003). However, CYP1A1 mRNA was induced to a lower extent in MCF-7 cells compared to HepG2 cells (Spink et al., 1994; McFadyen et al., 2003). Higher basal and induced levels of CYP1B1 in human MCF-7 cells may partly be explained by the high levels of ERalpha in breast cancer cells. Indeed, in the present study HepG2 cells transiently transfected with ERalpha resulted in higher basal CYP1A1 and CYP1B1 levels compared with normal HepG2 cells. Over-expression of ERalpha did however not change relative CYP1A1 and CYP1B1 mRNA levels induced by TCDD and the co-treatments compared with wild-type HepG2 cells. Nevertheless, the slight decrease in CYP1B1 mRNA observed with E2 in normal HepG2 cells was compensated in the presence of ERalpha (see also transfection results section 6.6).

6.2.2.2. CYP1A1 AND CYP1B1 EXPRESSION IN H4IIE

Rat hepatoma H4IIE cell line exerted highest CYP1A1 mRNA inductions by TCDD among the different cell models tested. H4IIE cells were reported to induce CYP1A1 mRNA, protein, and EROD activity after TCDD (0.001–8 nM, 24 h) treatment (Lai et al., 2004 and 2006). The protein synthesis inhibitor cycloheximide was shown to block the TCDD-induced degradation of the activated AhR/ARNT complex resulting in CYP1A1 mRNA superinduction in H4IIE and mouse hepatoma Hepa 1c1c7 (Lai et al., 2004; Ma et al., 2000). Normally, TCDD-mediated AhR activation is counteracted by a reduction of the nuclear AhR through degradation, which is mediated by the 26 S proteasome and involves ubiquitination of the AhR protein (Pollenz et al., 1994; Ma and Baldwin, 2000). In the present work, the high CYP1A1 mRNA induction levels after 20 h treatment in H4IIE cells were assumed to be associated with subsequent AhR degradation and may also account for a compensatory increase in AhR mRNA levels observed after 48 h treatment. Likewise, higher TCDD-mediated CYP1A1 protein at 48 h compared to 20 h may be associated with higher AhR mRNA levels at 48 h (see section 6.4).

The co-treatments of TCDD with E2 had no modulating effects on TCDD-induced CYP1A1 mRNA or protein expression. These results were not in accordance with the reported down-regulation of TCDD-induced (1.6 nM) CYP1A1 mRNA, protein, and EROD activity after co-treatment with E2 (50-100 µM) for 24 h (Lai et al., 2004). This E2-mediated suppressive effect could not be blocked by a protein synthesis inhibitor or by ER antagonists, suggesting the process being independent of a post-transcriptional way and not dependent on ER (Lai et al., 2004). Since considerably high E2 levels were used in the study of Lai and co-workers (2004) compared with the low concentrations used in the present work, the reported effects are considered to be rather due to cytotoxic effects. Moreover, the presence of ERalpha in H4IIE was not confirmed in this work as ERalpha mRNA was not detected (see section 6.5).

TCDD also induced CYP1B1 mRNA and protein levels in H4IIE. There was no effect on CYP1B1 levels observed for E2 alone, nor did it have a modulating effect on TCDD-induced levels. Lai and colleagues (2006) demonstrated that TCDD (1.6 nM) slightly increased CYP1B1 mRNA in H4IIE cells with no clear time-dependent relation (4, 8, 12, 24 h exposure). TCDD-dependent CYP1B1 mRNA increase was much lower than CYP1A1 induction (Lai et al., 2006), which was consistent with the results in the present study.

6.2.2.3. CYP1A1 AND CYP1B1 EXPRESSION IN RAT HEPATOCYTES

In primary rat hepatocytes TCDD-induced CYP1B1 mRNA expression was higher than CYP1A1 mRNA expression, which was however not evident in protein levels. Relatively high TCDD-mediated CYP1A1 mRNA increase was reflected in well-induced protein levels. This suggests that CYP1B1 protein may be less stable than CYP1A1 or that post-transcriptional processes play a role.

In vivo experiments showed parallel induction of CYP1A1 and CYP1B1 mRNA in the livers of intact and ovariectomized Sprague Dawley rats chronically exposed to TCDD (100 ng/kg bw/d, 30 weeks) as detected by RT-PCR (Tritscher et al., 1996). Higher induced CYP1A1 mRNA and protein levels compared with CYP1B1 were observed in the liver of female Sprague Dawley rats, that were chronically administered TCDD (up to 125 ng/kg bw, 30 weeks,) (Walker et al., 1999). Sprague-Dawley rats treated with a single oral dose of TCDD (25 µg/kg bw) showed increased CYP1B1 mRNA after 72 h in various tissues with the highest levels in the liver (Walker et al., 1995). These reports all indicate that despite low constitutive levels, CYP1B1 is well inducible by TCDD in the rat with the liver as the major target site.

Moreover, CYP1B1 mRNA but not CYP1A mRNA was found to be induced sex-specifically with higher levels in the livers and kidneys of TCDD-treated female Sprague Dawley rats (Walker et al., 1995). Likewise, results in rat hepatocytes from Wistar rats in the current study revealed higher induced CYP1B1 mRNA and protein levels in female-derived hepatocytes compared with male-derived cells (at least after 20 h) treated with TCDD and/or the co-treatments.

In the present work E2 alone was not able to induce CYP1A1 in rat primary hepatocytes. In contrast, CYP1B1 mRNA but not protein was slightly but significantly induced following treatment with E2, but only after 48 h treatment. Tsuchiya and co-investigators (2004) were the first to demonstrate that E2 alone (10 nM, 12 h) induced expression of human CYP1B1 mRNA in ER-positive MCF-7 breast cancer cells, which was found to be mediated by the direct interaction of ERalpha with an ERE in the 5’regulatory region of the human CYP1B1 gene. Likewise, E2 alone (100 nM) was reported to slightly but significantly in-

crease CYP1B1 mRNA but not CYP1A1 in ER-rich MCF-7 cells (Beischlag and Perdew, 2005). Based on findings of minimal induction of CYP1B1 by E2 in rat hepatocytes only after 48 h treatment in the present study, it can be suggested that E2 stimulates its own metabolism via induction of CYP1B1 and that a rather long treatment time is required. In concordance with that, the levels of CYP1A1 and CYP1B1 mRNA in TCDD-treated MCF-7 cells were shown to be lower and increased in cells maintained over several passages in normal E2-containing (i.e. 10 % FBS) medium compared to E2-deprived medium conditions. Additionally, this described E2-mediated effect was difficult to be observed after 48 h in culture under the same conditions. (Spink et al., 2003).

The co-treatments had no modulating effect on TCDD-induced CYP1A1 and CYP1B1 expression levels in rat hepatocytes. In *in vivo* experiments TCDD but not E2 induced CYP1A1 protein and activity in the liver of intact and ovariectomized Long Evans rats. TCDD-mediated CYP1A1 induction could be enhanced when the animals were exposed to a single dose of TCDD and E2 for several days. (Sarkar et al., 2000). This suggests enhancement of TCDD-mediated CYP induction after repeated dose of E2 *in vivo*.

Apart from the above described regulation of CYP1B1 by ERalpha, the control of CYP1B1 mRNA expression could involve transcriptional and post-transcriptional factors. Investigation of the upstream region of the 5'-flanking region of the human CYP1B1 gene, which contains basal regulatory elements and XREs, revealed the existence of positive and negative regulatory elements (Wo et al., 1997). Additionally, both mouse and rat CYP1B1 have been reported to be also regulated by cyclic AMP (cAMP)-mediated pathways. However, it is unclear if the same mechanism is present in human cells. (Brake and Jefcoate, 1995)

6.3. INDUCTION OF CYP1A ENZYME ACTIVITY

The EROD assay was used to determine CYP1A activity in order to evaluate the influence of estrogen on TCDD-inducible effects subsequent to gene expression. All three CYP1 enzymes exhibit EROD activity with the order of specific activities being CYP1A1 > CYP1A2 > CYP1B1, so that in the presence of CYP1A1 EROD activity primarily CYP1A1 activity is reflected (Doostdar et al., 2000).

Higher basal EROD levels were observed in primary rat hepatocytes than in hepatoma cell lines. These results were in accordance with former results (Knerr et al., 2006). Accordingly, EROD activities in HepG2 were also reported to be lower than in freshly isolated hu-

man adult hepatocytes (Grant et al., 1988), suggesting lower basal enzyme activities in tumorigenic cells.

In the current study treatment time for the EROD assay was set at 48 h, because results previously obtained in the laboratory showed that exposure to TCDD 1 nM reached its maximal efficacy after48 h treatment time in male rat hepatocytes, H4IIE, and HepG2 cell line (Zeiger et al. 2001).

High TCDD-mediated mRNA and protein induction levels in the different liver cell models were confirmed in induced EROD activity. Highest induced EROD activities were observed for male rat hepatocytes and HepG2 cell line. Concomitant to the results obtained with real-time RT PCR and Western Blot, E2 alone did not change CYP1A activity and the co-treatments had no effect on TCDD-induced enzyme activities.

In contrast to the results presented here, previously performed EROD studies in the laboratory demonstrated that TCDD-induced (1 nM) EROD activity was considerably higher in primary hepatocytes from male Wistar rats compared to HepG2 cells after 48 h treatment (Zeiger et al., 2001; Knerr et al., 2006). The difference in induced EROD levels between cells of human and rat origin was also found in human hepatocytes compared to rat hepatocytes, with the latter exhibiting higher TCDD-dependent EROD activity and CYP1A1 mRNA and protein expression (Xu et al., 2000). These differences compared to the results in the present study may be explained by different cell culture conditions. In the above stated studies treatments were performed in medium with high serum contents (10-20 %), wherea sin the current work the use of reduced serum conditions was shown to result in higher EROD activities in HepG2 cell line (see section 6.1). Additionally, Zeiger and colleagues (2001) as well as Knerr and colleagues (2006) treated the freshly isolated hepatocytes on the day of isolation, whereas in the present study hepatocytes were allowed to attach to collagenated plates overnight before the addition of test compounds. Moreover, the use of different EROD methods, and whether the test was performed in homogenized cells (Knerr et al., 2006) or in intact cells, as in the present study, may account for different inducibilities.

A gender difference was observed in the induction of CYP1A activity between hepatocytes from male and female Wistar rats. Hepatocytes from male rats showed significantly higher TCDD-induced but not basal EROD activities than female-derived hepatocytes. In fact, several studies indicated that mixed function oxidase activities are sex-dependent in the rat following induction, with males having higher activities than females (Croci and Williams, 1985; Probst and Hill, 1987; McQueen et al., 1986) (see also section 6.11.2). Determination of Phase 1 oxidative activities in hepatocytes from young adult male or

female Fischer F344 rats showed that basal liver activities of aryl hydrocarbon hydroxylase (AHH) was 5-fold higher in the male than in the female hepatocytes, with this difference being preserved during hepatocyte isolation process and during subsequent culture. Likewise, CYP contents in the male liver were higher than in the female liver. (Croci and Williams, 1985)

In the liver of female Long Evans rats, which were treated with a single doses of TCDD (100, 300, 1000 ng/kg bw), induced EROD activity were detected in both intact and ovariectomized female rats, and the highest dose of TCDD was able to decrease E2 serum levels in intact rats (Sarkar et al., 2000). A similar decrease in E2 levels by TCDD was also reported in the serum of female Holtzman rats (Chaffin et al., 1996) and in MCF-7 cell culture (Spink et al., 1990), and was attributed to enhanced hydroxylation of E2 to the respective 2-OHE2 and 4-OHE2 metabolites following CYP induction by TCDD. Using a low single dose of TCDD, which did not influence E2 serum levels, the co-treatment of E2 (administered daily for 11 days) and then TCDD in a single dose potentiated TCDD-induced CYP1A1 protein and activity, but E2 alone had no effect (Sarkar et al., 2000).This potentiation of CYP1A enzyme activity showed that E2 after repeated dose is able to affect the transactivation of the CYP1A1 gene in response to TCDD in order to stimulate its own metabolism. In contrast to the reported potentiating effect, E2 10 nM significantly reduced both basal and TCDD-induced (10 nM) CYP1A1 activity after 24 h in ER-rich MCF-7 breast cancer cells and to a lesser extent in HepG2 cells. These results confirmed that the hepatoma cell line is less sensitive to E2 than MCF-7 cells, which may be because of the lack of functional ERalpha in HepG2. (Coumoul et al., 2001). Overall, the different effects by the co-treatments are inconclusive. However, modulating effects by E2 are reported, which may depend on the origin of the cell type and culture conditions.

6.4. AHR MRNA STATUS AND TREATMENT EFFECTS

Since TCDD exerts most if not all of its carcinogenic effects via activation of the aryl hydrocarbon receptor signal transduction pathway followed by altered gene expression (Mimura and Fujii-Kuriyama, 2003), the effects on the receptor status in the four liver cell models were assessed by TaqMan real-time RT PCR. The findings clearly showed that Ah receptor mRNA was differentially expressed in the cells examined. Primary hepatocytes from male rats exhibited a higher constitutive level of AhR than rat hepatocytes from females, and HepG2 and H4IIE hepatoma cell lines after 20 h and 48 h in culture.

Higher AhR basal levels found in male rat hepatocytes compared to human and rat hepatoma cells may be due to a loss of natural receptor levels during cell transformation and

also correlated well with the lower CYP expression levels observed in hepatoma cells, showing that CYP expression is regulated according to AhR expression (see section 6.2). At the same time, it was reported that nuclear AhR levels in TCDD-treated rat hepatocytes were approximately 4 times higher than in TCDD-treated human hepatocytes, suggesting a species difference (Xu et al., 2000). However, binding affinity of tritium-labeled TCDD to nuclear AhR from rat and human hepatocytes was comparable (Xu et al., 2000). The observed sex difference with female-derived hepatocytes exhibiting lower basal AhR levels did not correlate with basal CYP expression, but may be related to lower induced CYP1A activities that were observed in females following possibly post-transcriptional changes after induction by an AHR agonist (see section 6.3).

Following treatments the results in the present work were generally in agreement with other groups that found that AhR mRNA was not changed by treatment with TCDD 2 nM or low affinity AhR agonists such as 3-MC (0.1 and 25 µM) after 48 h treatment in human HepG2 or mouse Hepa-1 hepatoma cell lines (Giannone et al., 1998; Mc Fadyen et al., 2003). In H4IIE cells, which expressed lowest basal AhR mRNA levels, TCDD and the co-treatments increased AhR mRNA levels, but only after 48 h exposure and without a difference in induction levels by the different treatments. This increase was suggested to be a time-dependent compensating effect for the relatively low basal AhR levels avoiding the AhR to become the limiting factor for CYP expression in this cell line. Moreover, also E2 alone at the low concentration of 10 nM induced AhR expression in H4IIE after 48 h treatment. A similar response was reported in MCF-7 cells treated with E2 1 nM for 72 h, but only when cells were cultured over several passages in E2-containing medium, i.e. medium supplemented with serum (Spink et al., 2003). This may imply a possible role for E2 on AhR responsiveness under certain cell culture conditions, possibly also suggesting a role for ERalpha. However, in the case of H4IIE cells the observed increase in AhR mRNA cannot be explained by the presence ERalpha, as H4IIE cells were not found to possess ERalpha mRNA (see section 6.5). Still, slightly increased AhR mRNA was also found in ER-positive female-derived rat hepatocytes after 48 h treatment with TCDD 1 nM and the co-treatment TCDD 1 nM/ E2 100 nM. Taken together, it is suggested that the increase in AHR might be subsequent to treatment with an AhR ligand to stimulate mRNA expression, which could be a response to compensate for AHR protein degradation processes often observed in cultured cells as a regulation of AHR following its activation (Ma and Baldwin, 2000).

Investigation of the AhR mRNA status in ERalpha-transfected HepG2 showed significantly increased AhR mRNA following treatments with TCDD 10 nM and the co-treatment TCDD 10 nM/E2 10 nM. Moreover, relative induction levels following treatment with E2 100 nM

or TCDD 10 nM were significantly enhanced in transfected HepG2 compared with wild-type HepG2 cells. Basal AhR mRNA levels were not affected by the presence of ERalpha in HepG2, indicating a treatment-dependent effect on AhR mRNA. Likewise, endogenous AhR protein and mRNA expression of AhR and ARNT was reported to be unaffected by over-expression of ERalpha in HuH7 human hepatoma cell line (MacPherson et al. 2009). The occurrence of enhanced relative AhR mRNA following treatment may correlate with enhanced CYP1B1 mRNA amounts in ERalpha-transfected HepG2 as described before (see section 6.6), supporting the role for ERalpha in the regulation of AhR.

In ER-positive MCF-7 cells (Spink et al., 2003) and ER negative mouse Hepa-1 cells (Giannone et al., 1998; Pollenz et al. 1994) TCDD treatment caused a reduction in immunoreactive AhR protein levels, which could be explained by AHR degradation. *In vivo* results showed that AhR protein levels in the liver of E2- and/or TCDD-treated intact and ovariectomized female Long Evans rats after single dose were not changed (Sarkar et al., 2000). As the focus of this study was on the implicated effector molecules of the AhR activation pathway, the levels of receptor protein were not investigated.

6.5. ERALPHA STATUS AND TREATMENT EFFECTS

In order to better characterize the effects of CYP1A1 and CYP1B1 induction and possible E2-mediated effects, it was important to determine the ERalpha status in the different liver cell models. There was no measurable ERalpha mRNA detected in rat H4IIE and human HepG2 cell lines using the sensitive TaqMan qPCR method. In contrast, rat primary hepatocytes exhibited low but measurable ERalpha mRNA levels with no sex-difference. In the course of a research internship extremely low but measurable mRNA levels of the ERbeta subtype were detected in rat hepatocytes from male rats (female rats were not performed), but ERbeta was expressed at much lower rates (two magnitudes lower) than ERalpha. The presence of both ER subtypes reflects the physiological situation of the liver (Pearce and Jordan, 2004). As expected transfection of ERalpha in HepG2 showed considerably high basal mRNA receptor levels and was used as a good model to compare effects of high ERalpha levels compared to rat hepatocytes with low ERalpha levels. HepG2 cells did not express functional ERalpha, but low expression evels of ERbeta mRNA were detected in HepG2 cells (Iwanari et al., 2002).
Treatments with TCDD and/or E2 did not alter mRNA receptor levels in male-derived rat hepatocytes and in transiently transfected ERalpha HepG2 cells. In contrast, female-derived rat hepatocytes showed decreased mRNA levels after treatments with E2 10 nM and the corresponding co-treatments of E2 10 nM with TCDD, which werehowever not

confirmed in translation processes. ERalpha protein levels were not changed by treatments with TCDD and/or E2 in rat hepatocytes. Similarly, in *in vivo* experiments the amount of constitutive nuclear ER was not affected in the liver of E2- and/or TCDD-treated (single dose) intact female Long-Evans rats, whereas in ovariectomized rats ER protein was increased upon single E2 treatment and the co-treatment, suggesting a stabilizing effect of E2 on hepatic ER levels (Sarkar et al., 2000).

Contrary to the liver tissue, TCDD-dependent antagonizing effects on estradiol-mediated increased uterine ER protein levels weres observed in rats after single dose treatment with E2 and/or TCDD (Romkes and Safe, 1988) and may be associated with enhanced regulation of AhR responsiveness to regulate E2 levels via CYP-mediated metabolism. Furthermore, from numerous investigations in ER-rich human breast cancer cell lines or endometrial carcinoma cells it was reported that TCDD did not affect changes of ERalpha at transcription processes, but down-regulated nuclear ERalpha protein levels (Jana et al., 1999 and 2001; Wang et al., 1993; Harris et al., 1990). The decrease in ERalpha levels was described to be due to a a rapid proteasome-dependent degradation of ERalpha protein induced by TCDD as observed in T47D, ZR-75, and MCF-7 human breast cancer cells (Safe et al., 2000). This antagonizing effect by TCDD was postulated as a possible mechanism of dioxin-related anti-estrogenic effect (Wormke et al., 2003). In turn, E2-deprivation in cultured MCF-7 cells was shown to increase ERalpha levels but reduce AhR mRNA levels. This was known as as negative feedback mechanism in the regulation of ERalpha expression in hormone-dependent tissues. (Pink and Jordan, 1996; Jeng et al., 1998)

6.6. OVER-EXPRESSION OF ERALPHA

6.6.1. ESTRADIOL-ENHANCED AHR-MEDIATED TRANSCRIPTIONAL ACTIVITY VIA ERALPHA

Activation of over-expressed ERalpha acted as a modulator of AhR activity and enhanced AhR-mediated transcriptional activity. HepG2 cells transfected with a XRE luciferase reporter encoding for rat CYP1A1 induced TCDD-dependent reporter gene activity in the absence and in the presence of the human ERalpha expression vector. Co-treatment of TCDD 1 nM with E2 10 nM further increased AhR-regulated transcription only in the presence of constitutively expressed ERalpha, suggesting a role of ERalpha in the enhancement of AhR signaling. E2 alone had no effect on AhR-mediated transcriptional activity. 8-Methoxypsoralen (8-MOP), a binding inhibitor of activated AhR/ARNT complex (AhRC) to dioxin response elements, was able to completely inhibit TCDD-induced XRE-driven lucife-

rase activity (Jin et al., 2004). Thus, activated AhRC was required for these transactivation processes.

Thes results in the present study were consistent with reports from other research groups. Accordingly, induction of luciferase by TCDD (20 nM, 18 h) in HepG2 cells transfected with pXRE$_3$-luc was decreased when cells were co-transfected with respective silencing siRNAs for AhR and ARNT. Moreover, expression of the target protein CYP1A1 was also decreased. (Abdelrahim et al., 2003)
As previously described, TCDD (10 nM) -bound AhR recruited ERalpha to CYP1A1 and CYP1B1 promotor occupancy shortly after ligand addition (60-120 min), which could be enhanced by additional treatment with E2 10 nM in ERalpha- and AhR-positive MCF-7 and T47D human breast cancer cells. In these experiments, E2 alone (10 nM) had no effect on promoter occupancy of ERalpha at CYP1A1, suggesting that the recruitment was dependent on both activated AhR and activated ERalpha (Matthews et al., 2005). Indeed, co-treatment of TCDD 1 nM with E2 10 nM further enhanced AhR-regulated transcription only in the presence of constitutively expressed ERalpha, suggesting a role of ERalpha in the enhancement of AhR signaling in HepG2.

The importance of the presence of ERalpha for AhR-mediated transactivation has been widely reported in breast cancer cells and hormone-related cancer cell lines. Vickers and co-workers were the first who pointed out that for a series of ER-positive and ER-negative breast cancer cell lines only the former cells were Ah-responsive as determined by the induction of CYP1A1 gene expression by TCDD (Vickers et al., 1989). ER-negative MDA-MB-231 cells restored TCDD-dependent (10 nM, 48 h) gene expression after transient transfection with ERalpha and the increase in transcriptional activity was more pronounced than the slight induction observed in non-ERalpha-transfected MDA-MB-231 cells. In return, down-regulation of the ER in MCF-7 cells by the anti-estrogen ICI 164,384 was accompanied by loss of Ah responsiveness. (Thomsen et al., 1994). Human uterine endometrial carcinoma KLE cells, that are defective in translocating ER into the nucleus but express high levels of AhR, could only induce CYP1A1 by TCDD after transient transfection of normal ERalpha expression plasmid along with TCDD-responsive pGL3-XRE-LUC, suggesting that nuclear translocation of ER was essential for CYP1A1 induction (Jana et al., 1999).

Similar effects to those observed in ERalpha-transfected HepG2 cell line in the current work were obtained by other research groups in human hepatoma cell line HuH7 after ER was transfected (Matthews et al., 2005; McPherson et al., 2009). Just like HepG2 cells HuH7 are responsive to AhR but do not possess ERalpha. Increasing amounts of ERalpha

expression plasmid in HuH7 cells resulted in a dose-dependent potentiation of TCDD-induced luciferase reporter gene activity after 24 h co-treatment of TCDD with E2 1 nM or 10 nM. Opposite to ERalpha-dependent effects, the expression of ERbeta did not affect AhR activity in HuH7 cells, suggesting ER subtype selectivity. (Matthews et al., 2005). This finding is important since HepG2 cells do not possess ERalpha, as confirmed in the lack of ERalpha mRNA, but were reported to have ERbeta (Iwanari et al., 2002). A recent study investigated the effects of stable siRNA–mediated knockdown of ER subtypes on CYP mRNA expression in HC11 mouse mammary epithelial cells (Wihlén et al., 2009). Suppression of ERalpha reduced, but knockdown of ERbeta enhanced TCDD-induced CYP1A1 expression in the non-tumorigenic HC11 cells. TCDD-induced CYP1B1 mRNA expression was reduced at either ERalpha or ERbeta knockdown in the mouse cell line. In turn, siRNA-mediated knockdown of ERalpha in MCF-7 breast cancer cell line had no effect on the transcription of CYP1A1 or CYP1B1 genes. (Wihlén et al., 2009). Consequently, the role of ER subtype in AhR-mediated regulation of target genes may be species-specific or depend on the origin of the cell type with respect to non-tumorigenic versus tumorigenic cells. In human breast cancers co-expression of both ERalpha and ERbeta was associated with lower aggressiveness of breast tumors (Järvinen et al., 2000), since generally ERbeta inhibits most but not all of ERalpha-mediated signaling to balance proliferative action via ERalpha (Williams et al., 2008; Matthews et al., 2003). Additionally, in the context of AHR-regulation ARNT was recently reported to function as a potent ERbeta co-activator (Ruegg et al., 2008). This highly interesting finding suggested an AhR/ERbeta cross talk, which may serve as an alternative mechanism for AhR-signaling via competing for limited pools of ARNT (Wihlén et al., 2009).

In the present work, despite the enhanced TCDD-induced CYP1A1 luciferase activity by E2 in ERalpha-transfected HepG2 cells, neither TCDD-induced CYP1A1 nor CYP1B1 mRNA and protein was considerably affected by the co-treatments (TCDD 1 nM/10 nM + E2 10 nM/100 nM). Relative inductions of CYP1A1 and 1B1 mRNA by the co-treatments or TCDD alone were not different in ERalpha-transfected HepG2 cells compared with non-transfected HepG2. This suggested that post-transcriptional changes may occur. Similarly, other reports showed that co-treatment with E2 increased the recruitment of ERalpha to CYP1A1 and CYP1B1 promotors without having an effect on the transcription of those genes in HC11 cells (Wihlén et al., 2009). In contrast, ERalpha expression increased the AhR regulation of TCDD-induced CYP1A1 and CYP1B1 mRNA expression in transiently transfected HuH-7 cells compared to control vector cells (MacPherson et al., 2009). Whereas there was no TCDD-mediated increase in relative expression levels observed for

CYP1A1 and CYP1B1 mRNA, at least the absolute amounts of CYP1A1 and CYP1B1 mRNA were elevated when ERalpha was over-expressed in HepG2 cells in the present work.

The observed potentiation of TCDD-induced transcriptional activity via E2 in transfected HepG2 cells might occur through protein/protein interactions between ERalpha and AhR as a proposed mechanism of AhR/ER cross talk (Figure 101, mechanism 3). Ligand-activated or unliganded ERalpha was reported to modulate AhR transcriptional activity by occupying AhR-responsive promotors and thus potentiate AhR-transcriptional activity. Chromatin immunoprecipitation (ChIP) assays confirmed the ability of TCDD to induce recruitment of ERalpha to the AhR target genes CYP1A1 and CYP1B1 in transiently ERalpha-transfected HuH7 cells (MacPherson et al., 2009). Additionally, the binding of ERalpha to these two CYP isoforms was even observed in control cells, but the occupancy of ERalpha to AhR target genes could further be increased in response to TCDD treatment. Deleting the functional ERalpha AF-1 domain had no effect, whereas an ERalpha AF-2 mutant did not increase the promotor occupancy at CYP1A1 and CYP1B1. The implication of the AF-2 domain in TCDD-induced recruitment of ERalpha to AHR-regulated target genes could further be supported in HuH7 using the selective anti-estrogens 4-hydroxytamoxifen (4OHT), preferentially inhibiting AF-2, or ICI 182,780 (ICI), which inhibits the activity of both functional domains. In their study TCDD alone further enhanced transcriptional activity of pCYP1A1-Luc and pCYP1B1-Luc, the latter to an even greater extent, in the presence of co-transfected wild-type ERalpha in HuH7 cells compared to vector control cells. There was no impact on TCDD-mediated increase reported in HuH7 cells transfected with either ERalpha AF-1 mutant or ERalpha AF-2 mutant, implicating the role of both domains of ERalpha for increased AhR-mediated CYP1A1 and CYP1B1 gene expression. (Mac Pherson et al., 2009)

The ERalpha-dependent and TCDD-mediated increase seen with HuH7 (MacPherson et al., 2009), but not with HepG2 in the present study is assumed to be due to cell-specific differences in responsiveness of AHR signaling, including AHR-dependent expression of other proteins.

Since the enhanced response in HuH7 cells was more pronounced for CYP1B1, further experiments of CYP1B1-dependent transcriptional activity should be examined using HepG2 cells. Furthermore, a species-specific difference may also play a role since transcriptional activity in the present study was investigated using rat CYP1A1-Luc reporter gene whereas human-regulated CYP1B1- and CYP1A1-plasmid constructs were used in the study conducted by MacPherson and colleagues. In agreement with the present work

using HepG2 cells, basal levels of CYP1A1-dependent luciferase activity were not influenced by the expression of ERalpha in HuH7 cells.

However, the expression of ERalpha significantly increased basal levels of the CYP1B1 luciferase activity levels in HuH7 cell line, supporting the role of ERalpha in the regulation of the human CYP1B1. (MacPherson et al., 2009). Moreover, the enhanced recruitment of ERalpha by the co-treatment (TCDD 10 nM + E2 10 nM) was found to be about 6-fold higher to the CYP1B1 promotor than to the CYP1A1 promotor in MCF-7 cells after 60 min treatment (Matthews et al., 2005). The increased CYP1B1 promotor occupancy may in part be explained by E2-dependent recruitment of ERalpha to a hERE located in the proximal promotor region of CYP1B1 (Tsuchiya et al., 2004). Tsuchiya and co-investigators demonstrated that E2 alone (10 nM, 12 h) induced the expression of human CYP1B1 mRNA in ER-positive MCF-7 cells but not in ER-negative MDA-MB-435 human breast cancer cells or human endometrial carcinoma Ishikawa cells. In the present work, there was no increase in CYP1B1 mRNA observed by E2 alone (10 and 100 nM, 20 h) in hERalpha-transfected HepG2 cells. However, the E2-induced concentration-dependent decrease of CYP1B1 mRNA in wild-type HepG2 was compensated by over-expressionof ERalpha. Moreover, rat primary hepatocytes, exhibiting low levels of ERalpha compared to ERalpha-rich MCF-7 cells, showed a slight induction of CYP1B1 mRNA but not CYP1A1 mRNA following exposure to E2 only after 48 h, supporting the role of CYP1B1 as a key enzyme in ERalpha-dependent AHR-regulation.

However, the ER-dependent potentiating effect by the co-treatment observed in the luciferase activity assay was not reflected in CYP1A1 and CYP1B1 mRNA levels in ERalpha-transfected HepG2 cells, nor in mRNA, protein, and CYP1A activity (only measured after 48 h) levels in primary rat hepatocytes from male and female rats, which express low levels of ERalpha. In order to address the role of CYP1B1 regulation via endogenous and over-expressed ERalpha, it appears essential to further examine the effects of TCDD and/or E2 on CYP1B1 activity in HepG2 cells and rat hepatocytes.

Moreover, TCDD and/or E2 did not modify ERalpha mRNA expression levels neither for transiently transfected HepG2 cells at 20 h, nor for male rat hepatocytes. Contrarily, in female rat hepatocytes decreased ERalpha mRNA levels were observed, which were associated with E2 10 nM treatment and respective co-treatments with TCDD. The slight changes in ERalpha mRNA in female rat hepatocytes were however not reflected in protein levels. The redirection of ERalpha protein to AhR target genes is used as a regulation system of AhR and ERalpha signaling. In this context, the investigation of luciferase activity in primary rat hepatocytes bearing low endogenous levels of ERalpha are strongly rec-

ommended to clarify if the potentiating effect of the co-treatment is due to over-expressed ERalpha levels or may also be observed in the presence of low endogenous receptor levels.

In the literature there are conflicting results regarding ERalpha modulation of the AhR-mediated transcription, which may be dependent on the cell-type and cell culture conditions. Apart from potentiating effects of co-treatments, also repressive effects or no effects by the co-treatment of TCDD and E2 were reported. In human embryonic kidney HEK-293 cells transfected with CYP1A1 promotor-driven luciferase co-transfected with both AhR and ERalpha expression plasmids, TCDD (2 nM, 20 h) activated CYP-dependent transcription, which could be diminished in the presence of E2 100 nM (Beischlag and Perdew, 2005). In another study, TCDD (1 nM, 24 h) caused a robust increase of CYP1A1 mRNA levels and CYP1A1 reporter gene activity, which could both significantly be decreased by co-treatment with E2 in ERalpha-transfected Hepa-1 and MCF-7 cells. Inhibitory effects on AhR transcription were suggested as an inhibitory effect of E2–bound ER dimer by blocking the binding of TCDD-AhR complex to the XRE. (Kharat and Saatcioglu, 1996). HepG2 and human breast cancer MCF-7 cells induced transcriptional activity of CYP1A1 but not CYP1B after treatment with TCDD 10 nM for 24 h, and a weak regression of this inductive effect was observed after the co-treatment with E2 10 nM. Additionally, E2 10 nM alone decreased CYP1A1 but not CYP1B1 promotor activity in MCF-7 cells, whereas in HepG2 cells only a trend towards a decrease was obtained by single E2 treatment. (Coumoul et al., 2001). MCF-7 cells and mouse hepatoma Hepa1c1c7 cells transiently transfected with an Ah-responsive plasmid containing the 5’-regulatory region of the human CYP1A1 gene significantly induced chloramphenicol acetyltransferase (CAT) activity after treatment with TCDD 10 nM for 24 h, whereas co-treatmentwith TCDD 10 nM + E2 1 nM did not affect the response. (Hoivik et al., 1997)

Effects of ERalpha recruitment to AHR target genes are also dependent on the specificity of AhR ligands. No effect of E2 on induced AhR-activation by AhR ligands other than TCDD has been reported. Accordingly, the weaker AhR ligand 3-methylcholanthrene (3-MC, 1 nM) effectively activated AhR-dependent transcription through XRE reporter plasmid transfected into MCF-7 cells, whereas the co-treatment of both 3-MC and E2 (10 nM) did not potentiate XRE-mediated transcription of 3-MC alone. In this case, 3-MC induced the recruitment of AhR/ARNT but not ERalpha to the CYP1A1 promotor XRE. (Ohtake et al., 2003). TCDD is a very stable AhR agonist that persistently activates AhR, whereas 3-MC has a lower binding affinity to the AhR and is susceptible to metabolism (Denison and Nagy, 2003). Different agonist properties explain distinct reaction patterns accordingly. The co-planar prototype AhR ligand PCB 126 recruited ERalpha to AhR regulated promo-

tors whereas the non-co planar PCB 104, which does not activate AhR, did not enhance promotor occupancy of ERalpha at CYP1A1 in T47 D cells (Matthews et al., 2007).

Altogether, the reported conflicting results of the effect of TCDD + E2 on TCDD-induced AhR-mediated gene expression can possibly be influenced by cell type and culture conditions. Results of the present work in HepG2 cells suggest that ERalpha with its ligand E2 plays a crucial role in mediating the effects on AhR transcription. The variability in AF-1 and AF-2 activity among different cell lines may contribute to the variability in the reported effects of ERalpha and E2 on the regulation of TCDD-induced CYP1A1 gene expression. The cofactor composition of ERalpha may also exhibit cell type specificity causing distinct changes in AHR-complex mediated transcription. Proteins that interact with AF-1 or AF-2 region of ERalpha may be important topics for future investigations of the ERalpha-mediated enhancement of AhR activity. In the present study, using HepG2 hepatoma cells, the proposed recruitment of ERalpha by TCDD to CYP1A1 and its enhancement by E2 is assumed to represent a feedback mechanism in estrogen signaling, since the induction of CYP1A1 as well as CYP1B1 result in the rapid oxidative metabolism of E2 (Figure 101, mechanism 1). Enhanced E2 metabolism has been shown to be associated with the tumorigenic potential of E2, as the formed main hydroxylated metabolites have a genotoxic potential via direct and indirect mechanism (Cavalieri et al., 2006).

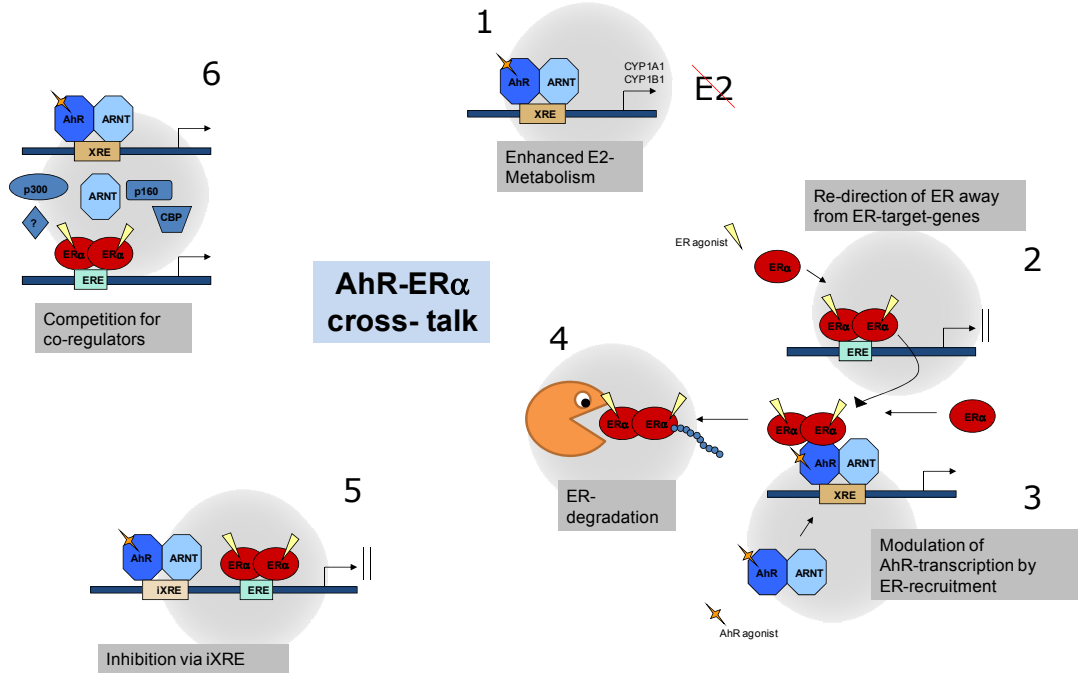

Figure 101: Proposed mechanisms of AhR/ERalpha cross talk via dioxin-mediated interaction of ER with AhR. Mechanisms: 1) Enhanced oxidative E2 metabolism via induction of CYP1A1 and CYP1B1. 2) Redirection of liganded or unliganded ERalpha from ER regulated genes to AhR regulated genes by the activated AhR serving at the same time as a regulation for ER protein levels. 3) Regulation of AhR-mediated transcription by recruitment of liganded or unliganded ER to AhR target genes. 4) Proteasomal degradation of ER. 5) Inhibition of E2-induced genes via inhibitory iXREs. 6) Competition for shared co-activators becoming limiting factors for target gene expression (according to Safe and Wormke, 2003; Matthews and Gustaffson, 2006)

6.6.2. TCDD-REPRESSED E2-MEDIATED ERALPHA SIGNALING

Transient co-transfection in HepG2 cells with vitellogenin-ERE-luciferase reporter and ERalpha expression vector showed that TCDD 1nM was able to significantly reduce luciferase activity induced by E2 10 nM. Data are consistent with results observed in breast cancer cells such as MCF-7, which expresses both ER and AhR receptors endogenously (Kharat and Saatcioglu, 1996; Ohtake et al., 2003). The less stable AHR agonist 3-methylcholanthrene (3-MC, 1 µM) decreased ERE-mediated transcription in the presence of E2 (10 nM) without binding directly to ERalpha or ERbeta in MCF-7 (Ohtake et al., 2003). The same anti-estrogenic response was also reported in mouse hepatoma Hepa-1 cells transiently transfected with ERalpha. The sequential treatment with TCDD and E2 resulted in a decrease in vitellogenin-ERE-mediated E2-induction. In turn, a mutant Hepa-1 cell line lacking functional AhR failed to exert an effect on E2-dependent ER signaling

pathway by TCDD. (Kharat and Saatcioglu, 1996). The co-treatment of different TCDD concentrations (10 nM – 0.01 nM) with E2 decreased E2-induced $pERE_3$-mediated luciferase activity in a concentration-dependent manner in ERalpha- and AhR-positive ZR-75 human breast cancer cells (Wormke et al., 2003). In general, TCDD is strongly anti-estrogenic in cells in which the levels of ER cannot be down regulated due to the constitutive expression of this receptor e.g. due to a transfected ER expression vector. It was reported that the subdomains of the transactivation domain of the AhR are responsible for the repressing E2-induced estrogen receptor transcriptional activity (Reen et al., 2002).

Several studies have shown that TCDD-activated AhR inhibited E2-induced reporter gene activity in cells transfected with an ERE-containing construct. Similarly, the expression of E2-induced genes/proteins and their related activities, such as plasminogen activator (Gierthy et al., 1987), cathepsin D (Krishnan et al., 1995), c-fos (Duan et al., 1999), or pS2 (Zacharewski et al., 1994) was decreased in a number of breast and endometrial cancer cells. Several mechanisms for inhibitory AhR/ERalpha cross talk have been proposed (Safe and Wormke, 2003; Matthews and Gustaffson, 2006). A functional AhR complex, that can translocate to the nucleus and inhibit the ERE binding activity of ERs, is required for the anti-estrogenic action of TCDD (Kharat and Saatcioglu, 1996). A further plausible explanation of the anti-estrogenic results of TCDD in the presence of E2 was suggested to be the direct interaction of the AhRC with critical promotor regions of E2-responsive genes, the so called inhibitory XREs (iXREs), thus resulting in the inhibition of ER target genes(Figure 101, mechanism 5). Functional iXREs have been identified, e.g. in the pS2, cathepsin D, and c-fos promotors (Safe and Wormke, et al., 2003; Gillesby et al., 1997; Krishnan et al., 1995; Duan et al., 1999)

In hormone-dependent tissues expressing high ER levels, such as breast and endometrium, treatment with E2 was associated with increased cell proliferation. In MCF-7 cells E2 10 nM induced several genes, proteins, or related activities that are involved in cell cycle progression, e.g. cyclin D1, E2F1, cyclin-dependent kinases-2, -4, and-7 activities (Wang et al., 1998). Exposure to E2 is accompanied by an increased percentage of cells in S phase and a decreased percentage in G0/G1 phase. It was shown that hormone-induced effects on cell cycle progression could be reversed by TCDD, so that the AhR/ER inhibitory cross talk may play an important role in inhibiting proliferative activity by E2 in hormone-dependent tissues. (Safe et al., 2000). In rat hepatocytes E2 showed a co-mitogenic effect on DNA synthesis stimulated through various growth factors, such as epidermal growth factor (EGF) or hepatocyte growth factor (Ni and Yager, 1994). However, estrogens were found to enhance the co-mitogenic actions of TCDD in rat hepatocytes (Schrenk et al.,

1992). This indicates a different mechanism in the liver than in hormone-dependent tissues, which may depend on tissue-specific ER receptor levels. The role of endogenously expressed ERalpha on ERE-mediated transcriptional activation in the liver has to be checked in further experiments using rat hepatocytes from male and female rats.

The inhibitory cross talk between AhR and ERalpha was explained to be an outcome of the enhancement of AhR-mediated proteasomal degradation of ERalpha after E2/TCDD co-treatment (Figure 101, mechanism 4) in order to limit the levels of available ERalpha (Wormke et al., 2003; Ohtake et al., 2009). Thus, in breast cancer cell lines co-treatment of E2/TCDD could induce a decrease of ERalpha protein levels. Decreased ERalpha protein was also observed in cells treated with the pure anti-estrogen ICI 182 780, which itself also induced proteasome-dependent degradation of ERalpha (Wijayaratne et al, 2001). Western blot analysis of three ER-positive human breast cancer cell lines (ZR-75, MCF-7, and T47D) showed that treatment with TCDD and the co-treatment of TCDD + E2 increased the proteolytic degradation of ERalpha and AhR. E2 alone only induced degradation of ERalpha but not of AhR. Transfection of ZR-75 cells with siRNA for AhR inhibited TCDD-induced but not E2-induced degradation of ERalpha protein, showing that AhR is required for TCDD-induced ERalpha degradation. (Wormke et al., 2003)

The recruitment of liganded or unliganded ERalpha to AhR target genes as described in section 6.6.1 (Figure 101, mechanism 3) supports AhR-induced inhibitory effects on ER signaling. Consequently, when ERalpha acts as a co-regulator of AhRC activity the pool of receptors regulating estrogen-responsive promotors may be reduced. This interaction is also associated with a time-dependent reduction in the recruitment of ERalpha to estrogen target gene promotors (Figure 101, mechanism 2). ERalpha may then be targeted for degradation via enhanced formation of ubiquinated forms of ERalpha and subsequent proteasomal degradation (mechanism 4, Figure 101) (Wormke et al., 2003). Whatever the mechanisms involved, the results in the present study in HepG2 cell line support the notion that TCDD is not a direct ERalpha antagonist but induces the inhibitory cross talk between liganded AhR and ERalpha. It is suggested that activated AhRC is directly involved in the anti-estrogenic action of TCDD.

However, TCDD alone did not induce transcriptional activity through ERE when ERalpha was constitutively expressed in HepG2. Contrarily, it was already shown that AhR agonists alone, i.e. 3-MC (100 nM and 1 µM), beta-naphthoflavone (100 nM and 1 µM), and TCDD (10 nM and 100 nM), were able to induce ERE-mediated transcription in MCF-7 cells (for 3-MC) and in Ishikawa cells for all three compounds) when ER (ERalpha or ERbeta) and AhR/ARNT were transiently co-expressed (Ohtake et al., 2003). Others reported that

TCDD (30 nM) exhibited estrogenic activity only in MCF-7 cells transfected with AhR siRNA (Abdelrahim et al., 2003). The authors concluded that due to the high affinity for AhR TCDD acts like an ERalpha agonist only in AhR-deficient cell context or in cells with high ERalpha/AhR protein ratio as obtained in ERalpha-transfected HepG2 cells. Likewise, this AhR/ERalpha inhibitory cross talk was not observed in AhR-deficient MCF-7 cells after TCDD treatment (Moore et al., 1994). However, AhR agonists with low receptor affinity such as 3-MC or PCBs were shown to directly activate ERalpha independent from AhR. (Abdelrahim et al., 2003 and 2006). Matthews and co-workers were unable to show direct activation of ERalpha by TCDD in competitive binding assays using baculovirus-expressed ERalpha proteins (Matthews et al., 2007). Thus, another possible mechanism for the reported activation of ERalpha by TCDD was proposed to be via indirect mechanisms involving kinase activation or other signal transduction pathways, which lead to increased ERalpha activity (Mac Pherson et al., 2009).

The functional association of activated AhRC with the two transactivation functions of ERwere examined with specific ER mutants. Experiments with ER-negative human endometrial cancer Ishikawa cells, which were transfected with ER mutants selectively inhibiting functional domains AF-1 or AF-2, revealed that AF-1 regions of ERalpha and ERbeta were required for the changes of ERE-mediated transcription by AhR/ARNT. There was no modulation of the AF-2 function detected. Furthermore, the ligand-bound AhR/ARNT complex modulated unliganded ERs (ERalpha and ERbeta) by association with its N-terminal A/B regions. Transfection assays with an ERalpha mutant lacking these AhR-interacting regions revealed that responsiveness for AhR/ARNT and for E2 addresses different regions of the estrogen receptor AF-1 function. (Ohtake et al., 2003)

In the present study in HepG2 TCDD-mediated decrease in E2-induced ERE-dependent signaling was reversed by the pure anti-estrogen ZK 191 703. ZK 191 703 modulates ER signaling by preventing interaction with the two activation functions AF-1 and AF-2 within the ERalpha and ERbeta structure. Additionally, the pure anti-estrogen destabilizes ER and induces its degradation (personal communication with K.H. Fritzemeier, Bayer Schering). Taken together, these results suggest an activation of estrogen receptor pathway and exclude a non-genomic pathway. The weak increase of luciferase activity induced by E2 treatment in ERalpha-negative HepG2 cells was inhibited by the ZK 191 703 anti-estrogen and may be explained by low endogenous levels of ER protein. ERalpha mRNA was not detected in HepG2 in the present work. Therefore, it was suggested that HepG2 cells express low levels of functional ERbeta. Iwanari and co-workers reported that HepG2 cells express ERbeta but not ERalpha mRNA (Iwanari et al., 2002). Thus, the role of ERbeta in HepG2 will have to be elucidated in further experiments.

The AhR antagonist 8-methoxypsoralen, applied under conditions that were shown to inhibit TCDD-mediated CYP1A EROD activity (Baumgart et al., 2005), did not affect E2-induced activity or its decrease by the co-treatments in the current work. 8-MOP is known to prevent binding of the ligand-activated AhR/ARNT complex to the respective AHR-dependent XREs but does not downregulate AHR protein (Jin et al., 2004). Contrarily, alpha-naphthoflavone, another widely used AhR antagonist, successfully blocked the estrogenic action of 3-MC in Ishikawa cells transiently transfected with ERalpha and AhR expression plasmids, suggesting that AhRC is involved (Ohtake et al., 2003). Alpha-naphthoflavone was shown to act as a partial antagonist of TCDD-induced CYP1A1 gene expression by directly competing for cytosolic receptor binding sites (Merchant et al., 1990). The effects of alpha-naphthoflavone in the mechanism of inhibition of TCDD in E2-induced ERE-mediated transcriptional activity have to be further investigated in HepG2 cells to clarify the role of AhR.

The exact molecular mechanisms of action of the inhibitory AHR/ER cross talk still need to be defined, but they may certainly include competition for common nuclear co-regulatory proteins that between ER and AHR transactivation functions comprising e.g. p300, ARNT, CBP, or members of the p160 family (Figure 101, mechanism 6) (Matthews and Gustafsson, 2006). There are some co-regulatory proteins that have been reported to be recruited by both AhR and ER such as the p300/CRB co-activator. P300 was recruited to ERalpha only in the presence of E2. Furthermore, p300 also associated with3-MC-bound AhR/ARNT and unliganded ERalpha to form a complex in MCF-7 cells. (Ohtake et al., 2003). The role of competition for common nuclear regulatory proteins including co-activators and co-repressors depend on the cell-context and the expression of the co-regulatory proteins that interact with ER and AhR.

6.7. TCDD- AND E2-MEDIATED ROS FORMATION LINKED TO CYP INDUCTION

Persistent expression of CYP via AhR-mediated mechanism was linked to induction of oxidative stress which is one plausible mechanism contributing at least partly to TCDD-induced carcinogenesis (Senft et al., 2002b; Chen et al., 2004). There is established evidence of an association between induction of CYP activity and ROS formation, which results from the catalytic site of the CYP mono-oxygenase system via uncoupling as described in section 2. Superoxide anion radicals are predominantly released, which can dismutate to H_2O_2. Subsequent increased ROS generation may result in the induction of oxidative DNA damage. (Kuthan and Ullrich, 1982). Even in the absence of a substrate, CYP reductase was reported to serve as a relevant source of ROS (Kuthan and Ullrich, 1982; Bosterling and Trudell, 1981; Wyde et al., 2001). Using reconstituted membrane vesicle systems containing purified rabbit liver microsomal NADPH-CYP reductase and CYP enzymes such as CYP2E1, generation of superoxide, hydrogen peroxide, and hydroxyl radical was observed (Ingelman-Sundberg and Johansson, 1984).

TCDD-induced CYP1A1 activity was associated with increased leakage of oxygen radicals in the mouse hepatoma cell line Hepa1c1c7 (Park et al., 1996). Single administration of TCDD induced production of superoxide anion by peritoneal lavage cells in AhR-responsive C57BL/6J mice and in female Sprague-Dawley rats but not in AHR-defective mice (Alsharif et al., 1994b). Moreover, the AhR-mediated induction of oxidative stress was correlated with the potency of AHR ligands, revealing that TCDD-mediated ROS production was more pronounced compared to AhR ligands with lower potency such as PCB (Sawyer and Safe, 1982; Alsharif et al., 1994b).

E2-dependent ROS generation may arise during its metabolism via catalyzed redox cycling between the catechol estrogens and their corresponding quinone forms (Liehr et al., 1986; Li et al., 1994). Since the formation of the respective catechol estrogens is catalyzed by CYP1A1 and CYP1B1, it was hypothesized that TCDD-mediated CYP induction may further elevate ROS production via enhanced E2 metabolism in the presence of E2.

In the present study ROS formation was determined in the H_2DCDA fluorescence assay. Basal levels of ROS were significantly higher in rat hepatocytes compared to the hepatoma cell lines, which may correlate with generally higher basal CYP1 levels in the primary rat hepatocyte culture (see section 6.2.1).

H4IIE cells constituted a good cell model to investigate ROS formation induced by TCDD In contrast to rat hepatoma cell line HepG2 cell line. TCDD and the co-treatments but not E2

alone considerably induced ROS formation in rat H4IIE. Increased ROS formation by the co-treatments did not differ from single TCDD treatments, indicating a TCDD-mediated increase. The positive control TBH extensively increased ROS formation in all cell models, but was most prominent in H4IIE.

In human HepG2 cell line TCDD alone did not show any effect on ROS levels. However, a minor increase was observed following exposure to two co-treatments after 48 h.

Female-derived rat hepatocytes were able to induce ROS only after 48 h following exposure to TCDD, E2, or the respective co-treatment. It may be speculated that the lack of any oxidative stress response mediated by single treatment with TCDD in male-derived cells can be attributed to higher endogenous E2 concentrations in the hepatocytes from female rats. Anyway, in hepatocytes from both sexes E2 alone at the highest concentration of 100 nM and the respective co-treatment of TCDD 1 nM with E2 100 nM gave rise to significantly enhanced ROS production, but only at the longer treatment time of 48 h. Thus, increased ROS production by E2 may correlate with induced CYP1B1 mRNA by E2 in rat hepatocytes after 48 h treatment, indicating that the E2-mediated effect may be a long-term treatment effect *in vitro*.

Results in HepG2 were consistent with previously obtained studies that reported the failure of TCDD (1 nM, 48 h) to increase ROS levels. However, contrary to the results in the present work, male hepatocytes from Wistar rats were shown to significantly increase ROS formation after treatment with TCDD. (Knerr et al., 2006). Knerr and co-workers (2006) measured ROS formation in microsomes, whereas in the present work cracked cells were used, suggesting that oxidation reactions during processing of cells may have an impact. Moreover, different cell culture conditions may account for the different response in PHm. In the previously performed study phenol red-containing medium was used and cells were kept in medium supplemented with 10% FBS even during treatments over 48 h. This standard culture in FBS-rich medium, thus E2-containing medium, may have had a positive effect in the stimulation of ROS. Based on the minimal E2 standard culture conditions used in the present work (see section 6.1), it is noteworthy that elevated oxidative stress response was found only after exposure to E2 100 nM and the co-treatment of TCDD 1 nM with E2 100 nM, suggesting a role of long-term E2 treatment in the formation of ROS *in vitro*. Likewise, *in vivo* results showed enhanced H_2O_2 generation in isolated liver microsomes after sub-chronic administration of E2 to Wistar rats (Barth et al., 2000).

The results of studies in breast-cancer cell lines, which attempted to ascribe a role of ERalpha to TCDD and/or E2-mediated effects on ROS production, were inconsistent. The

effects were rather cell model-specific and appeared to depend on the experimental conditions used. Non-tumorigenic human mammary epithelial cells (MCF-10A) showed TCDD-mediated (10 nM, 72 h) induction of CYP1A1 and CYP1B1 protein and mRNA, which was related to increased ROS generation. Moreover, in MCF-10A cells E2 alone did not influence intracellular ROS levels, but the co-treatment dramatically enhanced TCDD-mediated ROS accumulation. (Chen et al., 2004). Enhanced ROS formation after exposure to TCDD (0.001–10 nM 48 h) was detected in ER-negative MDA-MD 231 cells and in ER-positive MCF-7 cells only in the presence of an ER antagonist, supporting a protective role of ERalpha in TCDD-mediated oxidative stress (Lin et al., 2007). In contrast, in another study MCF-7 cells but not ER-negative MDA-2231 showed increased sensitivity towards E2-mediated (10 nM, 18 h) oxidative DNA damage, which could be blocked by an anti-estrogen (Mobley and Brueggemeier, 2004).

The role of ERalpha-dependent ROS formation in transiently transfected HepG2 cells was compared with non-responsive ER-negative HepG2 cells in the present work. Even though over-expression of ERalpha in HepG2 cells was found to be responsible for increased basal CYP1A1 and CYP1B1 mRNA levels, none of the treatments with TCDD and/or E2 for 20 h influenced ROS formation compared to non-transfected cells. These results suggested that ERalpha is not implicated or at least is not the only determinant in human hepatoma cells. Thus, the non-responsiveness of human hepatoma cells compared to rodent cells towards ROS formation may also be a species-specific effect. Human hepatocytes should be tested in future experiments to rule this out. Furthermore, the effects of over-expressed ERalpha in HepG2 cell line on ROS production should also be investigated after 48 h treatment to be in line with ROS-inducing effects observed in primary rat hepatocytes.

The CYP1 inhibitor 8-MOP efficiently blocked all TCDD- and E2-induced elevated ROS levels in all cell models, supporting the link between CYP1 induction and ROS increase. However, since EROD activity was well induced by TCDD in both HepG2 and H4IIE cell line, TCDD-dependent ROS formation in H4IIE but not in HepG2 cannot be solely explained by CYP1A1 induction. It is noteworthy, that HepG2 cell line exerted the lowest basal and induced CYP1B1 mRNA and protein compared to the cells of rat origin. Measurements of specific CYP1B1 activity to compare with CYP1A1 activity results will further elucidate the implication of CYP1B1 as a key enzyme in E2 metabolism. Since even control levels of ROS where diminished by the inhibitor 8-MOP, it can be assumed that CYP1 expression also influenced steady state levels of ROS in the liver cell models. Similarly, in human breast cancer cell lines MCF-7 and MDA-MB-231 TCDD-induced (10 nM, 2-72 h) oxidative stress,

as determined by the H_2DCFDA assay, was almost completely blocked in the presence of alpha-naphthoflavone (0.15 µM), another AhR inhibitor (Lin et al., 2007).

Overall, these experiments suggest that the status of AhR and its mediated gene expression modulate TCDD-induced ROS formation in hepatoma cells and primary rat hepatocytes. The effects of E2 alone in rat hepatocytes cannot completely be explained by metabolic conversion of E2 via CYPs. E2 did not induce CYP1A1 and only induction of CYP1B1 mRNA but not protein was observed. The impact of CYP1B1 activity will help to better identify its role in the oxidative stress response. Moreover, it is also hypothesized that estradiol induces changes in antioxidant status via ER-mediated cell proliferation. In this proposed mechanism a controlled increase in ROS accompanied by increasing sensitivity to DNA damage may act to potentiate cell growth. (Davies, 1999; Mobley and Bruegge-meier, 2004)

6.7.1. ROLE OF NADPH IN ROS FORMATION

In the present study the role of NADPH, which is the obligatory cofactor needed for NADPH-CYP-reductase-mediated single electron transfer onto the CYP protein, was investigated. The chemical reductive processes for the formation of ROS are primarily mediated by reduced pyridine nucleotides such as NADH and NADPH (Shen et al., 2005). For this reason, ROS formation in cells with and without the addition of the reducing agent NADPH was investigated in the H_2DCFDA assay.

In hepatoma cells NADPH-independent ROS formation did not differ from control levels, suggesting that NADPH is a negligible factor for the induced ROS formation observed in H4IIE cells. Contrarily, NADPH-independent formation of ROS was significantly decreased in rat hepatocytes derived from both sexes. In the rat primary culture, NADPH may play an important role in the activation of the CYP mono-oxygenase system. It was reported that the expression of human NADPH-CYP reductase in cultured V79 Chinese hamster cells increased basal levels of oxidative DNA damage after depletion of GSH (Heine et al., 2006). Therefore, it would additionally be interesting to investigate the role of NADPH-CYP reductase as a stimulator of ROS formation in the liver cell models in order to fully elucidate the role of the mono-oxygenase system in the TCDD- or E2-induced oxidative stress response.

6.8. CELLULAR TGSH LEVELS

GSH is the major antioxidant molecule occurring in all mammalian cell types and functioning as a redox buffer. It is also implicated in the detoxifying reactions during the oxidative E2 metabolism. (Cavalieri et al., 2006). It was important to investigate alterations of tGSH (oxidized and reduced form) in order to understand its role in the TCDD and/or E2-dependent oxidative stress response (see section 6.7).

6.8.1. GSH STATUS

The maintenance of an optimal GSH redox state is essential for limiting the level of oxidative cell damage. Variations in GSH can thus have critical consequences in numerous cell processes and steady state levels of ROS would rise. (Rebrin and Sohal, 2008). In mammalian cells under physiological conditions more than 95% of the intracellular glutathione is present as the reduced thiol form (GSH), termed as GSH status, since glutathione reductase will rapidly reduce any oxidized glutathione (DeLeve and Kaplowitz, 1991; Gallagher et al., 1994). In the present work GSH status ranged between 85% and 93% in hepatoma cell lines and male-derived rat hepatocytes, the latter showing the highest GSH status. The lowest GSH status, which was slightly beneath 80%, was found in female-derived rat hepatocytes, indicating a slight shift to a pro-oxidative redox state or a general stress response in these primary cultured cells. The availability of GHS to various tissues is predominantly determined by its synthesis in the liver. Therefore, GSH concentrations in the liver are very high, up to 7-8 mM in the rat liver. (Halliwell and Gutteridge, 1999). The different liver cell models revealed relatively high basal tGSH levels after 20 h cell culture, ranging from about 35 to 75 µM/mg protein.

6.8.2. TGSH LEVELS AFTER TREATMENTS

Following treatments with TCDD and/or E2 for 20 h there were no significant modifications of tGSH levels observed in all four cell models, except for increased tGHS levels in HepG2 after exposure to the co-treatment of E2 10 nM + TCDD 1 nM. This increase was associated with significantly increased GSH levels, whereas GSSG levels remained unchanged. In the absence of other statistically significant changes, only a trend for increasing tGSH levels after treatment with TCDD and the co-treatments was observed in HepG2 cells, and occasionally also in the other liver cell models.

Treatments with the known reference compound menadione for 1 h showed a trend for a decline in tGSH levels, which might be indicative of depleted GSH depots. Menadione is a redox cycler resulting in oxidative stress in isolated rat hepatocytes after 30 min treat-

ment (Morrison et al., 1984; Di Monte et al., 1984). Menadione was observed to deplete GSH without an increase in the levels of GSSG, a mechanism of action which was predominantly mediated by arylation rather than oxidative stress (Seung et al., 1998).

Elevated GSH levels following dioxin treatment have been reported in mammalian systems, suggesting that TCDD evokes a reducing thiol status (e.g. Senft et al., 2002a; Shertzer et al., 1998; Lin et al., 2007). Dioxin-treated female C57BL/6 mice (15 µg/kg bw, 3 consecutive days) showed increased H_2O_2 production in the liver which was associated with elevated mitochondrial GSH levels, whereas GSSG levels did not change. Additionally, mitochondrial GPx and GR were increased in parallel in the liver of dioxin-treated female mice, thus explaining the lack of GSSG increase (Senft et al., 2002a). In contrast, in another *in vivo* study exposure of female C57 BL/6J mice to a low dose of TCDD (5 µg/kg bw, 3 consecutive days), which still resulted in increased CYP1A1 activity, led to a pro-oxidant shift (Shertzer et al., 1998). In rats the depletion of GSH has been shown to result in increased PAH-induced oxidative liver damage in rats (Vuchetich et al., 1996). A single low dose of TCDD was sufficient in Sprague Dawley rats to induce ROS production, inhibit cytosolic GPx activity, and decrease mitochondrial tGSH (Stohs et al., 1986; Stohs et al., 1991). Additionally, TCDD was shown to induce GSTYa and GSTP activity in HepG2 cells and liver parenchymal cells from Wistar rats respectively (Rushmore et al., 1990; Aoki et al., 1992).

Estradiol was also associated with changes in GSH levels, mainly producing a reducing cell environment. During oxidative estradiol metabolism the correspondent quinone forms can undergo conjugation with GSH alone or catalyzed by GSTP1, thus reducing the level of reactive DNA-damaging E2 quinones (Hachey et al., 2003; Parl et al., 2009). Exposure to E2 increased GSH contents in the liver of male and female mice. These effects were associated with increased activities of GR and glutathione synthetase, indicating that increased recycling of oxidized GSSG and increased GSH synthesis contribute to it. (Liu et al., 2004). Treatment with E2 10 nM for 18 h increased GPx enzyme activity as well as SOD isoforms in ER-positive MCF-7 human breast cancer cells as a response of E2-mediated oxidative DNA damage (Mobley and Brueggemeier, 2004).

Besides ROS generation, which can occur during E2 metabolism, E2-induced changes in antioxidant status were also hypothesized to be part of a controlled redox-sensitive mechanism to stimulate cell proliferation via ER-mediated signaling. (Davies, 1999; Mobley and Brueggemeier, 2004;) However, the relevance for estrogen receptor in E2-mediated oxidative stress response is not yet much elucidated, but ER appears to be involved in

intracellular changes due to oxidative stress. Thus, the effects of TCDD and/or E2 in transiently transfected HepG2 cells on GSH levels may be further investigated.

In other cell lines such as human breast cancer MCF-7 and MDA-MB-231 breast cancer cells, GSH depletion was observed during the first 1-5 h of treatment with TCDD (Lin et al., 2007). The short lack of GSH depletion at 20 h in the hepatic cell models in this study may be due to the long treatment time. It is speculated that monitoring of GSH and GSSG levels at shorter treatment times than 20 h would perhaps have shown a transient decrease in the reducing agent, which then stabilizes over time resulting in increased GSH levels as a defense against persisting oxidative stress associated with CYP induction (see section 6.7).

Under the conditions of the assay in the present study the trend of TCDD or E2-mediated increased tGSH levels most probably associated with increased reduced form of GSH was consistent with the majority of the available *in vitro* and *in vitro* studies in the liver. However, in order to be able to fully assess the mechanism of ROS formation in TCDD- or E2-treated cells, activities of GR, GPx, and GST should be investigated in future experiments to better clarify the role of GSH in TCDD-induced E2 metabolism in the different liver cell models. The effects of GSH deficiency by the use of GSH-depleting chemicals are an additional possibility to evaluate the influence of high tGSH levels in the liver cells, particularly with regard to ROS formation and also oxidative DNA damage. GHS-deficient mouse models are also a good tool to investigate the role of GSH in TCDD- and/or E2-treated animals *in vivo* (Dalton et al., 2004).

6.9. EFFECTS OF TCDD AND/OR E2 ON COMT EXPRESSION

The most common detoxification pathway in E2 metabolism is the methylation of CEs by COMT, which preferably methylates 2-OHE2 and thus prevents the production of the genotoxic estrogen quinones (Ball and Knuppen, 1980; Goodman et al., 2002). Differential expression of COMT may play a role in differences of activation for oxidative DNA damage.

In the present study primary rat hepatocytes possessed much higher basal mRNA COMT levels compared to hepatoma cell lines, as detected by qPCR. The over-expression of ERalpha in transfected HepG2 cells did not have an influence on basal COMT mRNA compared to normal HepG2 cells. Differences in expression levels between primary and tumorigenic cells may be due to the fact that higher COMT levels are conserved in normal

tissues compared to cancer cells. In the breast for example COMT is less expressed in human breast carcinoma tissues than in normal female breast tissue (Rogan et al. 2003; Singh et al., 2005; Wen et al., 2007). Generally, COMT mRNA expression levels in the liver were at least ten-fold higher compared to normal human mammary gland and MCF-7 breast cancer cell line (Lehmann and Wagner, 2008). In normal human liver the expression profile of E2 detoxifying enzymes showed that mainly COMT was expressed, but also GST yielded high expression levels. Less frequent E2-metabolizing enzymes in the human liver were UDPGTs, SULTs, and low amounts of QR. (Lehmann and Wagner, 2008)

In the present study it was important to elucidate if E2 stimulates its own methylation or whether TCDD, which induced the CYPs responsible for E2 activation, concomitantly induced Phase 2 enzymes for detoxification. In HepG2 cells COMT mRNA was significantly decreased following exposure to E2 100 nM, TCDD, and the co-treatment of E2 100 nM with TCDD 1 nM for 20 h. COMT decrease could be related to the decreased CYP1B1 mRNA levels observed after 20 h, suggesting interplay of both genes to regulate E2 metabolism. After 48 h this diminishing effect was reversed and significantly induced COMT mRNA levels were observed for most of the co-treatments. H4IIE cells showed no treatment-dependent effects on COMT mRNA. In male rat hepatocytes a stimulation of COMT mRNA by both E2 10 nM and/or TCDD 10 nM was observed after 48 h. In contrast, in female rat hepatocytes TCDD resulted in a significant decrease in COMT after 20 h and 48 h and a general trend for a decrease could be observed for all the co-treatments. Thus, in female-derived rat hepatocytes inhibitory effects triggered by TCDD could be presumed.

HepG2 cells were reported to possess extensive metabolic capacities for the deactivation of catechol estrogens. The detoxification systems were shown to be more complex in HepG2 than in breast cancer MCF-7 cells. Therefore, HepG2 cells were protected from 4-OHE2-mediated oxidative DNA damage. (Gerstner et al., 2008). COMT was shown to mainly catalyze the formation of 2-methoxy E2/1 in both HepG2 and MCF-7 cell line. However, in contrast to MCF-7 cells, HepG2 cells were also able to preferentially glucuronize 4-OHE2/E1. (Gerstner et al., 2008). The most active UDPGT for the elimination of 4-OHE2/E1 in human liver is UDPGT2B7 isoenzyme (Pfeiffer et al., 2006).

Catechol metabolites of PCBs were shown to be potent inhibitors of COMT protein and activity in MCF-7 cells and are likely to contribute to reduced clearance of estradiol catechol metabolites. The effect of PCB metabolites on reduction of COMT expression is hypothesized to run via interaction with the ER, since the effect was abolished by the antiestrogen ICI 182 780. (Ho et al., 2008). It was also speculated that enhanced formation of

CE after exposure of liver cells to TCDD and E2may inhibit COMT expression via interaction with ERalpha. Therefore, it was interesting to investigate the effects of ERalpha on COMT expression in transiently transfected HepG2 cells compared to wild-type HepG2 cells after 20 h treatment. In contrast to the above reported results, COMT-decreasing effects were observed in ER-negative HepG2 cells by treatment with the high E2 concentration and/or TCDD. This decrease was compensated in the presence of ERalpha. The co-treatments even resulted in slightly increased COMT mRNA levels in transfected HepG2 cells. Thus, the amount of COMT mRNA was induced by TCDD+E2 when ERalpha was over-expressed.

Consequently, in human HepG2 cells the presence of remarkable amounts of ERalpha protein was associated with the activation of COMT mRNA, providing a good basis for detoxification of CYP-mediated CE metabolites. Treatment-related COMT induction was also observed in PHm, which possess low ERalpha levels, but also in ER-negative HepG2 after 48 h. This implies that parallel to CYP1A1 and CYP1B1 mRNA expression, COMT can be induced also independent of ERalpha status. Additionally, TCDD-dependent decrease of COMT mRNA in female-derived hepatocytes cannot be solely explained by ERalpha status, but may also be due to a sex difference. Furthermore, ERbeta could be implicated in the regulation of COMT expression.

Based on these results it can concluded that COMT mRNA levels cannot be taken as the only measure of investigation. The enzyme activity of COMT has to be investigated in future studies to fully characterize the effects of TCDD and E2 on the major Phase 2 enzyme in E2 metabolism in the liver cell models. Moreover, examination of the expression profile and enzymatic activities of the other major enzymes involved in the metabolism of catechol estrogens such as GSTs or UDPGTs will allow to better characterize the antioxidant status of the different liver cell models.

6.10. INDUCTION OF FPG-SENSITIVE DNA STRAND BREAKS IN THE COMET ASSAY

6.10.1. EFFECTS OF TCDD AND/OR E2 AND E2-METABOLITES

In all liver cell models TCDD, E2, and the co-treatments did not induce DNA strand break formation in the alkaline comet assay after 20 h treatment. The application of the excision repair glycosylase FPG enabled to provide evidence for DNA repair process based on

oxidative DNA modifications, which may have occurred but are not repaired by the intrinsic repair systems (Collins, 2004).

Basal DNA migration was significantly enhanced after the use of FPG. This finding was not surprising, since basal levels of endogenous oxidative DNA base modifications such as 8-oxo-G have been observed in all types of untreated mammalian cells (ESCODD, 2002). They reflect a steady state between a continuous generation of ROS-mediated modifications during cellular oxygen metabolism and DNA repair processes (Epe, 2002).

In the presence of FPG, TCDD or E2 caused a significant increase in DNA strand break formation only in primary rat hepatocytes. Pronounced FPG-sensitive DNA strand breaks following single treatments of TCCD or E2 occurred without a significant concentration dependency. The co-treatments did not further enhance this effect. Consequently, TCDD- and E2-induced DNA strand breaks in primary rat hepatocytes are mainly indicative of oxidative DNA damage.

There are no studies available in the literature using comet assay with FPG in liver cell models after exposure to TCDD or E2. However, in breast cancer cell lines TCDD was shown to induce DNA strand breaks in the alkaline comet assay. This effect was associated with increased ROS formation. (Lin et al., 2007)

Regarding the liver, a number of *in vitro* and *in vivo* studies in liver cells or tissue investigated the role of oxidative DNA modifications by quantification of the 8-oxo-dG as the most important biomarker for oxidative DNA damage. Consistent with our results at 20 h, it was reported that TCDD 1 nM (48 h) induced 8-oxo-dG in genomic DNA of primary rat hepatocytes from male rats but not in DNA of HepG2 cells. A slight increase in HepG2 cells did not reach statistical significance and was not considered relevant. (Knerr et al., 2006). Park and colleagues (1996) reported increased excretion of 8-oxo-G following treatment of mouse hepatoma Hepa1c1c7 cells with TCDD (0.5 nM, 48 h).

In vivo results revealed that long-term treatment of intact Sprague Dawley rats but not ovariectomized rats over 30 weeks with TCDD resulted in increased 8-oxo-dG levels in liver nuclear DNA. This increase was even more pronounced in DEN-initiated animals, suggesting the role of TCDD as a liver tumor promoter and supporting the hypothesis that estrogens may lead to increased oxidative DNA damage via increased metabolism of endogenous estrogens to catechols. (Tritscher et al., 1996)

Likewise, supplementation of E2 to ovariectomized rats enhanced the formation of 8-oxo-dG adducts in TCDD-treated DEN-initiated rats (Wyde et al., 2001). Consequently, ovarian hormones like estrogens have been linked to increase the tumor-promoting actions of

TCDD in female Sprague Dawley rats compared to ovariectomized rats (Lucier et al., 1991). Hence, the induction of 8-oxo-dG by TCDD appears to occur via chronic, sex-specific, and estrogen-dependent mechanism. Since CYP1B1 mRNA was reported to be more enhanced in the livers of female Sprague Dawley rats than in those of male rats (Walker et al., 1995), the mechanism of TCDD-increased estrogen metabolism may mainly depend on the metabolic activation of E2 to 4-OHE2.

Moreover, there may be a link between TCDD-induced oxidative DNA damage and apoptosis. The induction of oxidative stress and related oxidative DNA damage triggers transient cell cycle arrest as a defense mechanism. The temporary growth arrest via induction of the tumor-suppressor protein p53 enables the cell to eliminate damaged bases via DNA repair or to undergo programmed cell death. (Krokan et al., 1997). TCDD was reported to inhibit apoptosis, thus enhancing liver tumor formation and DNA-damaging effects. The prototype dioxin markedly reduced the rate of apoptosis in preneoplastic rat liver (Stinchcombe et al., 1995). Likewise, inhibition of UV- or 2-AAF-induced apoptosis by TCDD was observed in rat hepatocytes *in vitro* (Wörner and Schrenk, 1996).

In the current study E2 alone also increased FPG-sensitive DNA damage in rat hepatocytes but not in the hepatoma cell lines. This increase may result from DNA adduct formation or free radical formation following redox cycling of the estradiol metabolites (Cavalieri et al., 2006). Likewise, the direct effects of the two main E2 metabolites showed induced DNA fragmentation only in rat hepatocytes and only after FPG application. Induction of FPG-dependent DNA lesions predominantly represent oxidized DNA bases, which may arise from redox cycling between the catechol estrogens and the respective quinone forms, thus damaging the cells (Cavalieri et al., 2006).

E2 and its two main metabolites induced FPG-sensitive DNA damage to the same extent after 20 h treatment. Thus, both 4-OHE2 and 2-OHE2 contribute to E2-mediated ROS and oxidative damage. This was consistent with the finding that in primary rat hepatocytes E2 also induced ROS formation in the H_2DCFDA assay. However, the effects of E2 cannot completely be explained by metabolic conversion of E2 via CYPs, because E2 did not induce CYP1A1, and CYP1B1 mRNA induction was only observed following 48 h treatment. The impact of CYP1B1 activity will help to better identify its role in DNA damage. It was hypothesized that E2 induces changes in antioxidant status via ER-mediated cell proliferation. In this mechanism a controlled increase in ROS accompanied by increasing sensitivity to DNA damage may act to potentiate growth (Davies, 1999; Mobley and Brueggemeier, 2004). The effects of E2 and the E2 metabolites in the comet assay using HepG2 cells

transiently transfected with ERalpha would be a good tool to further investigate the role of ERalpha.

ER-rich MCF-7 cells showed induced DNA damage after exposure to E2 as low as 0.1 nM and 10 nM in the comet assay even without FPG (Rajapakse et al., 2005; Yared et al., 2002). MCF-7 cells treated with the catechol metabolites 2- and 4-OHE2 showed increased tail moments in the normal comet assay starting at concentrations of 100 nM. The 4-OHE2-mediated effect at 100 nM was slightly more pronounced than the effect by E2 at the same concentration, whereas 2-OHE2 100 nM increased mean tail moments to the same extent as E2. (Rajapakse et al., 2005). Similar findings were obtained in the ER-negative MDA-MB-231 cells in the normal comet assay, indicating that the ERalpha status is not relevant to these effects. (Rajapakse et al., 2005)

The genotoxic effects of the catechol estrogens are dependent on the cell's metabolic capabilities. In accordance with the results in the present study, there was no induction of FPG-sensitive DNA strand breaks observed in HepG2 cells after 2 h treatment with the catechol estrogens 2-OHE2 and 4-OHE2, determined in the alkaline unwinding assay in the absence of FPG (Gerstner et al., 2008). In MCF-7 cells 4-OHE2 but not 2-OHE2 slightly induced DNA strand breaks in the alkaline unwinding assay. This effect was assumed to be due to the lack of UDPGT2B7, which specifically glucurinates the reactive 4-OHE2 in HepG2 (Pfeiffer et al., 2006; Gerstner et al., 2008). Accordingly, in E2-treated MCF-7 cells the inhibition of COMT led to an increase in oxidative DNA damage mediated by the catechol estrogens (Lavigne et al., 2001). Likewise, COMT inhibitors led to higher levels of catechol estrogens, resulting in increased formation of the CE-mediated depurinating DNA adducts 4-OHE2-1-N3Ade and 4OHE2-1-N7Gua (Lu et al., 2007).

More complex activities of Phase 2 enzymes in the hepatoma cell line, which may have occurred due to the cell transformation, may also be responsible for the differences in oxidative DNA damage between hepatoma cells and the primary rat hepatocytes and will have to be further investigated.

Though E2 alone and TCDD alone were able to induce FPG-sensitive DNA damage in rat hepatocytes, no potentiating effect and no sex-specific response could be observed in rat hepatocytes in the present work. Lu and co-investigator showed that induction of CYP1B1 by pre-treatment with TCDD dramatically increased E2 metabolism in human ER-negative MCF-10F breast epithelial cells, which led primarily to the 4-hydroxylated metabolite. In MCF-10F cells, which were only treated with E2, the metabolism of E2 was very low (Lu et al., 2007). Thus, another experimental design, i.e. pre-treatment with TCDD and subsequent treatment with E2 instead of simultaneous treatment with both compounds, might

enable to better investigate the effects of preceding TCDD-mediated CYP induction on metabolic activation of estradiol.

6.10.2. EFFECTS OF MMS AND MENADIONE

FPG protein is known for its high sensitivity for detecting 8-oxo-G and other damaged purines, but it also detects AP sites and ring-opened N-7 guanine adducts (Collins et al., 1996, 1997; Epe et al., 1993; Tchou et al., 1994; Li et al., 1997).

In the present study the methylating agent MMS was used as a positive control in the comet assay. For all the liver cell models the FPG digestion step strongly enhancedMMS-induced DNA damage, confirming the alkylating agent as a substrate for FPG-sensitive sites. A close relationship between the FPG-dependent enhancement of DNA-damaging effects in the comet assay and the amount of N-7 alkylation was observed for the alkylating agents MMS, ethyl methanesulfonate, and ethylnitrosourea (Speit et al., 2004). The predominant adduct in double-stranded DNA resulting from MMS exposure is 7-methylguanine. The N7 position of guanine possesses the highest nucleophilic potential in DNA and is the preferential site of action of the electrophilic methylating agents. (Wyatt and Pittman, 2006). Comparison of effects between H_2O_2 and MMS showed that the enhancement of MMS-induced FPG-sensitive DNA damage was even stronger than the enhancement of the reactive oxygen compound, determined in whole blood samples or isolated human lymphocytes. Alkali treatment of 7-methylguanine during lysis step may result in ring-opened derivatives which can be repaired by the bacterial FPG repair enzyme. (Speit et al., 2004). In mammalian cells N-7-guanine-alkylated DNA is recognized by MPG (methylpurine DNA glycosylase), which is a DNA glycosylase that initiates BER (Wyatt and Pittman, 2006).

The second positive control used in the present study, menadione, led to extensive DNA fragmentation in the comet assay, which was nevertheless not further increased by FPG. Menadione is a representative quinone that resulted in a concentration-dependent induction of DNA strand breaks after treatment of rat primary hepatocytes (1–50 µM, 30 min) (Morrison et al., 1984; Di Monte et al., 1984). Quinones exert their toxic effects by two major mechanisms, i.e. oxidative stress as a consequence of ROS formation due to enzymatic redox cycling or decreased GSH levels due to sulfhydryl arylation (Thor et al., 1982; Rossi et al., 1986). In platelets prepared from plasma of Sprague Dawley rats menadione depleted GSH preferably via arylation, without an increase in the levels of GSSG. This effect indicated that menadione-mediated GSH decrease is predominantly mediated by arylation rather than oxidative stress (Seung et al., 1998) if GSH is available. Based on

these reported effects, the preference of menadione towards arylation in the presence of high amounts of GSH (see section 6.8.1) is suggested. Thus, the results of the present study support the idea that oxidative stress is not the primary mechanism for menadione toxicity in the rat liver cell models.

Generally, the enhanced DNA effects in the comet assay with FPG after exposure to genotoxic agents should not be regarded per se as evidence for the presence of oxidative damage. The mode of action of the agent should be considered as an important determinant for interpretation of FPG-sensitive DNA damage.

6.11. DNA REPAIR ACTIVITY IN THE UDS ASSAY

6.11.1. EFFECTS OF TCDD AND/OR E2

DNA repair activity induced by oxidative DNA modifications is predominantly performed by excision repair mechanism (mainly BER), which can be measured with the UDS assay. Using the LSC technique, hydroxyurea (HU) has to be used as an inhibitor of the scheduled DNA synthesis. The use of HU is indeed recommended in the OECD Guideline of the UDS assay *in vitro* (No. 482) in dividing cultures (OECD-Guideline, 1986).

In the present study lower UDS background activity in hepatoma cells compared with primary rat hepatocytes can be explained by the additional treatment with hydroxyurea. Primary rat hepatocytes are practically non-dividing and less than 0.05% of the cells enter the S phase of the cell cycle (Mitchell et al., 1983). However, the relatively high background level of incorporated tritium-labeled thymidine in rat hepatocytes and high standard deviations in PHm may reflect this minimal rate of replicative DNA synthesis. This may be checked in further experiments applying HU in appropriate non-toxic concentration to primary hepatocyte cultures. Under the same conditions used HU inhibited replicative DNA synthesis more efficiently in H4IIE cells than in HepG2 cells, leading to 99% and 91% inhibition respectively. HU depletes the pools of dNTP by inactivating ribonucleotide reductase, an enzyme needed for scheduled DNA synthesis (Skoog and Nordenskjöld, 1971; Thelander and Reichard, 1979). HU itself can exert genotoxic effects. Treatment with HU concentration of 10 mM for 1 h was found to be non-genotoxic in HepG2 cell line and effectively inhibited DNA replication. (Severin et al., 2003). In general terms, hepatocytes are recommended for UDS testing, since they exhibit appropriate metabolism, and the liver is often a prime target in rodent bioassays (Madle et al., 1994).

The treatments with TCDD and/or E2 showed no induction in DNA repair activity in hepatoma cells in the present study. These results were consistent with the negative results in the comet assay with and without FPG.

Rat primary hepatocytes did not result in a clear DNA repair induction following treatments. There was a slight tendency of an increasing effect observed in PHm, leading to a minimal non-statistical increase in repair activity for E2 or TCDD single treatments. Female-derived rat hepatocytes showed a significant increase following exposure to E2. However, this statistical effect represents only a small increase.

Studies on the induction of UDS in cultured hepatocytes from male Holtzman rats (with HU) resulted in a weak positive response after treatment with E2 at high doses in the range from 1 µM to 10 mM for 18 h (Althaus et al., 1982). Negative results in rat hepatocytes (with HU application) from male Fischer F.344/N rats have also been reported after 16 h exposure to E2 (Blakey and White, 1985). Unpublished results from Organon were reported to exert a positive UDS response in female-rat hepatocytes treated with E2 (Joosten et al., 2004).

Generally, the evaluation of a positive result in the UDS assay with strong and known carcinogens was identified as the increase over the negative control levels of [3H]-thymidine. Suggestions were also offered how to distinguish a marginally positive result from a negative result. In this context it was considered that a dose- or concentration-related increase in UDS is acceptable evidence of a positive response. (Williams, 1976). Others interpreted positive responses as those in which a reproducible, statistically significant increase in the [3H]-thymidine incorporation above that of the negative control could be demonstrated for at least one concentration of the test chemical (Martin et al., 1978). Optimally it was recommended that both criteria should be met to consider a test substance-related effect in UDS induction (Mitchell et al., 1983).

Accordingly, the obtained results in PHm showed very high variability in the four independent experiments. Further experiments in PHm are required to be able to demonstrate a reproducibility of the results. Currently, the trend for increased UDS activity by TCDD and E2 observed in PHm in the present study was not considered to be test substance-related. Likewise, in order to be able to draw a valid conclusion from the statistically significant increases in [3H]-thymidine incorporation by E2 10 and 100 nM observed in PHf, a dose-response relationship over at least 3 concentrations also in a wider range of concentrations should be carried out. Additionally, the influence of HU in rat hepatocytes culture on DNA activity following exposure to TCDD or E2 needs to be checked and to be compared with current results.

Contrarily to male-derived hepatocytes, female-derived hepatocytes failed tu induce a positive response with reference compounds. A sex-specificity in genotoxic response has often been reported in the UDS assay. This occurrence was presumably due to a different expression of enzyme systems catalyzing metabolic activation and detoxification of indirect mutagens and is further discussed in section 6.11.2. That is also the reason why male rat hepatocytes are generally recommended to be used in the *in vivo* standard genotoxicity testing (Madle et al., 1994). However, hepatocytes from female rats may be more appropriate for certain classes of chemicals, e.g. steroid hormones (Topinka et al., 1993; Martelli et al., 2003).

The LSC-based UDS variant is less sensitive than the autoradiography approach. In the autoradiography-based UDS assay S-phase cells can easily be recognized (extremely high numbers of nuclear silver grains) and excluded from counting (Mitchell et al., 1983; Fautz et al., 1991; Madle et al., 1994). This can be important for minimal numbers of S-Phase cells present in rat hepatocytes, because they can yield high background incorporation rates, lowering the sensitivity in LSC-based UDS testing, especially when the effect of weak DNA repair inducing agents shall not be missed. In future experiments the autoradiography UDS variant should be performed to better characterize the effects of TCDD and/or E2 on DNA repair mechanisms.

6.11.2. EFFECTS OF DIRECT AND INDIRECT GENOTOXINS

For the purpose of obtaining appropriate positive controls in the UDS assay, several genotoxic agents with a direct damaging mechanism or requiring metabolic activation were tested. The known mutagen 4-nitroquinoline N-oxide (NQO) and the alkylating agent methyl methanesulfonate are often used as appropriate positive controls in the UDS assay, because they do not require metabolic conversion of cells (Mitchell et al., 1983; Wyatt and Pittman, 2006).

In the present study NQO was found to be an appropriate positive control for the LSC-based UDS assay in HepG2. HepG2 cells have been reported to induce NQO-mediated UDS activity in a dose-dependent manner with its maximum at 2 µM (Naji-Ali et al., 1994). In their study cytotoxicity was starting at a concentration of 2.5 µM after 24 h treatment in HepG2 cells. The human hepatoma cell line was also reported to induce UDS activity after 24 h treatment with MMS at concentrations up to 50 µM (Naji-Ali et al., 1994), which also induced strand breaks in the comet assay in the present study. HepG2 cell line is a useful tool for the detection of genotoxins and has been widely used in genotoxicity

testing and toxicology screening as an alternative to human hepatocytes (Valentin-Severin et al., 2003; Knasmüller et al., 1998; Naji-Ali et al., 1994).

In rat H4IIE cell line NQO failed to induce UDS activity, which was even diminished at concentrations above 4 µM most probably due to cytotoxic effects. Secondly, the alkylating agent MMS was only able to show a positive response after 4 h treatment. In the Alamar blue Assay (data not shown) MMS 100 µM did not appear to affect cell viability after 20 h and 48 h treatment up to 200 µM in H4IIE cells. Nevertheless, MMS 100 µM may have altered the integrity of the cells over time possibly by affecting the intrinsic DNA repair system. This may explain the different response of MMS in the UDS and the comet assay in H4IIE cells. The unchanged DNA repair level by MMS at the longer 20 h exposure time may indicate that enzymatic DNA repair systems are already saturated over time. Alternatively, DNA lesions may have formed but are no longer repaired.

Both NQO and MMS were able to considerably increase [3H]-thymidine incorporation in male-derived rat hepatocytes. However, various concentrations of the hepatic carcinogen 2-actylaminofluorene (2-AAF) failed to induce UDS activity at 4 h. This indicates that possibly a longer treatment time may be necessary for metabolic activation of 2-AAF by CYP 1A2 (Edwards et al., 1990). Treatments with 2-AAF for 18 h were reported to induce DNA repair in male rat hepatocytes from Wistar rats in the autoradiography-based UDS (Schehrer et al., 2000). 2-AAF also gave a strong positive response in the LSC-based UDS assay with male rat hepatocytes from different strains (e.g. Wistar and Sprague-Dawley). However, the range of the positive response with 2-AAF was observed to be variable among different rat strains, probably due to strain variation in the capacity for biotransformation. (Fautz et al., 1991). Since the lowest observed effective concentrations for 2-AAF were lower in the autoradiography-based UDS assay, it was suggested that this method was slightly more sensitive than the LSC assay (Fautz et al., 1991).

Moreover, a sex-specific response in UDS activity was apparent in the present study. Several kinds of positive controls did not affect DNA repair activity in female-derived hepatocytes. Treatment with MMS at the concentration resulting in FPG-sensitive DNA fragmentation in the comet assay did not change DNA repair levels. Higher concentrations of MMS after 20 h (100–150 µM) as well as different concentrations of MMS, 2-AAF, and NQO after 4 h even significantly reduced UDS activity. The reduction most probably indicated either a cytotoxic response in these cells, effects on cell integrity thus affecting intrinsic repair enzymes, or the inappropriateness of these cells to exert DNA repair for certain kinds of test compounds. Nevertheless, female rat hepatocytes from three different strains (Fischer F344, Lewis, DA) were shown to induce UDS after treatment with 2-

AAF (18–20 h). Generally, exposure to 2-AAF 100 mM was toxic in all three strains and resulted in a stable or diminished UDS induction. However, sensitivity towards cytotoxic effects varied between the different rat strains. (Mc Queen and Way, 1991)

Reports are available showing lower sensitivity in response in female-derived rat hepatocytes in the DNA repair assay. Hepatocytes from Sprague Dawley and Fischer F344 rats treated with different concentrations of 2-AAF for 20 h showed lower UDS activity in female rat hepatotcytes than in male rat hepatocytes. Additionally, the response diminished with increasing age in both sexes. (Probst and Hill, 1987). Lower DNA repair activity with 2-AAF in female rats was associated with lower activities of a sulfotransferase, which is required for the formation of the reactive DNA-binding intermediate (Beland et al., 1982; Irving, 1975; Probst and Hill, 1987; McQueen et al., 1986). In Fischer F344 rats the activities of Phase 1 aryl hydrocarbon hydroxylases were shown to be lower in liver and hepatocytes from females than in those from males (Croci and Williams, 1981).

Consequently, in the present study there was a sex-dependent difference in response in the UDS assay in rat hepatocytes. This effect was predominantly obvious as a lack of induction by various reference compounds in PHf, while a positive response was found in PHm. Thus, the interpretation of the UDS results in hepatocytes from Wistar rats is difficult and the use of appropriate positive controls in the female rat hepatocytes will have to be investigated in more detail in this rat strain.

Taken together, the lack of clearly induced UDS activity by TCDD and E2 and the co-treatments in all cell models would be consistent with negative results observed in the normal alkaline comet assay. The induced formation of strand breaks by TCDD and/or E2 in rat hepatocytes of both sexes in the comet assay with FGP was not reflected in the UDS assay. The exogenous addition of the bacterial FPG repair enzyme to the DNA of the cells in the comet assay allows detection of specific DNA modifications, which remain unrepaired by the intrinsic repair system and can then be converted into additional DNA strand breaks subsequent to excision of the respective DNA stretch. The DNA repair measured in the UDS assay reflects directly the endogenous repair. It is assumed, that the intrinsic repair enzymes may be the limiting factor to repair the oxidative lesions observed in the comet assay.

In order to gather more insights into the genotoxic action of TCDD and/or E2 via indirect metabolic mechanisms, other DNA strand break assays such as the alkaline unwinding or alkaline elution technique may be performed. These assays can also be carried out by adding additional steps of specific DNA repair enzymes such as FPG (Hartwig et al., 1996; Pflaum et al., 1997). Together with the comet assay or the UDS assay, these tests have in

common that they are not restricted to certain cell lines or cell systems but can be used for measuring genetic damage in various target organs *in vitro* and *in vivo* (Kasper et al., 2007; ICH, 2008).

6.12. FPG-SENSITIVE DNA MODIFICATIONS IN REPAIR-DEFICIENT MICE AFTER SINGLE TCDD EXPOSURE

The effects of a single exposure of TCDD on 8-oxo-G formation and the implication of BER-mediated DNA repair processes were observed in repair-deficient OGG1$^{-/-}$/csb$^{mut/mut}$ mice compared to wild-type C57BL/6 mice. OGG1 protein is the mammalian repair enzyme initiating the base excision repair of the oxidative 8-oxo-G DNA modifications and related purine modifications (Klungland et al., 1999; Minowa et al., 2000). The cockayne syndrome B (csb) protein is involved in the transcription-coupled nucleotide excision repair and is part of a backup repair mechanism for 8-oxo-G (Osterod et al., 2002). Oxidative DNA modifications contribute to the mutagenic potential of cells and the efficiency of the DNA repair systems may play a major role in the initiation steps of carcinogenesis. Oxidative DNA damage dependent on the acute exposure to the environmental contaminant TCDD in the light of BER-mediated DNA repair pathway was further elucidated by means of the alkaline elution technique modified with an additional FPG treatment step.

FPG-sensitive background levels of DNA modifications were about 2-fold increased in the repair-deficient mice compared to the wild-type mice, suggesting a role for this repair mechanism by preventing accumulation of endogenous 8-oxo-dG in the liver. Previous results obtained in Prof. Epe's laboratory showed increased background levels of FPG-sensitive oxidative DNA modifications in OGG1$^{-/-}$/csb$^{mut/mut}$, which was about 3.4-fold higher than the 2-fold increase in OGG1$^{-/-}$ mice (Osterod, 2002). The combined defect of OGG1 and csb gave rise to the highest level of FPG-dependent oxidative DNA modifications, pointing out the importance of the csb protein in the pathways involved in the repair of these lesions (Osterod et al., 2002).

According to the age of the mice (3-7 months) used in the present study, the steady state levels of FPG-sensitive DNA modification in primary hepatocytes isolated from repair-deficient and wild-type mice were in the same range as with the results obtained in the course of a previously performed age-dependent investigation of FPG-sensitive DNA modification (Osterod et al., 2002).

Nevertheless, a single dose of TCDD (1 µg/kg bw) did not have any effect on FPG-sensitive DNA modifications in hepatocytes 96 h after exposure, neither in repair-deficient animals

nor in wild-type animals compared to control animals. Hence, it is assumed that following single exposure to TCDD, no TCDD-mediated oxidative DNA base modifications were formed. Further experiments following long-term exposure to TCDD in the repair-deficient mice need to be investigated in order to check if it is a repeated dose effect.

Female B6C3F1 mice were administered TCDD once by gavage (0.001, 0.01, 0.1, 1, 10, or 100 µg/kg bw) and sacrificed 7 days later (Slezak et al., 2000). Hepatic production of superoxide anion, measured as the reduction of cytochrome c, demonstrated a significant increase of oxidative stress, but only at the higher dose levels of 10 or 100 µg/kg TCDD. Furthermore, tGSH was increased at both of these dose levels. Significant increases in TBARS (Thiobarbituric Acid Reactive Substances), another parameter of oxidative stress measuring lipid peroxidation, were observed only at the highest dose of 100 µg/kg TCDD. (Slezak et al., 2000)

Shertzer and co-workers (1998) reported that acute TCDD exposure (5 µg/kg bw i.p., 3 consecutive days) produced a sustained oxidative stress response in female C57BL/6J mice. This was determined by elevated urinary excretion of 8-oxo-dG, a repair by-product of oxidative DNA damage, and persisted for at least 8 weeks after administration. Significant increases in the ratio of oxidized to reduced hepatic glutathione (GSSG/GSH) were also reported 1 week and 8 weeks after administration. This prolonged oxidative stress response may be related to the elevated CYP1 levels that persisted over the time course of 8 weeks after the high-dose acute exposure to TCDD. (Shertzer et al., 1998)

TCDD-treated female C57BL/6 mice (15 µg/kg bw i.p., 3 consecutive days) showed elevated mitochondrial H_2O_2 production 1 week up to 8 weeks after exposure. Moreover, dioxin treatment augmented mitochondrial GSH but not GSSG, which may be explained by increased glutathione reductase (GR) activity. (Senft et al., 2002a)

AhR$^{(-/-)}$, Cyp1a1$^{(-/-)}$, and Cyp1a2$^{(-/-)}$ knockout mice of the C57BL/6J background were administered TCDD (15 µg/kg bw, i.p., 3 consecutive days) and were sacrificed after 1 week. CYP1A1 $^{(-/-)}$, CYP1A2 $^{(-/-)}$, but not AhR $^{(-/-)}$ knockout animals showed increased GSH and GR activities as a consequence of TCDD administration, implicating a role of AhR function in the TCDD-dependent oxidative stress response.(Senft et al., 2002b)

The investigation of the role of CYPs in TCDD-induced oxidative stress was further investigated in CYP1A1$^{(-/-)}$ and CYP1A2$^{(-/-)}$ knockout mice after single administration of TCDD (5 µg/kg bw, sacrifice after one week). CYP1A1$^{(-/-)}$ mice displayed markedly lower levels of H_2O_2 production in both induced and non-induced liver microsomes compared with those from wild-type mice and CYP1A2$^{(-/-)}$ mice. CYP1A2 was suggested to act as an electron

acceptor by preventing the uncoupled electron transfer from NADPH to O_2. (Shertzer et al., 2004b)

Likewise, it was demonstrated that the induction of hepatic 8-oxo-dG adducts by TCDD in Sprague Dawley rats were only observed following chronic exposure but not acute exposure. Single dose treatment with TCDD (1000 and 3000 ng/kg bw) at doses resulting in liver burden showed no difference in 8-oxo-dG adducts between the control and treated female Sprague-Dawley rats 4 days after exposure. (Wyde et al., 2001)

Taken together, based on the reported mouse studies a dosing protocol of high acute TCDD doses such as higher than or equal to 5 µg/kg bw or administration over 3 consecutive days and sacrifice of the animals 1 week after exposure has been shown to be sufficient to intensify the dioxin-mediated oxidative stress response. The lack of response in the present study in the repair-deficient mice as well as wild-type mice following a single dose of 1 µg/kg bw TCDD suggested that the dioxin dose was probably too low to result in a manifested oxidative stress and FPG-sensitive DNA modifications. Further experiments with the same knockout mouse models and applying the well described dosing protocols in a concentration-dependent manner will have to be performed to better elucidate the role of the BER repair in the TCDD-mediated induction of oxidative DNA base modifications.

Thus, it is suggested that a single low dose of TCDD does not result in oxidative DNA modifications, but a threshold level has to be achieved. The lack of oxidative DNA damage in the presence of a single low dose of TCDD in the present study cannot be explained by the fact that DNA BER repair pathway is sufficiently working, since no modulating effect was seen in the repair-deficient mice either. High dose or low dose subchronic exposure appears to be necessary to detect increased dioxin-mediated oxidative stress responses in the liver.

7. SUMMARY AND CONCLUSION

There is extensive evidence that TCDD-activated AhR elicits anti-estrogenic activity by interfering with the regulation of estrogens and the estrogen-mediated ERalpha signaling pathway. Furthermore, TCDD and estradiol have been implicated in the induction of ROS as an initiating event and subsequent oxidative DNA damage, which could contribute to carcinogenesis.

The present study was conducted to shed light on the hypothesis that enhanced activation of estrogens by TCDD-induced CYP enzymes, mainly CYP1A1 and CYP1B1, leads to oxidative DNA damage in liver cells.

It was the first time that the effects on four different AhR-responsive liver cell models, rat H4IIE and human HepG2 hepatoma cell lines and primary hepatocytes from male and female rats, were investigated to elucidate the possible species- and sex-specific effects of TCDD-mediated CYP expression and subsequent oxidative DNA damage and its possible modulation by estradiol.

The effective induction of CYP1A1 and CYP1B1 by TCDD was demonstrated in all liver cell models. Despite of low basal levels in rat H4IIE and human HepG2 cell lines, CYP1A1 expression and activity was highly inducible in hepatoma cells. In contrast, basal and TCDD-induced CYP1B1 expression was more pronounced in cells of rat origin, and most pronounced in rat primary hepatocytes. Thus, rodent cells and especially non-tumorigenic liver cells appear to be better at stimulating the estradiol metabolism via the more reactive pathway involving the CYP1B1-mediated formation of the genotoxic 4-hydroxyestradiol.

CYP-dependent induction of ROS was only observed in rodent cells. Estradiol induced ROS only in rat hepatocytes, which was associated with a weak CYP1B1 mRNA induction. Thus, E2 itself was suggested to induce its own metabolism in primary rat hepatocytes resulting in the redox cycling of catechol estradiol metabolites leading to ROS formation. It was speculated that longer treatment times would be favorable to enhance this E2-mediated induction.

In this study, the role of TCDD and E2 on oxidative DNA damage was investigated for the first time *in vitro* in the comet assay in combination with FPG using liver cells. Both TCDD

and E2 were shown to induce FPG-sensitive oxidative DNA base modifications only in rat hepatocytes. Additionally, the direct oxidative DNA-damaging effect of the two main E2 metabolites, 4-OHE2 and 2-OHE2, were only observed in rat hepatocytes and revealed that E2 damaged the DNA to the same extent. The induction of oxidative DNA damage by E2 cannot completely be explained by the metabolic conversion of E2 via CYPs as E2 did not induce CYP1A1 and a weak CYP1B1 mRNA induction was only observed following 48 h treatment. The impact of CYP1B1 activity will help to better identify its role in this particular DNA damage. Moreover, other mechanisms of E2-induced changes in antioxidant status, possibly also involving ER-mediated cell proliferation, are interesting domains of further research.

The intrinsic base excision repair activity, which is responsible for the elimination of oxidative DNA base modifications, was not affected by the treatments in the hepatoma cell lines using the LSC-based UDS assay. Inconclusive results obtained with primary rat hepatocytes may be checked with the more sensitive autoradiography UDS variant to better characterize the effects of TCDD and/or E2 on DNA repair mechanisms. Furthermore, it is of interest to perform other DNA strand break assays *in vitro* such as the alkaline unwinding or alkaline elution technique in combination with FPG.

In an *in vivo* experiment, a single low dose of TCDD did not have an effect on FPG-sensitive oxidative DNA modifications 4 days after exposure, neither in wild-type nor in repair-deficient $OGG1^{-/-}/csb^{mut/mut}$ mice using the alkaline elution technique. This corroborates the theory that repeated dose exposure is necessary to detect a dioxin-mediated oxidative stress response in the liver. However, the *in vitro* results in the FPG-sensitive comet assay support that TCDD and also E2 possess a genotoxic potential through the indirect mechanism of oxidative DNA damage.

The high antioxidant status of GSH in the liver cells was not changed by exposure to TCDD and/or E2. Generally, there was a trend towards increased tGSH levels in all cell models, which was most probably associated with increased GSH levels and unchanged GSSG levels, creating a rather reducing cell environment.

The detoxification of catechol estrogens by COMT is the most common pathway to prevent the production of the genotoxic estrogen quinone forms. Higher amounts of basal COMT mRNA in rat hepatocytes than in hepatoma cell lines suggest a favorable expression in non-tumorigenic cells. The investigation of COMT-activity and those of other enzymes involved in the metabolism of catechol estrogens such as GPx, GST, or UDPGT will have to be carried out in the future to allow to fully characterize the metabolic capabilities of the liver cell models.

As a crucial point, the expression of low levels of endogenous ERalpha in rat hepatocytes and the lack of ERalpha in hepatoma cell lines was identified. Therefore, the effects of interference of ERalpha with AhR was examined in HepG2 transiently transfected with ERalpha. E2 enhanced the AhR-mediated transcriptional activity, which was dependent on ERalpha over-expression. This further increase of the co-treatment may be due to an ERalpha activity switching on AhR target genes in order to regulate E2 levels. In turn, TCDD reduced E2-mediated ERalpha signaling, which confirmed the anti-estrogenic action of TCDD. A modulation of the combined effects of TCDD with E2 was not observed in any of the other experiments. Thus, the role of low endogenous ERalpha levels has to be investigated in transfection experiments using rat primary hepatocytes to clarify whether the enhancement of AhR regulation by the co-treatment is due to an over-expression of ERalpha. The exact mechanisms of the AhR/ER cross talk are not yet fully understood and other unknown molecular mechanisms such as competition for common co-regulatory proteins are certainly a promising field for future investigations.

A sex-difference was observed. Lower TCDD-induced EROD activities and a lack of positive response in DNA repair activity in the presence of known genotoxins were noticeable in female rat hepatocytes. However, CYP1A1 and CYP1B1 expression and oxidative DNA damage was comparable between both sexes. Lower levels of Phase 1 enzyme activities implicated in the metabolic activation of certain compounds in female rat hepatocytes may explain these differences in response and should motivate to better characterize the sex-differences of Phase 1 enzyme activities, particularly CYP1B1 activity as a key enzyme in estradiol metabolism.

A general comparison between the responses observed in the different liver cell models revealed that the hepatoma cell lines were less responsive. The rat H4IIE data proved the cell line to be a good model for investigating TCDD-mediated ROS formation, which did however not result in FGP-sensitive oxidative DNA modifications. There were no E2-mediated effects observed in human and rat hepatoma cell lines, which both lacked ERalpha. In the human HepG2 cell line no oxidative DNA damage was found with either treatment condition. However, in HepG2 cells CYP1A activities were greatly induced being similar to the activities in male rat hepatocytes. Human hepatocytes may be used to check whether differences between human HepG2 cell line and rat hepatocytes were due to species-specific differences or the transformation of the cells to tumor cells.

Overall, rat primary hepatocyte cultures turned out to be the more adaptive cell model to investigate metabolism in the liver, reflecting a more realistic situation of the liver tissue. However, long-term culture effects would be very interesting especially with regard to

investigating the impacts of tumor promotors to better point out the effects of long-term exposures of estradiol in combination with TCDD *in vitro*. Furthermore, hepatoma cell lines can be used to permit to better examine molecular mechanisms. Indeed, during this work a cross talk between ERalpha with AhR was shown for the first time using human hepatoma HepG2 cell line by transiently transfecting ERalpha.

8. APPENDICES

8.1. SOLUTIONS AND BUFFERS

8.1.1. GENERAL SOLUTION

PBS (phosphate buffered saline, Ca^{2+} and Mg^{2+}-free), pH 7.4

Na_2HPO_4	0.923 g (6.5mM)
KH_2PO_4	0.204 g (1.5 mM)
NaCl	8.006 g (137 mM)
KCl	0.201 g (2.7 mM)
ddH_2O	ad 1 L

Adjust to pH 7.4, sterile filtration, store at room temperature

8.1.2. CELL CULTURE MEDIA

DMEM 10% FBS

DMEM w/o phenol red	87 mL
FBS	10 mL (10%)
Penicillin/streptomycin 100x	1 mL (1%)
L-Glutamine 200 mM	2 mL (4 mM)

store at 4 °C, prewarm at room temperature before use

DMEM 0.5% FBS

DMEM w/o phenol red	97 mL
FBS	0.5 mL (0.5%)
Penicillin/streptomycin 100x	1 mL (1%)
L-Glutamine 200 mM	2 mL (4 mM)

store at 4 °C, prewarm at room temperature before use

DMEM 0.5% FBS + hydroxyurea 10 mM

DMEM w/o phenol red	97 mL
FBS	0.5 mL (0.5%)
Penicillin/streptomycin 100x	1 mL (1%)
L-Glutamine 200 mM	2 mL (4 mM)
Hydroxyurea	76 mg (10 mM)

store at 4 °C, prewarm at room temperature before use

DMEM w/o FBS

DMEM w/o phenol red	97 mL
Penicillin/streptomycin 100x	1 mL (1%)
L-Glutamine 200 mM	2 mL (4 mM)

store at 4 °C, prewarm at room temperature before use

DMEM DCC FBS 10%

DMEM w/o phenol red	87 mL
DCC FBS	10 mL (10 %)
Penicillin/streptomycin 100x	1 mL (1%)
L-Glutamine 200 mM	2 mL (4 mM)

store at 4 °C, prewarm at room temperature before use

8.1.3. TREATMENT SOLUTIONS

For dissolving test chemicals in DMSO or Ethanol high quality anhydrous DMSO or EtOH p.a. were used.

TCDD stock solution 10^{-4} M

MW	322 g/L
TCDD	10^{-4} M

17beta- Estradiol (E2) stock solution 20mM

MW	272.39 g/L
E2	5.45 mg/mL

2-Hydroxyestradiol (2-OHE2) stock solution 13.8 mM

MW	288.4 g/L
2-OHE2	4 mg/mL

Store at -20 °C

4-Hydroxyestradiol (2-OHE2) stock solution 13.8 mM

MW	288.4 g/L
4-OHE2	4 mg/mL

Store at -20 °C

8-Methoxypsoralen (8-MOP) stock solution 100 mM

MW	216.2 g/L
8-MOP in DMSO	21.62 mg/mL

prepare protected from light, store at 4 °C

ZK°191°703 stock solution 10 mM

MW	623.782 g/L
ZK°191°703 in DMSO	6.238 mg/mL
store at 4 °C	

2-Acetylaminofluorene (2-AAF) stock solution 1 M

MW	223.3 g/L
2-AAF in DMSO	223.3 mg/mL

4-Nitroquinoline-N-oxide (NQO) stock solution 100 mM

MW	190.16 g/L
4-NQO in DMSO	19 mg/ mL
store at –20 °C	

Methyl methanesulfonate (MMS)

MW	110.13 g/L
density	1.3 g/mL at 25 °C
prepare freshly on the day of use	

8.1.4. PREPARATION OF RAT HEPATOCYTES

Heparin

1000 U/mL in 0.9% NacL

Pentobarbital solution

pentobarbital	33 mg
ddH_2O	ad 1 mL
Prepare prior to use	

HEPES

HEPES	23.83 g
ddH_2O	ad 100 mL
Adjust to pH 7.4	
sterile filtration	

Perfusion buffer I

Na Cl	31.5 g (0.1 M)
KCl	1.6 g (4 mM)
$MgSO_4 \cdot 7H_2O$	1.35 g (1 mM)
KH_2PO_4	0.75 g (1 mM)
$NaHCO_3$	9.05 g (20 mM)

HEPES	17.9 g (15 mM)
Glucose	7.5 g (8 mM)
EGTA	0.19 g (0.1 mM)
ddH_2O	ad 5L
Adjust to pH 7.4	
sterile filtration	

Perfusion buffer II

HEPES 1 M, pH 7.4	5 mL (10 mM)
DMEM/Ham's F12 (1:1)	ad 500 mL

Washing buffer

HEPES 1 M, pH 7.4	5 mL (10 mM)
Penicillin1000 U /Streptomycin 10 mg/L	5 mL (100 U/0.1 mg/mL)
FBS	100 mL (20%)
DMEM/Ham's F12 (1:1)	ad 500 mL

Glutamine solution, pH 7.6

L-Glutamin 48 mM	7 g/L
Sterile filtered and aliquoted	
Stored at –20 °C	

Insulin solution

Insulin (I-5500)	2 g/L
Dissolved in dist. H_2O by addition of 1 drop of 1 M NaOH	
Adjusted to pH 7.6 by 1 M HCl	
Sterile filtered and aliquoted	
Stored at –20°C	

EGTA solution

EGTA 125 mM	47.5 g/L
Dissolved in dist. H_2O by addition of 1 drop of 1 M NaOH	
Adjusted to pH 7.6 by 1 M HCl	
Sterile filtered and aliquoted	
Stored at –20°C	

8.1.5. PREPARATION OF MOUSE HEPATOCYTES

If not noted otherwise, solutions were prepared in bidistilled H_2O and autoclaved.

Glucose solution, pH 10

D (+) Glucose x H_2O	9 g/L (50 mM)

Krebs-Henseleit-buffer

NaCl 1000 mM	60 g/L
KCl 24 mM	1.75 g/L
KH_2PO_4 12 mM	1.6 g/L

Adjusted to pH 7.6 with NaOH

HEPES-buffer pH 8.5

HEPES (free acid) 250 mM	60 g/L

Adjusted to pH 8.5 with NaOH when used carbogen

Amino acid solution

L-Alanine 3.0 mM	0.27 g/L
L-Aspartit acid 1.0 mM	0.14 g/L
L-Asparagine 3.0 mM	0.40 g/L
L-Citrulline 1.5 mM	0.27 g/L
L-Cysteine 0.8 mM	0.14 g/L
L-Histidine 6.4 mM	1.0 g/L
L-Glutamic acid 6.8 mM	1.0 g/L
L-Glycin 13.3 mM	1.0 g/L
L-Isoleucine 3.0 mM	0.40 g/L
L-Leucine 6.1 mM	0.80 g/L
L-Lysine 7.1 mM	1.30 g/L
L-Methionine 3.7 mM	0.55 g/L
L-Ornithine 3.8 mM	0.65 g/L
L-Phenylalanine 3.3 mM	0.55 g/L
L-Proline 4.8 mM	0.55 g/L
L-Serine 6.2 mM	0.65 g/L
L-Threonine 11.3 mM	1.35 g/L
L-Tryptophan 3.2 mM	0.65 g/L
L-Tyrosine 3.0 mM	0.55 g/L
L-Valine 6.8 mM	0.80 g/L

Dissolved in distilled H2O
After stirring (20 min), pH was adjusted to 11 by addition of 10 N NaOH.
Thereafter, (10 min stirring) pH was adjusted to 7.6 by 37% HCl.
Solution was sterile filtered and kept at 4 °C for 2-3 months.

Glutamine solution, pH 7.6

L-Glutamin 48 mM	7 g/L
Sterile filtered and aliquoted	
Stored at –20 °C	

Insulin solution

Insulin (I-5500)	2 g/L
Dissolved in dist. H_2O by addition of 1 drop of 1 M NaOH	
Adjusted to pH 7.6 by 1 M HCl	
Sterile filtered and aliquoted	
Stored at –20°C	

EGTA solution

EGTA 125 mM	47.5 g/L
Dissolved in dist. H_2O by addition of 1 drop of 1 M NaOH	
Adjusted to pH 7.6 by 1 M HCl	
Sterile filtered and aliquoted	
Stored at –20°C	

$CaCl_2$ solution

$CaCl_2 \times 2H_2O$	129 mM

$MgSO_4$ solution

$MgSO_4 \times 7H2O$	100 mM

EGTA Buffer

Glucose solution	62 mL
Krebs-Henseleit buffer	10 mL
HEPES buffer	10 mL
Amino acid solution	15 mL
Glutamine solution	1 mL
Insulin solution	0.5 mL
EGTA solution	0.4 mL

Collagenase buffer

Glucose solution	77.5 mL
Krebs-Henseleit buffer	12.5 mL
HEPES buffer	12.5 mL
Amino acid solution	19 mL
$CaCl_2$ solution	5 mL
Glutamine solution	1.25 mL
Insulin solution	0.6 mL
Collagenase	62.5 mg

Collagenase was dissolved in the prewarmed mixture immediately before use.
$CaCl_2$ was added shortly before use.

Suspension buffer

Glucose solution	310 mL
Krebs-Henseleit buffer	50 mL
HEPES buffer	50 mL
Amino acid solution	75 mL
Glutamine solution	5 mL
Insulin solution	2.5 mL
$CaCl_2$ solution	4 mL
$MgSO_4$ solution	2 mL
BSA	1 g

Alkaline Elution

PBSCMF pH 7.5 (autoclaved)

NaCl	137 mM
KCl	2.7 mM
NaH_2PO_4	8.3 mM
KH_2PO_4	1.5 mM

BE_1-buffer pH 7.5 (autoclaved)

NaCl	100 mM
Tris/HCl	20 mM
Na_2EDTA	1 mM

BE_1/BSA-Puffer pH 7.5 (autoclaved)

NaCl	100 mM
Tris/HCl	20 mM
Na_2EDTA	1 mM
BSA	0.50 g/l

Lysis buffer pH 10.0 (with proteinase K)

Glycin	100 mM
Na_2EDTA	20 mM
SDS	2 %
Adjust pH with 2 N NaOH	
(400 mg/l proteinase K)	

Washing buffer pH 10.0 (autoclaved)

Na_2EDTA	20 mM
Adjust pH with 2 N NaOH	

Elution buffer pH 12.15

EDTA	20 mM
Adjust pH with Tetraethylammoniumhydroxid (TEAH)	

Bisbenzimide (Hoechst No. 33258)

stock solution	0.15 mM
Ad dist. H_2O	
aliquoted and stored at -20°C	

Phosphate buffer pH 6,0 (autoclaved)

NaH_2PO_4	68.1 mM
Na_2HPO_4	15.8 mM

Phosphate buffer pH 7,2 (autoclaved)

NaH_2PO_4	21.7 mM
Na_2HPO_4	93.0 mM
with bisbenzimide (1 % (v/v) stock solution)	
bisbenzimide stock solution is added immediately before use	

8.1.6. CYTOTOXICITY TEST: ALAMAR BLUE ASSAY

Resazurin stock solution (440 mM)

Resazurin	110.5 mg
DMF	in 1 mL

Store at 4°C for 1 week
Exclude from light

NaCl/P_i-Puffer

KH_2PO_4 1.1 mM	0.144 g
NaCl 154 mM	9 g
Na_2HPO_4 3.7 mM	0.528 g
ddH_2O	up to 1L

Store at 4°C

Resazurin-NaCl/Pi solution (440µM)

Resazurin stock solution	100µL
NaCl/Pi-Puffer	999.9 mL

Store at 4°C for up to 6 weeks
Exclude from light

Resazurin working solution

Dilute Resazurin - NaCl/Pi solution and phenol red-free DMEM (without supplementation of FBS) in the ratio 1:10 (v/v).
Prepare just before use and prewarm at room temperature.
Exclude from light.

8.1.7. CELLULAR ROS LEVELS: H_2DCFDA FLUORESCENCE ASSAY

H_2DCFDA stock solution (80 mM)

H_2DCFDA	38.98 mg / 1mL DMSO

Store at –20°C under dry nitrogen
Protect from light and oxygen

H_2DCFDA working solution (2 mM)

Dilute stock solution (80 mM) 1/40

H_2DCFDA 80mM	25 µL
DMSO	975 µL

Prepare freshly on the day of experiment

Borate buffer (10 mM), pH 8.0 (esterase enzyme buffer)

Boric acid	0.6183 g
ddH_2O	up to 1 L

Store at 4°C

Esterase (48.6 U/ mL)

Esterase 27 U/mg	9 mg
Borate buffer 10mM	5 mL

Keep on ice
Store at 4 °C for two weeks

Na-phosphate buffer (50 mM), pH 8.0

47.4 mM Na_2HPO_4; NaH_2PO_4 2.6 mM

$Na_2HPO_4 \cdot 2H_2O$	8.437 g
NaH_2PO_4 H_2O	359 mg
dd H2O	up to 1 L

store at 4 °C

NADPH (13.4 mM)

Na_4- NADPH	1 g
Na-phosphate buffer	89.23 mL

Keep on ice
Store at –80°C or at 4 °C after first thawing
protect from light

DCF standard solutions

Prepare the following solutions ins DMSO:
400x 5 nM, 10 nM, 25 nM, 50 nM, 100 nM, 250 nM, 500 nM, 1000 nM
Store at 4 °C

Tert-butylhydroperoxide (TBH) (400x250 µM)

TBH aqueous solution (70%)	13.7 µL
PBS	986.3 µL

Prepare freshly on the day of experiment
keep on ice

8.1.8. 7-ETHOXYRESORUFIN-O-DEETHYLASE (EROD) ASSAY

NaOH (0.1N)

NaOH	0.4 g
ddH_2O	100 mL

Na-acetate buffer (0.1 M), pH 4.5

Na-acetate trihydrate	1.361 g
ddH_2O	100 mL

Dicoumarol (2 mM) in NaOH (0.1 N)

Dicoumarol	33.629 mg
NaOH (0.1N)	50 mL

β-Glucuronidase (1000 U /mL) 574 000 U/g

β-Glucuronidase	34.8 mg
Na-acetate buffer (0.1 M)	20 mL

store at –20°C

7-Ethoxyresorufin (ER) stock solution (0.5 mM)

ER	5 mg
Methanol	41.459 mL

Prepare 1 mL aliquots
Protect from light
Store at -20°C

Resorufin stock solution (10 mM)

Resorufin sodium salt	23.5 mg
Methanol	10 mL

store at 4°C

Resorufin solutions (27µM and 2.7 µM)

Dilute resorufin stock solution (10 mM) 1/370,4: 13,5 µL / 5 mL MeOH
Dilute resorufin solution (27 µM) 1/10: 100 µL + 900 µL MeOH
store at 4°C

Na-phosphate (Napi-) buffer (50 mM), pH 8.0

Na_2HPO_4 47.4 mM; NaH_2PO_4 2,6 mM:

Na_2HPO_4 $2H_2O$	8,437 g
NaH_2PO_4 H_2O	359 mg
ddH_2O	up to 1 L

store at 4 °C

Fluorescamine solution (300 µg/mL)

fluorescamine	100 mg
acetonitrile	333.33 mL

protect from light
store at 4°C

BSA stock solution (1mg /mL)

BSA	10 mg/10 mL ddH_2O

store at –20°C

8.1.9. DETERMINATION OF TGSH AND GSSG

Solution A

KH_2PO_4	8,5 g
Na_2-EDTA	1.170 g
ddH_2O	up to 500 mL

store at 4 °C

Solution B

K_2HPO_4	10.875 g
Na_2-EDTA	1.170 g
ddH_2O	up to 500 mL

store at 4 °C

Phosphate buffer (solution A + B) pH 7.5

Solution A	15 mL
Solution B	85 mL

prepare freshly daily

$NaHCO_3$ 0.5% (w/v)

$NaHCO_3$	500 mg
ddH_2O	up to 100 mL

store at 4 °C

NADPH (20mM) in NaHCO3 0.5%

NADPH	18 mg / mL

prepare freshly daily
store on ice

DTNB (6mM)

DTNB	2.4 mg / mL phosphate buffer (solution A + B)

prepare freshly daily
protect from light

Glutathione reductase (GSR) (50 U /mL)

phosphate buffer (Solution A+B)	0.5 U/10 µL

prepare freshly daily
store on ice
vortex shortly prior to addition to reaction mixture

5-Sulfosalicylic acid (5-SSA)

5-SSA 10% (w/v)	10 g/100 mL ddH_2O
5-SSA 5% (w/v)	5 g/ 100 mL ddH_2O

store at 4 °C

Triethanolamine (TEA) (50 %)

TEA	10 mL
ddH_2O	10 mL

store at room temperature

8.1.10. QUANTIFICATION OF PROTEINS: BRADFORD ASSAY

BSA stock solution(0.5mg /mL)

BSA	0.5 mg/mL ddH'O

store at –20 °C

8.1.11. PREPARATION OF CELL HOMOGENATES

Lysis buffer

Tris 50mM	1.212 g
Na_2 EDTA $2H_2O$ 15 mM	1.116 g
NaCl 150 mM	0.438 g
Triton X-100 0.1%	200 µL
dd H2O	up to 200 mL

Adjust to pH 8.0
Store at 4°C

8.1.12. SEMI-QUANTITATIVE PROTEIN DETERMINATION

Isotonic Extraction Buffer 5x (IEB), ph 7.8

HEPES 50 mM	595.8 mg
sucrose 1.25 M	21.4 g
EGTA 5 mM	95.1 g
KCl 5 mM	465.9 mg
ddH_2O	up to 50 mL

Sterile filtration
Store at 4°C

Isotonic Extraction Buffer 1x

Dilute IEB 5x 1/5 with dd H2O

IEB 5x	100 µL
ddH_2O	400 µL

Add protease-inhibitor cocktail 0.1 % (v/v) just before use: 0.5 µL / 500 µL
Prepare freshly on the day of experiment
Keep on ice

Na-phosphate (NaPi-) buffer (50 mM), pH 7.6

$Na_2HPO_4 \cdot 2H_2O$ (1M)	42.25 mL
$NaH_2PO_4 \cdot H_2O$ (1M)	7.75 mL
dd H_2O	up to 1 L

8.1.13. SDS POLYACRYLAMIDE GEL ELECTROPHORESIS (SDS PAGE) AND IMMUNOBLOTTING

Electrophoresis buffer (10x)

Glycine 2M	720 g
Tris 250 mM	150 g
SDS (20% solution) 1% (v/v)	250 mL
ddH2O	up to 5L
Adjust to pH 8.4	

Tris/HCl (1.5 M)

Tris	18.2 g
ddH_2O	up to 100 mL
Adjust to pH 8.8	

Tris/HCl (0.5M)

Tris	6.1 g
ddH_2O	up to 100 mL
Adjust to pH 6.8	

Laemmli loading buffer (3x)

Tris/HCl (0.5 M, pH 6.8)	25 mL
SDS	0.62g
Glycerine	20 mL
Bromphenol blue	0.08 g
β-Mercaptoethanol	2.5 mL
ddH_2O	up to 100 mL
store at -20 °C	

Polyacrylamide gels

	Resolving gel (10%)	Stacking gel (4%)
Acrylamide (30%)	1.64 mL	0.25 mL
ddH2O	2.0 mL	1.2 mL
Tris (1.5 M, pH 8.8)	1.23 mL	-
Tris (0.5 M, pH 6.8)	-	0.5 mL
SDS (10 %)	49.2 µL	20 µL
APS (10 %)	24.6 µL	20 µL
TEMED	2.46 µL	2 µL

Blotting buffer

Glycine 39 M	5.8 g
Tris 48 mM	11.6 g
SDS (20% solution) 0.037%	3.75 mL
Methanol 20%	400 mL
ddH_2O	up to 2 L

TBS (20x)

NaCl 2.6 M	304 g
Tris/HCl 0.4 M	97 g
ddH2O	up to 2 L
Adjust to pH 7.4	

TBS-T (1x)

TBS 1x	2 L
Tween-20 0.3%	6 mL

Stripping buffer

Tris HCl (1M, pH 6.8) 62.5 mM	1.25 mL
SDS (20% solution) 2%	2 mL
β-mercaptoethanol 100 mM	142 µL
ddH_2O	up to 20 mL

Blocking buffer

TBS-T 1x	100 mL
Powdered milk 5%	5 g

Amido Black solution

Amido black 0.1% (v/v)	100 mg
Isopropanol 25% (v/v)	25 mL

Destaining solution

Isopropanol 25% (v/v)	25 mL
Acetic acid 10% (v/v)	10 mL
ddH_2O	up to 100 mL

8.1.14. TRANSIENT TRANSFECTION AND LUCIFERASE ACTIVITY

Reporter Lysis Buffer (RLB) 1x

RLB 5x	1 volume
ddH_2O	4 volumes

equilibrate 1x lysis buffer to room temperature before use
protect from light

Luciferase Assay Reagent

store at –80 °C
use at room temperature
protect from light

CPRG

CPRG	0.4 µL
$MgCl_2$ 100x	2 µL
Na-phosphate buffer 0.1 M	187.6 µL

Na-phosphate buffer 0.1 M

Na_2HPO_4 0.2M	41 mL
NaH_2PO_4	9 mL
ddH_2O	50 mL

8.1.15. COMET ASSAY (OXIDATIVE DNA DAMAGE)

If not indicated otherwise, all solutions for comet assay were prepared with autoclaved bidistilled water.

Lysis buffer, pH 10

NaCl	146.4 g (2.5 M)
Na2-EDTA	37.2 g (100 mM)
Tris	1.2 g (10 mM)
Adjust to pH 10	
NaOH	8.3 g
Na Lauryl Sarcosinate	10 g
ddH_2O	1 L

Store at 4 °C

Lysis solution

Lysis buffer	135 mL
DMSO	15 mL

Triton X-100	1.5 mL

Prepare freshly on the day of the experiment.

Denaturation and electrophoresis stock solutions

NaOH	40g/ 100mL (10N)
EDTA 2Na	7.4 g/ 100mL (200mM)

Store at room temperature

Denaturation and electrophoresis Buffer, pH13

NaOH 10nM	30 mL (300mM)
EDTA 2Na 200 mM	5 mL (1mM)
ddH2O	up to 1 litre

Prepare freshly on the day of the experiment with cold ddH2O.

Neutralization Buffer

Tris	48.5 g (0.4M)

Adjust to pH 7.5 with concentrated HCL

ddH_2O	up to 1 litre

store at 4 °C

Propidium iodide (PI) stock solution

DMSO	200 mg/mL

store at -20

PI working solution (5mg/L)

dilute stock solution 1/40 in ddH_2O

store at -20 °C

NMP Agarose (0.5 %) (w/v)

Agarose nMP	500mg
PBS w/o Ca and Mg	100mL

heat in microwave oven, maintain at 80 °C in a water bath to prepare nMP agarose layer

store at 4 °C

LMP agarose (0.7 %) (w/v)

LMP agarose	700mg
PBS w/o Ca_2+ and Mg_2+	100mL

heat in microwave, maintain at 37 °C in a water bath to prepare LMP agarose layer

store at 4 °C

FPG enzyme buffer stock solution (10x)

Hepes	95 g (400 mM)
KCl	74.6 g (1 M)
EDTA	1.96 g (5 mM)
BSA	2 g (2 mg/mL)
ddH_2O	up to 1L

adjust to pH 8 with KOH
store at -20 °C

FPG enzyme buffer (1x)

dilute buffer stock solution 1/10 with cold ddH_2O

FPG enzyme stock solution (100x)

dilute FPG 1x 1/100 with FPG enzyme buffer (1x) with addition of 10 % glycerol:

FPG enzyme 1x	10µL
glycerol	100µL
FPG enzyme buffer 1x	up to 1 mL

prepare aliquots of 25 µL or 40 µL
store at –80 °C
do not refreeze after thawing

FPG enzyme working solution (3000x)

dilute FPG aliquot (100x) 1/30 with enzyme buffer1x
keep on ice until added to the gels
do not refreeze working solution
keep at 4°C for 1 day

8.1.16. UNSCHEDULED DNA SYNTHESIS (UDS) ASSAY

Thymidine, [methyl] –3H
1 mCi /1 mL aqueous solution (37 MBq)
20.0 Ci /mmol (740 GBq/ mmol)
acitivity: 1µCi/µL

Lysis buffer, pH 8

Tris (10 mM)	0.06055 g
NaCL (40 mM)	1.1685 g
EDTA (1 mM)	0.1461 g
SDS (2 %)	10 g
Proteinase K (30 µg/mL)	15 mg
ddH_2O	up to 500 mL

add proteinase directly before experiment
store at 4°C

TCA 20%

TCA	20 g
ddH_2O	100 mL

Reagents	Distributors
Thymidine, [methyl] –3H-	Perkin Elmer
Trichloroacetic acid (TCA)	ICN Biochemicals
NaCL	Carl-Roth
SDS	Sigma, Applichem
Proteinase K	Sigma-Aldrich
Hydroxyurea	Sigma Aldrich
Ethanol p.a.	Merck
Microscint-O	Perkin Elmer

8.2. EQUIPMENT

Consumables/Equipment	Distributor
Camera Marlin F-046B	Allied Vision Technologies
Cannula Braunüle Vasocan 14G	B. Braun Melsungen AG
Centrifuge Beckman GS-6R	Beckmann, München
Centrifuge for microtubes Sigma 1K15	Sigma
Clean bench	Flow Laboratories, BDK
coplin jar	Fisher
Coulter Counter	Modell N Industry (Coulter Electronics LTD, Beds., England)
Eagle Eye II	Stratagene
Electrophoresis chamber (horizontal) Bio-Rad Sub cell GT Basic	Bio-Rad
Electrophoresis power supply Bio-Rad Power Pac 300	Bio-Rad
Filterholder (Alkal. Elution)	Swinnex SX 2500 (Millipore, Schwalbach)
Filters (Alkal. Elution)	Isopore Membranfilter, 2 cm, 25 mm, (Millipore, Schwalbach)
Filtration unit and vacuum pump	Millipore
Fluorescene microscope Axio II, c-0.5x	Zeiss
Fluorimeter	TKO 100, DNA Fluorimeter (Hoefer Scientific Instruments, San Francisco, USA)
Freezer	Liebherr
Frigerator	Liebherr
Hemocytometer	Carl-Roth
Homogenizer ultrasonic needle	B. Braun Melsungen AG
icycler	Bio-Rad
Immobilon-P Transfer (PVDF) membrane	Millipore
Incubator	Steri-Cult Incubator, Forma Scientific
Light Micrsoscope DM IRB	Leica
Lumi-Imager	Roche
Luminometer TopCountNT	Packard
Micro plate reader Fluoroscan Ascent FL,	Thermo Scientific, Labsystems
Micro plate reader MWG, Sirius HT injector	MWG
Microplate Scintillation and Luminescence Counter	TopCount NXT
Microplate spectrophotometer	MRX Dynex
Microscope Coverslide (24x24mm)	Menzel-Gläser
Microscope slides one side fully frosted (76x26 mm)	Menzel-Gläser
Omnifix-F 1mL	B. Braun Melsungen AG
pH-Meter 300	Beckman
Pipet aid	Hirschmann Laborgeräte
Pipettes (2.5, 10, 20, 100, 1000, 5000 µL)	Eppendorf, Gilson, Labnet
Power supply blotting: Power Pack P25	Biometra

Power supply SDS-PAGE: Mini Protean III Bio-Rad Power Pack	Bio-RAD
Pump BVP	Ismatec
Refrigerator at 4° C	Liebherr
Scales	Sartorius
Semi-Dry Blotter TE77	Hoefer
Shaker and incubator	Heidolph Titramax 100
Shaker S4	Elmi
Sterican 26G 0.45x12mm	B. Braun Melsungen AG
Sterile filters, 0,22 + 0,44 cm	Schleicher & Schüll, Dassel
Syringes (Alkal. Elution)	Becton Dickinson, Heidelberg
Thermoblock	Eppendorf
Thermostate T mA 6	Laudo, Dr. R. Wobser GmbH& Co. KG
Tubes for ultracentrifugation 2.0mL	Sarstedt
Ultracentrifuge Optima TL	Beckman
Water baths	Köttermann Labortechnik; Fisherbrand FBH 612

8.3. FIGURES

8.4. TABLES

8.5. REFERENCES

Arnaudeau S, Kelley W L, Walsh J V Jr., Demaurex N. (2001). Mitochondria recycle Ca2_ to the endoplasmic reticulum and prevent the depletion of neighboring endoplasmic reticulum regions. J. Biol. Chem. 276:29430–29439

Abdelrahim M, Smith R 3rd, Safe S. (2003). Aryl hydrocarbon receptor gene silencing with small inhibitory RNA differentially modulates Ah-responsiveness in MCF-7 and HepG2 cancer cells. Mol Pharmacol. 63(6):1373-81.

Adlercreutz H, Gorbach SL, Goldin BR, Woods MN, Dwyer JT, Hämäläinen E. (1994). Estrogen metabolism and excretion in Oriental and Caucasian women. J Natl Cancer Inst. 86(14):1076-82.

Agent Orange Association of Canada. http://www.agentorangecanada.com/stockholm.php (October 2009)

Agnez LF, Costa de Oliveira RL, Di Mascio P, Menck CF. (1996). Involvement of Escherichia coli exonuclease III and endonuclease IV in the repair of singlet oxygen-induced DNA damage. Carcinogenesis. 17(5):1183-5.

Ahlborg U G, Becking GC, Birnbaum LS, Brouwer A, Derks HJGM, Feeley M, Golog G, Hanberg A, Larsen JC, Liem AK et al. (1994). Toxic equivalency factors for dioxin-like PCBs: Report on WHO-ECEH and IPCS consultation. Chemosphere 28, 1049-1067.

Ahmad ME, Shadab GG, Hoda A, Afzal M. (2000). Genotoxic effects of estradiol-17beta on human lymphocyte chromosomes. Mutat Res.466(1):109-15.

Akerboom TPM and Sies H. (1981). Assay of glutathione, glutathione disulfide, and glutathione mixed disulfides in biological samples. Methods in Enzymology. 77: 373-382.

Alarid E T, Bakopoulos N, Solodin N. (1999). Proteasome-mediated proteolysis of estrogen receptor: a novel component in autologous downregulation.Mol. Endocrinol. 13:1522-1534.

Alia M, Ramos S, Mateos R, Bravo L, Goya L. (2005). Response of the antioxidant defense system to tert-butyl hydroperoxide and hydrogen peroxide in a human hepatoma cell line (HepG2). J Biochem Mol Toxicol. 19(2):119-28.

Alsharif NZ, Lawson T, Stohs SJ. (1994b). Oxidative stress induced by 2,3,7,8-tetrachlorodibenzo-p-dioxin is mediated by the aryl hydrocarbon (Ah) receptor complex. Toxicology. 92(1-3):39-51.

Alsharif NZ, Schlueter WJ, Stohs SJ. (1994a). Stimulation of NADPH-dependent reactive oxygen species formation and DNA damage by 2,3,7,8-tetrachlorodibenzo-p-dioxin in rat peritoneal lavage cells. Arch Environ Contam Toxicol. 26(3):392-7.

Althaus FR, Lawrence SD, Sattler GL, Longfellow DG, Pitot HC. (1982). Chemical quantification of unscheduled DNA synthesis in cultured hepatocytes as an assay for the rapid screening of potential chemical carcinogens. Cancer Res. 42(8):3010-5.

Anderson D, Dobrzyńska MM, Basaran N. (1997). Effect of various genotoxins and reproductive toxins in human lymphocytes and sperm in the Comet assay. Teratog Carcinog Mutagen. 17(1):29-43.

Anzenbacher P and Anzenbacherova E. (2001). Cytochromes P450 and metabolism of xenobiotics. Cell Mol Life Sci. 58:737-747

Aoki Y, Satoh K, Sato K, Suzuki KT. (1992). Induction of glutathione S-transferase P-form in primary cultured rat liver parenchymal cells by co-planar polychlorinated biphenyl congeners. Biochem J. 281 (Pt 2):539-43.

AppliChem Product Information. (2002). CheLuminate -HRP Pico Detect.

ATSDR. (1998). Toxicological Profile for Chlorinated Dibenzo-p-dioxins. Update. (Final report). NTIS Accesion No. PB99-121998. Atlanta, GA: Agency for Toxic Substances and Disease Registry. 729 pp.

Axelrod J and Tomchick R. (1958).Enzymatic O-methylation of epinephrine and other catechols. J. Biol. Chem. 233: 702-705

Axelrod J, Senoh S, Witkop B. (1958). O-Methylation of catechol amines in vivo. J Biol Chem. 233:697-701

Baker MA, Cerniglia GJ, Zaman A. (1990). Microtiter plate assay for the measurement of glutathione and glutathione disulfide in large numbers of biological samples. Anal Biochem. 190(2):360-5.

Ball P and Knuppen R. (1980). Catecholoestrogens (2-and 4-hydroxyoestrogens): chemistry, biogenesis, metabolism, occurrence and physiological significance. Acta Endocrinol Suppl (Copenh). 232:1-127.

Banduhn N and Obe G. (1985). Mutagenicity of methyl 2-benzimidazolecarbamate, diethylstilbestrol and estradiol: structural chromosomal aberrations, sister-chromatid exchanges, C-mitoses, polyploidies and micronuclei. Mutat Res. 156(3):199-218.

Barkhem T, Carlsson B, Nilsson Y, Enmark E, Gustafsson J-A, Nilsson S. (1998). Differential response of estrogen receptor a and estrogen receptor b to partial estrogen agonists/antagonists. Mol Pharmacol. 54:105-112.

Barnes DE, Lindahl T, Sedgwick B. (1993). DNA repair. Curr Opin Cell Biol. 5(3):424-33.

Barter RA and Klaassen CD. (1992). UDP-glucuronosyltransferase inducers reduce thyroid hormone levels in rats by an extrathyroidal mechanism. Toxicol Appl Pharmacol. 113(1):36-42.

Barth A, Landmann G, Liepold K, Zapf H, Müller D, Karge E, Klinger W. (1999). Influence of oestrogens on formation of reactive oxygen species in liver microsomes of differently aged male Wistar rats. Exp Toxicol Pathol. 51(4-5):282-8.

Barzilay G and Hickson ID. (1995). Structure and function of apurinic/apyrimidinic endonucleases. Bioessays. 17(8):713-9.

Bass DA, Parce JW, Dechatelet LR, Szejda P, Seeds MC, Thomas M.(1983). Flow cytometric studies of oxidative product formation by neutrophils: a graded response to membrane stimulation. J Immunol. 130:1910-7

Baum JK, Bookstein JJ, Holtz F, Klein EW. (1973). Possible association between benign hepatomas and oral contraceptives.Lancet. 2(7835):926-9.

Baumgart A, Schmidt M, Schmitz H-J, Schrenk D.(2005). Natural furocoumarins as inducers and inhibitors of cytochrome P450 1A1 in rat hepatocytes. Biochemical Pharmacology. 69: 657–667.

Becker-Follmann J and Baas D. (2004). PCR- Eine Methode, drei Schritte. BIOspektrum. 1:86.

Beckman KB and Ames BN. (1997). Oxidative decay of DNA. J Biol Chem. 272(32):19633-6.

Behr JP. (1996). L'éponge à protons: un moyen d'entrer dans une cellule auquel les virus n'ont pas pense´. Medecine/Sciences. 12: 56-59.

Beischlag TV and Perdew GH. (2005). ER alpha-AHR-ARNT protein-protein interactions mediate estradiol-dependent transrepression of dioxin-inducible gene transcription. J Biol Chem. 280(22):21607-11.

Beland FA, Dooley KL, Jackson CD. (1982). Persistence of DNA adducts in rat liver and kidney after multiple doses of the carcinogen N-hydroxy-2-acetylaminofluorene. Cancer Res. 42(4):1348-54.

Bellion P, Hofmann T, Pool-Zobel BL, Will F, Dietrich H, Knaup B, Richling E, Baum M, Eisenbrand G, Janzowski C. (2008). Antioxidant effectiveness of phenolic apple juice extracts and their gut fermentation products in the human colon carcinoma cell line caco-2. J Agric Food Chem. 56(15):6310-7

Bennett RA, Wilson DM 3rd, Wong D, Demple B. (1997). Interaction of human apurinic endonuclease and DNA polymerase beta in the base excision repair pathway. Proc Natl Acad Sci U S A. 94(14):7166-9.

Benzi G, Pastoris O, Marzatico F, Villa RF, Dagani F, Curti D. (1992). The mitochondrial electron-transfer alteration as a factor involved in the brain aging. Neurobiol Aging 13: 361-368.

Berry M, Metzger D, Chambon P. (1990). Role of the two activating domains of the oestrogen receptor in the cell-type and promoter context dependent agonistic activity of the anti-oestrogen 4-hydroxytamoxifen. EMBO J. 9:2811-2818.

Berthois Y, Katzenellenbogen JA, Katzenellenbogen BS. (1986). Phenol red in tissue culture media is a weak estrogen: implications concerning the study of estrogen-responsive cells in culture Proc Natl Acad Sci U S A. 83(8):2496-500.

Bertocci B, Miggiano V, Da Prada M, Dembic Z, Lahm HW, Malherbe P. (1991). Human catechol-O-methyltransferase: cloning and expression of the membrane-associated form. Proc Natl Acad Sci U S A. 88(4):1416-20.

Bhagwat M and Gerlt JA. (1996). 3'- and 5'-strand cleavage reactions catalyzed by the Fpg protein from Escherichia coli occur via successive beta- and delta-elimination mechanisms, respectively. Biochemistry. 35(2):659-65.

Bio-Rad (2006). Real-Time PCR Applications Guide. Bio-Rad Laboratories, Inc.

Bio-Rad. (1999). Protein Assay Technical Bulletin. Bio-Rad Laboratories, Inc.

Bissell DM and Guzelian PS. (1980). Phenotypic stability of adult rat hepatocytes in primary monolayer culture. Ann N Y Acad Sci. 349:85-98.

Bjeldanes LF, Kim JY, Grose KR, Bartholomew JC, Bradfield CA. (1991). Aromatic hydrocarbon responsiveness-receptor agonists generated from indole-3-carbinol in vitro and in vivo: comparisons with 2,3,7,8-tetrachlorodibenzo-p-dioxin. Proc Natl Acad Sci U S A. 88(21): 9543-7.

Blakey DC and White IN. (1985). Unscheduled DNA synthesis caused by norethindrone and related contraceptive steroids in short-term male rat hepatocyte cultures.Carcinogenesis. 6(8):1201-5.

Boiteux S and Radicella JP. (2000). The human OGG1 gene: structure, functions, and its implication in the process of carcinogenesis. Arch Biochem Biophys. 377(1):1-8.

Boiteux S, Gajewski E, Laval J, Dizdaroglu M. (1992). Substrate specificity of the Escherichia coli Fpg protein (formamidopyrimidine-DNA glycosylase): excision of purine lesions in DNA produced by ionizing radiation or photosensitization. Biochemistry. 31(1):106-10.

Bolton JL, Trush MA, Penning TM, Dryhurst G, Monks TJ. (2000). Role of quinones in toxicology. Chem Res Toxicol. 13(3):135-60

Bösterling B and Trudell JR. (1981). Spin trap evidence for production of superoxide radical anions by purified NADPH-cytochrome P-450 reductase. Biochem Biophys Res Commun. 98(2):569-75.

Bösterling B and Trudell JR. (1981). Spin trap evidence for production of superoxide radical anions by purified NADPH-cytochrome P-450 reductase. Biochem Biophys Res Commun. 98(2):569-75.

Boudjelal M, Wang Z, Voorhees JJ, Fisher GJ. (2000). Ubiquitin/ proteasome pathway regulates levels of retinoic acid receptor ? and retinoid X receptor ? in human keratinocytes. Cancer Res. 60:2247-2252

Bradford MM. (1976). A Rapid and Sensitive Method for the Quantitation of Microgram Quantities of Protein Utilizing the Principle of Protein-Dye Binding. Analytical Biochemistry. 72: 248-254.

Brake PB and Jefcoate CR. (1995). Regulation of cytochrome P4501B1 in cultured rat adrenocortical cells by cyclic adenosine 3',5'-monophosphate and 2,3,7,8- tetrachlorodibenzo-p-dioxin. Endocrinology. 136(11):5034-41

Brubacher JL and Bols NC. (2001). Chemically de-acetylated 29,79-dichlorodihydrofluorescein diacetate as a probe of respiratory burst activity in mononuclear phagocytes. Journal of Immunological Methods. 251: 81-91

Bruner SD, Norman DP, Verdine GL. (2000). Structural basis for recognition and repair of the endogenous mutagen 8-oxoguanine in DNA. Nature. 403(6772):859-66.

Burke MD and Mayer RT. (1974). Ethoxyresorufin: Direct fluorimetric assay of a microsomal O-dealkylation which is preferentially inducible by 3-methylcholanthrene. Drug Metab Dispos. 2:583-588

Butterworth BE, Smith-Oliver T, Earle L, Loury DJ, White RD, Doolittle DJ, Working PK, Cattley RC, Jirtle R, Michalopoulos G, et al. (1989). Use of primary cultures of human hepatocytes in toxicology studies. Cancer Res. 49(5):1075-84.

Cabaton N, Dumont C, Severin I, Perdu E, Zalko D, Cherkaoui-Malki M, Chagnon MC. (2009). Genotoxic, endocrine activities of bis(hydroxyphenyl)methane (Bisphenol F) and its derivatives in the HepG2 cell line. Toxicology. 255:15-24.

Cadet J, Bellon S, Berger M, Bourdat AG, Douki T, Duarte V, Frelon S, Gasparutto D, Muller E, Ravanat JL, Sauvaigo S. (2002). Recent aspects of oxidative DNA damage: guanine lesions, measurement and substrate specificity of DNA repair glycosylases. Biol Chem. 383(6):933-43.

Cadet J, Berger M, Douki T, Ravanat JL. (1997). Oxidative damage to DNA: formation, measurement, and biological significance. Rev Physiol Biochem Pharmacol. 131:1-87.

Cadet J, Bourdat AG, D'Ham C, Duarte V, Gasparutto D, Romieu A, Ravanat JL. (2000). Oxidative base damage to DNA: specificity of base excision repair enzymes. Mutat Res. 462(2-3):121-8.

Cavalieri E, Chakravarti D, Guttenplan J, Hart E, Ingle J, Jankowiak R, Muti P, Rogan E, Russo J, Santen R, Sutter T. (2006). Catechol estrogen quinones as initiators of breast and other human cancers: implications for biomarkers of susceptibility and cancer prevention. Biochim Biophys Acta. 1766(1):63-78.

Cavalieri E, Frenkel K, Liehr JG, Rogan E, Roy D. (2000). Estrogens as endogenous genotoxic agents-DNA adducts and mutations. J Natl Cancer Inst Monogr (27):75-93.

Cavalieri E, Frenkel K, Liehr JG. (2000). Chapter 4: Estrogens as Endogenous Genotoxic Agents-DNA Adducts and Mutations. J Natl Cancer Inst Monogr. 27:75-93

Cavalieri EL, Stack DE, Devanesan PD, Todorovic R, Dwivedy I, Higginbotham S, Johansson SL, Patil KD, Gross ML, Gooden JK, Ramanathan R, Cerny RL, Rogan EG. (1997). Molecular origin of cancer: Catechol estrogen-3,4-quinones as endogenous tumor initiators Proc Natl Acad Sci U S A. 94(20):10937-42.

Cerutti P, Ghosh R, Oya Y, Amstad P. (1994). The role of the cellular antioxidant defense in oxidant carcinogenesis. Environ Health Perspect. 102 Suppl 10:123-9.

Chaffin CL, Peterson RE, Hutz RJ. (1996). In utero and lactational exposure of female Holtzman rats to 2,3,7,8-tetrachlorodibenzo-p-dioxin: modulation of the estrogen signal. Biol Reprod. 55(1):62-7.

Chang CY and Puga A. (1998). Constitutive activation of the aromatic hydrocarbon receptor. Mol Cell Biol. 18(1):525-35.

Charles River Laboratories, http://info.criver.com/research_models_and_services/research_models/index.html (May 2009)

Chen ZH, Hurh YJ, Na HK, Kim JH, Chun YJ, Kim DH, Kang KS, Cho MH, Surh YJ. (2004). Resveratrol inhibits TCDD-induced expression of CYP1A1 and CYP1B1 and catechol estrogen-mediated oxidative DNA damage in cultured human mammary epithelial cells. Carcinogenesis. 25(10):2005-2013.

Cheng KC, Cahill DS, Kasai H, Nishimura S, Loeb LA. (1992). 8-Hydroxyguanine, an abundant form of oxidative DNA damage, causes G----T and A----C substitutions. J Biol Chem. 267(1):166-72.

Cheng Z, Rios GR, King CD, Coffman BL, Green MD, Mojarrabi B, Mackenzie PI, Tephly TR.(1998). Glucuronidation of catechol estrogens by expressed human UDP-glucuronosyltransferases (UGTs) 1A1, 1A3, and 2B7. Toxicol Sci. 45(1):52-7.

Ciolino HP, Daschner PJ, Wang TT, Yeh GC. (1998). Effect of curcumin on the aryl hydrocarbon receptor and cytochrome P450 1A1 in MCF-7 human breast carcinoma cells. Biochem Pharmacol. 56(2):197-206.

Ciolino HP, Daschner PJ, Yeh GC. (1999). Dietary flavonols quercetin and kaempferol are ligands of the aryl hydrocarbon receptor that affect CYP1A1 transcription differentially. Biochem J. 340:715-22.

Clayson DB, Mehta R, Iverson F. (1994). International Commission for Protection Against Environmental Mutagens and Carcinogens. Oxidative DNA damage--the effects of certain genotoxic and operationally non-genotoxic carcinogens. Mutat Res. 317(1):25-42.

Clemons M and Goss P. (2001). Estrogen and the risk of breast cancer. N Engl J Med. 344(4):276-85.

Colditz GA, Hankinson SE, Hunter DJ, Willett WC, Manson JE, Stampfer MJ, Hennekens C, Rosner B, Speizer FE. (1995). The use of estrogens and progestins and the risk of breast cancer in postmenopausal women. N Engl J Med. 332(24):1589-93.

Collins AR, Dobson VL, Dusinská M, Kennedy G, Stětina R. (1997). The comet assay: what can it really tell us? Mutat Res. 375(2):183-93.

Collins AR, Dusinska M, Gedik CM, Stetina R. (1996). Oxidative damage to DNA: Do we have a reliable biomarker? Environ Health Prospect. 104 (S3):465- 469.

Collins AR, Dusinská M, Horská A. (2001). Detection of alkylation damage in human lymphocyte DNA with the comet assay. Acta Biochim Pol. 48(3):611-4.

Collins AR, Dusinská M. (2002). Oxidation of cellular DNA measured with the comet assay. Methods Mol Biol. 186:147-59.

Collins AR, Duthie SJ, Dobson VL. (1993). Direct enzymic detection of endogenous oxidative base damage in human lymphocyte DNA. Carcinogenesis. 14(9):1733-5.

Collins AR, Mitchell DL, Zunino A, de Wit J, Busch D. (1997). UV-sensitive rodent mutant cell lines of complementation groups 6 and 8 differ phenotypically from their human counterparts. Environ Mol Mutagen. 29(2):152-60.

Collins AR, Oscoz AA, Brunborg G, Gaivão I, Giovannelli L, Kruszewski M, Smith CC, Stetina R. (2008). The comet assay: topical issues. Mutagenesis. 23(3):143-51.

Collins AR. (1999). Oxidative DNA damage, antioxidants, and cancer. Bioessays. 21(3):238-46.

Collins AR. (2004). The comet assay for DNA damage and repair: principles, applications, and limitations. Mol Biotechnol. 26(3):249-61.

Comet assay forum. www.cometassayindia.org (January 2009).

Compton SJ and Jones CG. (1985). Mechanism of Dye Response and Interference in the Bradford Protein Assay. Anal. Biochem. 151: 369.

Conner EM and Grisham MB.(1996). Inflammation, free radicals, and antioxidants. Nutrition. 12(4):274-277.

Cooke MS, Evans MD, Dizdaroglu M, Lunec J. (2003). Oxidative DNA damage: mechanisms, mutation, and disease. FASEB J. 17(10):1195-214.

Coumoul X, Diry M, Robillot C, Barouki R. (2001). Differential regulation of cytochrome P450 1A1 and 1B1 by a combination of dioxin and pesticides in the breast tumor cell line MCF-7. Cancer Res. 61(10):3942-8.

Croci T and Williams GM. (1985). Activities of several phase I and phase II xenobiotic biotransformation enzymes in cultured hepatocytes from male and female rats. Biochem Pharmacol. 34(17):3029-35.

Dace A, Zhao L, Park KS, Furuno T, Takamura N, Nakanishi M, West BL, Hanover JA., Cheng S. (2000). Hormone binding induces rapid proteasome-mediated degradation of thyroid hormone receptors. Proc. Natl. Acad. Sci. USA 97:8985-8990.

Dallner G and Ernster L. (1968). Subfractionation and composition of microsomal membranes: a review. J Histochem Cytochem. 16:611-632.

Dallner G. (1974). Isolation of rough and smooth microsomes - General. Methods in Enzymol. 31:191-201

Dalton TP, Chen Y, Schneider SN, Nebert DW, Shertzer HG. (2004). Genetically altered mice to evaluate glutathione homeostasis in health and disease. Free Radic Biol Med. 37(10):1511-26.

Davarinos NA, Pollenz RS. (1999). Aryl hydrocarbon receptor imported into the nucleus following ligand binding is rapidly degraded via the cytosplasmic proteasome following nuclear export. J. Biol. Chem. 274:28708-28715.

Davies KJ. (1999). The broad spectrum of responses to oxidants in proliferating cells: a new paradigm for oxidative stress. IUBMB Life. 48(1):41-7.

Dawling S, Roodi N, Mernaugh RL, Wang X, Parl FF. (2001). Catechol-O-methyltransferase (COMT)-mediated metabolism of catechol estrogens: comparison of wild-type and variant COMT isoforms. Cancer Res. 61(18):6716-22.

De Fries R and Mistuhashi M. (1995). Quantification of mitogen induced human lymphocyte proliferation: comparison of Alamar Blue assay to 3H-thymidine incorporation assay. J Clin Lab Anal. 9:89-95.

DeLeve LD and Kaplowitz N. (1991). Glutathione metabolism and its role in hepatotoxicity. Pharmacol Ther. 52(3):287-305.

Della Porta G, Dragani TA, Sozzi G. (1987). Carcinogenic effects of infantile and long-term 2,3,7,8-tetrachlorodibenzo-p-dioxin treatment in the mouse. Tumori. 73(2):99-107.

Denison MS and Heath-Pagliuso S. (1998). The Ah Receptor: A regulator of the Biochemical and Toxicological Actions of Structurally Diverse Chemicals. Bull Environ Contam Toxicol. 61:557-568

Denison MS and Nagy SR. (2003). Activation of the aryl hydrocarbon receptor by structurally diverse exogenous and endogenous chemicals. Annu Rev Pharmacol Toxicol. 43:309-34.

DePaolo LV and Masoro EJ. (1989). Endocrine Hormones in Laboratory Animals. In The Clinical Chemistry of Laboratory Animals. Eds. W. Loeb and F. Quimby. New York: Pergamon Press.

Deterding LJ, Prasad R, Mullen GP, Wilson SH, Tomer KB. (2000). Mapping of the 5'-2-deoxyribose-5-phosphate lyase active site in DNA polymerase beta by mass spectrometry.J Biol Chem. 275(14):10463-71.

Dhillon VS and Dhillon IK. (1995). Genotoxicity evaluation of estradiol. Mutat Res. 345(1-2):87-95.

Di Monte D, Ross D, Bellomo G, Eklöw L, Orrenius S. (1984). Alterations in intracellular thiol homeostasis during the metabolism of menadione by isolated rat hepatocytes. Arch Biochem Biophys. 235(2):334-42.

Diamond L, Kruszewski F, Aden DP, Knowles BB, Baird WM. (1980). Metabolic activation of benzo[a]pyrene by a human hepatoma cell line. Carcinogenesis. 1(10):871-5.

Dianov GL, Prasad R, Wilson SH, Bohr VA. (1999). Role of DNA polymerase beta in the excision step of long patch mammalian base excision repair. J Biol Chem. 274(20):13741-3.

Dizdaroglu M, Jaruga P, Birincioglu M, Rodriguez H. (2002). Free radical-induced damage to DNA: mechanisms and measurement. Free Radic Biol Med. 32(11):1102-15.

Donato MT, Gomez-Lechon MJ, Castell JV. (1993). A Microassay for Measuring Cytochrme P4501A1 and P4502B1 Activities in Intact Human and Rat Hepatocytes Cultured on 96-Well Plates. Analytical Biochemistry.213:29-33

Doostdar H, Burke MD, Mayer RT. (2000). Bioflavonoids: selective substrates and inhibitors for cytochrome P450 CYP1A and CYP1B1. Toxicology. 144(1-3):31-8.

Doostdar H, Demoz A, Burke MD, Melvin WT, Grant MH. (1990). Variation in drug-metabolizing enzyme activities during the growth of human Hep G2 hepatoma cells. Xenobiotica. 20(4):435-41.

Doostdar H, Duthie SJ, Burke MD, Melvin WT, Grant MH. (1988). The influence of culture medium composition on drug metabolising enzyme activities of the human liver derived HepG2 cell line. FEBS. 241: 15-18

Dragan YP and Schrenk D. (2000). Animal studies addressing the carcinogenicity of TCDD (or related compounds) with an emphasis on tumour promotion. Food Addit Contam. 17(4):289-302.

Dragan YP, Xu XH, Goldsworthy TL, Campbell HA, Maronpot RR, Pitot HC. (1992). Characterization of the promotion of altered hepatic foci by 2,3,7,8-tetrachlorodibenzo-p-dioxin in the female rat. Carcinogenesis. 13(8):1389-95.

Drevon C, Piccoli C, Montesano R. (1981). Mutagenicity assays of estrogenic hormones in mammalian cells. Mutat Res. 89(1):83-90.

DSMZ GmbH. http://www.dsmz.de (February 2009)

Du¸sinská, M. and Collins, A. (1996) Detection of oxidised purines and UV-induced photoproducts in DNA of single cells, by inclusion of lesion-specific enzymes in the comet assay. Altern. Lab. Anim. 24:405-411.

Duan R, Porter W, Samudio I, Vyhlidal C, Kladde M, Safe S. (1999). Transcriptional activation of c-fos protooncogene by 17beta-estradiol: mechanism of aryl hydrocarbon receptor-mediated inhibition. Mol Endocrinol. 13(9):1511-21.

Duncan T, Trewick SC, Koivisto P, Bates PA, Lindahl T, Sedgwick B. (2002). Reversal of DNA alkylation damage by two human dioxygenases. Proc Natl Acad Sci U S A. 99(26):16660-5.

Edwards RJ, Singleton AM, Murray BP, Sesardic D, Rich KJ, Davies DS, Boobis AR. (1990). An anti-peptide antibody targeted to a specific region of rat cytochrome P-450IA2 inhibits enzyme activity. Biochem J. 1990 Mar 1;266(2):497-504.

Eisenbrand G and Metzler M. (2002). Toxikologie für Natruwissenschaftler und Mediziner- Stoffe, Mechanismen, Prüfverfahren. Wiley VCH Verlag GmbH, Weinheim, Germany. 2nd edition

El Khissiin A and Leclercq G. (1999). Implication of proteasome in estrogen receptor degradation. FEBS Lett. 448:160-166.

Eldridge SR, Gould MN, Butterworth BE. (1992). Genotoxicity of environmental agents in human mammary epithelial cells. Cancer Res. 52(20):5617-21.

Emons G, Merriam GR, Pfeiffer D, Loriaux DL, Ball P, Knuppen R. (1987). Metabolism of exogenous 4- and 2-hydroxyestradiol in the human male. J Steroid Biochem. 28(5):499-504.

Epe B and Hegler J. (1994). Oxidative DNA damage: endonuclease fingerprinting. Methods Enzymol. 234:122-131

Epe B, Pflaum M, Häring M, Hegler J, Rüdiger H. (1993). Use of repair endonucleases to characterize DNA damage induced by reactive oxygen species in cellular and cell-free systems. Toxicol Lett. 67(1-3):57-72.

Epe B. (1996). DNA damage profiles induced by oxidizing agents. Rev Physiol Biochem Pharmacol. 1996;127:223-49.

Epe B. (2002). Role of endogenous oxidative DNA damage in carcinogenesis: what can we learn from repair-deficient mice? Biol Chem. 383(3-4):467-75.

ESCODD (European Standards Committee on Oxidative DNA Damage). (2002). Comparative analysis of baseline 8-oxo-7,8-dihydroguanine in mammalian cell DNA, by different methods in different laboratories: an approach to consensus. Carcinogenesis. 23 (12): 2129-2133

Eurogentec. (2007). QPCR Guide.

Fairbairn DW, Olive PL, O'Neill KL. 1995. The Comet assay: a comprehensive review. Mutat Res 339:37-59

Falbe J and Regitz M. (1995). Römpp Chemie Lexikon, 9. Auflage. G. Thieme Verlag Stuttgart New York.

Fautz R, Forster R, Hechenberger CM, Hertner T, von der Hude W, Kaufmann G, Madle H, Madle S, Miltenburger HG, Müller L, et al. (1991). Report of a comparative study of DNA damage and repair assays in primary rat hepatocytes with five coded chemicals. Mutat Res. 260(3):281-94.

Felgner PL, Gadek TR, Holm M, Richard R, Chan HW, Wenz M,Northrop JP, Ringold GM, Danielsen M. (1987). Lipofection: A highly efficient, lipid-mediated DNA-transfection procedure. Proc. Nati. Acad. Sci. USA. 84:7413-7417.

Fermentas Brochure. (2007). ExGen 500 Universal Transfection Reagent.

Fermentas Certificate of Analysis. (2004).ExGen 500 in vitro Transfection Reagent.

Ferrari S, Moro E, Pettenazzo, Behr JP, Zacchello F, Scarpa M.(1997). ExGen 500 is an efficient vector for gene delivery to lung epithelial cells in vitro and in vivo. Gene Therapy. 4:1100-1106.

Feser W, Kerdar RS, Blode H, Reimann R. (1996). Formation of DNA-adducts by selected sex steroids in rat liver. Hum Exp Toxicol. 15(7):556-62.

Forth W, Henschler D, Rummel W. (2005). Allgemeine und spezielle Pharmakologie und Toxikologie. Urban & Fischer Verlag, Elsevier GmbH, München, Germany. 9th edition

Fortini P, Parlanti E, Sidorkina OM, Laval J, Dogliotti E. (1999). The type of DNA glycosylase determines the base excision repair pathway in mammalian cells. J Biol Chem. 274(21):15230-6.

Fotsis T, Zhang Y, Pepper MS, Adlercreutz H, Montesano R, Nawroth PP, Schweigerer L. (1994). The endogenous oestrogen metabolite 2-methoxyoestradiol inhibits angiogenesis and suppresses tumour growth. Nature. 368(6468):237-9.

Fridovich I. (1995). Superoxide radical and superoxide dismutases. Annu Rev Biochem. 64:97-112

Gallagher EP, Kavanagh TJ, Eaton DL. (1994). Glutathione, oxidized Glutathione, and Mixed Disulfides in Biological Samples. Methods in Toxicology. 1b: 349-366.

Garland CF, Friedlander NJ, Barrett-Connor E, Khaw KT. (1992). Sex hormones and postmenopausal breast cancer: a prospective study in an adult community. Am J Epidemiol. 135(11):1220-30.

Gedik CM, Ewen SWB, Collins AR. (1992). Single-cell gel electrophoresis applied to the analysis of UV-C damage and its repair in human cells. Int J Radiat Biol. 62:313-320.

Gerstner S, Glasemann D, Pfeiffer E, Metzler M. (2008). The influence of metabolism on the genotoxicity of catechol estrogens in three cultured cell lines. Mol Nutr Food Res. 52(7):823-9.

Giannone JV, Li W, Probst M, Okey AB. (1998). Prolonged depletion of AH receptor without alteration of receptor mRNA levels after treatment of cells in culture with 2,3,7,8-tetrachlorodibenzo-p-dioxin. Biochem Pharmacol. 55(4):489-97.

Gierthy JF, Lincoln DW, Gillespie MB, Seeger JI, Martinez HL, Dickerman HW, Kumar SA. (1987). Suppression of estrogen-regulated extracellular tissue plasminogen activator activity of MCF-7 cells by 2,3,7,8-tetrachlorodibenzo-p-dioxin. Cancer Res. 47(23):6198-203.

Gillesby BE, Stanostefano M, Porter W, Safe S, Wu ZF, Zacharewski TR. (1997). Identification of a motif within the 5' regulatory region of pS2 which is responsible for AP-1 binding and TCDD-mediated suppression.Biochemistry. 36(20):6080-9.

Glickman MH AND Cichanover A. (2002). The Ubiquitin-Proteasome Proteolytic Pathway: Destruction for the Sake of Construction. Physiol Rev. 82: 373-428

Glutathione and Glutathione Disulfide in Large Numbers of Biological Samples. Analytical Biochemistry. 190: 360-365

Gonzalez FJ and Gelboin HV. (1994). Role of human cytochromes P450 in the metabolic activation of chemical carcinogens and toxins. Durg Metab Rev. 26:165-183

Goodman JE, Jensen LT, He P, Yager JD. (2002). Characterization of human soluble high and low activity catechol-O-methyltransferase catalyzed catechol estrogen methylation. Pharmacogenetics. 12(7):517-28.

Gradelet S, Astorg P, Leclerc J, Chevalier J, Vernevaut MF, Siess MH. (1996). Effects of canthaxanthin, astaxanthin, lycopene and lutein on liver xenobiotic-metabolizing enzymes in the rat. Xenobiotica. 26(1):49-63.

Grant MH, Duthie SJ, Gray AG, Burke MD. (1988). Mixed function oxidase and UDP-glucuronyltransferase activities in the human Hep G2 hepatoma cell line. Biochem Pharmacol. 37(21):4111-6.

Grant MH, Melvin MAI, Shaw P, Melvin WT, Burke MD. (1985). Studies on the maintenance of cytochromes P-450 and b5, monooxygenases and cytochrome reductases in primary cultures of rat hepatocytes. FEBS Lett. 190(1):99-103.

Greenwald P, Caputo TA, Wolfgang PE. (1977). Endometrial cancer after menopausal use of estrogens. Obstet Gynecol. 50(2):239-43.

Griffith OW. (1980). Determination of Glutathione and Glutathione Disulfide Using glutathione reductase and 2-Vinylpyridine. Anal. Biochem. 106:207-212.

Grossman MH, Creveling CR, Rybczynski R, Braverman M, Isersky C, Breakefield XO. (1985). Soluble and particulate forms of rat catechol-O-methyltransferase distinguished by gel electrophoresis and immune fixation. J Neurochem. 44(2):421-32.

Hachey DL, Dawling S, Roodi N, Parl FF. (2003). Sequential action of phase I and II enzymes cytochrome p450 1B1 and glutathione S-transferase P1 in mammary estrogen metabolism. Cancer Res. 63(23):8492-9.

Hall JM, Couse JF, Korach KS. (2001). The Multifaceted Mechanisms of Estradiol and Estrogen Receptor Signaling The Journal Of Biological Chemistry. 276(40): 36869-36872

Halliwell B and Gutteridge JMC. (1999). Free Radicals in Biology and Medicine. Oxford University Press, Oxford, New York. 3rd edition.

Han X and Liehr JG. (1994). 8-Hydroxylation of guanine bases in kidney and liver DNA of hamsters treated with estradiol: role of free radicals in estrogen-induced carcinogenesis. Cancer Res. 54(21):5515-7.

Hankinson O. (1995). The aryl hydrocarbon receptor complex. Annu Rev Pharmacol Toxicol. 35:307-340.

Harris M, Zacharewski T, Safe S.(1990). Effects of 2,3,7,8-tetrachlorodibenzo-p-dioxin and related compounds on the occupied nuclear estrogen receptor in MCF-7 human breast cancer cells. Cancer Res. 50(12):3579-84.

Hartwig A and Schwerdtle T. (2002). Interactions by carcinogenic metal compounds with DNA repair processes: toxicological implications. Toxicol Lett. 127(1-3):47-54.

Hartwig A, Dally H, Schlepegrell R. (1996). Sensitive analysis of oxidative DNA damage in mammalian cells: use of the bacterial Fpg protein in combination with alkaline unwinding. Toxicol Lett. 88(1-3):85-90.

Hasspieler B, Haffner D, Stelljes M, Adeli K. (2006). Toxicological assessment of industrial solvents using human cell bioassays: assessment of short-term cytotoxicity and long-term genotoxicity potential. Toxicology and Industrial Health.22: 301-315

Hayashi N, Hasegawa K, Komine A, Tanaka Y, McLachian JA, Barrett JC, Tsutsui T. (1996). Estrogen-induced cell transformation and DNA adduct formation in cultured Syrian hamster embryo cells. Mol Carcinog. 16(3):149-56.

Hayes CL, Spink DC, Spink BC, Cao JQ, Walker NJ, Sutter TR. (1996). 17 beta-estradiol hydroxylation catalyzed by human cytochrome P450 1B1. Proc Natl Acad Sci U S A. 93(18):9776-81.

Health Protection Agency. http://www.hpacultures.org.uk/collections/ecacc.jsp (October, 2009).

Heath-Pagliuso S, Rogers WJ, Tullis K, Seidel SD, Cenijn PH, Brouwer A, Denison MS. (1998). Activation of the Ah receptor by tryptophan and tryptophan metabolites. Biochemistry. 37(33):11508-15

Heine T, Glatt H, Epe B. (2006). Human cytochrome P450 reductase can act as a source of endogenous oxidative DNA damage and genetic instability. Free Radic Biol Med. 40(5):801-7.

Henderson LM and Chappell JB. (1993). Dihydrorhodamine 123: a fluorescent probe for superoxide generation? Eur J Biochem. 217(3):973-80.

Hengstler JG, Utesch D, Steinberg P, Platt KL, Diener B, Ringel M, Swales N, Fischer T, Biefang K, Gerl M, Böttger T, Oesch F. (2000). Cryopreserved primary hepatocytes as a constantly available in vitro model for the evaluation of human and animal drug metabolism and enzyme induction. Drug Metab Rev. 32: 81-118.

Highman B, Greenman DL, Norvell MJ, Farmer J, Shellenberger TE. (1980). Neoplastic and preneoplastic lesions induced in female C3H mice by diets containing diethylstilbestrol or 17 beta-estradiol. J Environ Pathol Toxicol. 4(5-6):81-95.

Highman B, Roth SI, Greenman DL. (1981). Osseous changes and osteosacomas in mice continuously fed diets containing diethylstilbestrol or 17 beta-estradiol. J Natl Cancer Inst. 67(3):653-62.

Ho PW, Garner CE, Ho JW, Leung KC, Chu AC, Kwok KH, Kung MH, Burka LT, Ramsden DB, Ho SL. (2008). Estrogenic phenol and catechol metabolites of PCBs modulate catechol-O-methyltransferase expression via the estrogen receptor: potential contribution to cancer risk. Curr Drug Metab. 9(4):304-9.

Hoivik D, Willett K, Wilson C, Safe S. (1997). Estrogen does not inhibit 2,3,7, 8-tetrachlorodibenzo-p-dioxin-mediated effects in MCF-7 and Hepa 1c1c7 cells. J Biol Chem. 272(48):30270-4.

Hoivik D, Wilson C, Wang W, Willett K, Barhoumi R, Burghardt R, Safe S. (1997b). Studies on the relationship between estrogen receptor content, glutathione S-transferase pi expression, and induction by 2,3,7,8-tetrachlorodibenzo-p-dioxin and drug resistance in human breast cancer cells. Arch Biochem Biophys. 348(1):174-82.

Holland PM, Abramson RD, Watson R, Gelfand DH. (1991). Detection of specific polymerase chain reaction product by utilizing the 5' - 3' exonuclease activity of Thermus aquaticus DNA polymerase. Proc Natl Acad Sci USA. 88:7276.

Howell SJ, Johnston SRD, Howell A. (2004). The use of selective estrogen receptro modulators ans selective estrogen receptor down-regulators in breast cancer. Best Practice & Research Clinical Endocrinology & Metabolism. 18: 47-66

Huff J, Lucier G, Tritscher A. (1994). Carcinogenicity of TCDD: experimental, mechanistc, and epidemiologic evidence. Annu Rev Pharmacol Toxicol. 34:343-372.

Huseby RA. (1980). Demonstration of a direct carcinogenic effect of estradiol on Leydig cells of the mouse. Cancer Res. 40(4):1006-13.

IARC Monographs on the Evaluation of Carcinogenic Risks to Humans. (1987). Overall Evaluations of Carcinogenicity: An Updating of IARC Monographs Volumes 1-42. Supplement No. 7, 284

IARC Monographs on the Evaluation of Carcinogenic Risks to Humans. (1997). Polychorinated dibenzo-para-dioxins and polychlorinated dibenzofurans. Volume 69

IARC Monographs on the Evaluation of Carcinogenic Risks to Humans. (1999). Hormonal Contraception and Postmenopausal Hormonal Therapy. Volume 72, 399

ICH (Internatioanl conference on harmonisation of technical requirements for registration of pharmaceuticals for human use). (2008). Guidance on Genotoxicity Testing and Data Interpretation for Pharmaceuticals Intended for Human Use-S2 (R1). Current step 2 version. EMEA/CHMP/ICH/126642/2008

Ingelman-Sundberg M and Johansson I. (1984). Mechanisms of hydroxyl radical formation and ethanol oxidation by ethanol-inducible and other forms of rabbit liver microsomal cytochromes P-450. J Biol Chem. 259(10):6447-58.

Irving CC. (1975). Comparative toxicity of N-hydroxy-2-acetylaminofluorene in several strains of rats. Cancer Res. 35(11 Pt 1):2959-61.

Iwanari M, Nakajima M, Kizu R, Hayakawa K, Yokoi T. (2002). Induction of CYP1A1, CYP1A2, and CYP1B1 mRNAs by nitropolycyclic aromatic hydrocarbons in various human tissue-derived cells: chemical-, cytochrome P450 isoform-, and cell-specific differences. Arch Toxicol. 76(5-6):287-98.

Jana NR, Sarkar S, Ishizuka M, Yonemoto J, Tohyama C, Sone H. (1999). Role of estradiol receptor-alpha in differential expression of 2,3,7, 8-tetrachlorodibenzo-p-dioxin-inducible genes in the RL95-2 and KLE human endometrial cancer cell lines. Arch Biochem Biophys. 368(1):31-9.

Jana NR, Sarkar S, Ishizuka M, Yonemoto J, Tohyama C, Sone H. (2000). Comparative effects of 2,3,7,8-tetrachlorodibenzo-p-dioxin on MCF-7, RL95-2, and LNCaP cells: role of target steroid hormones in cellular responsiveness to CYP1A1 induction. Mol Cell Biol Res Commun. 4(3):174-80.

Järvinen TA, Pelto-Huikko M, Holli K, Isola J. (2000). Estrogen receptor beta is coexpressed with ERalpha and PR and associated with nodal status, grade, and proliferation rate in breast cancer. Am J Pathol. 156(1):29-35.

Jeffery DR and Roth JA. (1984).Characterization of membrane-bound and soluble catechol-O-methyltransferase from human frontal cortex. J Neurochem. 42(3):826-32.

Jeng MH, Shupnik MA, Bender TP, Westin EH, Bandyopadhyay D, Kumar R, Masamura S, Santen RJ. (1998). Estrogen receptor expression and function in long-term estrogen-deprived human breast cancer cells. Endocrinology. 139(10):4164-74.

Jin DQ, Jung JW, Lee YS, Kim JA. (2004). 2,3,7,8-Tetrachlorodibenzo-p-dioxin inhibits cell proliferation through arylhydrocarbon receptor-mediated G1 arrest in SK-N-SH human neuronal cells. Neurosci Lett. 363(1):69-72.

Joosten HF, van Acker FA, van den Dobbelsteen DJ, Horbach GJ, Krajnc EI. (2004). Genotoxicity of hormonal steroids. Toxicol Lett. 151(1):113-34.

Kang YK, Guermah M, Yuan CX, Roeder RG. (2002). The TRAP/Mediator co-activator complex interacts directly with estrogen receptors alpha and beta through the TRAP220 subunit and directly enhances estrogen receptor function in vitro. Proc Natl Acad Sci U S A. 99(5):2642-7.

Kasper P, Uno Y, Mauthe R, Asano N, Douglas G, Matthews E, Moore M, Mueller L, Nakajima M, Singer T, Speit G; IWGT Workgroup. (2007). Follow-up testing of rodent carcinogens not positive in the standard genotoxicity testing battery: IWGT workgroup report. Mutat Res. 627(1):106-16. Epub 2006 Nov 22.

Kato S, Endoh H, Masuhiro Y, Kitamoto T, Uchiyama S, Sasaki H, Masushige S, Gotoh Y, Nishida E, Kawashima H, Metzger D, Chambon P. (1995). Activation of the estrogen receptor through phosphorylation by mitogen-activated protein kinase. Science. 270(5241):1491-4.

Kelley, M. K., Engqvist-Goldstein, A., Montali, J. A., Wheatley, J. B., Schmidt, D. E., Jr., and Kauvar, L. M. (1994) Variability of glutathione S-transferase isoenzyme patterns in matched normal and cancer human breast tissue. Biochem. J., 304: 843-848

Kelly SA, Havrilla CM, Brady TC, Abramo KH, Levin ED. (1998). Oxidative Stress in Toxicology: Established Mammalian and Emerging Piscine Model Systems. Env Health Perspec. 106 (7): 375-384

Kennedy SW and Jones SP. (1994). Simultaneous Measurement of Cytochrome P4501A Catalytic Activity and Total Protein Concentration with a Fluorescence Plate Reader. Analytical Biochemistry. 222:217-223

Kennedy SW, Jones SP, Bastien LJ. (1995). Efficient Analysis of Cytochrome P4501A Catalytic Activity, Porphyrins, and Total Proteins in Chicken Embryo Hepatocyte Cultures with a Fluorescence Plate Reader. Analytical Biochemistry.226:362-370

Keston AS, Brandt R. (1965). The fluorometric analysis of ultramicro quantitites of hydrogen peroxide. Anal Biochem. 11:1-5

Key TJ and Pike MC. (1988). The dose-effect relationship between 'unopposed' oestrogens and endometrial mitotic rate: its central role in explaining and predicting endometrial cancer risk. Br J Cancer. 57(2):205-12.

Kharat I and Saatcioglu F. (1996). Antiestrogenic effects of 2,3,7,8-tetrachlorodibenzo-p-dioxin are mediated by direct transcriptional interference with the liganded estrogen receptor. Cross-talk between aryl hydrocarbon- and estrogen-mediated signaling.J Biol Chem. 271(18):10533-7.

Kirkman H. (1959). Estrogen-induced tumors of the kidney. IV. Incidence in female Syrian hamsters. Natl Cancer Inst Monogr. 1:59-91.

Klauber N, Parangi S, Flynn E, Hamel E, D'Amato RJ. (1997). Inhibition of angiogenesis and breast cancer in mice by the microtubule inhibitors 2-methoxyestradiol and taxol. Cancer Res. 1997 Jan 1;57(1):81-6.

Klungland A, Rosewell I, Hollenbach S, Larsen E, Daly G, Epe B, Seeberg E, Lindahl T, Barnes DE. (1999). Accumulation of premutagenic DNA lesions in mice defective in removal of oxidative base damage. Proc Natl Acad Sci U S A. 96(23):13300-5.

Knasmüller S, Mersch-Sundermann V, Kevekordes S, Darroudi F, Huber WW, Hoelzl C, Bichler J, Majer BJ. (2004). Use of human-derived liver cell lines for the detection of environmental and dietary genotoxicants; current state of knowledge. Toxicology 198 (2004) 315-328

Knasmüller S, Parzefall W, Sanyal R, Ecker S, Schwab C, Uhl M, Mersch-Sundermann V, Williamson G, Hietsch G, Langer T, Darroudi F, Natarajan AT. (1998). Use of metabolically competent human hepatoma cells for the detection of mutagens and antimutagens. Mutat Res. 402(1-2):185-202.

Knerr S, Schaefer J, Both S, Mally A, Dekant W, Schrenk D. (2006). 2,3,7,8-Tetrachlorodibenzo-p-dioxin induced cytochrome P450s alter the formation of reactive oxygen species in liver cells. Mol Nutr Food Res. 50(4-5):378-84.

Knowles BB, Howe CC, Aden DP. (1980). Human hepatocellular carcinoma cell lines secrete the major plasma proteins and hepatitis B surface antigen. Science. 209(4455):497-9.

Kobayashi A, Numayama-Tsuruta K, Sogawa K, Fujii-Kuriyama Y. (1997). CBP/p300 functions as a possible transcriptional coactivator of Ah receptor nuclear translocator (Arnt). J. Biochem. (Tokyo) 122:703-710.

Kobayashi A, Sogawa K, Fujii-Kuriyama Y. (1996). Cooperative Interaction between AhR Arnt and Sp1 for the Drug-inducible Expression of CYP1A1 Gene. The Journal of Biological Chemistry. 271(21):12310-6.

Kochhar TS .(1985). Inducibility of chromosome aberrations by steroid hormones in cultured Chinese hamster ovary cells. Toxicol Lett. (2-3):201-6

Kociba RJ, Keyes DG, Beyer JE, Carreon RM, Wade CE, Dittenber DA, Kalnins RP, Frauson LE, Park CN,Barnard SD, Hummel RA, Humiston CG. (1978). Results of a two-year chronic toxicity and oncogenicity study of 2,3,7,8-tetrachlorodibenzo-p-dioxin in rats. Toxicol. Appl. Pharmacol. 46(2):279-303.

Kohn KW, Erickson LC, Ewig RAG, Friedman CA (1976). Fractionation of DNA from mammalian cells by alkaline elution. Biochemistry.15:4629-4637

Kong LY, Szaniszlo P, Albrecht T, Liehr JG. (2000). Frequency and molecular analysis of hprt mutations induced by estradiol in Chinese hamster V79 cells. Int J Oncol. 17(6):1141-9.

Kress S and Greenlee WF. (1997). Cell-specific Regulation of Human CYP1A1 and CYP1B1 Genes. Cancer Research. 57:1264-1269

Krishnan V, Porter W, Santostefano M, Wang X, Safe S. (1995). Molecular mechanism of inhibition of estrogen-induced cathepsin D gene expression by 2,3,7,8-tetrachlorodibenzo-p-dioxin (TCDD) in MCF-7 cells. Mol Cell Biol. 15(12):6710-9.

Krokan HE, Standal R, Slupphaug G. (1997). DNA glycosylases in the base excision repair of DNA. Biochem J. 325 (Pt 1):1-16.

Krusekopf S, Kleeburg U, Hildebrandt AG, Ruckpaul K. (1997). Effects of benzimidazole derivatives on cytochrome P450 1A1 expression in a human hepatoma cell line. Xenobiotica. 27(1): 1-9.

Kubista M, Andrade JM, Bengtsson M, Forootan A, Jonak J, Lind K, Sindelka R, Sjoback R,Sjogreen B, Strombom L, Stahlberg A, Zoric N. (2006). The real-time polymerase chain reaction. Molecular Aspects of Medicine. 27: 95.

Kubota Y, Nash RA, Klungland A, Schär P, Barnes DE, Lindahl T. (1996). Reconstitution of DNA base excision-repair with purified human proteins: interaction between DNA polymerase beta and the XRCC1 protein. EMBO J. 15(23):6662-70.

Kuiper GG, Enmark E, Pelto-Huikko M, Nilsson S, Gustafsson J-A. (1996). Cloning of a novel receptor expressed in rat prostate and ovary. Proc. Natl. Acad. Sci. U.S.A. 93: 5925-5930

Kuthan H and Ullrich V. (1982). Oxidase and oxygenase function of the microsomal cytochrome P450 monooxygenase system. Eur J Biochem. 126(3):583-8.

Laborda J. (1991). 36b4 cDNA used as an estradiol-independent mRNA control is the cDNA for human acidic ribosomal phosphoprotein PO. Nucleic Acids Research. 19: 3998.

Lachman HM, Papolos DF, Saito T, Yu YM, Szumlanski CL, Weinshilboum RM. (1996). Human catechol-O-methyltransferase pharmacogenetics: description of a functional polymorphism and its potential application to neuropsychiatric disorders. Pharmacogenetics. 6(3):243-50.

Lai KP, Mak NK, Wei X, Wong RNS, Wong MH, Wong CKC. (2006). Bifunctional modulating effects of an indigo dimer (bisindigotin) to CYP1A1 induction in H4IIE cells. Toxicology.226:188-196

Lai KP, Wong MH, Wong CKC. (2004). Modulation of AhR-Mediated CYP1A1 mRNA and EROD Activities by 17b-Estradiol and Dexamethasone in TCDD-Induced H4IIE Cells. Toxicological Sciences. 78:41-49.

Lang R and Reimann R. (1993). Studies for a genotoxic potential of some endogenous and exogenous sex steroids. I. Communication: examination for the induction of gene mutations using the Ames Salmonella/microsome test and the HGPRT test in V79 cells. Environ Mol Mutagen. 21(3):272-304.

Lavigne JA, Goodman JE, Fonong T, Odwin S, He P, Roberts DW, Yager JD. (2001). The effects of catechol-O-methyltransferase inhibition on estrogen metabolite and oxidative DNA damage levels in estradiol-treated MCF-7 cells. Cancer Res. 61(20):7488-94.

Lavigne JA, Helzlsouer KJ, Huang HY, Strickland PT, Bell DA, Selmin O, Watson MA, Hoffman S, Comstock GW, Yager JD. (1997). An association between the allele coding for a low activity variant of catechol-O-methyltransferase and the risk for breast cancer. Cancer Res. 1997 Dec 15;57(24):5493-7.

LeBel CP, Ischiropoulos H, Bondys SC. (1992). Evaluation of the Probe 2',7'-Dichiorofluorescin as an Indicator of Reactive Oxygen Species Formation and Oxidative Stress.Chem. Res. Toxicol. 5: 227-231

Ledirac N, Delescluse C, de Sousa G, Pralavorio M, Lesca P, Amichot M, Bergé JB, Rahmani R. (1997). Carbaryl induces CYP1A1 gene expression in HepG2 and HaCaT cells but is not a ligand of the human hepatic Ah receptor. Toxicol Appl Pharmacol. 144(1):177-82.

Lee AJ, Cai MX, Thomas PE, Conney AH, Zhu BT. (2003). Characterization of the oxidative metabolites of 17beta-estradiol and estrone formed by 15 selectively expressed human cytochrome p450 isoforms. Endocrinology. 144(8):3382-98.

Lee AJ, Kosh JW, Conney AH, Zhu BT. (2001). Characterization of the NADPH-dependent metabolism of 17beta-estradiol to multiple metabolites by human liver microsomes and selectively expressed human cytochrome P450 3A4 and 3A5. J Pharmacol Exp Ther. 298(2):420-32.

Lee AJ, Mills LH, Kosh JW, Conney AH, Zhu BT. (2002). NADPH-dependent metabolism of estrone by human liver microsomes. J Pharmacol Exp Ther. 300(3):838-49.

Lehmann L and Wagner J. (2008). Gene Expression of 17beta-Estradiol-metabolizing Isozymes: Comparison of Normal Human Mammary Gland to Normal Human Liver and to Cultured Human BreastAdenocarcinoma Cells. Adv Exp Med Biol. 617:617-24

Lekas P, Lok Tin K, Lee C, Prokipcak RD. (2000). The human cytochrome P450 1A1 mRNA is rapidly degraded in HepG2 cells. Archives of Biochemistry and Biophysics. 384:311-318

Leo C and Chen JD. (2000). The SRC family of nuclear receptor coactivators. Gene. 245(1):1-11.

Lew H, Pyke S, Quintanilha A. (1985). Changes in the glutathione status of plasma, liver and muscle following exhaustive exercise in rats. FEBS Lett. 185(2):262-6.

LGC Standards, http:// www.lgcstandards-atcc.org (March 2009)

Li JJ and Li SA. (1987). Estrogen carcinogenesis in Syrian hamster tissues: role of metabolism. Fed Proc. 46(5):1858-63.

Li Q, Laval J, Ludlum DB. (1997). Fpg protein releases a ring-opened N-7 guanine adduct from DNA that has been modified by sulfur mustard. Carcinogenesis. 18(5):1035-8.

Li W, Harper PA, Tang BK, Okey AB. (1998). Regulation of cytochrome P450 enzymes by aryl hydrocarbon receptor in human cells: CYP1A2 expression in the LS180 colon carcinoma cell line after treatment with 2,3,7,8-tetrachlorodibenzo-p-dioxin or 3-methylcholanthrene. Biochem Pharmacol. 56(5):599-612.

Li Y, Trush MA, Yager JD. (1994). DNA damage caused by reactive oxygen species originating from a copper-dependent oxidation of the 2-hydroxy catechol of estradiol. Carcinogenesis. 15(7):1421-7.

Lie YS and Petropoulos CJ. (1998). Advances in quantitative PCR technology: 5' nuclease assays. Curr Opin Biotechnol. 9 (1):43.

Liehr JG, Fang WF, Sirbasku DA, Ari-Ulubelen A. (1986). Carcinogenicity of catechol estrogens in Syrian hamsters. J Steroid Biochem. 24(1):353-6.

Liehr JG, Hall ER, Avitts TA, Randerath E, Randerath K. (1987). Localization of estrogen-induced DNA adducts and cytochrome P-450 activity at the site of renal carcinogenesis in the hamster kidney. Cancer Res. 47(8):2156-9.

Liehr JG. (2001). Genotoxicity of the steroidal oestrogens oestrone and oestradiol: possible mechanism of uterine and mammary cancer development. Human Reproduction Update. 7: 273-281

Lin PH, Lin CH, Huang CC, Chuang MC, Lin P. (2007). 2,3,7,8-Tetrachlorodibenzo-p-dioxin (TCDD) induces oxidative stress, DNA strand breaks, and poly(ADP-ribose) polymerase-1 activation in human breast carcinoma cell lines. Toxicol Lett. 172(3):146-58.

Lin PH, Lin CH, Huang CC, Fang JP, Chuang MC. (2008). 2,3,7,8-Tetrachlorodibenzo-p-dioxin modulates the induction of DNA strand breaks and poly(ADP-ribose) polymerase-1 activation by 17beta-estradiol in human breast carcinoma cells through alteration of CYP1A1 and CYP1B1 expression. Chem Res Toxicol. 21(7):1337-47

Lindl T. (2002). Zell-und Gewebekultur. Elsevier Spektrum Akademischer Verlag, Heidelberg, 5th edition

Liu H, Wang H, Shenvi S, Hagen TM, Liu RM. (2004). Glutathione metabolism during aging and in Alzheimer disease. Ann N Y Acad Sci. 1019:346-9.

Loft S and Poulsen HE. (1996).Cancer risk and oxidative DNA damage in man. J Mol Med. 74(6):297-312. Review. Erratum in: J Mol Med 75(1):67-8.

Lottspeich F and Engels JW. (2006). Bioanalytik. Spektrum Akademischer Verlag, Heidelberg-Berlin, 2. Auflage.

Lu F, Zahid M, Saeed M, Cavalieri EL, Rogan EG. (2007). Estrogen metabolism and formation of estrogen-DNA adducts in estradiol-treated MCF-10F cells. The effects of 2,3,7,8-tetrachlorodibenzo-p-dioxin induction and catechol-O-methyltransferase inhibition. J Steroid Biochem Mol Biol. 105(1-5):150-8.

Lucier GW, Tritscher A, Goldsworthy T, Foley J, Clark G, Goldstein J, Maronpot R. (1991). Ovarian hormones enhance 2,3,7,8-tetrachlorodibenzo-p-dioxin-mediated increases in cell proliferation and preneoplastic foci in a two-stage model for rat hepatocarcinogenesis. Cancer Res. 51(5):1391-7.

Ma Q and Baldwin KT. (2000). 2,3,7,8-tetrachlorodibenzo-p-dioxin-induced degradation of aryl hydrocarbon receptor (AhR) by the ubiquitin-proteasome pathway. Role of the transcription activaton and DNA binding of AhR. J Biol Chem. 275(12):8432-8.

Ma Q, Renzelli AJ, Baldwin KT, Antonini JM. (2000). Superinduction of CYP1A1 gene expression. Regulation of 2,3,7, 8-tetrachlorodibenzo-p-dioxin-induced degradation of Ah receptor by cycloheximide. J Biol Chem. 275(17):12676-83.

MacPherson L, Lo R, Ahmed S, Pansoy A, Matthews J. (2009). Activation function 2 mediates dioxin-induced recruitment of estrogen receptor alpha to CYP1A1 and CYP1B1. Biochem Biophys Res Commun. 385(2):263-8.

Madle S, Dean SW, Andrae U, Brambilla G, Burlinson B, Doolittle DJ, Furihata C, Hertner T, McQueen CA, Mori H. (1994). Recommendations for the performance of UDS tests in vitro and in vivo. Mutat Res. 312(3):263-85.

Mailander PC, Meza JL, Higginbotham S, Chakravarti D. (2006). Induction of A.T to G.C mutations by erroneous repair of depurinated DNA following estrogen treatment of the mammary gland of ACI rats. J Steroid Biochem Mol Biol. 101(4-5):204-15.

Malherbe P, Bertocci B, Caspers P, Zürcher G, Da Prada M. (1992). Expression of functional membrane-bound and soluble catechol-O-methyltransferase in Escherichia coli and a mammalian cell line.J Neurochem. 58(5):1782-9

Mangelsdorf DJ, Thummel C, Beato M, Herrlich P, Schütz G, Umesono K, Blumberg B, Kastner P, Mark M, Chambon P, Evan RM. (1995). The Nuclear Receptor Superfamily: The Second Decade. Cell. 83: 835-839

Martelli A, Mattioli F, Angiola M, Reimann R, Brambilla G. (2003). Species, sex and inter-individual differences in DNA repair induced by nine sex steroids in primary cultures of rat and human hepatocytes. Mutat Res. 536(1-2):69-78.

Martin C, Martinez R, Navarro R, Ruiz-Sanz JI, Lacort M, Ruiz-Larrea MB. (2001). tert-Butyl hydroperoxide-induced lipid signaling in hepatocytes: involvement of glutathione and free radicals. Biochem Pharmacol. 62(6):705-12.

Martin CN, McDermid AC, Garner RC. (1978). Testing of known carcinogens and noncarcinogens for their ability to induce unscheduled DNA synthesis in HeLa cells. Cancer Res. 38(8):2621-7.

Matthews J and Gustafsson JA. (2003). Estrogen signaling: a subtle balance between ER alpha and ER beta. Mol Interv. 3(5):281-92.

Matthews J and Gustafsson JA. (2006). Estrogen receptor and aryl hydrocarbon receptor signaling pathways. Nucl Recept Signal. 4:e016.

Matthews J, Wihlén B, Heldring N, MacPherson L, Helguero L, Treuter E, Haldosén LA, Gustafsson JA. (2007). Co-planar 3,3',4,4',5-pentachlorinated biphenyl and non-co-planar 2,2',4,6,6'-pentachlorinated biphenyl differentially induce recruitment of oestrogen receptor alpha to aryl hydrocarbon receptor target genes. Biochem J. 406(2):343-53.

Matthews J, Wihlén B, Thomsen J, Gustafsson JA. (2005). Aryl hydrocarbon receptor-mediated transcription: ligand-dependent recruitment of estrogen receptor alpha to 2,3,7,8-tetrachlorodibenzo-p-dioxin-responsive promoters. Mol Cell Biol. 25(13):5317-28.

McCullough AK, Dodson ML, Lloyd RS. (1999). Initiation of base excision repair: glycosylase mechanisms and structures. Annu Rev Biochem. 1999;68:255-85.

McFadyen MC, Rooney PH, Melvin WT, Murray GI. (2003). Quantitative analysis of the Ah receptor/cytochrome P450 CYP1B1/CYP1A1 signalling pathway. Biochem Pharmacol. 65(10):1663-74.

McKenna NJ and O'Malley BW. (2002). Combinatorial Control Review of Gene Expression by Nuclear Receptors and Coregulators. Cell. 108: 465-474

McKinnon RA, Hall PD, Quattrochi LC, Tukey RH, McManus ME. (1991). Localization of CYP1A1 and CYP1A2 messenger RNA in normal human liver and in hepatocellular carcinoma by in situ hybridization. Hepatology. 14(5):848-56.

McLemore TL, Adelberg S, Liu MC, McMahon NA, Yu SJ, Hubbard WC, Czerwinski M, Wood TG, Storeng R, Lubet RA, et al. (1990). Expression of CYP1A1 gene in patients with lung cancer: evidence for cigarette smoke-induced gene expression in normal lung tissue and for altered gene regulation in primary pulmonary carcinomas. J Natl Cancer Inst. 82(16):1333-9.

McQueen CA and Way BM. (1991). Sex and strain differences in the hepatocyte primary culture/DNA repair test. Environ Mol Mutagen. 18(2):107-12.

McQueen CA and Williams GM. (1987). The hepatocyte primary culture/DNA repair test using hepatOcytes from several species. Cell Biol. Toxicol. 3:209-218.

McQueen CA, Miller MJ, Williams GM. (1986). Sex differences in the biotransformation of 2-acetylaminofluorene in cultured rat hepatocytes. Cell Biol Toxicol. 2(2):271-81.

Meister A and Anderson ME. (1983). Glutathione. Annu Rev Biochem. 52:711-60.

Merchant M, Arellano L, Safe S. (1990). The mechanism of action of alpha-naphthoflavone as an inhibitor of 2,3,7,8-tetrachlorodibenzo-p-dioxin-induced CYP1A1 gene expression. Arch Biochem Biophys. 281(1):84-9.

Merk O and Speit G. (1999). Detection of crosslinks with the comet assay in relationship to genotoxicity and cytotoxicity. Environ Mol Mutagen. 33(2):167-72.

Meyer BK and Perdew GH. (1999). Characterization of the AhR-hsp90-XAP2 core complex and the role of the immunophilin-related protein XAP2 in AhR stabilization. Biochemistry. 38(28):8907-17.

Michaels ML, Cruz C, Grollman AP, Miller JH. (1992). Evidence that MutY and MutM combine to prevent mutations by an oxidatively damaged form of guanine in DNA. Proc Natl Acad Sci U S A. 89(15):7022-5.

Michiels C, Raes M, Toussaint O, Remacle J. Free Radic Biol Med. (1994). Importance of Se-glutathione peroxidase, catalase, and Cu/Zn-SOD for cell survival against oxidative stress. 17(3):235-48.

Mimura J and Fujii-Kuriyama Y. (2003). Functional role of AhR in the expression of toxic effects by TCDD. Biochimica et Biophysica Acta. 1619:263-268

Mimura J, Ema M, Sogawa K, Fujii-Kuriyama Y. (1999). Identification of a novel mechanism of regulation of Ah (dioxin) receptor function. Genes Dev. 13 (1):20-25.

Minowa O, Arai T, Hirano M, Monden Y, Nakai S, Fukuda M, Itoh M, Takano H, Hippou Y, Aburatani H, Masumura K, Nohmi T, Nishimura S, Noda T. (2000). Mmh/Ogg1 gene inactivation results in accumulation of 8-hydroxyguanine in mice. Proc Natl Acad Sci U S A. 97(8):4156-61.

Mitchell AD, Casciano DA, Meltz ML, Robinson DE, San RH, Williams GM, Von Halle ES. (1983). Unscheduled DNA synthesis tests. A report of the U.S. Environmental Protection Agency Gene-Tox Program. Mutat Res. 123(3):363-410.

Mobley JA and Brueggemeier RW. (2004). Estrogen receptor-mediated regulation of oxidative stress and DNA damage in breast cancer. Carcinogenesis. 25(1):3-9.

Mobley JA, Bhat AS, Brueggemeier RW. (1999). Measurement of oxidative DNA damage by catechol estrogens and analogues in vitro. Chem Res Toxicol. 1999 Mar;12(3):270-7.

Moennikes O, Loeppen S, Buchmann A, Andersson P, Ittrich C, Poellinger L, Schwarz M. (2004). A constitutively active dioxin/aryl hydrocarbon receptor promotes hepatocarcinogenesis in mice. Cancer Res. 64(14):4707-10.

Moore M, Wang X, Lu YF, Wormke M, Craig A, Gerlach JH, Burghardt R, Barhoumi R, Safe S. (1994). Benzo[a]pyrene-resistant MCF-7 human breast cancer cells. A unique aryl hydrocarbon-nonresponsive clone. J Biol Chem. 269:11751–11759.

Morita T, Asano N, Awogi T, Sasaki YF, Sato S, Shimada H, Sutou S, Suzuki T, Wakata A, Sofuni T, Hayashi M. (1997). Evaluation of the rodent micronucleus assay in the screening of IARC carcinogens (groups 1, 2A and 2B) the summary report of the 6th collaborative study by CSGMT/JEMS MMS. Collaborative Study of the Micronucleus Group Test. Mammalian Mutagenicity Study Group.Mutat Res. 389(1):3-122. Erratum in: Mutat Res 1997 Jul 14;391(3):259-67.

Morrison H, Jernström B, Nordenskjöld M, Thor H, Orrenius S. (1984). Potential exogenous sources of ROS consists of generation during irrradiotion by UV light, X-ray, and by gamma-rays. Biochem Pharmacol. 33(11):1763-9.

Mortelmans K, Haworth S, Speck W, Zeiger E. (1984). Mutagenicity testing of agent orange components and related chemicals. Toxicol Appl Pharmacol. 75(1):137-46.

Mullis KB and Faloona FA. (1987). Specific synthesis of DNA in vitro via a polymerase-catalyzed chain reaction. Methods Enzymol. 155: 335

Murray GI, Barnes TS, Sewell HF, Ewen SW, Melvin WT, Burke MD. (1988). The immunocytochemical localisation and distribution of cytochrome P-450 in normal human hepatic and extrahepatic tissues with a monoclonal antibody to human cytochrome P-450. Br J Clin Pharmacol. 25(4):465-75.

Murray GI, Melvin WT, Greenlee WF, Burke MD. (2001). Regulation, function, and tissue-specific expression of cytochrome P450 CYP1B1. Annu Rev Pharmacol Toxicol. 41:297-316.

Murray GI, Taylor MC, McFadyen MC, McKay JA, Greenlee WF, Burke MD, Melvin WT. (1997).Tumor-specific expression of cytochrome P450 CYP1B1. Cancer Res. 57(14):3026-31.

Murray GI. (2000). The role of cytochrome P450 in tumour development and progression and its potential in therapy. J Pathol. 192:419-426

Nagasawa H, Mori T, Nakajima Y. (1980). Long-term effects of progesterone or diethylstilbestrol with or without estrogen after maturity on mammary tumorigenesis in mice. Eur J Cancer. 16(12):1583-9.

Nagayama J, Nagayama M, Iida T, Hirakawa H, Matsueda T, Masuda Y. (1994). Effects of highly toxic organochlorine compounds retained in human body on induction of sister chromatid exchanges in cultured human lymphocytes. Chemosphere. 29 (9-11):2349-54.

Naji-Ali F, Hasspieler BM, Haffner D, Adeli K. (1994). Human bioassays to assess environmental genotoxicity: development of a DNA repair assay in HepG2 cells. Clin Biochem. 27(6):441-8.

Nakama A, Kuroda K, Yamada A. (1995). Induction of cytochrome P450-dependent monooxygenase in serum-free cultured Hep G2 cells. Biochem Pharmacol. 50(9):1407-12.

Nakama A. Modulation by extracellular matrices of monooxygenase and CYP1A1 induction in Hep G2 cells in serum-free culture. Cytotechnology. 31(1-2):205-211.

Nash HM, Bruner SD, Schärer OD, Kawate T, Addona TA, Spooner E, Lane WS, Verdine GL. (1996). Cloning of a yeast 8-oxoguanine DNA glycosylase reveals the existence of a base-excision DNA-repair protein superfamily. Curr Biol. 6(8):968-80.

Nash RA, Caldecott KW, Barnes DE, Lindahl T. (1997). XRCC1 protein interacts with one of two distinct forms of DNA ligase III. Biochemistry. 36(17):5207-11.

Nebert DW and Dalton TP. (2006). The role of cytochrome P450 enzymes in endogenous signalling pathways and environmental carcinogenesis. Nat Rev Cancer. 6(12):947-60.

Nebert DW, Dalton TP, Okey AB, Gonzalez FJ. (2004). Role of aryl hydrocarbon receptor-mediated induction of the CYP1 enzymes in environmental toxicity and cancer. J Biol Chem. 279(23):23847-50

Ni N and Yager JD. (1994). Comitogenic effects of estrogens on DNA synthesis induced by various growth factors in cultured female rat hepatocytes. Hepatology. 19(1):183-92.

Nilsen H and Krokan HE. (2001). Base excision repair in a network of defence and tolerance. Carcinogenesis. 22(7):987-98.

Nilsson S and Gustafsson J-A. (2000). Estrogen receptor transcription and transactivation: Basic aspects of estrogen action. Breast Cancer Res. 2:360-366

Nishioka K, Ohtsubo T, Oda H, Fujiwara T, Kang D, Sugimachi K, Nakabeppu Y. (1999). Expression and differential intracellular localization of two major forms of human 8-oxoguanine DNA glycosylase encoded by alternatively spliced OGG1 mRNAs. Mol Biol Cell. 10(5):1637-52.

Noble RL, Hochachka BC, King D. (1975). Spontaneous and estrogen-produced tumors in Nb rats and their behavior after transplantation. Cancer Res. 35(3):766-80.

NTP (National Toxicology Program). (1982a). Carcinogenesis Bioassay of 2,3,7,8-Tetrachlorodibenzo-p-dioxin (CAS No. 1746-01-6) in Osborne-Mendel Rats and B6C3F1 Mice (Gavage Study). Natl Toxicol Program Tech Rep Ser. 209:1-195.

NTP (National Toxicology Program).(1982b). Carcinogenesis Bioassay of 2,3,7,8-Tetrachlorodibenzo-p-dioxin (CAS No. 1746-01-6) in Swiss-Webster Mice (Dermal Study).Natl Toxicol Program Tech Rep Ser. 201:1-113.

O'Brien J, Wilson I, Ortan T, Pognan F. (2000). Investigation of the Alamar Blue (resazurin) fluorescent dye for the assessment of mammalian cell cytotoxicity. Eru. J. Biochem. 267: 5421-5426.

O'Connor TR, Graves RJ, de Murcia G, Castaing B, Laval J. (1993). Fpg protein of Escherichia coli is a zinc finger protein whose cysteine residues have a structural and/or functional role. J Biol Chem. 268(12):9063-70.

OECD Guideline for Testing of Chemicals. (1986). Genetic Toxicology: DNA Damage and Repair/Unscheduled DNA Synthesis in Mammalian Cells in vitro. No. 482.

Ohtake F, Fujii-Kuriyama Y, Kato S. (2009). AhR acts as an E3 ubiquitin ligase to modulate steroid receptor functions.Biochem Pharmacol. 77(4):474-84.

Ohtake F, Takeyama K, Matsumoto T, Kitagawa H, Yamamoto Y, Nohara K, Tohyama C, Krust A, Mimura J, Chambon P, Yanagisawa J, Fujii-Kuriyama Y, Kato S. (2003). Modulation of oestrogen receptor signalling by association with the activated dioxin receptor. Nature. 423(6939):545-50.

Olafsdottir K and Reed DJ. (1988). Retention of oxidized glutathione by isolated rat liver mitochondria during hydroperoxide treatment. Biochim Biophys Acta. 964(3):377-82.

Olive PL and Banath JP. (2006). The comet assay: a method to measure DNA damage in individual cells. Nat Protoc. 1(1):23-9.

Olive PL, Banath J P, Durand RE. (1990). Heterogeneity in radiation-induced DNA damage and repair in tumor and normal cells measured using the "comet" assay. Radiat Res. 122: 86-94.

Olive PL. (1989). Cell proliferation as a requirement for development of the contact effect in Chinese hamster V79 spheroids. Radiat Res. 117:79-92.

Olsen JR. (1994). Pharmacokinetics of dioxin and related chemicals. In Dioxins and Health. A. Schecter, ed. New York Plenum Press: 163-167

Oshiro Y, Balwierz PS, Piper CE. (1986). Absence of a genotoxic response from steroids in the rat primary hepatocyte unscheduled DNA synthesis assay. Environ Mutagen. 8(3):461-5.

Osterod M, Hollenbach S, Hengstler JG, Barnes DE, Lindahl T, Epe B. (2001). Age-related and tissue-specific accumulation of oxidative DNA base damage in 7,8-dihydro-8-oxoguanine-DNA glycosylase (Ogg1) deficient mice.Carcinogenesis. 2001 Sep;22(9):1459-63.

Osterod M, Larsen E, Le Page F, Hengstler JG, Van Der Horst GT, Boiteux S, Klungland A, Epe B. (2002). A global DNA repair mechanism involving the Cockayne syndrome B (CSB) gene product can prevent the in vivo accumulation of endogenous oxidative DNA base damage. Oncogene. 21(54):8232-9.

Östling O and Johanson KJ. (1984). Microelectrophoretic study of radiation-induced DNA damages in individual mammalian cells. Biochem. Biophys. Res. Commun., 123: 291.

Paech K, Webb P, Kuiper GG, Nilsson S, Gustafsson J-A, Kushner PJ, Scanlan TS. (1997). Differential ligand activation of estrogen receptors ERalpha and ERbeta at AP1 sites. Science. 277:1508-1510.

Palmer JR, Rosenberg L, Kaufman DW, Warshauer ME, Stolley P, Shapiro S. (1989). Oral contraceptive use and liver cancer. Am J Epidemiol. 130(5):878-82.

Park JY, Shigenaga MK, Ames BN. (1996). Induction of cytochrome P4501A1 by 2,3,7,8-tetrachlorodibenzo-p-dioxin or indolo(3,2-b)carbazole is associated with oxidative DNA damage. Proc Natl Acad Sci U S A. 93(6):2322-7.

Park S, Kim AJ, Lee M. (2009). Synergic effects of a-tocopherol and b-carotene on tert-butylhydroperoxide-induced HepG2 cell injury. Toxicology and Industrial Health 25: 311-320

Parl FF, Dawling S, Roodi N, Crooke PS. (2009). Estrogen metabolism and breast cancer: a risk model. Ann N Y Acad Sci. 1155:68-75.

Pastore A, Federici G, Bertini E, Piemonte F. (2003). Analysis of glutathione: implication in redox and detoxification. Clin Chim Acta. 333:19-39

Pearce ST and Jordan VC. (2004). The biological role of estrogen receptors alpha and beta in cancer. Crit Rev Oncol Hematol. 50(1):3-22.

Perdew GH and Babbs CF. (1991).Production of Ah receptor ligands in rat fecal suspensions containing tryptophan or indole-3-carbinol. Nutr Cancer. 1991;16(3-4):209-18.

Pettersson K and Gustafsson J-A. (2001). Role of estrogen receptor ? in estrogen action. Annu. Rev. Physiol. 63, 165-192

Pfaffl MW. (2001). A new mathematical model for relative quantification in real-time RT-PCR. Nucleic Acids Research. 29: 2002.

Pfaffl MW. (2004). Real-time RT-PCR: Neue Ansätze zur exakten mRNA Quantifizierung. BIOspektrum. 1:92.

Pfaffl MW. http://www.gene-quantification.info/ (January 2009)

Pfeiffer E, Graf E, Gerstner S, Metzler M. (2006). Stimulation of estradiol glucuronidation: a protective mechanism against estradiol-mediated carcinogenesis? Mol Nutr Food Res. 50(4-5):385-9

Pflaum M, Will O, Epe B. (1997). Determination of steady-state levels of oxidative DNA base modifications in mammalian cells by means of repair endonucleases. Carcinogenesis. 18(11):2225-31.

Pham T.A., Hwung Y.P., Santiso-Mere D., McDonnell D.P., O'Malley BW (1992) Liganddependent and -independent functions of the transactivation regions of the human estrogen receptor in yeast. Mol Endocrinol6:1043-1050

Pink JJ and Jordan VC. (1996). Models of estrogen receptor regulation by estrogens and antiestrogens in breast cancer cell lines. Cancer Res. 56: 2321-2330

Pitot HC, Goldsworthy T, Campbell HA, Poland A. (1980). Quantitative evaluation of the promotion by 2,3,7,8-tetrachlorodibenzo-p-dioxin of hepatocarcinogenesis from diethylnitrosamine.Cancer Res. 40(10):3616-20.

Pitot HC, Peraino C, Morse PA Jr, Potter VR. (1964). Hepatomas in tissue culture compared with adapting liver in vivo. Natl. Cancer Inst. Monogr. 13:229

Pohl RJ and Fouts JR. (1980). A rapid method for aassaying the metabolism of 7-ethoxyresorufin by microsomal subcellular fractions. Anal Biochem. 107:150-155.

Poland A and Knutson JC. (1982). 2,3,7,8-tetrachlorodibenzo-p-dioxin and related halogenated aromatic hydrocarbons: examination of the mechanism of toxicity. Annu Rev Pharmacol Toxicol. 22:517-554.

Poland A, Glover E, Kende AS. (1976). Stereospecific, high affinity binding of 2,3,7,8-tetrachlorodibenzo-p-dioxin by hepatic cytosol. Evidence that the binding species is receptor for induction of aryl hydrocarbon hydroxylase. J Biol Chem. 251(16):4936-46.

Pollenz RS, Sattler CA, Poland A. (1994). The aryl hydrocarbon receptor and aryl hydrocarbon receptor nuclear translocator protein show distinct subcellular localizations in Hepa 1c1c7 cells by immunofluorescence microscopy. Mol Pharmacol.45(3):428-38.

Probst GS and Hill LE. (1987). Influence of age, sex and strain on the in vitro induction of unscheduled DNA synthesis in rat hepatocyte primary cultures. Cell Biol Toxicol. 3(2):113-25.

Promega Technical Bulletin. (2006). Luciferase Assay System.

Pryor WA. (1986). Oxy-radicals and related species: their formation, lifetimes, and reactions. Annu Rev Physiol. 48:657-67.

Pylkkänen L, Jahnukainen K, Parvinen M, Santti R. (1991). Testicular toxicity and mutagenicity of steroidal and non-steroidal estrogens in the male mouse. Mutat Res. 261(3):181-91.

Racky J, Schmitz H-J, Kauffmann H-M, Schrenk D. (2004). Single nucleotide polymorphism analysis and functional characterization of the human Ah receptor (AhR) gene promoter. Archives of Biochemistry and Biophysics. 421:91-98

Rajapakse N, Butterworth M, Kortenkamp A. (2005). Detection of DNA strand breaks and oxidized DNA bases at the single-cell level resulting from exposure to estradiol and hydroxylated metabolites. Environ Mol Mutagen. 45(4):397-404.

Randerath K, Putman KL, Randerath E, Zacharewski T, Harris M, Safe S. (1990). Effects of 2,3,7,8-tetrachlorodibenzo-p-dioxin on I-compounds in hepatic DNA of Sprague-Dawley rats: sex-specific effects and structure-activity relationships. Toxicol Appl Pharmacol. 103(2):271-80.

Rao MS, Subbarao V, Prasad JD, Scarpelli DG. (1988). Carcinogenicity of 2,3,7,8-tetrachlorodibenzo-p-dioxin in the Syrian golden hamster.Carcinogenesis. 9 (9):1677-9.

Rebrin I and Sohal RS. (2008). Pro-oxidant shift in glutathione redox state during aging. Adv Drug Deliv Rev. 60(13-14):1545-52.

Reen RK, Cadwallader A, Perdew GH. (2002). The subdomains of the transactivation domain of the aryl hydrocarbon receptor (AhR) inhibit AhR and estrogen receptor transcriptional activity. Arch Biochem Biophys. 408(1):93-102.

Reuber MD.(1961). A transplantable bile-secreting hepatocellular carcinoma in the rat. J Natl. Cancer Inst. 26:791

RNeasy Mini Handbook. (2006). Qiagen.

Rogan EG, Badawi AF, Devanesan PD, Meza JL, Edney JA, West WW, Higginbotham SM, Cavalieri EL. (2003). Relative imbalances in estrogen metabolism and conjugation in breast tissue of women with carcinoma: potential biomarkers of susceptibility to cancer. Carcinogenesis. 24(4):697-702.

Romkes M and Safe S.(1988). Comparative activities of 2,3,7,8-tetrachlorodibenzo-p-dioxin and progesterone as antiestrogens in the female rat uterus. Toxicol Appl Pharmacol. 1988 Mar 15;92(3):368-80.

Rosenfeld MG, Lunyak VV, Glass CK. (2006). Sensors and signals: a co-activator/co-repressor/epigenetic code for integrating signal-dependent programs of transcriptional response. Genes Dev. 20(11):1405-28

Rossi L, Moore GA, Orrenius S, O'Brien PJ. (1986). Quinone toxicity in hepatocytes without oxidative stress. Arch Biochem Biophys. 251(1):25-35.

Rozen S and Skaletsky HJ. (2000). Primer3 on the WWW for general users and for biologist programmers. In: Krawetz S, Misener S (eds). Bioinformatics Methods and Protocols: Methods in Molecular Biology. Humana Press, Totowa, NJ. pp 365-386.

Rüegg J, Swedenborg E, Wahlström D, Escande A, Balaguer P, Pettersson K, Pongratz I. (2008).The transcription factor aryl hydrocarbon receptor nuclear translocator functions as an estrogen receptor beta-selective coactivator, and its recruitment to alternative pathways mediates antiestrogenic effects of dioxin. Mol Endocrinol. 304-16.

Rushmore TH, King RG, Paulson KE, Pickett CB. (1990). Regulation of glutathione S-transferase Ya subunit gene expression: identification of a unique xenobiotic-responsive element controlling inducible expression by planar aromatic compounds. Proc Natl Acad Sci U S A. 87(10):3826-30.

Safe S and Wormke M. (2003). Inhibitory aryl hydrocarbon receptor-estrogen receptor alpha cross-talk and mechanisms of action. Chem Res Toxicol. 16(7):807-816

Safe S, Wang F, Porter W, Duan R, McDougal A. (1998). Ah receptor agonists as endocrine disruptors: antiestrogenic activity and mechanisms. Toxicol Lett. 102-103:343-7.

Safe S, Wormke M, Samudio I. (2000). Mechanisms of Inhibitory Aryl Hydrocarbon Receptor-Estrogen Receptor Crosstalk in Human Breast Cancer Cells. J Mammary Gland Biol Neoplasia. 5(3):295-306.

Safe S. (2001). Molecular biology of the Ah receptor and its role in carcinogenesis. Toxicology Letters. 120: 1-17.

Salmon M. (2002). La PCR en temps réel. Le technoscope de Biofutur 219.

Sambrook J, Fritsch EF, Maniatis T. (1989). Molecular cloning- a laboratory manual. Cold Spring Harbor Laboratory Press, 2nd edition.

Sar M and Welsch F. (1999). Differential expression of estrogen receptor-beta and estrogen receptor-alpha in the rat ovary. Endocrinology. 140(2):963-71.

Sarkar S, Jana NR, Yonemoto J, Tohyama C, Sone H. (2000). Estrogen enhances induction of cytochrome P-4501A1 by 2,3,7, 8-tetrachlorodibenzo-p-dioxin in liver of female Long-Evans rats. Int J Oncol. 16(1):141-7.

Sassa S, Sugita O, Galbraith RA, Kappas A. (1987). Drug metabolism by the human hepatoma cell, Hep G2. Biochem Biophys Res Commun. 143(1):52-7.

Sato Y, Sakakibara Y, Oda T, Aizu-Yokota E, Ichinoseki K. (1992). Effect of estradiol and ethynylestradiol on microtubule distribution in Chinese hamster V79 cells. Chem Pharm Bull (Tokyo). 40(1):182-4.

Savas U, Carstens CP, Jefcoate CR. (1997). Biological oxidations and P450 reactions. Recombinant mouse CYP1B1 expressed in Escherichia coli exhibits selective binding by polycyclic hydrocarbons and metabolism which parallels C3H10T1/2 cell microsomes, but differs from human recombinant CYP1B1.Arch Biochem Biophys. 347(2):181-92.

Saville B, Wormke M, Wang F, Nguyen T, Enmark E, Kuiper G, Gustafsson J-A, Safe S. (2000). Ligand-, cell-, and estrogen receptor subtype (alpha/beta)-dependent activation at GC-rich (Sp1) promoter elements. J. Biol. Chem. 275:5379-5387.

Sawyer T and Safe S. (1982). PCB isomers and congeners: induction of aryl hydrocarbon hydroxylase and ethoxyresorufin O-deethylase enzyme activities in rat hepatoma cells. Toxicol Lett. 13(1-2):87-93.

Schaefer S, Baum M, Eisenbrand G, Dietrich H, Will F, Janzowski C. (2006). Polyphenolic apple juice extracts and their major constituents reduce oxidative damage in human colon cell lines. Mol Nutr Food Res. 50(1):24-33.

Schehrer L, Regan JD, Westendorf J. (2000). UDS induction by an array of standard carcinogens in human and rodent hepatocytes: effect of cryopreservation. Toxicology. 147(3):177-91.

Schenkman JB and Jansson I. (2003). The many roles of cytochrome b5. Pharmacology and Therapeutics. 97:139-152

Schmidt JV and Bradfield CA. (1996). Ah receptor signaling pathways. Annu Rev Cell Dev Biol. 12:55-89.

Schmitz S. (2009). Der Experimentator Zellkultur. Elsevier Spektrum Akademischer Verlag Heidelberg, 2nd edition.

Schnitzler R, Foth J, Degen GH, Metzler M. (1994). Induction of micronuclei by stilbene-type and steroidal estrogens in Syrian hamster embryo and ovine seminal vesicle cells in vitro. Mutat Res. 311(1):84-93.

Schrenk D, Karger A, Lipp HP, Bock KW. (1992). 2,3,7,8-Tetrachlorodibenzo-p-dioxin and ethinylestradiol as co-mitogens in cultured rat hepatocytes. Carcinogenesis. 13(3):453-6.

Schütze N, Vollmer G, Tiemann I, Geiger M, Knuppen R. (1993). Catecholestrogens are MCF-7 cell estrogen receptor agonists. J Steroid Biochem Mol Biol. 46(6):781-9.

Seglen PO. (1976). Preparation of isolated rat liver cells. Meth. Cell Biol. 13:29-83.

Seis H, ed. (1991).Oxidative stress: Oxidants and Antioxidants. Academic Press, London. 2nd edition.

Senft AP, Dalton TP, Nebert DW, Genter MB, Hutchinson RJ, Shertzer HG. (2002a). Dioxin increases reactive oxygen production in mouse liver mitochondria. Toxicol Appl Pharmacol. 178(1):15-21.

Senft AP,Dalton TP,Nebert DW, Genter MB, Puga A, Hutchinson RJ, J. Kerzee K, Uno S., Shertzer HG. (2002b). Mitochondrial Reactive Oxygen Production is Dependent on the Aromatic Hydrocarbon Receptor. Free Radical Biology & Medicine. 33: 1268–1278.

Seung SA, Lee JY, Lee MY, Park JS, Chung JH. (1998). The relative importance of oxidative stress versus arylation in the mechanism of quinone-induced cytotoxicity to platelets. Chem Biol Interact. 113(2):133-44.

Severin I, Padieu M, Lhuguenot JC, Chagnon MC. (2003). Toxic interaction between hydroxyurea and 1-beta-D-arabino-furanosylcytosine on the DNA of a human hepatoma cell line (HEPG2). Toxicol Lett. 145(3):303-11.

Shen D, Dalton TP, Nebert DW, Shertzer HG. (2005). Glutathione Redox State Regulates Mitochondrial Reactive Oxygen Production. 280(27): 25305-25312

Shen D, Dalton TP, Nebert DW, Shertzer HG. (2005). Glutathione Redox State Regulates Mitochondrial Reactive Oxygen Production. Journal of Biological Chemistry. 280:25305–25312

Shertzer HG, Clay CD, Genter MB, Chames MC, Schneider SN, Oakley GG, Nebert DW, Dalton TP. (2004a). Uncoupling-mediated generation of reactive oxygen by halogenated aromatic hydrocarbons in mouse liver microsomes. Free Radic Biol Med. 2004 Mar 1;36(5):618-31

Shertzer HG, Clay CD, Genter MB, Schneider SN, Nebert DW, Dalton TP. (2004b). Cyp1a2 protects against reactive oxygen production in mouse liver microsomes. Free Radic Biol Med. 36(5):605-17.

Shertzer HG, Nebert DW, Puga A, Ary M, Sonntag D, Dixon K, Robinson LJ, Cianciolo E, Dalton TP. (1998). Dioxin causes a sustained oxidative stress response in the mouse. Biochem Biophys Res Commun. 253(1):44-8.

Shimada T, Hayes CL, Yamazaki H, Amin S, Hecht SS, Guengerich FP, Sutter TR. (1996). Activation of chemically diverse procarcinogens by human cytochrome P-450 1B1. Cancer Res.:2979-84.

Shou M, Korzekwa KR, Brooks EN, Krausz KW, Gonzalez FJ, Gelboin HV. (1997). Role of human hepatic cytochrome P450 1A2 and 3A4 in the metabolic activation of estrone. Carcinogenesis. 18(1):207-14.

Shull JD, Spady TJ, Snyder MC, Johansson SL, Pennington KL. (1997). Ovary-intact, but not ovariectomized female ACI rats treated with 17beta-estradiol rapidly develop mammary carcinoma. Carcinogenesis. 18(8):1595-601.

Sies H, Gerstenecker C, Menzel H, Flohé L. (1972). Oxidation in the NADP system and release of GSSG from hemoglobin-free perfused rat liver during peroxidatic oxidation of glutathione by hydroperoxides. FEBS Lett. 27(1):171-175

Sigma Protocol. (2005). Endoplasmic Reticulum Isolation Kit.

Silbernagel S and Despopoulos A. (2003). Taschenatlas der Physiologie. Georg Thieme Verlag Stuttgart, 6th edition.

Silkworth JB and Brown JF Jr. (1996). Evaluating the impact of exposures to environmental contaminants on human health. Clin Chem. 72:1345-1349

Singh NP, McCoy MT, Tice RR, Schneider EL. (1988). A simple technique for quantitation of low levels of DNA damage in individual cells. Exp Cell Res. 175: 184.

Singh S, Chakravarti D, Edney JA, Hollins RR, Johnson PJ, West WW, Higginbotham SM, Cavalieri EL, Rogan EG. (2005). Relative imbalances in the expression of estrogen-metabolizing enzymes in the breast tissue of women with breast carcinoma. Oncol Rep. 14(4):1091-6.

Singh SS, Hord NG, Perdew GH. (1996). Characterization of the activated form of the aryl hydrocarbon receptor in the nucleus of HeLa cells in the absence of exogenous ligand. Arch Biochem Biophys. 329(1):47-55.

Skoog L and Nordenskjöld B. (1971). Effects of hydroxyurea and 1-beta-D-arabinofuranosyl-cytosine on deoxyribonucleotide pools in mouse embryo cells. Eur J Biochem. 19(1):81-9.

Slezak BP, Hatch GE, DeVito MJ, Diliberto JJ, Slade R, Crissman K, Hassoun E, Birnbaum LS. (2000). Oxidative stress in female B6C3F1 mice following acute and subchronic exposure to 2,3,7,8-tetrachlorodibenzo-p-dioxin (TCDD). Toxicol Sci. 54(2):390-8.

Slupphaug G, Kavli B, Krokan HE. (2003). The interacting pathways for prevention and repair of oxidative DNA damage. Mutat Res. 531(1-2):231-51.

Sobol RW, Horton JK, Kühn R, Gu H, Singhal RK, Prasad R, Rajewsky K, Wilson SH. (1996). Requirement of mammalian DNA polymerase-beta in base-excision repair. Nature. 379(6561):183-6.

Speit G, Schütz P, Bonzheim I, Trenz K, Hoffmann H. (2004). Sensitivity of the FPG protein towards alkylation damage in the comet assay. Toxicol Lett. 146(2):151-8.

Spencer DL, Masten SA, Lanier KM, Yang X, Grassman JA, Miller CR, Sutter TR, Lucier GW, Walker NJ. (1999). Quantitative Analysis of Constitutive and 2,3,7,8-Tetrachlorodibenzo-p-dioxin-induced Cytochrome P450 1B1 Expression in Human Lymphocytes. Cancer Epidemiology, Biomarkers & Prevention. 8:139-146

Spink DC, Eugster HP, Lincoln DW 2nd, Schuetz JD, Schuetz EG, Johnson JA, Kaminsky LS, Gierthy JF. (1992). 17 beta-estradiol hydroxylation catalyzed by human cytochrome P450 1A1: a comparison of the activities induced by 2,3,7,8-tetrachlorodibenzo-p-dioxin in MCF-7 cells with those from heterologous expression of the cDNA. Arch Biochem Biophys. 293(2):342-8.

Spink DC, Hayes CL, Young NR, Christou M, Sutter TR, Jefcoate CR, Gierthy JF. (1994). The effects of 2,3,7,8-tetrachlorodibenzo-p-dioxin on estrogen metabolism in MCF-7 breast cancer cells: evidence for induction of a novel 17 beta-estradiol 4-hydroxylase. J Steroid Biochem Mol Biol. 51(5-6):251-258.

Spink DC, Katz BH, Hussain MM, Pentecost BT, Cao Z, Spink BC. (2003). Estrogen regulates Ah responsiveness in MCF-7 breast cancer cells. Carcinogenesis. 24(12):1941-50.

Spink DC, Lincoln DW 2nd, Dickerman HW, Gierthy JF. (1990). 2,3,7,8-Tetrachlorodibenzo-p-dioxin causes an extensive alteration of 17 beta-estradiol metabolism in MCF-7 breast tumor cells. Proc Natl Acad Sci U S A. 87(17):6917-21.

Sreerama L, Sladek NE. (1994). Identification of a methylcholanthrene-induced aldehyde dehydrogenase in a human breast adenocarcinoma cell line exhibiting oxazaphosphorine-specific acquired resistance. Cancer Res. 54(8):2176-85.

Stenchever MA, Jarvis JA, Kreger NK. (1969). Effect of selected estrogens and progestins on human chromosomes in vitro. Obstet Gynecol. 34(2):249-51.

Stinchcombe S, Buchmann A, Bock KW, Schwarz M. (1995). Inhibition of apoptosis during 2,3,7,8-tetrachlorodibenzo-p-dioxin-mediated tumour promotion in rat liver. Carcinogenesis. 16(6):1271-5.

Stohs SJ, Al-Bayati ZF, Hassan MQ, Murray WJ, Mohammadpour HA.(1986). Glutathione peroxidase and reactive oxygen species in TCDD-induced lipid peroxidation. Adv Exp Med Biol. 197:357-65.

Stohs SJ, Alsharif NZ, Shara MA, al-Bayati ZA, Wahba ZZ. (1991). Evidence for the induction of an oxidative stress in rat hepatic mitochondria by 2,3,7,8-tetrachlorodibenzo-p-dioxin (TCDD). Adv Exp Med Biol. 283:827-31.

Strahl BD and Allis CD. (2000). The language of covalent histone modifications. Nature. 403(6765):41-5.

Stucki M, Pascucci B, Parlanti E, Fortini P, Wilson SH, Hübscher U, Dogliotti E. (1998). Mammalian base excision repair by DNA polymerases delta and epsilon. Oncogene. 17(7):835-43.

Sun J, Meyers MJ, Fink BE, Rajendran R, Katzenellenbogen JA, Katzenellenbogen BS. (1999). Novel ligands that function as selective estrogens or antiestrogens for estrogen receptor-? or estrogen receptor-?. Endocrinology 140, 800-804 (1999).

Sutter TR, Tang YM, Hayes CL, Wo YY, Jabs EW, Li X, Yin H, Cody CW, Greenlee WF. (1994). Complete cDNA sequence of a human dioxin-inducible mRNA identifies a new gene subfamily of cytochrome P450 that maps to chromosome 2. J Biol Chem. (18):13092-9.

Tchou J, Bodepudi V, Shibutani S, Antoshechkin I, Miller J, Grollman AP, Johnson F. (1994). Substrate specificity of Fpg protein. Recognition and cleavage of oxidatively damaged DNA. J Biol Chem. 269(21):15318-24.

Tenhunen J, Salminen M, Lundström K, Kiviluoto T, Savolainen R, Ulmanen I. (1994). Genomic organization of the human catechol O-methyltransferase gene and its expression from two distinct promoters. Eur J Biochem. 223(3):1049-59.

Thelander L and Reichard P. (1979). Reduction of ribonucleotides. Annu Rev Biochem. 48:133-58.

Thermo Fischer Scientific Inc., http://www.nanodrop.com (January 009)

Thomas D, Scot AD, Barbey R, Padula M, Boiteux S. (1997). Inactivation of OGG1 increases the incidence of G . C-->T . A transversions in Saccharomyces cerevisiae: evidence for endogenous oxidative damage to DNA in eukaryotic cells. Mol Gen Genet. 254(2):171-8.

Thompson PA, Shields PG, Freudenheim JL, Stone A, Vena JE, Marshall JR, Graham S, Laughlin R, Nemoto T, Kadlubar FF, Ambrosone CB. (1998). Genetic polymorphisms in catechol-O-methyltransferase, menopausal status, and breast cancer risk. Cancer Res. 58(10):2107-10.

Thomsen JS, Wang X, Hines RN, Safe S. (1994). Restoration of aryl hydrocarbon (Ah) responsiveness in MDA-MB-231 human breast cancer cells by transient expression of the estrogen receptor. Carcinogenesis. 15(5):933-7.

Thor H, Smith MT, Hartzell P, Bellomo G, Jewell SA, Orrenius S. (1982). The metabolism of menadione (2-methyl-1,4-naphthoquinone) by isolated hepatocytes. A study of the implications of oxidative stress in intact cells. J Biol Chem. 257(20):12419-25.

Tice R.R., Vazquez M. (1999 revised). Protocol for the application of the pH>13 alkaline single cell gel (SCG) assay to the detection of DNA damage in mammalian cells. Exp. Cell Res. 175:184-191

Tice RR, Agurell E, Anderson D, Burlinson B, Hartmann A, Kobayashi H, Miyamae Y, Rojas E, Ryu J-C, Sasaki YF. (2000). Single-cell gel/comet assay: guidelines for in vitro and in vivo genetic toxicology testing. Environ Mol Mutagen. 35:206-221.

Toniolo PG, Levitz M, Zeleniuch-Jacquotte A, Banerjee S, Koenig KL, Shore RE, Strax P, Pasternack BS. (1995). A prospective study of endogenous estrogens and breast cancer in postmenopausal women. J Natl Cancer Inst. 87(3):190-7.

Topinka J, Andrae U, Schwarz LR, Wolff T. (1993). Cyproterone acetate generates DNA adducts in rat liver and in primary rat hepatocyte cultures. Carcinogenesis. 14(3):423-7.

Tóth K, Somfai-Relle S, Sugár J, Bence J. (1979). Carcinogenicity testing of herbicide 2,4,5-trichlorophenoxyethanol containing dioxin and of pure dioxin in Swiss mice. Nature. 278(5704):548-9.

Tritscher AM, Seacat AM, Yager JD, Groopman JD, Miller BD, Bell D, Sutter TR, Lucier GW. (1996). Increased oxidative DNA damage in livers of 2,3,7,8-tetrachlorodibenzo-p-dioxin treated intact but not ovariectomized rats. Cancer Letters. 98:219-225.

Tsuchiya Y, Nakajima M, Kyo S, Kanaya T, Inoue M, Yokoi T. (2004). Human CYP1B1 is regulated by estradiol via estrogen receptor. Cancer Res. 1;64(9):3119-25.

Tsuchiya Y, Nakajima M, Yokoi T. (2005). Cytochrome P450-mediated metabolism of estrogens and its regulation in human. Cancer Lett. 227(2):115-24.

Tsutsui T, Suzuki N, Fukuda S, Sato M, Maizumi H, McLachlan JA, Barrett JC. (1987). 17beta-Estradiol-induced cell transformation and aneuploidy of Syrian hamster embryo cells in culture.Carcinogenesis. 8(11):1715-9.

Tsutsui T, Tamura Y, Yagi E, Barrett JC. (2000). Involvement of genotoxic effects in the initiation of estrogen-induced cellular transformation: studies using Syrian hamster embryo cells treated with 17beta-estradiol and eight of its metabolites. Int J Cancer. 2000 Apr 1;86(1):8-14.

Tudek B, Van Zeeland AA, Kusmierek JT, Laval J. (1998). Activity of Escherichia coli DNA-glycosylases on DNA damaged by methylating and ethylating agents and influence of 3-substituted adenine derivatives. Mutat Res. 407(2):169-76.

Turteltaub KW, Felton JS, Gledhill BL, Vogel JS, Southon JR, Caffee MW, Finkel RC, Nelson DE, Proctor ID, Davis JC. (1990). Accelerator mass spectrometry in biomedical dosimetry: relationship between low-level exposure and covalent binding of heterocyclic amine carcinogens to DNA. Proc Natl Acad Sci U S A. 87(14):5288-92.

Tuschl G and Mueller SO. (2006). Effects of cell culture conditions on primary rat hepatocytes—Cell morphology and differential gene expression.Toxicology. 218:205–215

Tzukerman MT, Esty A, Santiso-Mere D, Danielian P, Parker MG, Stein RB, Pike JW, McDonnell DP. (1994). Human estrogen receptor transactivational capacity is determined by both cellular and promoter context and mediated by two functionally distinct intramolecular regions. Mol Endocrinol. 8(1):21-30.

Udenfried S, Stein S, Böhlen P, Dairman W, Leimgruber W, Weigele M. (1972). Fluorescamine: a reagent for assay of amino acids, peptides, proteins, and primary amines in the picomole range. Science 178:871-872.

Ulmanen I and Lundström K. (1991). Cell-free synthesis of rat and human catechol O-methyltransferase. Insertion of the membrane-bound form into microsomal membranes in vitro.Eur J Biochem. 202(3):1013-20.

Valentin I, Philippe M, Lhuguenot JC, Chagnon MC. (2001). Uridine uptake inhibition as a cytotoxicity test for a human hepatoma cell line (HepG2 cells): comparisons with the neutral red assay. Toxicology. 158:127-139.

Valentin-Severin I, Le Hegarat L, Lhuguenot JC, Lebon AM, Chagnon MC. (2003). Use of HepG2 cell line for direct or indirect mutagens screening: comparative investigation between comet and micronucleus assays. Mutat Res. 536:79 - 90.

Valentin-Severin I. (2002). Evaluation de la cytotoxicité et de la genotoxicité à l'aide d'une lignée cellulaire hepatique d'origine humaine 'HepG2'. Doctoral thesis at the University of Burgundy, Dijon, France.

Valentin-Severin I., Laignelet L., Lhuguenot J.C., Chagnon M.C. (2002). Uridine uptake inhibition assay: an automated micromethod for the screening of cytotoxicity. Toxicology. 171:207-213.

Valko M, Izakovic M, Mazur M, Rhodes CJ, Telser J. (2004). Role of oxygen radicals in DNA damage and cancer incidence. Mol Cell Biochem. 266(1-2):37-56.

Valko M, Rhodes CJ, Moncol J, Izakovic M, Mazur M. (2006). Free radicals, metals and antioxidants in oxidative stress-induced cancer. Chemico-Biological Interactions. 160:1-40

Van Aswegen CH, Purdy RH, Wittliff JL. (1989). Binding of 2-hydroxyestradiol and 4-hydroxyestradiol to estrogen receptors from human breast cancers. J Steroid Biochem. 32(4):485-92.

Van den Berg M, Peterson RE, Schrenk D. (2000). Human risk assessment and TEFs. Food Additives and Contaminants. 17:347-358.

Van der Horst GT, van Steeg H, Berg RJ, van Gool AJ, de Wit J, Weeda G, Morreau H, Beems RB, van Kreijl CF, de Gruijl FR, Bootsma D, Hoeijmakers JH. (1997). Defective Transcription-Coupled Repair in Cockayne Syndrome B Mice is Associated with Skin Cancer Predisposition. Cell. 89:425-435

Van der Kemp PA, Thomas D, Barbey R, de Oliveira R, Boiteux S. (1996). Cloning and expression in Escherichia coli of the OGG1 gene of Saccharomyces cerevisiae, which codes for a DNA glycosylase that excises 7,8-dihydro-8-oxoguanine and 2,6-diamino-4-hydroxy-5-N-methylformamidopyrimidine. Proc Natl Acad Sci U S A93(11):5197-202.

Vickers PJ, Dufresne MJ, Cowan KH. (1989). Relation between cytochrome P450IA1 expression and estrogen receptor content of human breast cancer cells. Mol Endocrinol. 3(1):157-64.

Vik DP, Amiguet P, Moffat GJ, Fey M, Amiguet-Barras F, Wetsd RA, Tack B. (1991). Structural features of the human C3 gene: intron/exon organization, transcriptional start site, and promoter region sequence. Biochemistry. 30:1080-l085

Viluksela M, Bager Y, Tuomisto JT, Scheu G, Unkila M, Pohjanvirta R, Flodström S, Kosma VM, Mäki-Paakkanen J, Vartiainen T, Klimm C, Schramm KW, Wärngård L, Tuomisto J. (2000). Liver tumor-promoting activity of 2,3,7,8-tetrachlorodibenzo-p-dioxin (TCDD) in TCDD-sensitive and TCDD-resistant rat strains. Cancer Res. 60(24):6911-20.

Vuchetich PJ, Bagchi D, Bagchi M, Hassoun EA, Tang L, Stohs SJ. (1996). Naphthalene-induced oxidative stress in rats and the protective effects of vitamin E succinate. Free Radic Biol Med. 21(5):577-90.

Wahba ZZ, Lawson TW, Murray WJ, Stohs SJ. (1989). Factors influencing the induction of DNA single strand breaks in rats by 2,3,7,8-tetrachlorodibenzo-p-dioxin (TCDD). Toxicology. 58(1):57-69.

Walker NJ, Gastel JA, Costa LT, Clark GC, Lucier GW, Sutter TR. (1995). Rat CYP1B1: an adrenal cytochrome P450 that exhibits sexdependent expression in livers and kidneys of TCDD-treated animals. Carcinogenesb. 16: 1319-1327

Walker NJ, Portier CJ, Lax SF, Crofts FG, Li Y, Lucier GW, Sutter TR. (1999). Characterization of the Dose-Response of CYP1B1, CYP1A1, and CYP1A2 n the liver of Female Sprague-Dawley Rats Following Chronic Exposure to 2,3,7,8-Tetrachlorodibenzo-p-dioxin. Toxicology and Applied Pharmacology. 154:279-286

Walker NJ, Wyde ME, Fischer LJ, Nyska A, Bucher JR. (2006). Comparison of chronic toxicity and carcinogenicity of 2,3,7,8-tetrachlorodibenzo-p-dioxin (TCDD) in 2-year bioassays in female Sprague-Dawley rats. Mol Nutr Food Res. 50(10):934-44.

Walter P, Green S, Greene G, Krust A, Bornert JM, Jeltsch JM, Staub A, Jensen E, Scrace G, Waterfield M, et al. (1985). Cloning of the human estrogen receptor cDNA. Proc Natl Acad Sci U S A. 82(23):7889-7893.

Wang H and Joseph JA. (1999). Quantifying Cellular Oxidative Stress by Dichlorofuorescein assay using microplate reader.Free Radical Biology & Medicine.27: 612-616

Wang S and Hankinson O. (2002). Functional involvement of the Brahma/ SWI2-related gene 1 protein in cytochrome P4501A1 transcription mediated by the aryl hydrocarbon receptor complex. J. Biol. Chem. 277:11821-11827.

Wang S, Ge K, Roeder RG, Hankinson O. (2004). Role of mediator in transcriptional activation by the aryl hydrocarbon receptor. J. Biol. Chem. 279:13593-13600.

Wang W, Smith R 3rd, Safe S. (1998). Aryl hydrocarbon receptor-mediated antiestrogenicity in MCF-7 cells: modulation of hormone-induced cell cycle enzymes. Arch Biochem Biophys. 356(2):239-48.

Wang X, Porter W, Krishnan V, Narasimhan TR, Safe S. (1993). Mechanism of 2,3,7,8-tetrachlorodibenzo-p-dioxin (TCDD)-mediated decrease of the nuclear estrogen receptor in MCF-7 human breast cancer cells. Mol Cell Endocrinol. 96(1-2):159-66.

Warner M, Eskenazi B, Mocarelli P, Gerthoux PM, Samuels S, Needham L, Patterson D, Brambilla P. (2002). Serum dioxin concentrations and breast cancer risk in the Seveso Women's Health Study. Environ Health Perspect. 110(7):625-8.

Weatherman RV. (2006). Untangling the estrogen receptor web. Nature Chemical Biology. 2(4): 175-176

Weisz J, Bui QD, Roy D, Liehr JG. (1992). Elevated 4-hydroxylation of estradiol by hamster kidney microsomes: a potential pathway of metabolic activation of estrogens. Endocrinology. 131(2):655-61.

Wen W, Ren Z, Shu XO, Cai Q, Ye C, Gao YT, Zheng W. (2007). Expression of cytochrome P450 1B1 and catechol-O-methyltransferase in breast tissue and their associations with breast cancer risk. Cancer Epidemiol Biomarkers Prev. 16(5):917-20.

Whitlock JP Jr, Okino ST, Dong L, Ko HP, Clarke-Katzenberg R, Ma Q, Li H. (1996). Cytochromes P450s. Induction of cytochrome P4501A1: a model for analyzing mammalian gene transcription. FASEB Journal. 10(8):809-18.

Whitlock JP Jr. (1999). Induction of cytochrome P450 1A1. Annu. Rev. Pharmacol. Toxicol. 39:103-25

WHO Consultation. (1998). Executive Summary. Assessment of the health risk of dioxins: re-evaluation of the Tolerable Daily Intake (TDI). WHO European Centre for Environment and Health International Programme on Chemical Safety

WHO. (2009). Fact sheet N°297. http://www.who.int/mediacentre/factsheets/fs297/en/.

Wihlén B, Ahmed S, Inzunza J, Matthews J. (2009). Estrogen receptor subtype- and promoter-specific modulation of aryl hydrocarbon receptor-dependent transcription. Mol Cancer Res. 7(6):977-86.

Wijayaratne AL and McDonnell DP. (2001). The Human Estrogen Receptor-_ Is a Ubiquitinated Protein Whose Stability Is Affected Differentially by Agonists, Antagonists, and Selective Estrogen Receptor Modulators Journal of Biological Chemistry. 276: 35684-35692,

Wijayaratne AL, NagelL SC, Paige LA, Christensen DJ, Norris JD, Fowlkes DM, McDonnell DP. (1999). Comparative Analyses of Mechanistic Differences Among Antiestrogens Endocrinology Vol. 140, No. 12 5828-5840

Wilhelm J and Pingoud A. (2003). Real-time Polymerase Chain Reaction. ChemBioChem. 4: 1120.

Wilkening S and Bader A. (2003). Influence of culture time on the expression of drug-metabolizing enzymes in primary human hepatocytes and hepatoma cell line HepG2. J Biochem Mol Toxicol. 17(4):207-13.

Wilkening S, Stahl F, Bader A. (2003). Comparison of primary human hepatocytes and hepatoma cell line Hepg2 with regard to their biotransformation properties. Drug Metab Dispos. 31(8):1035-42.

Williams C, Edvardsson K, Lewandowski SA, Ström A, Gustafsson JA. (2008). A genome-wide study of the repressive effects of estrogen receptor beta on estrogen receptor alpha signaling in breast cancer cells. Oncogene.27(7):1019-32.

Williams GM, Bermudez E, Scaramuzzino D. (1977). Rat hepatocyte primary cell cultures. III. Improved dissociation and attachment techniques and the enhancement of survival by culture medium. In Vitro. 13(12):809-17.

Williams GM. (1976). Carcinogen-induced DNA repair in primary rat liver cell cultures; a possible screen for chemical carcinogens. Cancer Lett. 1(4):231-5.

Williams GM. (1977). Detection of chemical carcinogens by unscheduled DNA synthesis in rat liver primary cell cultures. Cancer Res. 37(6):1845-51.

Wo YY, Stewart J, Greenlee WF. (1997). Functional analysis of the promotor for the human CYP1B1 gene. J Biol Chem. 272:26702-26707

Wood ML, Dizdaroglu M, Gajewski E, Essigmann JM. (1990). Mechanistic studies of ionizing radiation and oxidative mutagenesis: genetic effects of a single 8-hydroxyguanine (7-hydro-8-oxoguanine) residue inserted at a unique site in a viral genome.Biochemistry.29(30):7024-32.

Wood RD, Mitchell M, Lindahl T. (2005). Human DNA repair genes, 2005. Mutat Res. 577(1-2):275-83.

Wormke M, Stoner M, Saville B, Walker K, Abdelrahim M, Burghardt R, Safe S. (2003). The aryl hydrocarbon receptor mediates degradation of estrogen receptor alpha through activation of proteasomes. Mol Cell Biol. 23(6):1843-55.

Wörner W and Schrenk D. (1996). Influence of liver tumor promoters on apoptosis in rat hepatocytes induced by 2-acetylaminofluorene, ultraviolet light, or transforming growth factor beta 1. Cancer Res. 56(6):1272-8.

Wu X, Li J, Li X, Hsieh CL, Burgers PM, Lieber MR. (1996). Processing of branched DNA intermediates by a complex of human FEN-1 and PCNA. Nucleic Acids Res. 24(11):2036-43.

Wyatt MD and Pittman DL. (2006). Methylating agents and DNA repair responses: Methylated bases and sources of strand breaks. Chem Res Toxicol. 19(12):1580-94.

Wyde ME, Wong VA, Kim AH, Lucier GW, Walker NJ. (2001). Induction of hepatic 8-oxo-deoxyguanosine adducts by 2,3,7,8-tetrachlorodibenzo-p-dioxin in Sprague-Dawley rats is female-specific and estrogen-dependent. Chem Res Toxicol. 14(7):849-55.

Wysowski DK, Comstock GW, Helsing KJ, Lau HL. (1987). Sex hormone levels in serum in relation to the development of breast cancer. Am J Epidemiol. 125(5):791-9.

Xu L, Li AP, Kaminski DL, Ruh MF. (2000). 2,3,7,8 Tetrachlorodibenzo-p-dioxin induction of cytochrome P4501A in cultured rat and human hepatocytes. Chem Biol Interact. 124(3):173-89.

Yager JD and Liehr JG. (1996). Molecular mechanisms of estrogen carcinogenesis. Annu Rev Pharmacol Toxicol. 36:203-32.

Yager JD and Shi YE. (1991). Synthetic estrogens and tamoxifen as promoters of hepatocarcinogenesis. Prev Med. 20(1):27-37.

Yager JD. (2000). Endogenous estrogens as carcinogens through metabolic activation. J Natl Cancer Inst Monogr. (27):67-73.

Yared E, McMillan TJ, Martin FL. (2002). Genotoxic effects of oestrogens in breast cells detected by the micronucleus assay and the Comet assay. Mutagenesis. 17(4):345-52.

Zacharewski TR, Bondy KL, McDonell P, Wu ZF. (1994). Antiestrogenic effect of 2,3,7,8-tetrachlorodibenzo-p-dioxin on 17 beta-estradiol-induced pS2 expression. Cancer Res. 54(10):2707-13.

Zacharia LC, Piché CA, Fielding RM, Holland KM, Allison SD, Dubey RK, Jackson EK. (2004). 2-hydroxyestradiol is a prodrug of 2-methoxyestradiol. J Pharmacol Exp Ther. 309(3):1093-7.

Zahid M, Kohli E, Saeed M, Rogan E, Cavalieri E. (2006). The greater reactivity of estradiol-3,4-quinone vs estradiol-2,3-quinone with DNA in the formation of depurinating adducts: implications for tumor-initiating activity. Chem Res Toxicol. 19(1):164-72.

Zeiger M, Haag R, Höckel J, Schrenk D, Schmitz HJ.(2001).Inducing Effects of Dioxin-like Polychlorinated Biphenyls on CYP1A in the Human Hepatoblastoma Cell Line HepG2, the Rat Hepatoma Cell Line H4IIE, and Rat Primary Hepatocytes: Comparison of Relative Potencies. Toxicological Sciences. 63: 65-73

Zhu BT and Liehr JG. (1993). Inhibition of the catechol-O-methyltransferase-catalyzed O-methylation of 2- and 4-hydroxyestradiol by catecholamine: implications for the mechanism of estrogen-induced carcinogenesis. Arch Biochem Biophys. 304(1):248-56.

8.6. CURRICULUM VITAE

Personal Data	
	Manuela Göttel Diplom Lebensmittelchemikerin (Food chemist) Born 21 January 1981 in Mainz, Germany

Education	
Jun 2000	**Allgemeine Hochschulreife (University Entrance Exams)** Elisabeth-Langgässer-Gymnasium, Alzey, Germany
Oct 2000–Apr 2005	**Food Chemistry Studies** Technische Universität Kaiserslautern, Germany
Feb–Apr 2004	**Research Internship** "Role of docosahexaenoic (DHA) acid and diacylglycerol containing DHA on the increase in free intracellular calcium concentrations in Jurkat T cell line" Department of Physiology and Immunology, University of Burgundy, Dijon, France
Oct 2004–Apr 2005	**Diploma Thesis** "Untersuchung der Genexpression fremdstoffmetabolisierender Enzyme unter dem Einfluss des Apfelsaftextraktes AS03B an zwei humanen Kolonkarzinomzelllinien" Technische Universität Kaiserslautern, Germany
Apr 14th 2005	**Diploma Degree Food Chemist and First State Examination**
May 2005–Dec 2009	**Doctoral Thesis** "The Role of 17beta-Estradiol on 2,3,7,8-Tetrachlorodibenzo-*p*-dioxin-mediated Oxidative DNA Damage in Liver Cell Models" Technische Universität Kaiserslautern, Germany
Oct 2006–May 2007	**Research Work in the course of the PhD Program** Department of Food Toxicology, ENSBANA, University of Burgundy, Dijon, France

Employment	
Since March 2009	**Regulatory Toxicologist** Product Safety Crop Protection BASF, Ludwigshafen, Germany

Further Qualifications	
Oct 2002–Jun 2006	**Supplementary Course of Studies "Technical French"** Technische Universität Kaiserslautern, Germany
Oct 2005–Jun 2008	**Supplementary Course of Studies "Technical English"** Technische Universität Kaiserslautern, Germany
Since Jan 2006	**Participation in the Toxicology Training Program "Fachtoxikologe DGPT"** Deutsche Gesellschaft für experimentelle und klinische Pharmakologie und Toxikologie (DGPT)

Scholarships	
Oct 2000–Sep 2001	**Novice Scholarship** Fachbereich Chemie, Technische Universität Kaiserslautern, Germany
May 2005–Mar 2007	**Doctoral Scholarship** Landesgraduiertenförderungsgesetz (LGFG) Rheinland-Pfalz
Oct 2006–Mar 2007	**Foreign Exchange Scholarship** Deutscher Akademischer Austauschdienst (DAAD)